

**MOLECULAR BASIS OF PATHOGENESIS OF
DYSTONIA AMONG INDIAN PATIENTS**

**Thesis submitted for the degree of
DOCTOR OF PHILOSOPHY (SCIENCE)
in GENETICS**

SUBHAJIT GIRI

S. N. Pradhan Centre for Neurosciences

University of Calcutta

2017

Acknowledgement

To begin with, I would love to convey my deepest gratitude to Prof. Jharna Ray for providing me such an excellent opportunity to work on Neurogenetics field of Dystonia in her laboratory. I am appreciative towards her enthusiastic support and constant supervision throughout this study. Her advices, technical suggestions and thoughts made me enlightened and developed as a scientist.

Another person who inspired me to be a geneticist is Prof. Kunal Ray. Being an associated collaborator of Prof. Jharna Ray, he took my interview during my joining to the laboratory. His challenging questions regarding human genetics instigated me to explore this particular field. I am indebted to his academic and technical support throughout these days.

I am also thankful to our clinical collaborator, Prof. Shyamal Kumar Das and Dr. Charulata Savant Sankhla for their constant support regarding sample collection and providing the invaluable clinical reports of the Dystonia patients. With a special note, Prof. Shyamal Kumar Das granted us to attend the movement disorder clinic and educated us how to diagnose the different types of Dystonia and other movement disorders.

With my deepest gratitude, I was very lucky to have an opportunity to work with Prof. Mark S. LeDoux at The Department of Neurology, University of Tennessee Health Science Centre, Memphis, USA as a Fulbright-Nehru doctoral research fellow for nine months. It was an absolutely productive and enjoyable tenure of my doctoral program. I am really thankful to him to use the enormous laboratory resources and academic materials to pursue my endeavours. I am also thankful to the lab members of Prof. Mark S. LeDoux - Dr. Xianfeng Xiao, Dr. Satya Vemula, Dr. Esther M Marquez-Lona, Dr. Yu Zhao, Dr. Mohammad Moshahid Khan and Dr. Yi Xue; Dr. David Kakhniasvili and Dr. Daniel Johnson of Molecular Resource Centre and all other teaching and non-teaching staff of UTHSC.

Acknowledgement

I have been greatly indebted in a loving way to my family members. I have received a great support from my father, Mr. Jagannath Giri who supported me throughout my life with great care both financially and mentally. I am thankful to almighty to be a son of my deceased mother, Late Sandhya Rani Giri who was my friend, philosopher and a teacher in a true sense. Without their love, care and belief on me, I won't be able to achieve anything in my life and I am really happy to make them proud. I am also thankful to my beloved wife, Mrs. Sanchita Das for her support, compassion and love to me and being around during my all ups and downs in my life.

I would like to express my gratitude to my past and present laboratory colleagues Dr. Gautami Das, Dr. Tamal Sadhukhan, Dr. Tufan Naiya, Dr. Arindam Biswas, Ms. Dipanwita Sadhukhan, Ms. Arunibha Ghosh, Ms. Arunima Bhaduri, Mr. Prosenjit Pal and Mr. Shubhrajit Roy for being supportive colleagues with their best intentions. I am also thankful to Dr. Mainak Sengupta and Dr. Krishnadas Nandogopal of Department of Genetics, University of Calcutta for their all academic and administrative supports.

I am thankful to the Calcutta Consortium of Human Genetics (CCHuGe) to integrate me during my Ph.D tenure as an active student member and providing me the opportunity to discuss and present the different aspects of Human Genetics which was really enriched my knowledge and broaden my horizon of expertise. I have fortunate enough to have the friendships of some of the CCHuGe members Dr. Santu Kumar Saha, Dr. Sweta Sharma, Mrs. Amrapali Bhattacharya and Ms. Chirantani Mukherjee with a special note for keeping me motivated to complete my thesis write-ups.

I would like to thank all the associated teaching and non-teaching staff of Calcutta University and especially in our department with a special note to Mr. Sowbhagya Chowdhury and Mr. Kundan Dubey. I would like to express my sincere gratitude to all the administrative personnel in Calcutta University for their immense support regarding the administrative requirements.

Thesis Outline

Acknowledgement.....	I-II
Chapter 1: Introduction.....	1-10
Chapter 2: The genetics of dystonia.....	11-71
2.1: Introduction.....	12
2.2: The DYT loci.....	14
2.2.1: <i>DYT1-TOR1A</i>	14
2.2.2: <i>DYT2-HPCA</i>	19
2.2.3: <i>DYT3-TAF1</i>	21
2.2.4: <i>DYT4-TUBB4A</i>	24
2.2.5: <i>DYT5a/DYT14-GCH1</i>	26
2.2.6: <i>DYT5b-TH</i>	32
2.2.7: <i>DYT6-THAP1</i>	34
2.2.8: <i>DYT8-MR1</i>	39
2.2.9: <i>DYT9/DYT18-SLC2A1</i>	41
2.2.10: <i>DYT10-PRRT2</i>	43
2.2.11: <i>DYT11-SGCE</i>	46
2.2.12: <i>DYT12-ATP1A3</i>	52
2.2.13: <i>DYT16-PRKRA</i>	54
2.2.14: <i>DYT23-CIZ1</i>	56
2.2.15: <i>DYT24-ANO3</i>	57
2.2.16: <i>DYT25-GNAL</i>	59
2.2.17: <i>DYT26- KCTD17</i>	61

Thesis outline

2.2.18:	<i>DYT27-COL6A3</i>	63
2.3:	Common molecular pathway for dystonia pathogenesis.....	64-70
2.3.1	Cellular proliferation and apoptosis.....	65
2.3.2	Transcriptional regulation and gene expression.....	66
2.3.3	Response to cellular stress.....	67
2.3.4	Synaptic functions and neurotransmission.....	68
Chapter 3:	Screening of <i>TOR1A</i> and <i>THAP1</i> gene variants in primary pure dystonia patients.....	71-110
3.1	Introduction.....	72-74
3.2	Materials & Methods.....	75-90
3.2.1	Patients & Controls.....	75
3.2.2	Genetic screening study.....	76
3.2.3	Statistical and <i>in silico</i> analysis.....	88
3.3	Results.....	90-105
3.3.1	Identification of nucleotide variants in <i>TOR1A</i> gene.....	90
3.3.2	Primary torsion dystonia due to the <i>TOR1A</i> Δ GAG in an Indian family.....	90
3.3.3	Case control association study of identified <i>TOR1A</i> SNPs.....	93
3.3.4	Identification of nucleotide variants in <i>THAP1</i> gene.....	99
3.3.5	Clinical characterization of patients	103
3.3.6	Association study of rs11989331 (IVS2-87 A>G).....	104
3.3.7	Gene-gene interaction for <i>TOR1A</i> and <i>THAP1</i> SNPs	104
3.4	Discussion.....	106-110

Chapter 4:	Functional characterization of <i>THAP1</i> missense variants in cell culture based model.....	111-148
4.1:	Introduction.....	112-116
4.2	Materials and methods.....	117-139
4.2.1	Generation of <i>THAP1</i> mutant constructs by site-directed mutagenesis.....	117
4.2.2	Immunocytochemistry and confocal microscopy.....	124
4.2.3	Cycloheximide chase assay/western blot.....	125
4.2.4	Actinomycin D chase assay/qRT-PCR.....	127
4.2.5	Dual - Luciferase assay	133
4.3	Results.....	140-145
4.3.1	Generation of different <i>THAP1</i> mutant constructs.....	140
4.3.2	Subcellular localization of mutant THAP1 protein.....	141
4.3.3	Mutant THAP1 protein stability determination.....	142
4.3.4	Mutant <i>THAP1</i> mRNA stability assay.....	143
4.3.5	Effect of <i>THAP1</i> mutation over <i>TOR1A</i> transcription.....	145
4.4	Discussion.....	146-148
Chapter 5:	Whole genome gene expression analysis of primary dystonia patients having <i>THAP1</i> mutation by RNA-sequencing.....	149-233
5.1	Introduction.....	150
5.2	Materials & Methods.....	151-181
5.2.1	Selection of patient and control subjects.....	151

5.2.2	Fibroblast cell culture	153
5.2.3	Isolation and purification of total RNA from fibroblast samples.....	155
5.2.4	Sequencing library preparation for RNA-seq.....	158
5.2.5	RNA-seq data analysis.....	181
5.3	Results.....	182-230
5.3.1	Quality and quantity determination of isolated total RNA samples.....	182
5.3.2	The sequencing quality determination.....	185
5.3.3	Identification of differentially expressed genes in <i>THAP1</i> mutant dystonia patients compared to controls.....	217
5.4	Discussion.....	231-232
Chapter 6:	Whole cell quantitative proteomic profiling of primary dystonia patients having <i>THAP1</i> mutation by LC-MS/MS.....	233-269
6.1	Introduction.....	234
6.2	Materials & Methods.....	235-248
6.2.1	Selection of patient and control subjects.....	235
6.2.2	Fibroblast cell culture.....	235
6.2.3	Whole cell lysate preparation from fibroblast samples.....	235
6.2.4	Protein concentration determination	236
6.2.5	Sample preparation with TMT™ Isobaric Mass Tagging.....	238
6.2.6	Protein sequencing through Orbitrap Fusion™ Lumos™ Tribrid™ Mass Spectrometer.....	247
6.2.7	Statistical analysis.....	248
6.3	Results	249-268
6.4	Discussion.....	269

Thesis outline

Chapter 7: Conclusion.....	270-276
7.1: Summary of findings.....	271
7.2: Future direction.....	274
References.....	277-344
Appendix I.....	345
Appendix II.....	346-347
Appendix III.....	348-349
Reprints of publications	

List of Tables

Table 1:	Classification of dystonia.....	4
Table 2:	Prevalence rate of dystonia reported in different world population.....	6
Table 3:	The DYT loci.....	15
Table 4:	Genetic rare variants of <i>TOR1A</i> gene found in primary dystonia patients.....	17
Table 5:	Mutations found in <i>GCH1</i> gene in DRD patients.....	29
Table 6:	Mutations found in <i>TH</i> gene in DRD patients.....	34
Table 7:	Mutations found in <i>THAP1</i> gene in primary DYT6 dystonia patients...	37
Table 8:	Mutations found in <i>SLC2A1</i> gene in PED patients.....	42
Table 9:	Mutations found in <i>PRRT2</i> gene in PKD patients.....	45
Table 10:	Mutations found in <i>SGCE</i> gene in myoclonus dystonia patients.....	49
Table 11:	Mutations found in <i>ATP1A3</i> gene in RDP patients.....	53
Table 12:	Mutations found in <i>GNAL</i> gene in PTD patients.....	61
Table 13:	<i>TOR1A</i> Δ GAG mutation found on different ethnic population.....	73
Table 14:	Clinical diagnosis and demographics of Indian primary dystonia patients recruited for <i>TOR1A</i> genetic study.....	77
Table 15:	Clinical diagnosis and demographics of Indian primary dystonia patients recruited for <i>THAP1</i> genetic study.....	78
Table 16:	Primer sequences and amplification conditions for <i>TOR1A</i> gene regions.....	81
Table 17:	Primer sequences and amplification conditions for <i>THAP1</i> gene regions.....	82
Table 18:	List of Buffers and solutions used for gel electrophoresis.....	84
Table 19:	Sequencing reaction composition.....	85
Table 20:	Thermocycler condition for DNA sequencing.....	86
Table 21:	PCR primers and restriction enzymes were used for genotyping.....	89
Table 22:	<i>TOR1A</i> nucleotide variants identified in primary dystonia patients....	91
Table 23:	Clinical parameters of individuals harbouring <i>TOR1A</i> Δ GAG mutation.....	91
Table 24:	Allele and genotype frequency of rs1801968.....	95
Table 25:	Allele and genotype frequency of rs3842225.....	95
Table 26:	Allele and genotype frequency of rs1182.....	96

List of Tables

Table 27:	Allele and genotype frequency of rs13300897.....	96
Table 28:	rs1182-rs3842225 haplotypic association study.....	98
Table 29:	rs1801968-rs1182-rs3842225 haplotypic association study.....	98
Table 30:	<i>THAP1</i> Nucleotide Variants in Indian primary dystonia patients.....	102
Table 31:	Clinical characteristics of patients having <i>THAP1</i> genetic variants.....	102
Table 32:	Allele and genotype frequency of rs11989331.....	104
Table 33:	Best predictive gene-gene interaction models identified by multifactor dimensionality reduction analysis.....	105
Table 34:	Comparison of the different approach for functional characterization of <i>THAP1</i> gene variants reported in literature.....	113
Table 35:	<i>In-silico</i> prediction for pathogenicity of the selected <i>THAP1</i> variants for functional characterization.....	116
Table 36:	Primer sequences used for site-directed mutagenesis to generate different <i>THAP1</i> mutant constructs.....	118
Table 37:	SDM reaction composition.....	119
Table 38:	Thermocycler condition for SDM.....	119
Table 39:	KLD reaction composition.....	119
Table 40:	Sanger sequencing reaction composition for plasmid sequencing.....	123
Table 41:	Thermocycler condition for plasmid DNA sequencing.....	123
Table 42:	Primer sequences used for TaqMan based qRT-PCR.....	128
Table 43:	qPCR reaction component.....	129
Table 44:	Reaction components for single reverse transcription reaction.....	133
Table 45:	Reaction condition of thermal cycler for cDNA conversion.....	133
Table 46:	Primer sequences for amplification of <i>TOR1A</i> core promoter.....	135
Table 47:	Reaction component for ligation reaction by T4 DNA ligation.....	136
Table 48:	<i>THAP1</i> genotype and pathogenicity values of patient and control fibroblast samples.....	152
Table 49:	The quality and concentration determined for total RNA samples.....	182
Table 50:	Significant up-regulated genes in primary dystonia patients having <i>THAP1</i> mutation compared to controls.....	219

List of Tables

Table 51:	Significant down-regulated genes in primary dystonia patients having <i>THAP1</i> mutation compared to controls.....	220
Table 52:	Ingenuity pathway analysis (IPA) to identify top affected disease network.....	225
Table 53:	Disease and function annotation of significant up and down regulated genes.....	226
Table 54:	Expression level of dystonia related genes in the <i>THAP1</i> mutant dystonia patients & control fibroblast samples.....	230
Table 55:	Preparation of elution solutions for TMT-labeled peptides.....	245
Table 56:	Preparation of diluted peptide digest assay standards.....	246
Table 57:	Significant up-regulated proteins in primary dystonia patients having <i>THAP1</i> mutation compared to controls.....	250
Table 58:	Significant down-regulated proteins in primary dystonia patients having <i>THAP1</i> mutation compared to controls.....	259
Table 59:	Ingenuity pathway analysis (IPA) to identify top affected molecular pathway.....	264
Table 60:	Disease and function annotation of significant up and down regulated proteins.....	266

List of Figures

Figure 1:	Metabolic pathway for BH ₄ , dopamine, serotonin and other monoamines.....	28
Figure 2:	Identification of <i>TOR1A</i> ΔGAG mutation in an Indian family.....	94
Figure 3:	Genotyping of <i>TOR1A</i> SNPs for case-control association study.....	97
Figure 4:	Haplotype analysis of common <i>TOR1A</i> gene variants.....	98
Figure 5:	Identification of THAP1 gene variants in Indian primary dystonia patients.....	100
Figure 6:	The secondary mRNA structure prediction of <i>THAP1</i>	101
Figure 7:	NEB Q5 Site-Directed Mutagenesis kit overview.....	117
Figure 8:	Format of the DLR™ Assay using a luminometer.....	139
Figure 9:	Representative chromatogram of <i>THAP1</i> SDM reaction products....	140
Figure 10:	Subcellular localization of wild type & mutant THAP1 protein.....	141
Figure 11:	THAP1 mutant protein stability determination by cycloheximide chase/western blot assay.....	142
Figure 12:	<i>THAP1</i> mutant mRNA stability assay by actinomycin D treatment followed by TaqMan based qRT-PCR.....	144
Figure 13:	Effect of <i>THAP1</i> missense changes on <i>TOR1A</i> repression as measured by dual luciferase assay.....	145
Figure 14:	TruSeq RNA sample preparation v2 workflow for eukaryote transcriptome library construction.....	158
Figure 15:	TruSeq RNA sample preparation v2 mRNA purification and fragmentation workflow.....	159
Figure 16:	Representative electropherogram of the RNA samples from fibroblast samples.....	182
Figure 17:	The representative chromatograms of RNA electrophoresis in Agilent 2000 Bio-analyzer for individual RNA samples.....	184
Figure 18:	Representative figures of RNA sequencing quality of sample ML-1.....	188
Figure 19:	Representative figures of RNA sequencing quality of sample ML-2.....	190
Figure 20:	Representative figures of RNA sequencing quality of sample ML-3.....	192

List of Figures

Figure 21:	Representative figures of RNA sequencing quality of sample ML-4.....	194
Figure 22:	Representative figures of RNA sequencing quality of sample ML-5.....	196
Figure 23:	Representative figures of RNA sequencing quality of sample ML-6.....	198
Figure 24:	Representative figures of RNA sequencing quality of sample ML-7.....	200
Figure 25:	Representative figures of RNA sequencing quality of sample ML-8.....	202
Figure 26:	Representative figures of RNA sequencing quality of sample ML-9.....	204
Figure 27:	Representative figures of RNA sequencing quality of sample ML-10.....	206
Figure 28:	Representative figures of RNA sequencing quality of sample ML-11.....	208
Figure 29:	Representative figures of RNA sequencing quality of sample ML-12.....	210
Figure 30:	The alignment of raw RNA-seq reads of ML1 and visualization of mutant allele of <i>THAP1</i> (c.50 A>G) through NextGENe® software.....	211
Figure 31:	The alignment of raw RNA-seq reads of ML2 and visualization of mutant allele of <i>THAP1</i> (c.395 T>C) through NextGENe® software.....	212
Figure 32:	The alignment of raw RNA-seq reads of ML3 and visualization of mutant allele of <i>THAP1</i> (c.153C>G) through NextGENe® software.....	213
Figure 33:	The alignment of raw RNA-seq reads of ML8 and visualization of mutant allele of <i>THAP1</i> (c.161 G>A) through NextGENe® software.....	214
Figure 34:	The alignment of raw RNA-seq reads of ML10 and visualization of mutant allele of <i>THAP1</i> (c.46 A>G) through NextGENe® software.....	215

List of Figures

Figure 35:	The alignment of raw RNA-seq reads of ML11 and visualization of mutant allele of <i>THAP1</i> (c.446 T>C) through NextGENe® software.....	216
Figure 36:	Heat map of differentially expressed genes (DEG).....	222
Figure 37:	Scatter plot of differentially expressed genes (DEG).....	223
Figure 38:	Volcano plot of differentially expressed genes (DEG).....	224
Figure 39:	Ingenuity interactome analysis of up and down regulated genes enriched in disease network 1.....	227
Figure 40:	Ingenuity interactome analysis of up and down regulated genes enriched in disease network 2.....	228
Figure 41:	Ingenuity interactome analysis of up and down regulated genes enriched in disease network 3.....	229
Figure 42:	Chemical structure of the TMT Label Reagents.....	239
Figure 43:	Spin column conditioning and sample fractionation workflow.....	243
Figure 44:	Top canonical pathways as identified by Ingenuity Pathway Analysis.....	268

List of Abbreviations

µg:	Microgram
µl:	Microliter
°C:	Degree celcius
2D-DIGE:	2 dimensional-Difference gel electrophoresis
AAA+:	ATPases Associated with diverse cellular Activities
ACN:	Acetonitrile
AD:	Autosomal dominant
ANO3:	Anoctamin 3
AP2B2:	AP2 adaptor complex β-2 adaptin subunit
AP-3:	Adaptor protein complex 3
AR:	Autosomal recessive
ATP1A3:	ATPase Na ⁺ /K ⁺ Transporting Subunit Alpha 3
AURKA:	Aurora kinase A
BBB:	Bead Binding Buffer
BCA:	Bicinchoninic acid
BCP:	1-bromo-3-chloropropane
BDS:	bis die sumendum (twice a day)
BFIE:	Benign familial infantile epilepsy
BH:	Benjamini-Hochberg
BH4:	Tetrahydrobiopterin
BIRC5:	Baculoviral IAP Repeat Containing 5
BIS:	Benign infantile seizures
BSA:	Bovine serum albumin
BWB:	Bead Washing Buffer
CACNA1B:	Calcium Voltage-Gated Channel Subunit Alpha1 B
CADD:	Combined annotation dependent depletion
CCNB1:	Cyclin B1
CDK2:	Cyclin-dependent kinase 2
CDKN1:	Cyclin-Dependent Kinase Inhibitor 1
cDNA:	Complimentary DNA
ChIP:	Chromatin immunoprecipitation
CHK1:	Cell Cycle Checkpoint Kinase 1
CIZ1:	CDKN1A Interacting Zinc Finger Protein 1
CNS:	Central nervous system
COL6A3:	Collagen Type VI Alpha 3 Chain
cSNP:	Coding single nucleotide polymorphism
CT:	Computed tomography
CTE:	End Repair Control
CVC:	Cross-validation consistency
DAPI:	4',6-diamidino-2-phenylindole

Abbreviations

DAT:	Dopamine transporter
DAXX:	Death Domain Associated Protein
DBS:	Deep brain stimulation
DR2:	Dopamine receptor D ₂
DEG:	Differentially expressed genes
DICER:	Helicase with RNase motif
DMEM:	Dulbecco's Modified Eagle Medium
DMSO:	Dimethyl sulfoxide
DNC:	Dentate nucleus of the cerebellum
dNTP:	Deoxynucleotide triphosphate
DPBS:	Dulbecco's phosphate buffer saline
DRD:	Dopa-responsive dystonia
DSC:	Disease specific changes
DSF:	Differential scanning fluorimetry
DTI:	Diffusion Tensor Imaging
EDTA:	Ethylenediamine tetraacetic acid
EEG:	Electroencephalogram
ELB:	Elution Buffer
EMSA:	Electrophoretic mobility shift assay
EPF:	Elute, Prime, Fragment Mix
ER:	Endoplasmic reticulum
ERAD:	Endoplasmic reticular associated degradation
ERP:	End Repair Mix
ETD:	Electron transfer dissociation
Exol:	Exonuclease I
FATHMM:	Functional Analysis Through Hidden Markov Models
FBS:	Fetal Bovine Serum
FDR:	False discovery rate
fMRI:	Functional Magnetic Resonance Imaging
GCH1:	GTP cyclohydrolase 1
GLUT1:	Glucose transporter 1
GNAL:	G Protein Subunit Alpha L
GPi:	Globus pallidus interna
HAGH:	Hydroxyacyl glutathione hydrolase
HCD:	Higher energy collision dissociation
HCF-1:	Host cell factor 1
HCl:	Hydrochloric acid
HEPA:	High efficiency particulate air
HM:	Hemiplegic migraine
HMMR:	Hyaluronan Mediated Motility Receptor
HPCA:	Hippocalcin
HRP:	Horseradish peroxidase
HWE:	Hardy-Weinberg equilibrium
ICCA:	Infantile convulsions and choreoathetosis

Abbreviations

ICMR:	Indian Council for Medical Research
IPA:	Ingenuity Pathway Analysis
ITC:	Isothermal titration calorimetry
IVS:	Intervening sequence
KCl:	Potassium chloride
KCTD17:	Potassium Channel Tetramerization Domain Containing 17
KH ₂ PO ₄ :	Potassium dihydrogen phosphate
KLC1:	Kinesin light chain 1
LA:	Luria agar
LAP1:	Lamin associated polypeptide 1
LAR II:	Luciferase Assay Reagent II
LC-MS/MS:	Liquid chromatography-tandem mass spectrometry
LD:	Linkage disequilibrium
LTD:	Long term depression
LULL1:	Torsin-1A-interacting protein 2
MAD2:	Mitotic arrest deficient 2
MAF:	Minor allele frequency
MC:	Mutation cluster
MCS:	Multiple cloning sequences
MD:	Myoclonus dystonia
MDRpt:	Multifactor dimensionality reduction –permutation testing
MetaSVM:	Ensemble score by Support Vector Machine
miRNA:	microRNA
ml:	Mililiter
MR1:	Major Histocompatibility Complex, Class I-Related
mRNA:	Messenger RNA
Na ₂ HPO ₄ :	Disodium hydrogen phosphate
NaCl:	Sodium chloride
NCV:	Nerve conduction velocity
NE:	Nuclear envelope
NLS:	Nuclear localization signal
NOS:	Nitric oxide synthase
O-GlcNAC:	O-linked N-acetylglucosaminyltransferase
OMIM:	Online Mendelian Inheritance in Man
ORF:	Open reading frame
PACT:	Protein ACTivator of the interferon induced protein kinase
PAGE:	Polyacrylamide gel electrophoresis
PAH:	Phenylalanine hydroxylase
PAWR:	Prostate apoptosis response-4 protein
PBS:	Phosphate buffered saline
PCNA:	Proliferating cell nuclear antigen
PCR:	Polymerase chain reaction
PE:	Prediction error

Abbreviations

PED:	Paroxysmal exercise induced dyskinesia
PET:	Positron Emission Tomography
PKD:	Paroxysmal kinesigenic dyskinesia
PLB:	Passive lysis buffer
PML:	Promyelocytic Leukemia
PMM:	PCR Master Mix
PNKD1:	Paroxysmal nonkinesigenic dyskinesia 1
PPC:	PCR Primer Cocktail
PPN:	Pedunculopontine nuclei
pRb:	Protein retinoblastoma
PRKRA:	Protein Kinase, Interferon-Inducible Double-Stranded RNA-Dependent Activator
PRRT2:	Proline-rich transmembrane protein 2
PTD:	Primary torsion dystonia
PVDF:	Polyvinylidene fluoride
qPCR:	Quantitative polymerase chain reaction
qRT-PCR:	Quantitative reverse transcription polymerase chain reaction
RDP:	Rapid-onset dystonia-parkinsonism
RFLP:	Restriction Fragment Length Polymorphism
RIN:	RNA Integrity Number
RIPA:	Radioimmunoprecipitation assay
ROS:	Reactive oxygen species
RPB:	RNA Purification Beads
RPM:	Rotation per minute
RRM1:	Ribonucleotide Reductase Catalytic Subunit M1
RRM2:	Ribonucleotide Reductase Regulatory Subunit M2
RSB:	Resuspension Buffer
RT:	Room temperature
sAHP:	Slow afterhyperpolarization
SAP:	Shrimp Alkaline Phosphatase
SCX:	Strong cation exchange
SDS:	Sodium dodecyl sulphate
SEM:	Standard error of mean
SGCE:	Epsilon sarcoglycan
SIFT:	Sorting intolerant from tolerant
SILAC:	Stable isotope labeling with amino acids in cell culture
siRNA:	small interfering RNA
SLC2A1:	Solute Carrier Family 2 Member 1
SNAP-25:	Synaptosomal-associated protein 25
SNARE:	SNAP (Soluble NSF Attachment Protein) REceptor
SNP:	Single nucleotide polymorphism
SPR:	Sepiapterin reductase
SRM:	Selective reaction monitoring
SSM:	Second Strand Master Mix

Abbreviations

STL:	Stop Ligation Buffer
SVA:	Short interspersed nuclear element, Variable number of tandem repeats and Alu composite retrotransposon
TAE:	Tris/Acetic acid/EDTA
TAF1:	TATA-Box Binding Protein Associated Factor 1
TBA:	Testing balanced accuracy
TBE:	Tris/Borate/EDTA
TBP:	TATA-box binding protein complex
TCEP:	Tris (2-carboxyethyl) phosphine
TCHP:	Trichoplein
TDS:	ter die sumendum (thrice a day)
TEA:	Triethylamine
TEAB:	Triethyl ammonium bicarbonate
TFA:	Trifluoroacetic acid
TFIID:	Transcription factor IID
TGF β :	Transforming growth factor beta
TH:	Tyrosine Hydroxylase
THAP1:	THAP Domain Containing, Apoptosis Associated Protein 1
TMEM16C:	Transmembrane Protein 16C
TMT:	Tandem mass tag
TNF- α :	Tumor necrosis factor alpha
TOR1A:	Torsin-1A
tRNA:	Transfer RNA
TUBB4A:	Tubulin Beta 4A Class IVa
UTR:	Untranslated region
VBM:	Voxel-based morphometry
VMAT2:	Vesicular monoamine transporter 2
WR:	Working reagents
XDP:	X-linked dystonia-parkinsonism
XR:	X-linked recessive
β -ME:	β -mercaptoethanol



DYSTONIA

DYSTONIA

CHAPTER 1

INTRODUCTION

1.1 Definition of Dystonia

Dystonia is the third most common movement disorder following Essential Tremor and Parkinson's disease (1). The definition of dystonia first proposed by the Dystonia Medical Research Foundation in 1984 and recently been updated by an international team of movement disorder scientists (2).

“Dystonia is a movement disorder characterized by sustained or intermittent muscle contractions causing abnormal, often repetitive, movements, postures, or both. Dystonic movements are typically patterned, twisting, and may be tremulous. Dystonia is often initiated or worsened by voluntary action and associated with overflow muscle activation.”

Dystonia results from involuntary concomitant contraction of agonist and antagonist muscles. It is an inadequately understood medical condition for proper treatment and management of symptoms.

1.2 History

The term “Dystonia” was first introduced in 1911 by a German neurologist, Hermann Oppenheim, Berlin. He reported a medical condition in four Jewish children with muscle spasm in limbs and trunk with abnormal twisting postures. The condition was progressive and certain postures became fixed. These symptoms were distinguished as a new medical term “*dystonia musculorum deformans*” and “*dysbasia lordotica progressiva*” (3, 4). Later in 1944, a German-American neurologist, Ernst Herz, described the cases of primary dystonia (5), where the patients have co-contraction of agonist and antagonist muscles. Very recently in 1976, the dystonia has been established as a neurological condition, which can be originated from the dysfunction of central neural circuits (6, 7). Thereafter, a

significant advancement in clinical research and medical management has been achieved.

1.3 Classification of Dystonia

Dystonia has been classified clinically based on i) age of onset; ii) etiology and iii) distribution of affected anatomical parts (8). Recent revised classification has been reported to provide important information for better treatment and laboratory research investigations (2). A brief outline of the the updated classification is depicted in the Table 1.

The classification based on age of onset is very important for diagnosis and prognosis. Sporadic forms of idiopathic dystonia usually emerge as late onset dystonia (≥ 26 years), while the genetic and familial dystonias could appear as early onset dystonia (≤ 26 years). The childhood onset dystonias could be progressed towards the focal to generalized dystonia (9, 10). The classification based on the involvement of anatomical parts is also very crucial for diagnosis and management of the disease. The treatment strategies for adult onset focal dystonia could be much different from young onset generalized dystonia. Upper and lower limbs, cervical region, larynx, trunk, orofacial regions are the most common body parts that could be affected either individually or in combination. Depending on the involvement of above mentioned body parts, dystonias could be classified as focal, segmental, multifocal, generalized and hemidystonia. The Dystonic symptoms could be present in the same extent throughout the day as a persistent one or it could be triggered by specific activity (task specific dystonia).

Table 1: Classification of Dystonia.

Criteria for Classification	Description
Age of onset	<ul style="list-style-type: none"> • Infancy (birth to 2 years) • Childhood (3 – 12 years) • Adolescence (13–20 years) • Early adulthood (21–40 years) • Late adulthood (>40 years)
Anatomical distribution	<ul style="list-style-type: none"> • Focal: Single body part is affected (Blepharospasm, Writer’s cramp, laryngeal dystonia, cervical dystonia). • Segmental: Two or more adjacent body parts are affected (Cranial dystonia). • Multifocal: Two or more non-contiguous body regions are affected. • Generalized: Two or more body parts along with the trunk are affected. • Hemidystonia: Body parts of one side are affected.
Temporal pattern	<ul style="list-style-type: none"> • Persistent: Dystonic symptoms persist throughout the day. • Action-specific: Dystonia triggered by certain activity. • Diurnal fluctuations: Circadian variation of severity and occurrence of dystonia. • Paroxysmal: Abrupt episodes of Dystonic symptoms induced by trigger.
Disease course	<ul style="list-style-type: none"> • Static • Progressive
Associated features	<ul style="list-style-type: none"> • Isolated dystonia or combined with another movement disorder (Isolated dystonia and combined dystonia). • Occurrence of other neurological or systemic manifestations.
Recognition of dystonia syndromes	<ul style="list-style-type: none"> • Early-onset generalized isolated dystonia • Focal or segmental isolated dystonia with onset in adulthood • Dystonia-parkinsonism • Myoclonus dystonia
Etiology	<ul style="list-style-type: none"> • Primary: Dystonia is the only manifestation with the exception of tremor and pain. • Dystonia Plus: Dystonic symptoms in addition to other neurological features, such as, Parkinsonism or myoclonus without neurodegeneration • Heredodegenerative: A group of neurodegenerative disorders, where dystonia is one of the prominent symptoms, e.g. Wilson’s disease • Secondary: Dystonia with identifiable causes, such as, brain lesions or drug effects.

The Dystonic symptoms may show a circadian variation, where it could be aggravated at the late afternoon or evening. This diurnal variation is a prominent clinical feature of a specific Dystonic form “Dopa-responsive dystonia”. An inducible sudden episodic attack of dystonia may be observed in the paroxysmal Dystonic forms, which could be triggered by exercise or consumption or other triggering factors.

Based on etiology, dystonia may be classified as primary, dystonia plus syndrome, secondary and hereditary degenerative dystonia. Primary dystonia only manifest the Dystonic symptoms excluding any other neurological condition. Dystonia plus syndrome could be generated with the occurrence of Parkinsonism or myoclonus without any sign and symptoms of neurodegeneration. In certain neurological diseases including neurodegenerative diseases, Dystonic symptoms are present as prominent characteristics. This group of dystonias are termed as hereditary degenerative dystonia. Secondary dystonias could be evolved by the exogenous causes, such as, brain lesions and drug effect.

1.4 Epidemiology & Prevalence

Although the epidemiological studies on dystonia are limited, despite that it has been revealed that the prevalence of late-onset dystonia is more frequent than the early-onset dystonia in the world population. The prevalence estimates of primary dystonia vary widely across the world population ranging from 2 - 50 cases per million for early onset and 30 - 7320 cases per million for late onset dystonia (11) (Table 2). This wide range of variation in prevalence rate could be explained by the fact that inappropriate sample size and diverse methodologies chosen for such epidemiological studies. A recent meta analysis demonstrated that the focal dystonia

Introduction

Table 2: Prevalence rate of dystonia reported in different world population.

Country (Years of study)	Study design/ Data source	Population sample	Age	Cases found	Prevalence (95% CI)	Reference
Eight European countries (1996-1997)	Neurology service based	57,92,937	>20 years	677	117 (108-126)	(12)
Italy (2000)	Population sample	707	>50 years	6	7320 (3190–15640)	(13)
Serbia (2001)	Neurology and non-neurology service based	16,02,226	All ages	165	136 (116-159)	(14)
Norway (1999–2002)	Neurology and non-neurology service based	5,08,726	All ages	129	254 (212–301)	(15)
Egypt (1988–1990)	Door to door	42,000	All ages	4	100 (26–243)	(16)
Israel (1949–1959)	Record-linkage system	4,55,169	<20 years	11	24 (12–43)	(17)
China (1983)	Door to door	63,195	All ages	3	50 (10–150)	(18)
Japan (2000)	Neurology and non-neurology service based	14,59,130	All ages	147	101 (84.5–118)	(19)
Japan (1988–1993)	Neurology-service based	2,45,000	All ages	15	61 (34–101)	(20)
USA (1952–1980)	Record-linkage system	4,06,976	All ages	17	295 (172–479)	(21)
Italy (1987–1999)	Neurology and non-neurology service based	67,606	All ages	9	133 (61–253)	(22)
USA (1990)	Service based	14,66,800	<28 years	73	50 (39–63)	(23)
Germany (1996–1997)	Neurology-service based	18,07,000	All ages	182	101 (84–119)	(24)
England (1993–2002)	Record-linkage system	1,01,766	All ages	43	430 (306–569)	(25)
Thailand (2005-2010)	Neurology-service based	10,39,595	All ages	207	199 (172-226)	(26)
Iceland (2003)	Administrative database	2,88,201	All ages	107	371 (304-449)	(27)
Italy (2005)	Neurology-service based	16,52,332	All ages	53	322 (230-408)	(28)
India (2003-2004)	Door to door	52,377	All ages	23	439 (284-648)	(29)
Columbia (2007-2012)	Neurology-service based	62,21,742	All ages	874	712 (487-937)	(30)
Italy (2001-2002)	Neurology-service based	5,41,653	>17 years	69	137 (102–166)	(31)
Japan (2003)	Neurology-service based	11,66,967	All ages	177	151 (68–144)	(32)
Japan (2000-2003)	Neurology-service based	2,47,973	>50 years	34	137 (91–183)	(33)

is more prevalent than other forms of primary dystonia (34). Among focal dystonias, cervical dystonia is more prevalent in Europe (67.1/million) and USA but not in Japan (25.2/million). Though in India, the prevalence rate of limb dystonia is highest as a form of writer's cramp and writing tremor followed by Blepharospasm and cervical dystonia (29). Blepharospasm has been reported as the prevalent focal dystonia in Italy (28, 31) and Japan (19).

1.5 Pathophysiology of dystonia

Histopathological evaluation and structural MRI of primary dystonia patients revealed no gross neurodegeneration of brain. However, neurophysiological studies and the beneficial use of deep brain stimulation (DBS) at the pars interna of globus pallidus (GPI) strongly suggest the involvement of basal ganglia for dystonia pathophysiology. With the advancement of the functional neuroimaging and electrophysiological techniques, various studies reported the functional abnormalities of cortico-striatal-thalamic-cortical loop, which could be responsible for development of certain clinical features (35). Functional neuroimaging (fMRI & PET) and structural imaging of gray matter by Voxel-based morphometry (VBM) and white matter by diffusion tensor imaging (DTI) were effectively helpful to identify the functional abnormalities in sensorimotor network for primary and secondary dystonia (36). VBM studies reported an increase in the grey matter volume in the globus pallidus internus, nucleus accumbens and prefrontal cortex in focal hand dystonia patients (37) as well as other primary dystonias (38). Enlargement in putamen also observed in blepharospasm (39) and focal hand and cranial dystonia (40). Diffusion tensor imaging studies identified altered fractional anisotropy and mean diffusivity in the corpus callosum, putamen, right caudate and pre-frontal cortical areas of white

matter region for cervical dystonia patients (41-43). White matter microstructural abnormality was also observed in cases of blepharospasm (44) and spasmodic dysphonia patients (45). A wide range of functional abnormalities and metabolic alterations in different brain regions involved specifically in sensorimotor networks were also been observed by PET imaging and fMRI studies (46, 47). These alterations were observed both in task specific (48, 49) and task free conditions (50, 51) due to increased or decreased activation of the motor network. Abnormal sensorimotor plasticity was also observed in cases of writer's cramp patients (52-54) and also for the blepharospasm patients with abnormal plasticity in the blink reflex circuits of brain stem (55).

Though dystonia is believed to be a basal ganglia disorder, new line of evidences suggest a pivotal pathophysiological role of cerebellum in dystonia pathogenesis (56). The first indications were reported as the secondary cervical dystonia patients have structural brain lesions in cerebellum (57). PET imaging studies have also revealed the abnormal cortico-striatal-pallido-thalamocortical (CSPTC) and cerebellar-thalamo-cortical pathways in carriers of *DYT1* and *DYT6* mutations (58, 59). A very recent study reported that targeted knock down of *DYT1* gene in cerebellum is sufficient to induce the abnormal motor symptoms in mouse model, but not in basal ganglia (60). This could be generated by the abnormal activity of the Purkinje cells and neurons of the deep cerebellar nuclei.

1.6 Thesis outline

The overall objectives of this thesis is to identify the genetic factors responsible for idiopathic primary dystonia pathogenesis in Indian primary dystonia

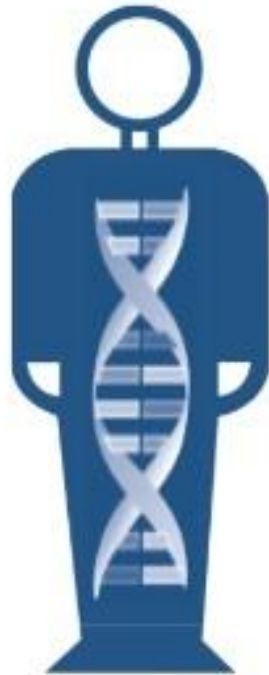
patients and functional characterization of the identified genetic variants for unraveling the cellular mechanism of disease development. The specific objectives are:

1. Screening of *TOR1A* gene including its promoter in primary dystonia patients.
2. Screening of *THAP1* gene in primary dystonia patients.
3. Functional analysis of identified *THAP1* mutants.
4. Effect of *THAP1* mutation on *TOR1A* transcription.
5. Whole genome gene expression analysis in primary dystonia patients' samples having *THAP1* missense mutation to identify differentially expressed genes.
6. Whole cell proteomic analysis in primary dystonia patients' samples having *THAP1* missense mutation to identify the dysregulated molecular pathway(s).

In chapter 2, a detailed review on the genetic aspects of dystonia including clinical presentation, neuropathology, molecular genetics and molecular pathology has been discussed wherever applicable. The interconnection between different DYT genes and their shared molecular mechanism have also been discussed for a comprehensive understanding of the primary dystonia pathogenesis. Chapter 3 describes the identification of rare genetic variants in *TOR1A* and *THAP1* genes in primary dystonia patients. The common genetic variants of these two genes have also been assessed in case-control association studies. In chapter 4, the experimental details have been presented for the functional characterization of the *THAP1* missense mutations identified in primary dystonia patients. The detailed experimental evidences have been provided to understand the effect of missense variants on *THAP1* protein and mRNA stability, subcellular localization and

repression efficiency on *TOR1A* transcription. The experimental details and results of whole genome gene expression analysis of primary dystonia patients having *THAP1* mutation by RNA-sequencing have been discussed in chapter 5. The differentially expressed genes have been enriched for certain molecular pathways. These pathways were identified by bioinformatics analysis and depicted here. In chapter 6, the findings from whole cell quantitative proteomic analysis of primary dystonia patients having *THAP1* mutation by LC-MS/MS have been described. The aim of this study is to find out the pivotal dysregulated cellular pathways for which the up and down regulated proteins are involved. In the conclusive and final chapter 7, the summary of the findings and its implication towards the primary dystonia pathogenesis has been discussed which may lead to rethink the future research direction of primary dystonia.

Genetics of Dystonia



CHAPTER 2

THE GENETICS OF DYSTONIA

2.1 Introduction

The aetiology of dystonia is genetically complex, as the penetrance of certain genetic variant(s) requires the interaction of environmental factors to be causal for disease manifestation. The multifactorial inheritance of dystonia suggests that multiple genetic variants of variable penetrance may contribute to the susceptibility to the disorder (61, 62). In the recent era, the discovery of underlying genetic factor(s) has been expedited by 'next generation' sequencing. In past few years, seven new genes *HPCA* (63), *TUBB4A* (64, 65), *CIZ1* (66), *ANO3* (67), *GNAL* (68), *KCTD17* (69) & *COL6A3* (70) have been discovered to be associated as genetic contributor of primary dystonia and *PRRT2* has been recognized as the cause of paroxysmal kinesigenic dystonia (71). Present evidence suggests that there is a significant genetic contribution towards the pathogenesis of dystonia. Monogenic inheritance has mostly been found in early onset dystonia. However, late-onset dystonia, which represents the most number of dystonia cases, also appears to have a strong genetic basis. It was also found through family based clinical examination that the first-degree relatives of patients with focal dystonia have a relative risk of 36% at the most for developing the same or another form of dystonia (72, 73). Epidemiological studies demonstrated that adult onset dystonia may sometimes be inherited in an autosomal dominant manner with a low penetrance (72, 74, 75). There are several evidences which suggest that these dystonia genes (DYT genes) may act synergistically for a common pathway of disease pathogenesis (76, 77). The identification of these genes supports the probable involvement to the pathophysiology of dystonia through dopaminergic transmission and transcription abnormalities, whereas some of them may be implicated for ion channel abnormalities, microtubular or synaptic dysfunction. Thus the molecular mechanism

involved in dystonia due to the genetic variations of DYT genes is absolute pivotal to understand the disease pathogenesis.

In this chapter, a comprehensive overview of different forms of dystonia is attempted with special emphasis on molecular genetics, clinical and pathophysiology. The known findings are discussed for each DYT genes including the associated phenotype, neuropathology, molecular genetics and molecular pathology wherever applicable. The approach of this review is to comprehensively summarize the functions of each DYT genes individually and the possible interactions among them.

2.2 The DYT loci – genetic contributor of familial dystonia

So far, a total of 27 loci with well defined clinical phenotypes and 18 causal genes have been implicated for different types of dystonia (Table 3). These encompass several primary pure dystonia, primary plus dystonia, paroxysmal dystonia, dystonia plus syndromes, myoclonus dystonia and dystonia-parkinsonism. The monogenic forms of dystonia exhibit Mendelian inheritance though the disease pathogenesis is complex in nature.

2.2.1 *DYT1-TOR1A*

Clinical features:

DYT1 dystonia or primary torsion dystonia (PTD) is the most frequent form of dystonia and it has been the first clinically characterized form. Generally disease onset is in childhood or adolescence with involuntary posturing of the trunk, neck, or limbs (78, 79). Phenotypic characteristics of DYT1 dystonia include 1) disease onset before the age of 26 years and 2) disease begins from limbs and gradually progressed to other body parts except the cranio-cervical and oromandibular regions leading to generalized dystonia. However, in some cases dystonia does not generalize but remains focal or segmental (80, 81).

Neuropathology

The neuropathological assessment of four DYT1 dystonia patients having the pathogenic Δ GAG deletion revealed a perinuclear inclusion bodies in cholinergic neurons of the midbrain reticular formation, particularly in the pedunculopontine nuclei (PPN), and periaqueductal gray matter (82). The immunohistochemical study

Genetics of Dystonia

Table 3: The DYT loci.

Symbol	Locus	OMIM	Gene	Inheritance	Special features	Reference
DYT1	9q34.11	128100	<i>TOR1A</i>	AD	Early-onset torsion dystonia	(83, 84)
DYT2	1p35-p34.2	224500	<i>HPCA</i>	AR	Autosomal recessive primary isolated dystonia	(63, 85)
DYT3	Xq13.1	314250	<i>TAF1</i>	XR	X-linked dystonia parkinsonism	(86, 87)
DYT4	19p13.12-13	128101	<i>TUBB4A</i>	AD	Autosomal dominant whispering dysphonia	(64, 65, 88)
DYT5a/ DYT14	14q22.1- 14q22.2	128230	<i>GCH1</i>	AD	Autosomal dominant dopa-responsive dystonia	(89)
DYT5b	11p15.5	191290	<i>TH</i>	AR	Autosomal recessive dopa-responsive dystonia	(90)
DYT6	8p11.21	602629	<i>THAP1</i>	AD	Autosomal dominant craniocervical dystonia	(91)
DYT7	18p11	602124	<i>Unknown</i>	AD	Adult onset craniocervical dystonia	(92)
DYT8	2q35	118800	<i>MR1</i>	AD	Paroxysmal nonkinesigenic dyskinesia	(93)
DYT9/ DYT18	1p35-p31.3	601042	<i>SLC2A1</i>	AD	Episodic choreoathetosis/spasticity, Paroxysmal exercise induced dyskinesia	(94, 95)
DYT10	16p11.2-q12.1	128200	<i>PRRT2</i>	AD	Paroxysmal kinesigenic dyskinesia	(71, 96)
DYT11	7q21-7q31	159900	<i>SGCE</i>	AD	Myoclonus dystonia	(97)
DYT12	19q12-13.2	128235	<i>ATP1A3</i>	AD	Rapid onset dystonia parkinsonism	(98, 99)
DYT13	1p36.32-p36.13	607671	Unknown	AD	Autosomal dominant craniocervical/upper limb dystonia	(100)
DYT15	18p11	607488	Unknown	AD	Early onset myoclonus dystonia	(101)
DYT16	2q31.3	612067	<i>PRKRA</i>	AR	Young onset dystonia- parkinsonism	(102)
DYT17	20p11.2-q13.12	612406	Unknown	AR	Adolescent onset focal dystonia	(103)
DYT19	16q13-q22.1	611031	Unknown	AD	Episodic dyskinesia triggered by sudden movement	(104)
DYT20	2q31	611147	Unknown	AD	Paroxysmal nonkinesigenic dyskinesia 2	(105)
DYT21	2q14.3-q21.3	614588	Unknown	AD	Adult onset craniocervical dystonia progressed to generalized dystonia	(106)
DYT23	9q34.11	611420	<i>CIZ1</i>	AD	Adult onset cervical dystonia	(66)
DYT24	11p14.2	610110	<i>ANO3</i>	AD	Adult onset craniocervical dystonia	(67, 107)
DYT25	18p11.21	615073	<i>GNAL</i>	AD	Adult onset cervical dystonia	(68)
DYT26	22q12.3	616398	<i>KCTD17</i>	AD	Early onset myoclonus dystonia	(69)
DYT27	2q37.3	616411	<i>COL6A3</i>	AR	Early onset craniocervical segmental dystonia	(70)

OMIM: Online Mendelian Inheritance in Man; AD: Autosomal dominant, AR: Autosomal recessive, XR: X-linked recessive

identified the inclusions stained positively for ubiquitin, torsin-A, and lamin A/C. So it has been concluded that DYT1 dystonia is associated with impaired protein folding and possible disruption of the nuclear envelope, which could lead to the motor abnormalities in DYT1 dystonia. But there are two recent studies, which reported no gross abnormalities or no disease-specific pathological intracellular inclusions in DYT1 dystonia patients' brain (108, 109).

Molecular genetics

The clinical features of primary torsion dystonia, recognized in 1990 was the first dystonia locus (DYT1) and linked to chromosome 9q32-34 (110). Seven years later, the gene *TOR1A* was discovered for DYT1 locus, (84). The *TOR1A* consists of five exons spanning ~ 11.2 kb of DNA and encodes a 332 amino acid long 37.8 kDa protein, TorsinA. The specific mutation, a tri-nucleotide in-frame deletion c.904-906/907-909 Δ GAG found in exon 5 of *TOR1A* is the causal and almost exclusive cause of DYT1 dystonia. This mutation was found in almost all population throughout the world that has been studied for *TOR1A* mutation. Although the penetrance of this variant is reported to be 30% to 40% i.e. 30 to 40 individuals out of 100 having the variant would have DYT1 dystonia manifestation (111, 112). The penetrance of this mutation could be governed by the presence of a non-synonymous polymorphism, c. 646 G>C (p. D216H; dbSNP ID: 1801968) in exon 4 of *TOR1A* gene. The presence of the 216H allele *in-trans* position to the GAG deletion may reduce the risk of developing symptoms of dystonia by 10-fold to as little as 3% (113, 114). Apart from these two variants, several other genetic variants were found having different degrees of pathogenicity (Table 4). Over-expression of the Δ GAG allele in cellular model revealed perinuclear inclusion body formation, while the normal subcellular

localization of TorsinA is mainly in the lumen of endoplasmic reticulum (ER); although a small amount of TorsinA was also detected in the nuclear envelope (NE) (115-117). It has been found that the minor allele of rs1801968, 216H could form the same kind of perinuclear inclusions as that formed by Δ GAG, but in a much lower level (118). Moreover the presence of the 216H allele *in-cis* to the Δ GAG could reduce the formation of inclusions, showing a mutual cancelling effect (118). So it was also been proposed that the presence of 216D allele *in-cis* to Δ GAG may be enough to be penetrant (113), though this is not conclusive yet.

Table 4: Genetic rare variants of *TOR1A* gene found in primary dystonia patients.

Nucleotide change	Location	Amino acid change	Frequency	References
c.40_45 Δ GCGCCG	Exon 1	p. A14_P15 Δ	1/162	(119)
c. 361 G>A	Exon 2	p. E121K	1/162	(119)
c.385G>A	Exon 2	p. V129I	1/461	(120)
c.488 C>T	Exon 3	p. A163V	1/940	(121)
c.581A>T	Exon 3	p. D194V	1/201	(122)
c.613T>A	Exon 3	p. F205I	1/801	(123)
c.692 T>A	Exon 4	p. I231N	1/940	(121)
c.823A>G	Exon 5	p. K275E	1/1000	(124)
c.863G>A	Exon 5	p. R288Q	1/501	(125)
c. 904-906/907-909 Δ GAG	Exon 5	p. E302/303 Δ	-	Table 13
c.962C>T	Exon 5	p. T321M	1/940, 1/1000	(121, 124)
c.966_983 Δ 18	Exon 5	p. V322_Y328 Δ insV	1/24	(126)

The c.40_45 Δ GCGCCG (p. A14_P15 Δ) mutation was found in a 76 years old lady affected with cervical dystonia with dystonic tremor in hands and head (119). The other variant c. 361 G>A (p. E121K) was found in a patient affected with segmental dystonia consisting of cervical dystonia and spasmodic dysphonia. The functional analysis for p. A14_P15 Δ revealed a profound degradation through the autophagy-lysosome pathway, though it was unable to produce any perinuclear inclusions like Δ GAG mutation. Furthermore, this variant fall into the TorsinA oligomerization

domain predicted to inhibit it, but no such observation was found. The p.E121K resulted in a significant inclusion body formation, when the autophagy pathway was blocked by bafilomycin, an antibiotic inhibiting fusion between autophagosomes and lysosomes (119). The p.V129I variant was found in an adult onset (38 years) isolated cervical dystonia patient aged 55 years and was predicted to be a pathogenic variant (120).

Molecular pathology

TOR1A encodes the protein TorsinA, a member of AAA+ family of ATPases with diverse cellular activities (84). The TorsinA is expressed throughout the brain and restricted to neurons with the highest expression in cerebellum, hippocampus, frontal cortex, thalamus, substantia nigra pars compacta, locus ceruleus and Purkinje cells (127-131). Within the cells, TorsinA primarily found in the endoplasmic reticulum (ER) lumen as ATP-free state and nuclear envelop (NE) as ATP-bound active form (115-117). TorsinA is a homologue of Hsp100/Clp heat shock protein and is believed to function as a molecular chaperone for maintenance of different protein conformation and protein signaling cascades (132). TorsinA mediated protein degradation could be mediated by lysosomal AP-3 complex (133) and by proteosomal degradation pathway (134, 135). The loss of TorsinA normal activity by its mutant form could dysregulate the proteosomal degradation of misfolded protein and increase the ER stress (136). The increased expression and enzymatic activity of TorsinA was observed during cellular oxidative stress (116, 137) and experimentally overexpression of torsinA can protect from stress-induced cell death (138, 139). Moreover, the ΔE (ΔGAG) mutant of torsinA form the perinuclear inclusion bodies and resides primarily in the NE as punctate, which implicates the nuclear envelopes

dysfunction (140-142). TorsinA interacts with lamin associated polypeptide 1 (LAP1) in the NE and LULL1 in the NE/ER network (143). Along with the LAP1, torsinA form a complex with kinesin light chain 1 (KLC1) and then undergoes anterograde transport along microtubules in secretory pathway towards the axonal growth cone (144). In neuronal cell, torsinA is responsible for maintaining cell polarity through association with tau protein (145). It has been shown that ΔE torsinA could inhibit the neurite growth, which may affect the development of neuronal pathway (146). TorsinA localizes within transport vesicles (147) and help to transport membrane bound proteins through secretory pathway (148, 149); whereas ΔE torsinA could disrupt the vesicular transport of VMAT2 (Vesicular monoamine transporter 2) and DAT (Dopamine transporter) (141, 150). At neuronal synapses, torsinA binds to the Snapin, which is crucial for synaptic vesicle recycling and stabilization of certain synaptic protein including synaptotagmin-1 (151, 152). Synaptotagmin-1 is a Ca^{2+} sensor in presynaptic axonal membrane and involved in neurotransmitter release and exocytosis (153, 154), mutation of which could also develop dystonia (155).

2.2.2 *DYT2-HPCA*

Clinical features:

DYT2 is a childhood onset autosomal recessive form of primary dystonia which affects distal limbs first and then progress mildly to neck, orofacial, and craniocervical regions (79, 156). It was found first in a Spanish Gypsy family where the affected family members were affected either with generalized dystonia or branchial dystonia (157). The DYT2 dystonia was also found in Sephardic Jewish kindred, where three siblings were affected with childhood onset limb dystonia which

slowly progressed to generalized dystonia with predominant cranio-cervical involvement (85).

Molecular genetics

The segregation analysis in three consanguineous Spanish Gypsy families suggested autosomal recessive inheritance of the disorder (157). Homozygosity mapping and whole-exome sequencing in the Sephardic Jewish consanguineous kindred affected by autosomal recessive isolated dystonia identified a homozygous mutation (c. 225 C>A, p. N75K) in *HPCA* gene (63). In the same study, *HPCA* screening in an additional 150 patients affected with early-onset dystonia identified a compound heterozygous mutation (c. 212 C>A, p. T71N and c. 568 G>C, p. A190T) in a 64-year old women of Sri Lankan origin (63). In another genetic study, an Italian cohort of 73 patients with isolated dystonia (158), no *HPCA* mutation was identified suggesting the mutation in *HPCA* gene may be a rare cause of primary isolated dystonia. *HPCA* encodes for a plasma membrane associated neuron specific 23 kDa Ca²⁺-binding protein, Hippocalcin and it was first discovered in rat hippocampus (159). A cDNA clone encoding human hippocalcin isolated from a human hippocampus cDNA library showed a 100% amino acid identity between human sequence and rat sequence (160). *HPCA* gene consists of 3 exons spanning 7 kb on chromosomal region 1p35-p34.2 (161).

Molecular pathology

It has been shown that hippocalcin can bind to the the β -2 adaptin subunit of the AP2 adaptor complex (AP2B2) and the AP2-hippocalcin complex acts as a Ca²⁺ sensor that couples NMDA receptor dependent activation to regulated endocytosis of AMPA

receptors during long term depression (LTD) (162). Another study found that, mice deficient of hippocalcin did not elicit the sAHP (slow afterhyperpolarization) current after brief depolarizations. Expression of hippocalcin in rat cultured hippocampal neurons led to prominent sAHP currents, whereas neurons expressing hippocalcin lacking N-terminal myristoylation exhibited a small sAHP current similar to that recorded by intact neurons (163). Based on this background knowledge, it has been predicted for p. N75K variant that it might affect the Ca^{2+} binding by altering the semi-conservative residue in the EF-hand domain 2 of hippocalcin. A functional study has been undertaken where the *Hpca* on rat primary neurons and astrocytes was knocked down by shRNA and the hippocalcin deficiency driven cellular calcium homeostasis was measured by fura-2 fluorescence microscopy. In this experiment it was found that *HPCA* deficiency might inhibit voltage-dependent Ca^{2+} channels thus affecting the maintenance of membrane potential and cellular response to membrane depolarization (63).

2.2.3 ***DYT3-TAF1***

Clinical features

DYT3 dystonia represents an atypical dystonia named X-linked dystonia-parkinsonism (XDP) or “Lubag” syndrome, which is endemic for Filipino population (86, 164). DYT3 dystonia typically an adult-onset (first four decade of life) dystonia often associated with parkinsonian features and generalizes after few years of disease onset (164). XDP was first reported in a Filipino family which was also studied later for clinical study and genetic mapping (165-167). As it is X-linked, DYT3 predominantly affected the Filipino males rather than females (99:1 ratio). The mean age of onset for men is 39 years ranging from 12 to 64 years while for the women it

is 52 years ranging from 26 to 75 years (168). The clinical features of XDP is highly variable. Though it was traditionally diagnosed with dystonic features (169), the genetically confirmed XDP patients develop the parkinsonian features (170) which may include the cardinal features like resting tremor, bradykinesia, rigidity, and postural instability and levodopa responsiveness (171). The dystonic symptoms may include jaw dystonia, cervical dystonia in the form of retrocollis and torticollis, limb dystonia in advanced cases, tongue dystonia manifesting as either involuntary tongue protrusion or limitation in tongue protrusion and rarely laryngeal dystonia (172).

Neuropathology

The very first neuropathological study was done for two Filipino XDP patients and it was found that there was multifocal mosaic pattern of astrocytosis and neuronal loss in caudate and lateral putamen (173). Later it was studied in detail and two distinct pathological information was derived, which showed in the dystonic phase, the loss of striosomal inhibitory projections lead to disinhibition of nigral dopaminergic neurons while in the parkinsonian phase, severe and critical reduction of matrix-based projection may result in extranigral parkinsonism (174). There was a neuropathological study done on a XDP patient affected with severe generalized dystonia and Parkinsonism and confirmed the mosaic pattern of striatal gliosis along with a marked gliotic patches (175). This may be developed due to synaptic loss rather than neuronal loss because with synaptic immunostaining, the patchy areas showed poor synaptophysin staining. Detailed analysis of XDP post-mortem brain revealed a striking depleted striatosomes while the striatal matrix was moderately affected (176). More recent neuropathological study showed a neostriatal defect of

neuropeptide Y and suggested that the neuropeptide Y system may be involved in the progressive loss of striatal neurons (177).

Molecular genetics

XDP is an X-linked recessive disorder (178) for which linkage analysis and association studies assigned DYT3 to Xq13.1 (86). The specific gene for DYT3 dystonia is somewhat ambiguous, though *TAF1* is likely to be the candidate (179). *TAF1/DYT3* locus consists of 38 exons followed by additional five exons (exons d1-d5) which can be independently transcribed (180, 181). There are five XDP disease specific changes (DSC; DSC1, DSC2, DSC3, DSC10 & DSC12) and a 48 bp deletion in *TAF1/DYT3* locus were reported in Filipino patients and it was suggested that these changes could be potential pathogenic variants for XDP (180). Among these DSCs, DSC1 is located within an Alu repeat, DSC2 within a LINE2 repeat, and DSC10 within a LIMB2 repeat in intron 32 of *TAF1*. DSC12 is located in intron 18 of *TAF1*, whereas the 48-bp deletion is located in intron 2 of *TAF1*. The DSC3 (c. 94 C>T; p. R32C) is located in exon d4 and it's the only molecular alteration detected in a mature transcript within the XDP core haplotype (180). Recently using the advanced genomic sequencing strategies, a disease-specific short interspersed nuclear element, variable number of tandem repeats and Alu composite (SVA) retrotransposon insertion in intron 32 of *TAF1* were reported with significantly reduced expression of *TAF1* and *DDR2* (Dopamine receptor D₂) in the caudate nucleus of XDP patients (87).

Molecular pathology

The *TAF1* gene encodes for TAF1 protein, a component protein of the transcription factor IID (TFIID) of RNA polymerase II mediated transcription (182). TFIID binds directly to the TATA-box promoter elements and acts as scaffold for transcription initiation. TAF1 is an essential cofactor of the TFIID associated TATA-box binding protein complex (TBP) and it regulate the expression of several cell cycle related genes (183, 184). *TAF1* is thought to have a regulative role in G1/S and G2/M cell cycle progression by activating the transcription of cyclin D1 and cyclin A (185-187). This obvious role of *TAF1* in regulating cell cycle may explain the molecular mechanism of DYT3 dystonia-parkinsonism. It has been suggested that the decreased expression of the neuron-specific isoform of *TAF1* results in transcriptional dysregulation of many neuronal genes, including DRD2 (87). In a very recent study it was found that the DSC3 in *TAF1/DYT3* interferes with dopamine processing and function, as well as calcium metabolism leading to impaired vesicular neurotransmitter release (188).

2.2.4 DYT4-TUBB4A

Clinical features

DYT4 dystonia is an autosomal dominant whispering dysphonia followed by the involvement of other muscles of the neck or limbs. *DYT4* dystonia was first reported in large Australian kindred, where four consecutive generations were affected with whispering dysphonia along with generalized torsion dystonia (88, 189). A recent follow up study for the same family reported the development of tongue bradykinesia with swallowing problem soon after the onset of spasmodic dysphonia (190). All the patients developed an alcohol responsive laryngeal adductor dysphonia. Several

patients developed generalized dystonia or an unusual 'hobby horse gait,' with toe walking, stiff legs, and skipping gait.

Molecular genetics

Following family based linkage analysis and exome sequencing, a heterozygous mutation (c. 4C>G; p. R2G) was identified in *TUBB4A* gene (64) in a family previously reported by Parker et.al. (1985). This variant resides in the highly conserved residue in the autoregulatory MREI (methionine–arginine–glutamic acid – isoleucine) domain of β -tubulin, which was predicted to abrogate the autoregulatory capability of β -tubulin and interfere with proper assembly. In an independent and simultaneous study for the same family the p. R2G mutation was also identified by genomewide linkage analysis and genome sequencing in 2 family members (65). In the same study, screening of *TUBB4A* in 394 additional index dystonia patients identified another variant p. A271T in a 71 year old woman with onset of spasmodic dysphonia at the age of 60 years. Very recently in a genetic study, high-resolution melting and Sanger sequencing was done for *TUBB4A* gene in 575 dystonia patients affected with primary laryngeal, segmental and generalized dystonia. As no pathogenic variants in the *TUBB4A* gene was found, it has been suggested that variation in *TUBB4A* is not a significant cause of primary dystonia (191). The *TUBB4A* gene has been mapped to the chromosomal position 19p13.3.

Molecular pathology

The *TUBB4A* gene encodes a brain-specific beta-tubulin protein that is highly expressed in brain specifically in the cerebellum, putamen and white matter (192). The expression is highest in the cerebellum and white matter tract of cerebral cortex (64). Beta tubulins are essential components of the cytoskeletons, which is

responsible for maintaining neuron morphology and function. Beta tubulins are continuously incorporated and released in the dynamic microtubules and *TUBB4A* accounts for almost 50% of all β -tubulins in central nervous system (CNS) (193). It has been found that the c. 4C>G mutant *TUBB4A* mRNA expression was downregulated (65) and this mutation was predicted to have interference property for β -tubulin oligomerization. These could be sufficient to disrupt the microtubule structure in CNS and trigger the DYT4 pathogenesis. This may be an evidential clue to DYT1 dystonia as TorsinA interacts with microtubules and the microtubule associated synaptic transport (194). For the other mutation p. A271T, no functional study has been done yet.

2.2.5 *DYT5a/DYT14-GCH1*

Clinical features

DYT5 generally termed as Dopa-responsive dystonia (DRD) or Segawa syndrome, is an early onset autosomal dominant form of dystonia characterized by marked diurnal variation of symptoms in ~75% of the affected patients, parkinsonism and a dramatic therapeutic response to L-dopa (195-197). This has been first reported in 1976, where patients were reported to have postural and motor disturbances with marked diurnal fluctuation (195). The clinical spectrum may include generalized, segmental and focal dystonia through postural anomalies, parkinsonism, abnormal gait and involvement of limb dystonia and tremor (198-202). As the clinical presentation of DRD typically involve lower limb dystonia and gait disturbance, occasionally it leads to misdiagnosis as cerebral palsy or spastic paraparesis (198). Rarely, DRD patients may develop dystonic tremor or akinetic-rigid Parkinsonism during the course of their

disease progression (203, 204). In one recent study, major depression and sleep disorders has been reported, whereas obsessive–compulsive disorder was found in 25% of cases (205).

Neuropathology

There were no gross abnormalities found in the cases of DYT5 (Dopa responsive dystonia) dystonia. However, there were certain reports of hypopigmented neurons with lower level of dopamine in the substantia nigra (197, 206, 207). Biochemical examination on 2 DRD patients, it was found that a considerable decrease in brain tetrahydrobiopterin (BH4), neopterin and low levels of the tyrosine hydroxylase enzyme activity (208). These findings were complemented by a recent study, where neuroimaging, neurophysiological and biochemical evidences confirmed the decreased striatal dopamine and a decreased level of tyrosine hydroxylase is the main pathology of autosomal dominant DRD, as the structure of nigrostriatal dopaminergic neurons were perfectly normal (209). The deprivation of GTP cyclohydrolase I activity was found to be specific to females with a 4:1 predominance, as it was found to have a higher activity in male DRD patients compared to female DRD patients (89).

Molecular genetics

The locus DYT5a was mapped to the chromosomal position 14q22.1-q22.2 (197) and the corresponding gene *GCH1* was assigned using in-situ hybridization (89, 210). The *GCH1* gene is comprised of 6 exons (211). Genetic variations in *GCH1* gene could cause the autosomal dominant dopa-responsive dystonia and has a higher penetrance in females (~80%) compared to male (~40%-50%) patients (200, 212). *GCH1* encodes GTP cyclohydrolase, a rate-limiting enzyme in

tetrahydrobiopterin (BH4) synthesis pathway. BH4 acts as a cofactor for tyrosine hydroxylase (TH) enzyme involved in dopamine biosynthesis (Figure 1). The mutation in *GCH1* gene could hamper the BH4 biosynthesis in a dominant negative manner (213, 214). Missense, nonsense, splice site mutations, small and large deletion, whole exon or multiexonic deletions were found in DRD patients and till date a total of 168 mutations were identified (Table 5).

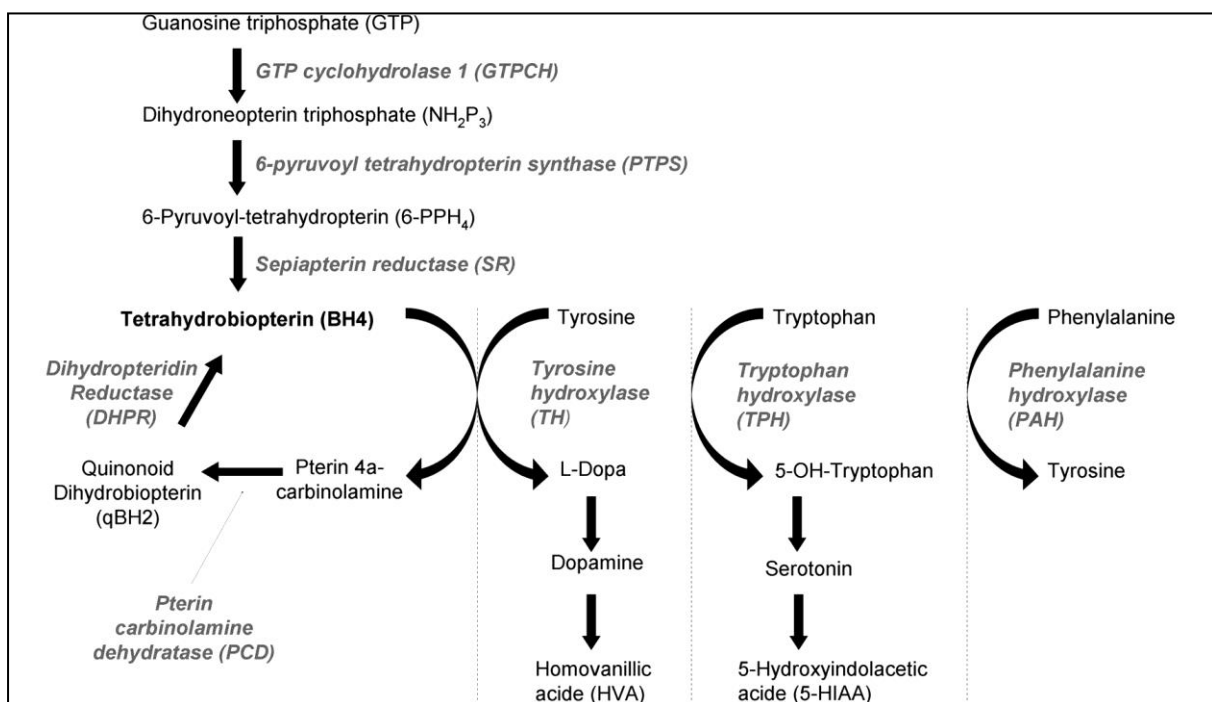


Figure 1: Metabolic pathway for BH4, dopamine, serotonin and other monoamines. (Figure courtesy: Clot et. al. 2009)

Table 5: Mutations found in *GCH1* gene in DRD patients.

Nucleotide variant	Exon No.	Amino acid change	Disease manifestation	Reference
Missense variants				
c.1 A>G	1	p. M1V	DRD	(215)
c.1 A>T	1	p. M1L	DRD	(216)
c.2 T>C	1	p. M6T	DRD	(217)
c.5 A>G	1	p. Q2G	DRD	(218)
c.68 C>T	1	p. P23L	DRD	(219-223)
c.206 C>T	1	p. T8C	DRD	(224)
c.212 T>A	1	p. L71Q	DRD	(225)
c.218 C>A	1	p. A73D	DRD	(226, 227)
c.221 C>T	1	p. A74V	DRD	(225)
c.236 T>C	1	p. L79P	DRD	(228)
c.239 G>A	1	p. S80E	DRD	(217)
c.241 T>C	1	p. S81P	DRD	(229)
c.245 T>C	1	p. L82P	DRD	(217)
c.248 G>C	1	p. G83A	DRD	(225)
c.260 A>C	1	p. Q87P	DRD	(230)
c.262 C>T	1	p. R88W	DRD	(89)
c.262 C>G	1	p. R88G	DRD	(222)
c.263 G>C	1	p. R88P	DRD	(225)
c.272 T>G	1	p. L91R	DRD	(222)
c.281 C>A	1	p. T94K	DRD	(222, 231, 232)
c.281 C>T	1	p. T94M	DRD	(233)
c.284 C>G	1	p. P95R	DRD	(234)
c.293 C>T	1	p. A98V	DRD	(204)
c.305 T>A	1	p. M102K	DRD	(235)
c.305 T>G	1	p. M102R	DRD	(236)
c.308 A>C	1	p. Q103P	DRD	(222)
c.309 G>C	1	p. Q103H	DRD	(227)
c.317 C>T	1	p. T106I	DRD	(237)
c.322 G>A	1	p. G108S	DRD	(238)
c.323 G>A	1	p. G108D	DRD	(222, 239)
c.323 G>T	1	p. G108V	DRD	(240)
c.328 C>G	1	p. Q110E	DRD	(241)
c.334 A>G	1	p. T112A	DRD	(241)
c.343 G>A	1	p. D115N	DRD	(220)
c.350 T>G	2	p. L117R	DRD	(242)
c.358 G>T	2	p. A120S	DRD	(241)
c.385 A>G	2	nk	DRD	(243)
c.400 G>A	2	p. D134N	DRD	(238)
c.401 A>T	2	p. D134V	DRD	(89)
c.401 A>G	2	p. D134G	DRD	(241)
c.402 T>C	2	p. I135T	DRD	(243)
c.404 T>A	2	p. I135K	DRD	(244)
c.410T>G	2	p. M137R	DRD	(245)
c.421T>C	2	p. C141R	DRD	(236)
c.423T>G	2	p. C141W	DRD	(232, 235)
c.431A>C	2	p. H144P	DRD	(240, 246, 247)
c.435G>T	2	p. L145F	DRD	(233)
c.454C>T	2	nk	DRD	(243)
c.458A>C	3	p. H153P	DRD	(225)
c.460A>G	3	p. I154V	DRD	(241)
c.463G>A	3	p. G155S	DRD	(245)
c.488T>G	3	p. L163R	DRD	(221)
c.510G>T	4	p. R170S	DRD	(204)
c.524A>G	4	p. Y175C	DRD	(238)
c.527G>C	4	p. S176T	DRD	(232, 235)
c.532A>G	4	p. R178G	DRD	(222)
c.534A>C	4	p. R178S	DRD	(248)
c.534A > T	4	p. R178S	DRD	(203)

Continued.....

Genetics of Dystonia

Nucleotide variant	Exon No.	Amino acid change	Disease manifestation	Reference
c.539A>G	4	p. Q180R	DRD	(203)
c.544C>G	5	p. Q182E	DRD	(223)
c.547G>A	5	p. E183K	DRD	(249)
c.550C>T	5	p. R184C	DRD	(222)
c.554T>G	5	p. L185R	DRD	(250)
c.557C>A	5	p. T186K	DRD	(240, 251, 252)
c.557C>T	5	p. T186I	DRD	(253)
c.571G>A	5	p. V191I	DRD	(204, 225)
c.586G>T	5	p. A196S	DRD	(201)
c.587C>A	5	p. A196D	DRD	(238)
c.593G>A	5	p. R198Q	DRD	(241)
c.595C>G	5	p. P199A	DRD	(254, 255)
c.595C>T	5	p. R199S	DRD	(256)
c.596C>T	5	p. P199L	DRD	(203)
c.601G>A	5	p. G201R	DRD	(222)
c.602G>A	5	p. G201E	DRD	(89)
c.604G>A	5	p. V202I	DRD	(222)
c.607G>A	5	p. G203R	DRD	(204, 225)
c.610G>A	5	p. V204I	DRD	(204, 227, 241)
c.614T>G	5	p. V205G	DRD	(227, 255)
c.617T>C	5	p. V206A	DRD	(227)
c.623C>A	5	p. A208E	DRD	(257)
c.625A>C	5	p. T209P	DRD	(258)
c.630C>G	6	p. H210Q	DRD	(259)
c.637A>G	6	p. M213V	DRD	(238)
c.640G>A	6	p. V214I	DRD	(226)
c.650G>T	6	p. G217V	DRD	(241)
c.661A>T	6	p. M221L	DRD	(227, 239)
c.662T>C	6	p. M221T	DRD	(239, 260)
c.669C>A	6	p. S223R	DRD	(222)
c.671A>G	6	p. K224R	DRD	(225, 241, 255, 258, 261)
c.677T>C	6	p. V226A	DRD	(230)
c.690G>A	6	p. M230I	DRD	(241)
c.701T>C	6	p. F234S	DRD	(225)
c.703C>T	6	p. R235W	DRD	(262)
c.721C>T	6	p. R241W	DRD	(225)
Nonsense mutations				
c.3G>C	1	p. M1*	DRD	(247)
c.22_23delinsTA	1	p. A8*	DRD	(222)
c.142C>T	1	p. Q48*	DRD	(263)
c.159del	1	p. W53*	DRD	(264)
c.166G>T	1	p. E56*	DRD	(225)
c.181G>T	1	p. E61*	DRD	(204, 221, 265)
c.193G>T	1	p. E65*	DRD	(266)
c.225C>A	1	p. Y75*	DRD	(221)
c.265C>T	1	p. E89*	DRD	(267-269)
c.287G>A	1	p. W96*	DRD	(270)
c.288G>A	1	p. W96*	DRD	(271)
c.328C>T	1	p. E110*	DRD	(241)
c.341C>A	1	p. S114*	DRD	(266)
c.341C>G	1	p. S114*	DRD	(272)
c.538C>T	4	p. E180*	DRD	(203, 236)
c.544C>T	5	p. E182*	DRD	(200, 221)
c.646C>T	6	p. R216*	DRD	(225)
c.670A>T	6	p. K226*	DRD	(220)
Truncating mutations				
c.3_4dup	1	p. E2GfsX66	DRD	(89)
c.62_63delinsAACC	1	p. G21EfsX47	DRD	(273)
c.149del	1	p. A50GfsX17	DRD	(199)
c.172_173delC	1	p. R59QfsX5	DRD	(274)

Continued.....

Genetics of Dystonia

Nucleotide variant	Exon No.	Amino acid change	Disease manifestation	Reference
c.233delT	1	p. I78TfsX2	DRD	(275)
c.260del	1	p. Q87RfsX31	DRD	(204)
c.309delG	1	p. Q103HfsX15	DRD	(200, 221)
c.329dup	1	p. E111GfsX13	DRD	(199)
c.351del	2	p. N118TfsX13	DRD	(199)
c.453+1G>C		p. D115fsX7	DRD	(276)
c.456_509+2del	3	p. V152DfsX6	DRD	(237)
c.456_541+2del	3	p. V152LfsX3	DRD	(237)
c.477delC	3	p. N159LfsX14	DRD	(221)
c.513_525del	4	p. I174DfsX14	DRD	(228)
c.631_632del	6	p. M211VfsX38	DRD	(199, 225)
c.654_655insT	6	p. Q219SfsX31	DRD	(222)
c.656_663del	6	p. K220QfsX27	DRD	(226)
c.695delG	6	p. G232VfsX14	DRD	(255)
c.726_727insTTCCC	6	p. E243FfsX5	DRD	(277)
c.729delG	6	p. E243DfsX3	DRD	(278)
Splice site mutations				
c.343+5G>C (IVS1+5G>C)	Intron 1		DRD	(204)
c.344-1G>A (IVS1-1G>A)	Intron 1		DRD	(266)
c.344-2A>G (IVS1-2A>G)	Intron 1		DRD	(204, 221, 279)
c.453+6G>T (IVS2+6G>T)	Intron 2		DRD	(233)
c.453+1G>A (IVS2+1G>A)	Intron 2		DRD	(280)
c.454-2A>G (IVS2-2A>G)	Intron 2		DRD	(279)
c.509+1G>T (IVS3+1G>T)	Intron 3		DRD	(221)
c.509+68A>G (IVS3+68A>G)	Intron 3		DRD	(215)
c.509+3A>G (IVS3+3A>G)	Intron 3		DRD	(238)
c.509+1G>A (IVS3+1G>A)	Intron 3		DRD	(281)
c.509+5G>A (IVS3+5G>A)	Intron 3		DRD	(282)
c.510-2G>A (IVS3-2G>A)	Intron 3		DRD	(199)
c.541+1G>C (IVS4+1G>C)	Intron 4		DRD	(221)
c.541+1G>A (IVS4+1G>A)	Intron 4		DRD	(222)
c.542-2A>C (IVS4-2A>C)	Intron 4		DRD	(238)
c.626+1G>A (IVS5+1G>A)	Intron 5		DRD	(237, 283)
c.626+5G>A (IVS5+5G>A)	Intron 5		DRD	(221)
c.626+1G>C (IVS5+1G>C)	Intron 5		DRD	(255)
c.626+4A>G (IVS5+4A>G)	Intron 5		DRD	(238)
c.626+1G>T (IVS5+1G>T)	Intron 5		DRD	(282)
c.627-6T>G (IVS5-6T>G)	Intron 5		DRD	(215)
c.627-2A>G (IVS5-2A>G)	Intron 5		DRD	(284)
Exon deletion				
c.1_509del	1	Ex1_Ex3del	DRD	(230)
c.1_541del	1	Ex1_Ex4del	DRD	(222)
c.1_753del	1	Ex1_Ex6del	DRD	(222, 285)
c.1_343del	1	Ex1del	DRD	(230)
c.344_541del	2	Ex2_Ex4del	DRD	(282)
c.344_453del	2	Ex2del	DRD	(253)
c.344_753del	2	Ex2_Ex6del	DRD	(285)
c.454_750del	3	Ex3_Ex6del	DRD	(238)
c.454_541del	3	Ex3_Ex4del	DRD	(237)
c.454_509del	3	Ex3del	DRD	(237)
c.510_753del	4	Ex4_Ex6del	DRD	(285)
c.542_753del	5	Ex5_Ex6del	DRD	(286)
Whole gene deletion				
c.?	3'UTR	p. GCH1del	DRD	(287)
c.-360delGCH1	3'UTR	p. GCH1del	DRD	(288)

NK: Not known, DRD: Dopa responsive dystonia, IVS: Intervening sequence, UTR: Untranslated region.

Molecular pathology

Mutations in *GCH1* may cause deficiency of GTPCH1 activity leading to inhibition of BH4 biosynthesis (89, 289). BH4 is an essential cofactor for normal activity of Nitric oxide synthase (NOS), Tyrosine hydroxylase (TH), Phenylalanine hydroxylase (PAH) and Tryptophan hydroxylase to synthesize nitric oxide, monoamines and dopamine, tyrosine and serotonin respectively. Thus mutation in *GCH1* gene could substantially reduce the production of monoamines and pivotal neurotransmitters like dopamine and serotonin (290). GCH1 activity is regulated by BH4-mediated feedback inhibition (291), where GCH1 feedback regulator protein (GFRP) interacts with GCH1 in presence of BH4 to inhibit the GCH1 activity. Though this mechanism is tissue specific as GFRP is expressed only in serotonergic neurons but not in dopaminergic ones (292). These tissue specific regulatory processes leading to significant higher GCH1 expression in serotonergic neurons other than monoaminergic neurons (293). GTPCH1 forms a homodecamer to be a functional unit, while any mutation could hamper the interaction and substantially decrease the GCH1 activity through dominant negative mechanism (214). This helps to make the GCH1 enzyme to be non-functional or dysfunctional which direct the severity of dopa responsive dystonia in patients.

2.2.6 *DYT5b-TH*

Clinical features

DYT5b dystonia is similar to DYT5a dystonia (Dopa responsive dystonia), often referred to as autosomal recessive Segawa syndrome. It can be developed due to deficiency of Tyrosine hydroxylase (*TH* deficiency), a rate-limiting enzyme in

dopamine biosynthetic pathway that convert tyrosine to dopamine. In cases of TH-deficient DRD, the lower limb dystonia is the prominent symptoms with difficulty in walking which can be progressed to generalized dystonia. The disease onset is generally from 6 months to 12 years (90). Certain parkinsonian features were observed in the form of bradykinesia, postural tremor and rigidity in the affected limbs. Pyramidal signs may be observed as hyperreflexia and spasticity. A diurnal fluctuation of symptoms was observed but relatively less frequent than DYT5a. Though psychomotor and intellectual ability are not affected, a TH-deficient DRD patient was found with impaired cognitive impairment (294). TH-deficient DRD patients also demonstrated excellent levodopa responsiveness even for extensive levodopa therapy (294, 295).

Molecular genetics

DYT5b locus was mapped to chromosomal position at 11p15.5 which consist the gene *TH* (296). The *TH* gene consists of 14 exons spanning ~8.5 kb (297) and the alternatively spliced 4 transcript variants of *TH* differentially expressed hroughout the nervous system (298, 299). The inheritance pattern of *TH* is autosomal recessive with complete penetrance. Till date, 14 pathogenic nucleotide variants were found (Table 6) in the cases of TH-deficient DRD patients, most of which occurred as missense mutations. Modification in amino acid sequences may hinder the catalytic activity; alter the structural integrity and/or substrate binding ability.

Molecular pathology

Crystal structure of Tyrosine hydroxylase revealed a a short α -helix containing carboxyl terminal responsible for tetramerization (300), a ~300 amino acid long

central catalytic domain containing catalytic iron atom (301) and a amino terminal regulatory domain (302). Tyrosine hydroxylase remain in cytosol and to some extent in plasma membrane for packing of chatecholamine into vesicles to synaptic export (303). Pathogenic mutations in these functionally important motifs are responsible for aberrant enzymatic activity of tyrosine hydroxylase which in turn hamper the biosynthesis of dopamine and other chatecholamines.

Table 6: Mutations found in *TH* gene in DRD patients.

Nucleotide variant	Exon No	Amino acid change	Disease manifestation	Reference
c.1-71C>T	3'UTR	-	DRD	(304)
c. 56C>G	1	p. S19C	DRD	(243)
c.698G>A	6	p. R233H	DRD	(305-309)
c.707C>T	6	p. L236P	DRD	(307, 310)
c.736C>T	6	p. H246Y	DRD	(311, 312)
c.739G>A	7	p. G247S	DRD	(312, 313)
c.826A>C	8	p. T276P	DRD	(295, 314)
c.901C>G	8	p. P301A	DRD	(282, 312)
c.956G>C	9	p. R319P	DRD	(282, 312)
c.1004C>T	9	p. A335V	DRD	(315)
c.1010G>A	9	p. R337H	DRD	(295, 314)
c.1282G>A	12	p. G428R	DRD	(243, 316)
c.1451G>A	14	p. R484H	DRD	(315)
c.1493A>G	14	p. D498G	DRD	(294, 307, 311, 317)

DRD: Dopa responsive dystonia, UTR: Untranslated region.

2.2.7 *DYT6-THAP1*

Clinical features

DYT6 dystonia or “idiopathic torsion dystonia of mixed type” is characterized by dystonic symptoms involved in cranio-cervical regions with secondary generalization to other body parts like orofacial region and upper limb(s). The symptoms start as focal dystonia and often progress to generalized dystonia. Laryngeal involvement is common as a form of dysphonia. Age of onset varies from early childhood to late

adulthood (91, 318, 319). DYT6 dystonia was first identified in an isolated Amish-Mennonite family with typical dystonic features in upper limbs, cranial and cervical muscles (320).

Neuropathology

DYT6 locus specified for a gene product THAP1 protein is expressed widely throughout the rat brain regions. The prominent expression was found in dopaminergic neurons in basal ganglia, thalamus, Purkinje cells and pyramidal cells in cerebral cortex, medium spiny neurons and cholinergic neurons of striatum and dorsal root ganglion (321). A recent knockin mouse model of pathogenic *THAP1* variant confirmed altered morphology and hypocellularity of projection neurons of cerebellar dentate nucleus (322). Functional anisotropy and diffusion tensor imaging of DYT6 dystonia patients revealed subgyral white matter of sensorimotor cortex was damaged (323). Another recent study reported the absence of any major neuropathological hallmark (324).

Molecular genetics

DYT6 dystonia transmits in an autosomal dominant fashion with reduced penetrance (~60%). The disease locus was mapped to the chromosomal position 8p11.21 (320) and harbor the specific gene *THAP1*. Mutations of *THAP1* were identified in DYT6 dystonia patients (91). *THAP1* gene consists of 3 exons spanning ~6.6 kb and encode a 213 amino acid long 24.9 kDa protein, Thanatos associated [THAP] domain containing apoptosis associated protein 1 (THAP1). The very first identified mutation in THAP1 gene was a double frameshift mutation (c. [134_135 insGGGTT; 137_139delAAC]) found in an Amish-Mennonite family (91). After discovery of the

responsible gene, there was several genetic studies done throughout the major world population and about 88 different genetic variants were found (Table 7). Though there was no strong genotype-phenotype correlation (325), a recent effort revealed mutations in THAP domain was associated with early age of onset with extensive anatomical distribution compared to non-THAP domain mutations (326).

Molecular pathology

THAP1 protein is a transcription factor, contains an N-terminal Zn²⁺ binding THAP domain followed by a proline rich domain, nuclear localization signal sequences buried in C-terminal leucine rich coiled-coil region (327, 328). The THAP domain is responsible for DNA binding and the coiled-coil domain helps in dimerization to form a functional unit (329). Mutation(s) in THAP domain may diminish the DNA binding ability and affinity (330) as determined by biophysical techniques followed by the transcriptional repression activity over *TOR1A* transcription (331, 332) as concluded by ChIP, EMSA and luciferase reporter assay. Mutations in coiled-coil domain resulted in impaired dimerization (329) and certain mutations throughout the protein alter the subcellular localization (329, 333, 334) from nuclear localization to diffused cytosolic localization. The truncating mutations could be implemented for non-sense mediated decay and splice site variant alter the splicing event followed by gene expression (335). THAP1 was found to control the transcription of genes involved in pRb/E2F pathway and influence the cell cycle and apoptotic pathway (327, 336). Interaction with HCF-1, an essential cofactor of THAP1 and O-GlcNAC transferase could help the transcriptional activities of THAP1 over certain pRb/E2F pathway genes like *RRM1* (337). THAP1 also interact with prostate apoptosis response-4

Table 7: Mutations found in *THAP1* gene in primary DYT6 dystonia patients.

Nucleotide variant	Exon No.	Amino acid change	Protein structure affected	Reference
Missense mutation				
c.1 A>G	1	p. M1?	THAP dom.	(338, 339)
c.15 C>G	1	p. C5W	L1-THAP dom.	(340)
c.16 T>C	1	p. S6P	L1-THAP dom.	(341)
c.17 C>T	1	p. S6F	L1-THAP dom.	(342)
c.20 C>A	1	p. A7D	L1-THAP dom.	(326)
c.23 A>G	1	p. T8C	L1-THAP dom.	(342)
c.25 G>T	1	p. Q9C	L1-THAP dom.	(343)
c.36 C>A	1	p. N12L	L1-THAP dom.	(318)
c.38 G>A	1	p. R13H	L1-THAP dom.	(344)
c.46 A>G	1	p. K16E	L1-THAP dom.	(326)
c.50 A>G	1	p. D17Q	L1-THAP dom.	(343)
c.57 C>T	1	p. P19P	L1-THAP dom.	(124)
c.61T>A	1	p. S21T	L1-THAP dom.	(318)
c.62 C>T	1	p. S21F	L1-THAP dom.	(339)
c.62 C>G	1	p. S21C	L1-THAP dom.	(326, 345)
c.68A>C	1	p. H23P	BS1-THAP dom.	(331)
c.70 A>G	1	p. K24Q	BS1-THAP dom.	(333)
c.77C>G	2	p. P26R	L2-THAP dom.	(342)
c.77 C>T	2	p. P26L	L2-THAP dom.	(333)
c.83 C>T	2	p. T28I	L2-THAP dom.	(339)
c.86G>A	2	p. R29Q	L2-THAP dom.	(346)
c.86G>C	2	p. R29P	L2-THAP dom.	(318)
c.89C>G	2	p. P30R	L2-THAP dom.	(347)
c.89 C>A	2	p. P30H	L2-THAP dom.	(348)
c.95T>A	2	p. L32H	L2-THAP dom.	(349)
c.115G>A	2	p. A39T	AH1-THAP dom.	(318)
c.151 A>G	2	p. S51G	L3-THAP dom.	(350)
c. 153 C>G	2	p. S51R	L3-THAP dom.	(124)
c.161G>A	2	p. C54Y	BS2-THAP dom	(332)
c.161G>T	2	p. C54F	BS2-THAP dom	(351)
c.167 A>G	2	p. E56G	AH2-THAP dom.	(352)
c.169 C>A	2	p. H57N	AH2-THAP dom.	(353)
c.173 T>C	2	p. F58S	THAP dom.	(348)
c.176 C>T	2	p. T59I	THAP dom.	(354)
c. 208 A>G	2	p. K70E	L4-THAP dom.	(325)
c.215 T>G	2	p. L72R	L4-THAP dom.	(341)
c.224 A>T	2	p. N75I	L4-THAP dom.	(351, 355)
c.238 A>G	2	p. I80V	AH4-THAP dom.	(326)
c.241T>C	2	p. F81L	AH4-THAP dom.	(91)
c.247T>C	2	p. C83R		(353)
c.266A>G	2	p. K89R		(318)
c.267 G>A	2	p. K89L		(351)
c.339 T>C	3	p. D113D		(351)
c.395 T>C	3	p. F132S		(343)
c.407 A>G	3	p. N136S		(325, 342)
c.408 C>G	3	p. N136K		(354)
c.410 A>G	3	p. Y137C		(353)
c.424 A>G	3	p. T142A	Coiled-coil dom.	(329)
c.427 A>G	3	p. M143V	Coiled-coil dom.	(124, 353, 356)
c.446 T>C	3	p. I149T	NLS	(343)
c.449 A>C	3	p. H150P	NLS	(351, 355)
c.489C>G	3	p.L163L	Coiled-coil dom.	(357)
c.496 G>A	3	p. A166T	Coiled-coil dom.	(343, 345)
c.506 G>A	3	p. R169Q	Coiled-coil dom.	(342)
c.508 T>C	3	p. C170R	Coiled-coil dom.	(358)
c.521A>G	3	p.E174G	Coiled-coil dom.	(357)
c.530 T>C	3	p. L177P	Coiled-coil dom.	(359)
c.539 T>C	3	p. L180S	Coiled-coil dom.	(351)

Continued.....

Genetics of Dystonia

Nucleotide variant	Exon No.	Amino acid change	Protein structure affected	Reference
c.559 C>A	3	p. Q187K	Coiled-coil dom.	(343)
c.574 G>A	3	p. D192N		(353)
Nonsense mutation				
c.7 C>T	1	p.Q3X	L1-THAP dom.	(342)
c.85 C>T	2	p.R29X	L2-THAP dom.	(318, 325, 345)
c.150 T>G	2	p.Y50X	L3-THAP dom.	(342)
c.289 C>T	2	p. Q97X	Proline rich region	(339)
c.370 C>T	3	p.Q124X		(353)
Small-in frame deletion				
c.207_209ΔCAA	2	p. N69_N69Δ	L4-THAP dom.	(341, 354)
c. 394_396 ΔTTC	3	p. F132 Δ		(329)
Small out-of-frame deletion				
c.2 ΔT	1	p. M1?	THAP dom.	(318)
c.20_33Δ	1	p. A7EfsX23	L1-THAP dom.	(341)
c.63_66 ΔTTTC	1	p. F22fsX71	L1-THAP dom.	(351)
c.174 ΔT	2	p. F58LfsX15	THAP dom.	(342)
c.197_198ΔAG	2	p. E66VfsX19	L4-THAP dom.	(353)
c.208-209 ΔAA	2	p.K70VfsX15	L4-THAP dom.	(356)
c.236 ΔC	2	p. T79KfsX41	AH4-THAP dom.	(342)
c.348 ΔT	3	p. I116MfsX4		(339)
c.377_378ΔCT	3	p. P126RfsX2		(360)
c.388_389ΔTC	3	p. V131FfsX3		(319, 353)
c.389_390ΔCA	3	p. S130CfsX4		(361)
c.413 ΔC	3	p. T138MfsX15		(348)
c.436_443Δ	3	p. R146DfsX9	NLS	(341)
c.460ΔC	3	p. Q154SfsX27	NLS	(318)
c.474 ΔA	3	p. K158NfsX23	NLS	(319)
c.570 ΔA	3	p. D191TfsX9	Coiled-coil dom.	(333)
Small out-of-frame insertion				
c.134_135insGGGTT c.137_139ΔAAC	2	p. F45fsX73		(91, 318)
c.109dup	2	p. E37GfsX10	AH1-THAP dom.	(339)
c.213dup	2	p. L72TfsX14		(357)
c.514dup	3	p. R172KfsX7	Coiled-coil dom.	(360)
c.109_132dup	2	p. Q37_N44dup	AH1-THAP dom.	(345)

protein (PAWR), a pro-apoptotic transcription factor present in a low amount in synapses and dendrites (362). Apoptotic triggers could elevate the amount of PAWR in neurons and induce the neuronal death in certain neurodegenerative disease like Parkinson's disease (363) and Alzheimer's disease (364). Though there was no evidence of neurodegeneration for DYT6 dystonia, dysregulated THAP1 activity may be involved in apoptosis and impaired cell proliferation in developing neurons (321).

2.2.8 DYT8-MR1

Clinical features

DYT8 dystonia is referred to as paroxysmal nonkinesigenic dyskinesia 1 (PNKD1), which is characterized by spontaneous intermittent attacks of dystonia, chorea and athetosis (93, 365-368). The symptoms generally start with the involvement of limbs and spread to other body regions. The attacks may occur at rest and often provoked by consumption of alcohol, caffeine and to a lesser extent by nicotine, hunger, exercise or emotional stress (369-373). The disease onset is generally in childhood and adolescence although the adult-onset cases were also reported (374-376). The episode of attack could last from minutes to hour and may happen several times a day to few times in a year.

Neuropathology

Though there are no certain neuropathological evidences exists, one study reported lesions of the basal ganglia in case of paroxysmal dyskinesia patients (377). As the patients were not screened for genetic mutations, the outcome of the study may not be evidential for PNKD1 neuropathology.

Molecular genetics

DYT8 locus was assigned to 2q33-35 (375) and the respective gene *MR-1* (Myofibrillogenesis regulator 1) was discovered, mutation of which could cause PNKD (93). The *MR-1* gene has 12 exons and the brain specific *MR-1* transcript give rise to a 385 amino acid long 42.9 kDa protein. Two individual heterozygous mutations, (p. A7V (c. 20 C>T) and p. A9V in exon 1 of *MR-1* were found in two PNKD1 patients (93). These mutations were also reported in a study, where p. A9V was found in 3 unrelated families with PNKD1 and the p. A7V in the affected individuals in 5 unrelated families (367). The p. A9V mutation was also found in a 15 year old Serbian boy (378) affected with PNKD1. Both the mutations were found in a large PNKD1 French and Irish family (365, 379). There was another mutation (p. A33P) in exon 2 of *MR-1* found in a proband of 3 generation family affected with PNKD1 (380). This mutation is located in the N-terminal mitochondrial targeting sequence and may hamper the normal subcellular localization of the *MR-1* gene product.

Molecular pathology

MR-1 protein is thought to be involved in the assembly of protein complexes of sarcomere in skeletal muscle and interacts with myosin regulatory light chain, myomesin 1 and β -enolase. The β -lactamase domain of MR-1 has similarities with Hydroxyacyl glutathione hydrolase (HAGH), a zinc metallohydrolase enzyme, which catalyses conversion of methylglyoxal to D-lactate (381, 382). Methylglyoxal is usually found in coffee, alcoholic beverages and could be generated due to oxidative stress. Impaired function of MR-1 thus might trigger the attacks by consumption of alcohol, caffeine and emotional stress (367). It was found that, the neuron specific

MR-1 may have GSH-producing activity similar to HAGH and mutant MR-1 could have the inability to do so (367). This is supported by the fact that the MR-1 deficient mice have significantly diminished cortical GSH levels (383). The similar observation was found while *PNKD* knock-out mice have decreased Pnkd-L (*PNKD* long isoform) protein as well as decreased level of GSH in cortex region (384). Glutathione acts as a major scavenger of free radicals generated by oxidative stress and is an indicator of cellular redox state. So these experimental evidences suggest a pivotal role of MR-1 to maintain the cellular redox state in brain.

2.2.9 *DYT9/DYT18-SLC2A1*

Clinical features

DYT9 is an autosomal dominant neurologic disorder characterized by childhood onset of paroxysmal choreoathetosis and progressive spastic paraplegia. This paroxysmal dyskinesia choreoathetosis is kinesigenic as it often triggered by physical exercise (95, 385-388). The phenotypic spectrum of DYT9 dystonia is variable enough including seizures, migraine headaches and episodic ataxia (95). DYT9 dystonia could often be presented with progressive spastic paraplegia and cognitive impairment. Dystonic tremor could also be associated with the disorder (389).

Molecular genetics

The DYT9 dystonia transmit as an autosomal dominant trait with incomplete penetrance. DYT9 locus is positioned on chromosome 1p31.3- p35 and a gene, *SLC2A1* was found to be the specific one by candidate gene approach (94). The *SLC2A1* comprised of 10 exons and gives rise to a 492 amino acid long 54 kDa protein GLUT1, Glucose transporter 1. Two missense and one 4-bp deletion

mutations in *SLC2A1* were first reported in paroxysmal exercise induced dystonia patients (94) of three individual families. There are certain other mutations specifically found in DYT9 dystonia patients through recent studies and listed in the Table 8.

Table 8: Mutations found in *SLC2A1* gene in PED patients.

Nucleotide variant	Exon No.	Amino acid change	Disease manifestation	References
c.138 G>C	1	p. Q46H	PED	(95)
c.274 C>T	1	p. R91W	PED	(390)
c.376 C>T	1	p. R126C	PED	(95)
c.493 G>A	1	p. V165I	PED	(391)
c.634 C>T	2	p. R212C	PED	(95)
c.950 A>C	4	p. N317T	PED	(392)
c.998 G>A	4	p. R333Q	PED	(390)
c.1002 G>A	4	p. A275T	PED	(94)
c.1119 G>A	5	p. G314S	PED	(94)
c. 1022_1033Δ	5	p. Q282_S285 Δ	PED	(94)

PED: Paroxysmal exercise induced dyskinesia

Molecular pathology

Mutation in *SLC2A1* gene could cause two types of disease conditions, Paroxysmal exercise induced dyskinesia (DYT9 dystonia) and GLUT1 deficiency syndrome. GLUT1 deficiency syndromes could be characteristically different from DYT9 dystonia as it is associated with epilepsy, microcephaly, spasticity and ataxia (393, 394). GLUT1 is expressed ubiquitously and has an excess expression on the endothelial cells of blood-brain barrier as it is responsible for glucose entry into the brain (395). Along with the glucose, GLUT1 also transport dehydroascorbic acid into mitochondria and brain, where it remains as ascorbic acid. It has been pointed out that oxidation of ascorbic acid is an important regulatory step for accumulation of different vitamins by the brain (395). So the normal GLUT1 function is essential for

elevated metabolic energy requisite of CNS and removal of free radicals generated from oxidative stress (396, 397). As the DYT9 dystonic symptoms are exercise induced, it can be explained by the impairment of glucose transport and subsequent deprivation of glucose metabolism in addition to the depletion of cellular glucose by physical exercise. The functional studies in *Xenopus* oocytes and in human erythrocytes have showed that the mutant form of GLUT1 could alter the intracellular sodium, potassium and calcium level and impaired glucose transport (94). These experimental evidences point out that DYT9 dystonia could be generated by energy deficit and improper synaptic communication due to the fluctuation in intracellular cation concentrations.

2.2.10 DYT10-PRRT2

Clinical features

DYT10 dystonia or Paroxysmal kinesigenic dyskinesia (PKD) is characterized by recurrent and brief attacks of involuntary movement triggered by sudden voluntary movement (398). It could be associated with other clinical symptoms like athetosis, ballism or dystonia. It has been reported that seizures could be present for the PKD patients (399). The onset of PKD could be childhood or early adolescence onset and the frequency and severity generally diminish in adulthood (96). Parkinsonian symptoms also been reported in a single study, where the patient responded well in dopamine therapy, suggesting abnormal dopamine signalling may have a role for PKD pathogenesis (400).

Molecular genetics

The DYT10 locus was mapped to chromosomal position 16p11.2 and family based linkage analysis followed by exome sequencing revealed *PRRT2* as the responsible gene, mutation of which could cause PKC (96). The *PRRT2* gene consists of 4 exons, where the first exon is non-coding. The mutations found in *PRRT2* are mostly clustered at exon 2 and exon 3 and the majority (>95%) of it are frameshift mutations creating truncated protein (401). The frameshift mutation could generate haploinsufficiency by nonsense mediated decay of the anomalous *PRRT2* mRNA. There are certain missense, nonsense, splice site mutations and large sub-microscopic deletions encompassing *PRRT2* gene also reported and listed in Table 9. In general the *PRRT2* mutations inherit as autosomal dominant fashion. But there is a certain report where a compound heterozygous mutation (c.510dupT and c.647C>G) was found in a male PKD patient, where his asymptomatic father and mother did harbour the individual mutation respectively (401). Also there were several *de-novo* mutations found in sporadic cases of PKD, suggesting the inheritance of *PRRT2* mutation could be variable (402-404). The c.649dupC (p.R217PfsX7) was found as the most common mutation of *PRRT2* which was also identified in different ethnic population with variable phenotypes (405, 406).

Molecular pathology

PRRT2 (Proline rich transmembrane protein-2) protein is found adequately in the CNS and is enriched in the cerebral cortex, hippocampus and cerebellum (96). It was also found that, *Prrt2* is widely expressed in mouse brain with a higher expression in cerebral cortex during the early developmental stages suggesting *Prrt2* could be essential for normal neurodevelopment (407). The *PRRT2* protein is a

Table 9: Mutations found in *PRRT2* gene in PKD patients.

Nucleotide variant	Exon No.	Amino acid change	Disease manifestation	References
c.117delA	2	p. V41YfsX49	PKD	(401)
c.133-136delCCAG	2	p.P45RfsX44	PKD	(406)
c. 186-187delGC	2	p. P63QfsX70	PKD	(408)
c.272delC	2	p.P91QfsX24	PKD	(405)
c.369-370insG	2	p.S124VfsX10	PKD	(409)
c.510-511insT	2	p.L171SfsX3	PKD	(401)
c.513-514ins	2	p.L171LfsX3	PKD	(410)
c.514-517delTCTG	2	p.S172RfsX3	PKD	(96)
c. 579 dupA	2	p. E194RfsX6	PKD	(401)
c.595G>T	2	p.Glu199X	PKD	(405)
c.604-607delTCAC	2	p.S202HfsX16	PKD	(405)
c.629-630insC	2	p.A211SfsX14	PKD, ICCA	(402, 407)
c. 647 C>G	2	p. P216R	PKD	(401)
c.649C>T	2	p.R217X	PKD	(401, 402, 411-414)
c.649delC	2	p. R217EfsX12	PKD, ICCA, HM	(402, 405, 411, 415)
c.649-650insC	2	p. R217PfsX8	PKD, ICCA, BFIE, HM	(71, 96, 401-403, 405, 407, 409-412, 415-433)
c.718C>T	2	p. R240X	ICCA, BIS, PKD	(405, 418, 423, 426)
c.776insG	2	p. A260X	PKD	(424)
c.796C>T	2	p. R266W	PKD	(71)
c.841T>C	2	p. W281R	PKD	(409)
c.859G>A	2	p. A287T	PKD	(409)
c.872C>T	2	p. A291V	PKD	(401)
c.913G>A	3	p. G305R	PKD	(405, 416)
c.913G>T	3	p.E305W	PKD	(410)
c.922C>T	3	p. R208C	PKD	(405, 409)
c.964delG	3	p. V322WfsX15	PKD	(409)
c.972delA	3	p. V325SfsX12	PKD	(96)
c.980-981insT	3	p. I327IfsX14	PKD	(418)
c.1011C>T	3	NK	PKD	(410)
c.1011-1012delCG+1-9del9bp	-	-	PKD	(409)
0.544 Mb deletion at 16p11.2 affecting approximately 30 genes	-	-	PKD	(400)
0.43 Mb deletion at 16p11.2 affecting 30 genes	-	-	PKD	(434)

PKD: Paroxysmal kinesigenic dyskinesia, ICCA: Infantile convulsions and choreoathetosis, BIS: Benign infantile seizures, BFIE: benign familial infantile epilepsy, HM: Hemiplegic migraine. NK: Not known

member of dispanin family of protein which are involved in cellular development, adhesion and signalling (435). It was also reported that dispanins are responsive to interferons which actually helps preferentially the neural stem cell differentiation into neurons and enhances the growth and number of neurons (436). PRRT2 also interacts with SNAP-25 of SNARE complex, which is vital for neurite projections and outgrowth (418, 437, 438). Along with these experimental evidences and brain-specific expression of PRRT2 at different developmental stages would lead to the idea that PRRT2 protein is involved in neuronal development and differentiation and truncating mutations of PRRT2 would impede the neurodevelopmental process.

2.2.11 *DYT11/ε-SGCE*

Clinical features

DYT11 or Myoclonus dystonia syndrome is childhood onset hyperkinetic movement disorder. The disease onset is generally during childhood or adolescence and rarely in adulthood (439). The clinical phenotype is characterized by mild to severe myoclonic jerk specifically precipitated as cervical dystonia or writer's cramp and associated with focal or segmental dystonia. Other anatomical parts like lower limbs and orofacial region could be affected and present in at least 25% of the patient pool (440-442). The myoclonus dystonia is alcohol responsive, where the symptoms are dramatically improved by consumption of alcohol (443). Psychiatric problems like depression and anxiety, obsessive–compulsive disorder, panic attacks and attention deficit hyperactivity disorder may be associated with myoclonus dystonia (444).

Molecular genetics

Myoclonus dystonia may develop due to mutation in *SGCE* gene (97). DYT11 dystonia has an autosomal dominant inheritance pattern with reduced penetrance as the *SGCE* gene is maternally imprinted. The disease penetrance of paternal transmission of gene mutation is 100%, the maternal inheritance has only 10-20% of penetrance. It could also be developed by maternal uniparental disomy following the inactivation of both the maternal genes (445). The DYT11 locus was mapped in chromosomal position 7q21 by linkage analysis (446, 447). The *SGCE* gene consists of 12 exons having a brain specific exon 11b (448) and encode a 437 amino acid long 49.8 kDa protein product ϵ -sarcoglycan. Till now, 116 different mutations were found in *SGCE* gene amongst the myoclonus dystonia patients worldwide. Those mutations include nonsense, missense, splice site variants, in-dels, small and large deletions (Table 10) leading to aberrant 'loss of function' ϵ -sarcoglycan protein generating haploinsufficiency (444). Most of the identified mutations are located in the transmembrane domain of ϵ -sarcoglycan. It was also found for certain missense mutations of *SGCE* gene, ubiquitination and proteosomal degradation was triggered for mutated aberrant ϵ -sarcoglycan protein molecules (449). Coexpression study with wildtype *TOR1A* and mutant *SGCE*, resulted in a reduction in aggregated mutant ϵ -sarcoglycan protein, suggesting the chaperone activity of Torsin1A over mutant ϵ -sarcoglycan protein (449).

Molecular pathology

The ϵ -sarcoglycan is widely expressed throughout the different brain regions and muscles both in embryonic and adult tissues (450, 451). It was found with high expression levels particularly in the substantia nigra, the cerebellar Purkinje cells and

monoaminergic neurons (452-455). The brain specific isoform of ϵ -sarcoglycan is generated from brain specific transcript, the protein responsible for alternative splicing to generate it was found to be neuron-specific at the time of neurogenesis (456). ϵ -sarcoglycan is a transmembrane protein consists of a signal peptide sequence, an extracellular domain with glycosylation site, a transmembrane domain and a cytoplasmic domain (457). The ϵ -sarcoglycan along with other isoforms (α -, β -, γ -, δ -, ζ - sarcoglycan) forms dystrophin–glycoprotein complex in muscles and brain and make the connection between cytoplasm and extracellular matrix (458, 459). As this complex is found at the neuromuscular junction, it may have a role in exchange of neuronal signal towards the muscle (460-462). Epsilon sarcoglycan has a high degree of homology with α -sarcoglycan and it can functionally express in certain tissues where the expression and functionality of α -sarcoglycan is limited (450, 463). Apart from ϵ -sarcoglycan, mutation in other isoforms (α -, β -, γ -, δ - sarcoglycan) would develop limb-girdle muscular dystrophies. Mutation in ϵ -sarcoglycan, thus create structural abnormality in the dystrophin–glycoprotein complex, which in turn impose impaired functionality in the cytoplasm and extracellular matrix of neurons.

Table 10: Mutations found in *SGCE* gene in myoclonus dystonia patients.

Nucleotide change	Exon	Amino acid change	Disease manifestation	References
c. -111-?_*275+?Δ	-	-	MD	(464)
c. -1067A>G	1	-	MD	(465, 466)
c. -1062A>G	1	-	MD	(465)
c. -911G>C	1	-	MD	(465)
c. 54G>A	1	NK	MD	(467)
c. 101T>C	1	p. L34S	MD	(468)
c. 107C>G	1	p. T36R	MD	(469)
c. 109+1G>A	Intron 1	-	MD	(470, 471)
c. 109+1G>T	Intron 1	-	MD	(472, 473)
c. 109+5G>C	Intron 1	-	MD	(474)
c. 164ΔC	2	p. G55VfsX31	MD	(475)
c. 179A>C	2	p. H60P	MD	(475-477)
c. 179A>G	2	p. H60R	MD	(478)
c. 208G>T	2	p. Q70X	MD	(479, 480)
c. 221ΔA	2	p. Y74SfsX12	MD	(479)
c. 222C>A	2	p. Y74X	MD	(481)
exon 2-exon11Δ	2	-	MD	(482)
Exon 2Δ	2	-	MD	(483)
c. 110-?_232+?Δ	2	NK	MD	(484)
c. 110-?_390+?Δ	2-3	NK	MD	(485)
c.110-?_662+?Δ	2-5	NK	MD	(485)
c. 232+1G>A	Intron 2	-	MD	(477, 479)
c. 232+1G>T	Intron 2	-	MD	(469)
c. 232+2 T>C	Intron 2	p. V37_P77Δ	MD	(479)
c. 233-1G>A	Intron 2	-	MD	(486-488)
c. 233-1G>T	Intron 2	-	MD	(479, 480)
c. 256ΔA	3	p. T86HfsX91	MD	(477)
c. 275T>C	3	p. M92T	MD	(479)
c. 278ΔG	3	p. G93VfsX39	MD	(487)
nk	3	p. D96N	MD	(489)
c. 289C>T	3	p. R97X	MD	(467, 471, 474, 480, 484, 490)
c. 298T>G	3	p. W100G	MD	(480)
c. 300G>A	3	p. W100X	MD	(479, 480)
c. 304C>T	3	p. R102X	MD	(475-477, 480, 484, 485, 487, 490)
c. 305G>A	3	p. R102P	MD	(491, 492)
c. 334G>A	3	p. G112R	MD	(493)
c. 344A>G	3	p. Y115C	MD	(479, 480)
c. 347G>A	3	p. G116Q	MD	(468)
c. 372ΔG	3	p. K125SfsX7	MD	(494)
c. 386T>C	3	p. I129T	MD	(491)
c. 391-3T>C	Intron 3	-	MD	(480)
c. 391-82_405Δ	Intron 3	-	MD	(490)
c. 391-79G>T	Intron 3	-	MD	(467)
c. 391-43A>C	Intron 3	-	MD	(495)
c. 391-42A>C	Intron 3	-	MD	(467)
c. 391-3T>C	Intron 3	-	MD	(467)
c. 391_405Δ	4	p. I131_N135Δ	MD	(490)
c. 402C>A	4	NK	MD	(493)
C. 444ΔT	4	p. N149IfsX2	MD	(471)
c. 444_447ΔTAAT	4	p. I148MfsX2	MD	(479, 480, 496)

Continued....

Genetics of Dystonia

Nucleotide change	Exon	Amino acid change	Disease manifestation	References
Exon 4-Exon 5Δ	4-5	p. I131RfsX19	MD	(497)
Exon 4-Exon 8Δ	4-8	-	MD	(498)
c. 463+1G>A	Intron 4	-	MD	(474)
c. 463+6T>C	Intron 4	-	MD	(487)
c. 464-317_663-802Δ	Intron 4	p. D155AfsX26	MD	(499)
c.464-?_662+?Δ	5	NK	MD	(499)
c. 481C>T	5	p. Q161X	MD	(500)
c. 483ΔA	5	p. A162QfsX8	MD	(490)
c. 488_497Δ	5	p. E163VfsX4	MD	(490)
c. 524T>C	5	p. L175S	MD	(477)
c. 524_531Δ	5	nk	MD	(482)
c. 529A>T	5	p. S177C	MD	(477)
c. 547_548ΔAG	5	p. R183GfsX191	MD	(501)
c. 551T>C	5	p. L184P	MD	(469, 502)
c. 564_576Δ	5	p. K188NfsX5	MD	(467)
c. 566ΔA	5	p. N189MfsX8	MD	(490)
c. 587T>G	5	p. L196R	MD	(503, 504)
c. 619_620ΔAG	5	p. R207GfsX9	MD	(476, 477)
c. 625insG	5	p. G209GfsX7	MD	(483)
c. 626dupG	5	p. R210QfsX7	MD	(466, 495)
c. 630_658Δ	5	p. V221GfsX20	MD	(474)
c. 639dupT	5	p. P214SfsX3	MD	(505)
Exon 5Δ	5	-	MD	(474, 499)
c. 662G>A	5	p. G221D	MD	(474, 506)
c. 662+1dup	5	NK	MD	
c. 663-1G>A	Intron 5	NK	MD	(487)
c. 663-6109_825+550Δ	Intron 5	p. V222LfsX13	MD	(499)
nk	6	p. G227V	MD	(507)
c. 697ΔT	6	p. S233LfsX14	MD	(471, 508)
c. 709C>T	6	p. R237X	MD	(480, 484, 504)
c. 734_737ΔAATT	6	p. Q245RfsX10	MD	(480, 487)
c. 742_745dup	6	p. S249MfsX2	MD	(479)
c. 745_746insTGTA	6	p. S249MfsX2	MD	(480)
c. 765_773Δ	6	p. I256_C258Δ	MD	(474)
c. 771_772ΔAT	6	p. T257TfsX1	MD	(469, 470, 474, 480, 492)
c. 788dupA	6	p. F262IfsX8	MD	(471)
c. 795ΔA	6	p. Q265HfsX24	MD	(470)
c. 808T>C	6	p. W270R	MD	(476, 477)
c. 810G>A	6	p. W270X	MD	(493)
c. 812G>A	6	p. C271Y	MD	(479)
c. 842ΔA	6	NK	MD	(482)
c. 856C>T	6	p. Q286X	MD	(476, 487, 490)
Exon 6Δ	6	-	MD	(499)
Exon 6-9Δ	6	-	MD	(477)
c. 825+1G>A	Intron 6	-	MD	(490)
c. 826-1G>A	Intron 6	-	MD	(493)
c. 907+1G>A	Intron 6	-	MD	(490)
c. 832_836Δ	7	p. T279AfsX17	MD	(485)
c. 835_839ΔACAAA	7	p. T279AfsX17	MD	(470, 474, 479, 480, 485, 503, 504)
c. 856C>T	7	p. Q286X	MD	(476, 477, 480, 487)
c. 884dupT	7	p. L295FfsX3	MD	(476, 477, 504, 509)
c. 885_886insT	7	p. P296SfsX2	MD	(476, 509)

Continued...

Genetics of Dystonia

Nucleotide change	Exon	Amino acid change	Disease manifestation	References
c. 940ΔT	7	p. Y313fsX318	MD	(510)
c. 946ΔG	7	p. D316lfsX318	MD	(477)
c. 966ΔT	7	p. V323CfsX11	MD	(466, 478)
c. 974ΔC	7	p. S325WfsX9	MD	(502)
c. 974_977ΔCGGC	7	p. S325X	MD	(477)
c. 1037+2T>C	Intron 7	-	MD	(476, 477)
c. 1037+5G>A	Intron 7	-	MD	(471, 474, 487)
c. 1114C>T	9	p. R372X	MD	(467, 471, 474, 479, 480, 484)
c. 1151ΔT	9	p. L384RfsX10	MD	(469)
c. 1053C>G	9	p. Y314X	MD	(474)
c. 1058_1062ΔCACCA	9	p. Q352fsX376	MD	(511)
c. 1253+811A>C	Intron 9	p. S418+14R	MD	(479)
c. 1294A>C	10	p. S432R	MD	(512)
Exon 1-12Δ	1-12	No transcript	MD	(464, 471, 474, 484)

MD: Myoclonus dystonia, NK: Not known

2.2.12 *DYT12-ATP1A3*

Clinical features

DYT12 is an autosomal dominant disorder named rapid-onset dystonia-parkinsonism (RDP) characterized by sudden onset of asymmetric dystonia accompanied with parkinsonism (513). The age of onset varied widely from early childhood to late adulthood. Affected individuals generally encounter slow progressive nonparoxysmal neurological problems in a rostrocaudal gradient (face>arm>leg) with prominent bulbar dysfunction, such as, dysarthria or dysphagia (514-516). The severity of the symptoms may aggravate by certain triggering components, such as, physical overexertion, trauma, heat, emotional agitation and consumption of alcohol (517).

The typical parkinsonian features may be present as bradykinesia and postural imbalance (518, 519). Psychiatric symptoms were also been associated as depression, social phobia, schizoid personality disorder and mental retardation (517, 520). Seizure has also been found in certain cases of RDP (521, 522).

Neuropathology

In RDP patients' brain, no certain neurophological abnormalities were found (517). Functional imaging reported no gross abnormalities (523, 524), while transcranial sonography identified bilateral hyperechogenicity of the substantia nigra with uncertain significance (525). In a very recent study, it was found for RDP patients that certain anatomical parts like globus pallidus, subthalamic nucleus, red nucleus, inferior olivary nucleus, cerebellar Purkinje and granule cell layers, and dentate nucleus were been affected (526). A loss of dorsal column fibers also been identified

in the spinal cord. So the neuronal cells in the complex motor and sensory regions been affected, as it has been found through this study.

Molecular genetics

Family based linkage analysis mapped the RDP locus at the chromosomal position 19q12-13.2 (98, 527). Mutations in *ATP1A3* gene were identified for Rapid-onset dystonia Parkinsonism patients (99) *ATP1A3* gene consists of 23 protein coding exons spanning 25 kb producing ~112 kDa neuron specific protein, ATPase Na⁺/K⁺ transporting subunit alpha 3 (528). DYT12 inherited in an autosomal dominant trait with incomplete penetrance. There were certain missense, insertion and deletion mutations reported to be found in RDP patients (Table 11) affecting the highly conserved N-terminal transmembrane domain of the protein. These mutations are generally loss of function in nature generating unstable and non-functional protein through haploinsufficiency (99).

Table 11: Mutations found in *ATP1A3* gene in RDP patients.

Nucleotide variants	Exon	Amino acid change	Disease manifestation	Reference
c. 821 T>C	MC 8	p. I274T	RDP	(99, 514, 529)
c. 829 G>A	MC 8	p. E277K	RDP	(99, 514, 515)
c. 946 G>A	MC8	p. G316S	RDP	(530)
c. 979_981 ΔCTG	MC 8	p. 327 ΔL	RDP	(531)
c. 1109 C>A	9	p. T370N	RDP	(532)
c. 1144 C>T	9	p. W382R	RDP	(532)
c. 1250 T>C	10	p. L417P	RDP	(532)
c. 1838 C>T	MC 14	p. T613M	RDP	(99, 514, 517, 519, 533-536)
c. 2051 C>T	15	p. S684F	RDP	(525)
c. 2267 G>A	MC 17	p. R756H	RDP	(522)
c. 2273 T>G	MC 17	p. I758S	RDP	(99)
c. 2338 T>C	MC 17	p. F780L	RDP	(99, 514)
c. 2401 G>T	MC 17	p. D801Y	RDP	(99, 514)
c. 2767 G>A	20	p. D923N	RDP	(516, 522, 537)
c. 3191_3193 dupTAC	23	p. 1013 dupY	RDP	(538)
c.*196_*198 dup	3' UTR		RDP	(538)

RDP: rapid-onset dystonia-parkinsonism, MC: Mutation cluster.

Molecular pathology

ATP1A3 expressed abundantly in the developing and mature central nervous system (CNS) and localises in the synapse (539, 540). The Na⁺/K⁺ ATPase maintain the Na⁺/K⁺ electrochemical gradient across the neuronal cell membrane and critical for generating the resting potential and osmotic homeostasis (541). The ATP1A3 (α 3 Na⁺/K⁺ ATPase) is believed to be a “reverse pump” of ATP1A1 (α 1 Na⁺/K⁺ ATPase), which can be activated by high intracellular sodium concentration after several action potential (542, 543). Mutations in ATP1A3 have a dominant negative effect, which causes inefficiency in ion transport capability of neurons and dysregulation in neurotransmitter exchange through synapse. These findings supportively suggest the rapid onset of dystonia-parkinsonism symptoms due to a triggering effect. It was found through animal experiment that an adverse interconnectivity through di-synaptic thalamic pathway between cerebellum and basal ganglia could cause the RDP (544). The cerebellar dysfunction could account for the dystonic symptoms and affect the basal ganglia to generate the parkinsonian features.

2.2.13 DYT16-PRKRA

Clinical features

DYT16 is an autosomal recessive young onset dystonia-parkinsonism disorder, which affects the axial, oromandibular and laryngeal region and might progressed to a generalized form. Disease onset was early childhood (2-12 years) to adolescence (18 years). Orofacial dystonia, dysphonia and speech problems are prominent

features. Bradykinesia and postural tremor could be present as parkinsonian features.

Molecular genetics

The DYT16 locus was mapped to the chromosomal position 2q31.3 and the specific gene was identified as *PRKRA* (102). It spans around 20Kb and consists of 8 exons to give rise to 313 amino acids long 34.4 kDa protein, Protein ACTivator of the interferon induced protein kinase (PACT). DYT16 inherits as autosomal recessive pattern. The first *PRKRA* mutation, a homozygous c. 665 C>T (p. P222L) in exon 7 was found in seven Brazilian patients (102). A heterozygous 2-bp deletion mutation (c. 266_267ΔAT; p. H89fsX20) was found in a 9 year old German patient affected with sporadic young onset dystonia parkinsonism (545). Later in another family based exome-sequencing study, the homozygous p. P222L mutation was found in two Polish siblings (546). Haplotype analysis indicated for a founder effect, which was in consistent with the findings from Brazil. In the same study, 3 other heterozygous rare variants (c. 100A>T; p. T34S, c. 305A>G; p. N102S and c. -14A>G) were found in 3 patients with adult onset focal or segmental dystonia with uncertain pathogenicity. Very recently, the p. P222L mutation was also found in Italian kindred having 3 brothers affected with young onset generalized dystonia (547).

Molecular pathology

PRKRA encoded PACT expresses in the brain regions specifically in Purkinje cells and external granular layer of cerebellum (548). PACT acts as an activator of RNA dependent protein kinase PKR, which is involved in antiviral defence mechanism,

signal transduction, cell proliferation and apoptosis (549, 550). During stress condition, *PRKRA* expresses and activates PKR followed by the activation of NF- κ B, which might activate the specific apoptotic pathway (551-553). Recently, the functional characterization of the p. P222L mutant PACT revealed that it activates PKR in excess in response to the ER stress. The mutant form also increased the PACT-PACT and PACT-PKR interaction leading to a robust activation of PKR followed by enhanced cellular death via apoptotic pathway (554).

2.2.14 *DYT23-CIZ1*

Clinical features

DYT23 dystonia is characterized by adult onset isolated cervical dystonia. The Dystonic symptoms precipitate in the neck region and might have the torticollis, anterocollis or retrocollis. Tremor in head and upper limbs can also be present in the patients (555).

Molecular genetics

The DYT23 dystonia inherits as autosomal dominant manner. The causative gene *CIZ1* was discovered for DYT23 dystonia by family based linkage analysis followed by whole exome sequencing (66). *CIZ1* gene localizes at the chromosomal position 9q34.11 and spans about 34.3 kb (556). It consists of 17 exons and produces 898 amino acid long 100kDa protein Cip1/CDKN1 interacting zinc finger proteins. Exome sequencing in a large Caucasian family, found an exonic splicing enhancer missense variant in exon 7 of *CIZ1* (c. 790A>G; p. S264G) and additional screening study in adult onset cervical dystonia patients also identified another two missense variants c.139C>T (p.P47S) and c.2015G>T (p.R672M). A recent genetic study from

Germany, found a novel missense variant c. 2357C>T (p. T786I) in a cervical dystonia patient (557). In an another study with 12 Chinese pedigrees affected with autosomal dominant cervical dystonia, there was no mutation found in *CIZ1* (558).

Molecular pathology

CIZ1 is a C2CH zinc-finger transcription factor, which interacts with CIP1 (p21/CDKN1A) of cyclin E, cyclin A, CDK2, PCNA and estrogen receptor- α (559) promoting DNA replication initiation and G1/S-phase transition (560, 561). *CIZ1* expresses ubiquitously and in brain, its highest expression was found in cerebellum, cerebral cortex, substantia nigra and putamen (562). *CIZ1* been identified to be associated with Alzhimers disease (563, 564) and rheumatoid arthritis (565) and overexpression of it could lead to the different types of cancers including lung (566), colon (567), gallbladder (568), breast (563), prostate carcinoma (569) and Ewing tumor (570). A recent functional study on transgenic *CiZ1* knock-out mouse model confirms certain motor abnormalities of gait and balance in the animal but the absence of Dystonic features (571). Whole genome gene expression in *CiZ1*^{-/-} mice revealed the down regulated genes are involved in cell cycle, cellular development, cell death and survival and cell morphology pathways. This study suggests the involvement of *CIZ1* in the post-mitotic differentiation of neurons and the dysregulated gene expression might compensate for the absence of Dystonic features in that particular mouse model.

2.2.15 *DYT24-ANO3*

Clinical features

The phenotypic spectrum of *DYT24* dystonia includes adult onset craniocervical dystonia with tremor predominantly in the upper limbs, head and laryngeal

musculatures. Presence of blepharospasm and writing tremor was reported in a British family (107). Another study also reported the cases of adult onset cervical dystonia along with oromandibular dystonia (67).

Molecular genetics

The specific gene for DYT24 locus, *ANO3*, was identified by family based linkage analysis followed by whole exome sequencing in a British kindred affected with autosomal dominant craniocervical dystonia (67). The *ANO3* gene was mapped on chromosome 11p14 as *TMEM16C*, a Ca^{2+} -activated Cl^- channels (CaCCs) (572). *ANO3* consists of 27 exons spanning 479.5 kb and encodes a 981 amino acids long 114.6 kDa protein, Anoctamin 3, a Ca^{2+} activated chloride channel. The first missense mutation found in two craniocervical dystonia patients was c. 1480A>T (p. R494W). In the same study, additional screening of *ANO3* in 188 cervical dystonia patients confirmed the presence of another five missense variants c. 161C>T (p. T54I), c. 1470G>C (p. W490C), c. 2053A>G (p. S685G), c. 2586G>T (p. L862N) and c. -190C>T (67). Another study identified two missense variants c. 2497A>G (p. I833V) and c. 2917G>C (p. G973R) in two probands affected with cervical dystonia (573). Another three variants, c. 704A>G (p. Y235C), c. 767A>G (p. N256S) and c. 2678C>T (p. P893L) were found in the control subjects in the same study. A genetic study from China reported the occurrence of a missense variant c. 2540C>T (p. Y847C) in two individual pedigrees (574). Another six silent variants were found c. -11G>T, c. 2478 (p. T826T), c. 2520T>G (p. R840R), c. 1158A>G (p. L386L), c. 1692A>C (p. A564A) and c. 2682C>T (p. P894P) in probands with the later three in controls. A recent case series study reported the previously identified three missense variants p. S685G, p. W490C and p. R494W (575). There was also a missense

variant c. 702C>G (p. C234W) found in a patient affected with hyperkinetic dysarthria and blepharospasm with complex motor tics (576).

Molecular pathology

Anoctamin 3 was reported to be expressed in cerebral cortex, cerebellum with highest expression in putamen and striatum (67). Recent studies suggest that Anoctamin 3 localizes at the ER membrane instead of cell surface (577). As Anoctamin 3 is a calcium activated chloride channel and ER is the main repository of intracellular Ca^{2+} , it can be postulated that ANO3 may control the ER driven calcium discharge. Recent functional assay of patient derived fibroblast sample indicated that mutant ANO3 could be responsible for faulty ER-driven calcium release (67). It was also shown that, Ca^{2+} -activated chloride channels may modulate the neuronal excitability through Na^{2+} activated potassium channel (578, 579). As ANO3 have the highest expression in striatum, dysfunction of mutant ANO3 could lead to abnormal excitability of striatal neuron followed by manifestation of dystonic symptoms.

2.2.16 DYT25-GNAL

Clinical features

DYT25 is an autosomal dominant adult onset focal dystonia primarily involved in neck region as cervical dystonia. The disease nature is progressive and could spread to other body parts as generalized dystonia. Laryngeal and facial muscles are the most affected regions in DYT25 dystonia (68).

Molecular genetics

DYT25 dystonia was found to be caused by mutation in *GNAL* gene, which was identified by family based linkage analysis followed by exome sequencing (68). The *GNAL* was mapped to chromosomal position 18p11 (580) and consists of 12 coding exons spanning ~196 kb. *GNAL* encodes for a 381 amino acid long 44.3 kDa protein Guanine nucleotide binding protein G α (olf). The promoter region of *GNAL* doesn't have any CCAAT or TATA boxes; instead it contains several transcription start sites. There were several *GNAL* gene variants found in adult onset focal/segmental dystonia patients and enlisted in Table 12. These variants include missense, nonsense, frameshift and deletion mutations, which could result in loss-of-function mutations.

Molecular pathology

GNAL encodes a protein, G α (olf), which was found in olfactory epithelium and is responsible for odorant signalling through olfactory receptor neurons (581). The brain specific expression of *GNAL* is restricted to caudate nucleus of basal ganglia, amygdala and cholinergic interneurons (580, 582, 583). In the brain, *GNAL* is the key mediator for coupling of adenylate cyclase to dopamine D1 receptors and adenosine A2a receptors (584). The role of G α (olf) in dopamine signalling is inevitable, though it might also be important for downstream signal transduction of A2A receptors following indirect pathway in striatopallidal neurons, which could potentially be involved in primary dystonia (585). Thus mutations of *GNAL* could potentially hamper the normal function towards the dopamine and adenosine neurotransmission. *GNAL* could also be involved in vesicular trafficking as longer splice variant of *GNAL* [XLG α (olf)] was found to localize in Golgi apparatus instead of plasma membrane and involved in endosome formation (586). Neurotransmitter signalling through

synaptic vesicles could be hindered by *GNAL* mutations, thus the striatal neurotransmission could be dysregulated (587, 588).

Table 12: Mutations found in *GNAL* gene in PTD patients.

Nucleotide variants	Exon	Amino acid change	Disease manifestation	Reference
c. 3G>A	1	p. M1?	PTD	(589)
c. 40C>T	1	p. Q14X	PTD	(590)
c. 61C>T	1	p. R21X	PTD	(68)
c. 66C>T	1	p. R22R	PTD	(590)
c. 139C>A	2	p. L47I	PTD	(590)
c. 166-167insA	3	p. S56KfsX16	PTD	(591)
c. 214C>G	3	p. P72A	PTD	(590)
c. 274-5T>C	Intron3		PTD	(68)
c. 304-312ΔCCTCCAGTT	4	p. P102-V104Δ	PTD	(68)
c. 283-284insT	4	p. S95fsX110	PTD	(68)
c. 284C>T	4	p. S95X	PTD	(592)
c. 289A>G	5	p. M97V	PTD	(591)
c. 399C>A	5	p. F133L	PTD	(593)
c. 409G>A	5	p. V137M	PTD	(68)
c. 436G>A	6	p. V146M	PTD	(573)
c. 463G>A	6	p. E155K	PTD	(68)
c. 514G>A	7	p. V172I	PTD	(594)
c. 591-592insA	8	p. R198fsX210	PTD	(68)
c. 591dupA	8	p. R198TfsX13	PTD	(589)
c. 628G>A	9	p. D210N	PTD	(595)
c. 637G>A	8	p. G213S	PTD	(596)
c. 682G>T	10	p. V228F	PTD	(589)
c. G>A	10	p. V234I	PTD	(597)
c. 733C>T	10	p. R245X	PTD	(589)
c. 878C>A	10	p. S293X	PTD	(68)
c. 932-7T>G	Intron 10	-	PTD	(592)
c. 1018G>A	11	p. G340S	PTD	(590)
c. 1057G>A	12	p. A353T	PTD	(596)
c. 1060G>A	12	p. V354M	PTD	(590)
c. 1061T>C	12	p. V354A	PTD	(598)
c. 1216C>T	12	p. R329W	PTD	(599)

PTD: Primary torsion dystonia.

2.2.17 *DYT26-KCTD17*

Clinical features

DYT26 dystonia is an autosomal dominant neurological disorder characterized by myoclonic jerks affecting the upper limbs. These symptoms are progressive in nature

and can spread predominantly towards the craniocervical regions, trunk or lower limbs. The disease onsets generally in first or second decades of life.

Molecular genetics

DYT26 locus was mapped at chromosomal position 22q12.3 and the specific gene was identified as *KCTD17* (69). *KCTD17* gene consists of 9 coding exons spanning 11.6 kb genomic region and encodes a 321 amino acids long 35.6 kDa protein, Potassium channel tetramerization domain containing 17 (KCTD17). Till date, only one missense mutation in exon 4 of *KCTD17* (c. 434G>A; p. R145H) was found in two British pedigrees affected with myoclonus dystonia (69). The mutation in *KCTD17* gene was identified by combined linkage analysis and whole exome sequencing study. The members of both the pedigrees were represented with myoclonus dystonic symptoms often with generalized dystonia. None of the patients did harbour the mutation(s) in *SGCE* gene, the common cause of myoclonus dystonia.

Molecular pathology

KCTD17 acts as a substrate adaptor, which interacts with trichoplein (TCHP) and CUL3-RING E3 ubiquitin ligases and promote the polyubiquitination and degradation of TCHP followed by Aurora kinase A (AURKA), which in turn helps ciliogenesis (600). *KCTD17* is abundantly expressed in the brain regions with the highest expression in putamen and thalamus region. Coexpression network analysis found *KCTD17* is a part of putamen gene network involved in post-synaptic dopaminergic transmission pathway, significantly enriched for dystonia related genes. Functional study in mutation bearing patients fibroblast sample revealed reduced ER dependent calcium signalling and reduced calcium storage in ER (69).

2.2.18 *DYT27-COL6A3*

Clinical features

DYT27 dystonia was reported as an autosomal recessive segmental or isolated dystonia primarily affecting craniocervical region and upper limbs. The age of onset could be in first two decades of life. Other symptoms were reported for DYT27 dystonia includes postural tremor, writer's cramp, oromandibular dystonia and laryngeal dystonia (70).

Molecular genetics

The disease locus was mapped to chromosomal position 2q37.3 (601) and the specific gene was found as *COL6A3* (70). The *COL6A3* gene consists of 43 coding exons spanning about 90.3 kb genomic region and gives rise to a 3177 amino acids long 343.6 kDa protein product, Collagen Alpha-3 (VI) chain. Mutation in this gene could cause Bethlem myopathy, Ullrich congenital muscular dystrophy 1 and DYT27. Using whole exome sequencing in a recessive dystonia affected German kindred, a compound heterozygous mutation [c. 9128G>A (p. R3043H) + c. 9245C>G (p. P3082R)] was found (70). Additional screening of 367 German patients identified two more compound heterozygous mutations [c. 8966-1G>C (p. V2989-K3077delinsQ) + c. 7502G>A (p. R2501H)] and [c. 8966-1G>C (p. V2989-K3077delinsQ) + c. 7660G>A (p. A2554T)]. Interestingly, all the patients having mutation in *COL6A3* gene did harbour a mutation in exon 41, which may cause disruption of this exon leading to pathogenicity to develop dystonic symptoms. Another study reported five missense rare variants (c. 9017A>G; p. K3006R, c. 9148G>A; p. A3050T, c. 9128G>A; p. R3043H, c. 9191C>T; p. S3064F, c. 9245C>G; p. P3082R), one silent

variant (c. 9012C>T; p. S3004S) and one compound heterozygous mutation [c. 9245C>G (p. P3082R) + c. 2195C>T (p. T732M)] in *COL6A3* gene among isolated dystonia patients and Parkinson's disease patients having dystonic features (602). The p. R3043H and the compound heterozygous mutation were found in two different German Parkinson's disease patients.

Molecular pathology

COL6A3 expresses ubiquitously while the expression analysis of mouse *Col6a3* revealed widespread expression throughout striatum and cerebellum with highest expression in brainstem and midbrain. In functional study based on zebrafish model, suppression of exon 41 ortholog resulted inefficient axonal outgrowth and neurodevelopmental problems (70). These findings implicate the dysfunction of extracellular matrix in brain could be a potential underlying pathogenesis of dystonia.

2.3 Common molecular pathway for dystonia pathogenesis

With the increasing numbers of newly identified dystonia related genes, it has been found that multiple *DYT* genes are responsible for a certain spectrum of dystonic manifestation. For example, cervical dystonia is a prominent clinical feature of the patients having mutation in any one of the genes including *TOR1A*, *THAP1*, *CIZ1*, *GNAL*, *ANO3*, *COL6A3* or in the unidentified genes in the locus *DYT7* or *DYT21* (Table 1). Dopa responsive dystonia with variable severity could be developed by mutation in *GCH1*, *TH* or *SPR* genes. Myoclonus dystonia could be occurred due to mutations in *SGCE*, *KCTD17* and *CACNA1B* genes or in the *DYT15* gene (603). Therefore, it is obvious that there should have certain common mechanism for the distinct dystonia pathogenesis.

2.3.1 Cellular proliferation and apoptosis

It has been found that several dystonia related genes, like *CIZ1*, *THAP1*, *GNAL* and *TAF1* are functionally responsible for cell cycle regulation and cellular proliferation. *CIZ1* and *GNAL* interacts with CIP1 (p21/CDKN1A) of cyclin E , cyclin A, CDK2, PCNA and estrogen receptor- α (559), while the *GNAL* binds to CSN5 associated with p27Kip1, which prevent the activation of cyclinE-CDK2 complex. *GNAL* targets the p27Kip1 for proteosomal degradation, thus promoting the G1/S cell cycle progression (604). Mutations in *CIZ1* and *GNAL* genes could inhibit the normal cellular function towards cell cycle regulation. Whole genome gene expression analysis also revealed that *Ciz1* knock out mice is deficient in expression of specific genes involved in cell cycle regulation, cellular proliferation and apoptotic pathway (571). *THAP1* also found to be a transcriptional regulator of cell cycle related genes specifically involved in pRb-E2F pathway (336). RNAi mediated *THAP1* knockdown demonstrated downregulation of eight pivotal pRb-E2F pathway genes: *RRM1*, *MAD2*, *BIRC5*, *HMMR*, *RRM2*, *CDC2*, *CCNB1* and *DLG7*. *THAP1* also interact with prostate apoptosis response-4 protein (*PAWR*), a pro-apoptotic transcription factor present in a low amount in synapses and dendrites (362) and dysregulated *THAP1* activity may be involved in apoptosis and impaired cell proliferation in developing neurons (321). Defect in neuronal *TAF1* (N-*TAF1*) has been implicated for *DYT3* pathogenesis (87) and it expresses significantly in medium spiny neurons and striatum (605). Mutations in *TAF1* could make it defective in function and affect the cell cycle control mechanism. *TAF1* phosphorylates p53 and induces G1/S phase transition and *TAF1* defective cell line exhibited ATR mediated phosphorylation of p53 and *CHK1*, which induced the cell cycle arrest (185).

2.3.2 Transcriptional regulation and gene expression

Certain dystonia related genes also involved in transcriptional regulation and could modulate the gene expression profile. THAP1, CIZ1 and TAF1 are transcription factors and directly involved in transcriptional machinery, mutation of which can alter the gene expression parameters. PRKRA and TOR1A could also influence the RNA expression and processing. PRKRA binds to the double stranded RNA molecules and activates several pathways like antiviral defence mechanism through NF- κ B pathway, ER mediated stress response and apoptotic pathway (549, 551, 553). PRKRA also regulates the gene expression as it can bind to the DICER and helps to produce small interfering RNAs (siRNA) and processing of miRNA from pre-miRNA (553). The transcriptional regulation by mutant torsinA could be mediated by inhibiting the normal structure and function of nuclear envelop through formation of perinuclear inclusion bodies (141). The distribution and structural integrity of nuclear pores on NE are crucial for RNA transport and subsequent gene expression (606, 607). Mutant torsinA binds to the NE structural components through lamina associated proteins LAP1 and LULL1 (140). It also binds to the KASH domain of nesprin-3 and build an interaction between nucleus and cytoplasm (77). This interaction is important for maintaining cell polarity and transcriptional process (608, 609). TorsinA was also found to be associated with transcriptional regulation through TGF β pathway (610). So, torsinA could regulate the transcriptional pathways in an indirect manner to influence the gene expression (194, 611). TAF1 acts as the most important functionally diverse subunit of transcription factor IID (TFIID), which is the pivotal regulator of genome wide expression of eukaryotic genes (612). TAF1 activates TFIID mediated transcription by phosphorylation of histone H2B-serine 33, which is essential for expression of genes involved in cell cycle progression and

development (613). Therefore, the loss of function mutations of these genes could dysregulate the transcriptional pathways to alter the gene expression parameters and could share a common mechanism for dystonia pathogenesis.

2.3.3 Response to cellular stress

There are several DYT gene products, which actively contribute to the cellular stress response pathway. Evidently, the gene products of *TOR1A*, *PRKRA*, *MR-1*, *THAP1*, *GCH1* and *SLC2A1* are involved directly in the cellular stress response mechanism. TorsinA, a molecular chaperone, resides in the ER lumen and helps in protein trafficking including the proteins like dopamine transporter. The ΔE mutant torsinA inhibits this trafficking and the protein processing through secretory pathway as is evident from the DYT1 dystonia patients fibroblast sample (149). This defective mechanism could be recovered by siRNA based allele specific knockdown of the mutant protein (614). It has also been shown that overexpression of torsinA could protect cells from ER stress, whereas downregulation of it could withdraw the protection (136, 614), suggesting the endurance of torsinA towards the ER stress in neuronal cells. TorsinA was found to be involved in endoplasmic reticulum associated degradation (ERAD) pathway, where misfolded proteins are degraded by proteasome (134, 615). PRKRA also involved in the regulation of ER mediated stress as reactive oxygen species (ROS) phosphorylates PRKRA, which activates PKR (551). This also activates the downstream NF- κ B signalling and translation inhibition, which can induce the apoptotic pathway (552, 553). SLC2A1 could contribute towards the oxidative stress response pathway as it helps in the transportation of dehydroascorbic acid across the blood-brain barrier and mitochondria (395, 616), where it reduced to ascorbic acid. This ascorbic acid helps

in scavenging the ROS and the functional dysregulation of SLC2A1 could hamper this process, which could lead to the oxidative stress. Another dystonia related gene product, GCH1, is responsible for production of an important neurotransmitter, dopamine. It has been found that increased bioavailability of dopamine could lead to the oxidative stress by auto-oxidation of dopamine followed by dopamine neurotoxicity (617). Excess dopamine and its metabolite Dopa quinones could form 5-cystinyl catechols on proteins and irreversibly alter the normal protein functions, which in turn may generate the oxidative stress (617, 618). Moreover, the increased expression of *GCH1* could be elevated by TNF- α and interferons (619, 620) and the transcription of *GCH1* could be activated by NF- κ B (621). It has been found that MR-1 could activate the NF- κ B signalling pathway, which in turn could downregulated the expression of TNF- α (622). MR-1 is a homolog of HAGH and in neurons MR-1 was implicated as a response mediator against the oxidative stress (367, 383). Another DYT gene product, THAP1 had also been reported as an enhancer of TNF- α induced apoptosis in PML nuclear bodies (362). So certain DYT gene products are involved in cytokine mediated cellular stress response pathway, whereas the cytokines are involved in synaptic plasticity regulation (436, 623). Alteration in cytokine production and functional deprivation can encourage the abnormality in synaptic plasticity, which has been implicated for dystonia pathogenesis (55, 624).

2.3.4 Synaptic functions and neurotransmission

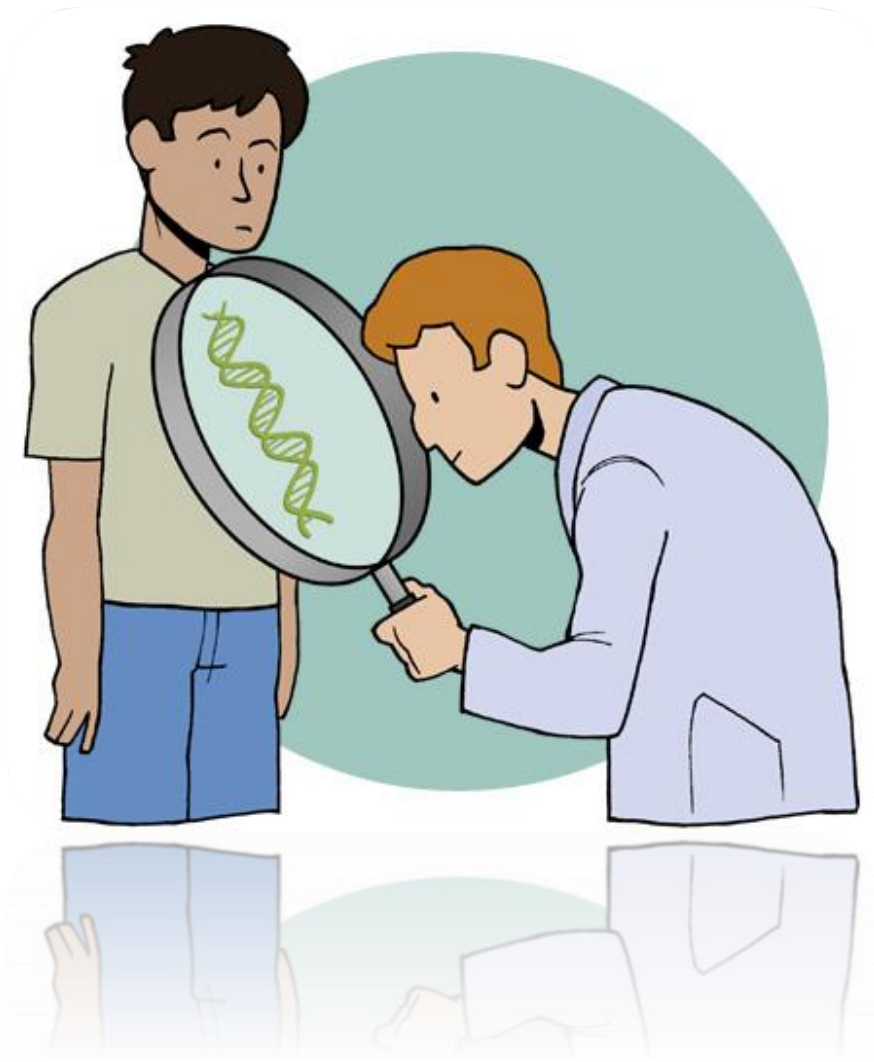
One of the most interesting pathways for idiopathic dystonia pathogenesis is defects in synaptic functions and neurotransmission. The most important one is dopamine signalling and some of the DYT proteins are found to be involved in it. The mutations in *GCH1* and *TH* genes have the defined roles in dopamine biosynthesis and

subsequent neurotransmission (89, 625). Functional deficit of GCH1 and TH could lead to reduction in dopamine level followed by dopa responsive dystonia. Thus, DRD can be well treated with the supplementation of L-dopa, which can maintain the presynaptic dopamine bio-availability (204). Moreover, reduction in D2 receptor (D2R) binding was reported for idiopathic dystonia patients (626, 627). TorsinA could have some effect on the dopamine neurotransmission as reduction in D2R binding was observed in manifesting and non-manifesting *TOR1A* ΔE mutation carriers (628, 629). Recent studies over transgenic hMT-CMV mice and DYT1 knock-in mice reported the decrease in numbers and elevation in size of dopaminergic neurons with reduced DA reuptake in substantia nigra (630, 631). It has also been observed that a potentially functional interaction of torsinA with dopamine transporter (DAT) and monoamine vesicular transporter (VMAT) (141, 150). TorsinA was found in vesicles of axons and presynaptic terminal as the enrichment occurs in the synaptosomal membranes (629). *In-vitro* functional studies in neuronal cell based model also reported that torsinA ΔE mutant could compromise the synaptic vesicle recycling (151, 152). Abnormal D2R binding was also found in manifesting and non-manifesting carriers of DYT6 dystonia patients carrying THAP1 mutations (632). THAP1 was found to regulate the expression of Par-4 (362), which can compete with calmodulin to bind D2Rs and modulate its activity (633). Impaired Par-4 activity leads to enhanced calmodulin binding and inefficient D2R function which can be influenced indirectly by mutations in THAP1.

Apart from primary isolated dystonia, altered D2R binding was also observed in dystonia plus syndromes like DYT11, DYT8 and DYT3 dystonia. Reduced level of D2R availability was reported in myoclonus dystonia patients with higher level of

endogenous dopamine (634). The studies done on transgenic SGCE knockout mouse model reported similar observations, where the striatal D2R was significantly decreased with a subsequent higher discharge of dopamine and its metabolites (635, 636). In contrast, an increase in striatal density of postsynaptic D2R was reported with reduced presynaptic DOPA decarboxylase activity and decreased level of dopamine (637, 638). Loss of dopamine signalling was also been reported in the patients affected with DYT3 dystonia. Significant downregulation of TAF1 and D2R were observed in the caudate, cerebral cortex and nuclear accumbens (87). Recently, it was found that TAF1 overexpression could lead to differential expression of genes involved in vesicular transport and dopamine metabolism (188), which suggested a direct involvement of TAF1 towards dystonia pathogenesis through alterations in neurotransmission.

Depletion in dopaminergic signalling was also found in DYT12 dystonia, where reduced homovalinic acid level was reported for symptomatic and asymptomatic carriers of ATP1A3 mutations (529, 639, 640). Mutations in ATP1A3 could lead to decreased Na⁺ affinity and efficacy of Na⁺ efflux which may cause abnormal synaptic functions (641). In a recent study using zebrafish model and selective inhibition of ATP1A3 resulted in dopaminergic neuronal cell death suggesting the pivotal role of ATP1A3 in neurotransmission and survival of neurons (642). On the other hand the DYT25 gene product G α (olf) has a more direct effect over neurotransmission where G α (olf) mediate the coupling of the adenylate cyclase to the dopamine type 1 receptors (D1R) and adenosine A2A receptors of medium spiny neurons (584). The loss-of-function mutations in *GNAL* gene could lead to impaired D1R activity and subsequent abnormal dopamine neurotransmission (582, 643).



CHAPTER 3

SCREENING OF *TOR1A* AND *THAP1* GENE VARIANTS IN PRIMARY PURE DYSTONIA PATIENTS

3.1 Introduction

TOR1A was identified as the very first primary dystonia related gene at least two decades ago (84), mutation of which could cause DYT1 dystonia. DYT1 dystonia is early onset primary pure dystonia typically manifested in early childhood and adolescence with autosomal dominant inheritance pattern. The tri-nucleotide deletion mutation c. 904-906/907-909 Δ GAG in *TOR1A* gene accounts almost exclusively for DYT1 dystonia pathogenesis. The majority of manifesting carrier of this variant develops generalized dystonia in a progressive nature. Though initially this variant was found in Ashkenazi Jews population, population based genetic screening revealed that this variant is most common cause of DYT1 dystonia in various world population (Table 13). In search of this variant among Indian primary dystonia patients, our laboratory performed a preliminary screening study and reported the absence of this variant in that particular study cohort (644). This study has been continued in an extended cohort of primary dystonia patients in India. Apart from this pathogenic variant, there are certain other variants were also found in *TOR1A* gene (Table 4), which was assessed to be pathogenic and causal (118, 123, 645). Moreover, a common variant c.646 G > C (rs1801968) in *TOR1A* gene was found to be a disease modifier in terms of penetrance as well as pathogenicity of Δ GAG mutation (113, 118). So, the genetic screening for *TOR1A* gene in Indian primary dystonia patients was indisputable. Until 2009, *TOR1A* was the only identified causal gene for primary dystonia. However, *THAP1* gene was identified as a causal gene for DYT6 dystonia primarily

Table 13: *TOR1A* ΔGAG mutation found on different ethnic population.

Population	<i>TOR1A</i> ΔGAG carrier / Total individuals screened	Reference
Europeans		
Caucasian	14/57 (24.5%)	Fasano et. al. 2006 (646)
Germans	6/256 (2.3%)	Grundmann et. al. 2003 (81)
	4/57 (7%)	Kamm et. al. 1999 (647)
	1/184 (0.5%)	Schmidt et. al. 2012 (648)
French	14/35 (40%)	Tuffery-Giraud et. al. 2001
	5/100 (5%)	Brassat et. al. 2000 (650)
Danish	14/51 (27.4%)	Lebre et. al. 1999 (651)
	3/107 (2.8%)	Hjermind et. al. 2002 (652)
Italian	5/30 (16.6%)	Zorzi et. al. 2002 (653)
Serbian	3/50 (6%)	Major et. al. 2001 (654)
British	22/150 (14.6%)	Valente et. al. 1998 (655)
Polish	17/63 (26.9%)	Gajos et. al. 2006 (656)
Irish	5/14 (35.7%)	O'Riordan et. al. 2002 (657)
Dutch	1/43 (2.3%)	Ritz et. al. 2009 (658)
Asian		
Indian	3/321 (0.9%)	Giri et. al. 2014 (659)
Iranian	10/63 (15.8%)	Akbari et. al. 2012 (660)
Japanese	6/178 (3.3%)	Matsumoto et. al. 2001 (661)
Korean	5/162 (3%)	Im et. al. 2004 (662)
Taiwanese	3/200 (1.5%)	Lin et. al. 2006 (663)
Chinese	7/17 (41.1%)	Yang et. al. 2009 (664)
	1/71 (1.4%)	Zhang et. al. 2010 (665)
Russian	24/39 (61.5%)	Slominsky et. al. 1999 (666)
South America		
Brazilian	2/88 (2.2%)	Camargo et. al. 2014 (667)

in Amish-Mennonite population (91). *DYT6* dystonia typically manifests as early-onset generalized or focal dystonia with cranio-cervical involvement, often progressive to adjacent muscles involving upper limb leading to segmental dystonia (668, 669). Mutation in *THAP1* gene is emerging as an important genetic factor for primary isolated dystonia, as about 88 distinct genetic variants have been reported in *THAP1* in *DYT1* negative families till date in different major population throughout

the world (Table 7). These variants are essentially non-recurrent missense showing greater diversity and widely distributed throughout the gene (318, 343). Moreover, frameshift, non-coding and homozygous mutations in *THAP1* have also been associated with dystonia (342, 343, 349). One third of these variants were found in adult-onset primary dystonia indicating the occurrence of DYT6 dystonia irrespective of age of onset (333, 343, 350, 353, 357, 670, 671).

Though the mutations in both the *TOR1A* and *THAP1* genes were identified for primary dystonia patients in the major world population, the genetic information for Indian primary dystonia patients is unavailable due to lack of thorough study. Thus this study is focused to explore the genetic variants of *TOR1A* and *THAP1* genes among the primary pure dystonia patients in India. Dystonia patients and control samples were screened for 5'-untranslated region (UTR), exon 4, exon 5 including 3'-UTR of *TOR1A* gene and also the entire *THAP1* gene including 5' & 3'-UTR.

3.2 Materials & Methods

3.2.1 Patients & Controls

This study was approved by 'Bioethics Committee for Animal and Human Research Studies, University of Calcutta' following the guidelines of Indian Council for Medical Research (ICMR). The patient samples were collected from the Movement Disorder Clinics of Bangur Institute of Neurosciences, Kolkata, India and Hinduja Hospital, Mumbai, India, where patients were examined for diagnosis. The control samples without any neurological problem were collected from different blood donation camp programs held in Kolkata. Both the patient and control samples were collected with their written informed consent.

A total of 303 index primary dystonia patients (Mean age: 40.91 ± 16.14) having mean age at onset: 35.65 ± 16.86 and 332 healthy control individuals were recruited for molecular genetics study for *TOR1A* gene. Among the 303 patients, 106 representing writer's cramp, 53 with cervical dystonia, 29 affected with generalized dystonia, 36 with blepharospasm and 48 patients with isolated limb dystonia. For *THAP1* gene screening, 227 index primary pure dystonia patients (mean age: 34.8 ± 16.6 and mean age at onset: 29.6 ± 17.4) and 254 controls (mean age: 41.2 ± 12.6) were recruited in this study. The patients recruited for *THAP1* screening includes 36 (15.85%) generalized, 163 (71.8%) focal, 17 (7.48%) segmental and 12 (5.28%) multifocal dystonia patients. Detailed demographics of patients are summarized in Table 14 and Table 15 for *TOR1A* and *THAP1* gene screening respectively. All patients underwent a standard neurological examination by movement disorder specialists following the criteria described by Fahn and Eldridge, 1976 (672). The patients were found to be negative for any secondary causes as per evidence from patients past history of diseased condition, neuroimaging (CT, MRI, etc) studies for

any brain lesions and other biochemical measurements (e.g. serum ceruloplasmin, uric acid, etc); none had K-F ring as verified by routine slit-lamp eye examination.

3.2.2 Genetic screening study

3.2.2.1 Genomic DNA isolation

10 ml of peripheral blood samples were collected in EDTA vials from both the patients and controls. Genomic DNA was isolated by conventional salting out method using sodium perchlorate followed by isopropanol precipitation (673). The experimental protocol is described below as used in the laboratory.

Composition of DNA extraction solutions & buffers:

a. Solution A (1 L):

- (a) Sucrose – 109.5 gm (final concentration, 0.32 M)
- (b) 1 (M) MgCl₂ – 5 ml (final concentration, 5 mM)

Distilled water (Elix grade) was added to make the volume up to 900 ml, autoclaved at 15 lb/sq. inch pressure and 121 °C temperature for 15 minutes and then 10 ml of Triton™ X-100 (Sigma-Aldrich) was added (final concentration 1%) after the solution cooled to room temperature. The volume was adjusted to 1000 ml with distilled water.

b. Solution B (100 ml):

- (a) 1 (M) Tris-Cl (pH 8.0) – 40 ml (final concentration 0.4 M)
- (b) 0.5 (M) EDTA (pH 8.0) – 12 ml (final concentration 0.05 M)
- (c) 1 (M) NaCl – 15 ml (final concentration 0.15 M)

Screening of *TOR1A* & *THAP1* genes in Indian primary dystonia patients

Table 14: Clinical diagnosis and demographics of Indian primary dystonia patients recruited for *TOR1A* genetic study.

Clinical Diagnosis (Dystonia Types)	Patients (n)	Sex		Disease Onset		Age Mean ± SD	Age at Onset Mean ± SD	Disease Duration Mean ± SD	Family History		
		M	F	Early	Adult				Positive	Negative	Unknown
Generalized	30	20	10	21	9	29.1 ± 16.7	21.6 ± 17.1	8.2 ± 9.5	5	25	0
Segmental	15	12	3	8	7	37.4 ± 17	30.0 ± 19.4	7.5 ± 13.8	2	11	2
Multifocal	3	3	0	0	3	54.0 ± 14.1	49.0 ± 17.4	5.0 ± 6.08	0	3	0
Focal	163										
Cervical	46	32	14	20	26	35.0 ± 15.0	31.3 ± 16.01	4.5 ± 3.8	2	40	4
Writer's Cramp	110	101	9	33	77	42.1 ± 15.7	37.3 ± 15.7	5.8 ± 7.0	28	81	1
Blepharospasm	34	21	13	2	32	51.3 ± 11.8	46.9 ± 12.1	3.7 ± 4.5	5	29	0
Limb	46	41	5	14	32	43.1 ± 16.9	30.5 ± 17.5	6.8 ± 8.2	8	35	3
Oromandibular	6	6	0	1	5	43.5 ± 11.7	42.1 ± 10.7	1.8 ± 1.1	0	6	0
Orofacial	8	6	2	1	7	44.7 ± 10.5	39.1 ± 14.9	5.8 ± 7.6	0	7	1
Others	5	5	0	3	2	36.6 ± 13.4	32.4 ± 14.4	4.2 ± 4.5	0	3	2

Screening of *TOR1A* & *THAP1* genes in Indian primary dystonia patients

Table 15: Clinical diagnosis and demographics of Indian primary dystonia patients recruited for *THAP1* genetic study.

Clinical Diagnosis (Dystonia Types)	Patients (n)	Sex		Disease Onset		Age Mean ± SD	Age at Onset Mean ± SD	Disease Duration Mean ± SD	Family History		
		M	F	Early	Adult				Positive	Negative	Unknown
Generalized	36	23	13	28	8	27.2 ± 9.5	19.2 ± 15.6	8.3 ± 9.5	8	27	1
Segmental	17	13	4	6	11	40.8 ± 16.2	32.0 ± 19.5	8.0 ± 12.6	2	14	1
Multifocal	11	9	2	3	8	47.8 ± 16.7	38.9 ± 16.7	8.9 ± 7.2	1	10	0
Focal	163										
<i>Cervical</i>	46	31	15	23	23	35.0 ± 15.0	31.3 ± 16.01	4.5 ± 3.8	4	39	3
<i>Writer's Cramp</i>	52	47	5	34	18	32.1 ± 15.0	27.0 ± 14.4	6.3 ± 8.0	13	37	2
<i>Blepharospasm</i>	10	7	3	2	8	48.5 ± 16.2	45.0 ± 17.9	3.5 ± 3.6	3	7	0
<i>Limb</i>	22	17	5	14	8	36.6 ± 17.6	30.0 ± 17.3	6.5 ± 8.0	3	18	1
<i>Oromandibular</i>	8	7	1	1	7	44.0 ± 9.9	42.5 ± 9.1	1.5 ± 1.1	0	8	0
<i>Orofacial</i>	5	5	0	1	4	46.6 ± 14.8	43.2 ± 18.1	3.4 ± 4.3	0	5	0
<i>Others</i>	20	15	5	14	6	24.6 ± 16.5	25.4 ± 16.9	4.6 ± 3.9	6	8	6

Distilled water (Elix grade) was added to make the volume to 90 ml, autoclaved at 15 lb/sq. inch pressure, 121 °C temperatures for 15 minutes. The solution was cooled to room temperature and then 5 ml of 20% SDS (final concentration 1%) was added. The volume was adjusted to 100 ml and mixed gently.

c. Solution C:

Sodium perchlorate – 70.23 g (final concentration 5 M)

Water was added to adjust the volume to 100 ml.

Detailed protocol for extraction of Genomic DNA from peripheral blood

- 1) To about 10 ml of fresh blood 40 ml of 0.9% NaCl was added and centrifuged at 2000 rpm for 10 minutes.
- 2) The supernatant was discarded carefully without disturbing the precipitate so that it did not dislodge.
- 3) To the precipitate, solution A was added (four times of the volume of the precipitate) and mixed well by turning up and down for 5 minutes.
- 4) Centrifuged at 2800 rpm for 5 minutes.
- 5) The supernatant was discarded carefully.
- 6) To the white precipitate, 1.5 ml of solution B was added and mixed well by swirling the tube until the precipitate turned smooth and silky.
- 7) 500 µl of solution C was added and mixed gently by turning up and down.
- 8) 2 ml of chilled chloroform was added and mixed gently by turning up and down.
- 9) Centrifuged at 2800 rpm for 5 minutes.

- 10) The aqueous layer (800 μ l) was taken into a 1.5 ml eppendorf tube and equal volume of chloroform was added and mixed again. Then it was centrifuged at 2800 rpm for 5 minutes.
- 11) The aqueous layer was taken (700 μ l) into a 1.5 ml eppendorf tube and equal volume of chilled isopropanol was added for the precipitation of DNA.
- 12) The precipitate was washed in 70% ethanol (1 ml) for 15 minutes.
- 13) The tubes were centrifuged at 13000 rpm for 10 minutes and the supernatant was discarded.
- 14) Steps 12 and 13 were repeated once more.
- 15) The DNA was allowed to air-dry at room temperature until the precipitate becomes translucent (care was taken not to make it completely dehydrated).
- 16) The DNA was dissolved in 500 μ l of TE buffer (10 mM Tris - HCl, 1 mM EDTA, pH 8.0) and stored at 4 $^{\circ}$ C.

Estimation for quantity and quality of DNA samples

Each genomic DNA samples were checked for quantity (A_{260nm}) and purity ($A_{260/280} = 1.8 - 2.0$) by using a UV-visible spectrophotometer following the standard protocol (674).

3.2.2.2 Primer design & polymerase chain reaction (PCR)

The web based program Primer3 (<http://bioinfo.ut.ee/primer3-0.4.0/>) was used to design the oligonucleotide primers for the genetic assays (675). The primers and the PCR conditions used for *TOR1A* & *THAP1* are listed in Table 16 and Table 17 respectively. PCR was carried out in a total volume of 25.0 μ l in 1X PCR buffer [10 mM Tris-HCl (pH 8.3), 50 mM KCl] containing 20 - 50 ng genomic DNA, 20 pM of

Screening of *TOR1A* & *THAP1* genes in Indian primary dystonia patients

Table 16: Primer sequences and amplification conditions for *TOR1A* gene regions.

	Primer sequence (5' to 3')	Anneling temp. (°C)	25mM Mg ²⁺ (μl)	Amplicon size (bp)	Cycle no. (cycle parameters)	Special requirement	Segment of the gene
Forward Reverse	GAGGGGACACAGTCTTGCTC CCACCCTGCTTGTTCTCGC	58	1.5		30 (30-30-30)	7 min hot-start, 10% DMSO (2.5 μl)	5' UTR
Forward Reverse	GCGGTCGGCGCGAGAACA CATGCCCTGGTCCTAGTTCAG	58	1	301	30 (30-30-30)	5 % DMSO	Exon 1
Forward Reverse	GCCAGGAGCTTACAGACCG CAACATAGAACTCCCAAATCTC	56	1.5	503	30 (30-30-30)		Exon 2
Forward Reverse	AGTGAAGCTGCGGTTCTTAGT AATCCCAGTGGGTAAGGACAG	58	1.5	352	30 (30-30-30)		Exon 3
Forward Reverse	CAGGGCTAGGACATGATGGA GTTACCTGGAGTTCATCAGC	56	1.5	390	30 (30-30-30)		Exon 4
Forward Reverse	CCCTGGAATACAAACACCTA CACATCAAACAGGAACATTCA	54	1.5	315	30 (30-30-30)		Exon 5
Forward Reverse	TCCTTCCCTGGAAGAGGAATC CCAGTAAAGATACATCACAGTC	56	1.5	386	30 (30-30-30)		3' UTR fragment 1 (for rs1182)
Forward Reverse	GGCCACACTGTCAACATTTG GCACATGCAAAATTTTATTGTA	56	2	321	30 (30-30-30)		3' UTR fragment 2 (for rs3842225)

Screening of *TOR1A* & *THAP1* genes in Indian primary dystonia patients

Table 17: Primer sequences and amplification conditions for *THAP1* gene regions.

	Primer sequence (5' to 3')	Anneling temp. (°C)	25mM Mg ²⁺ (µl)	Amplicon size (bp)	Cycle no. (cycle parameters)	Special requirement	Segment of the gene
Forward Reverse	CCACTTCGGCAACTCTGAAG GTGAGCGAAGCCTGCAACC	60	2 (5X Q sol.)	682	35 (30-30-30)	10% Glycerol (2.5 µl), 12 min hot-start, 68°C-61°C touchdown	Exon 1 & flanking sequence
Forward Reverse	CTGGAAAGTTTGGGTGCCTTTA AACTACAAGGTTCCAGGCACA	56	1.5	386	30 (30-30-30)		Exon 2 & flanking sequence
Forward Reverse	GCCACCTCTTCCTCACAA ATGTGGTATTGCCCCATTAGA	57	1.5	543	30 (20-20-20)	6.8% DMSO (1.7 µl)	Exon 3 & flanking sequence
Forward Reverse	TGGGGCAATACCACATATCC CAAGACAGTAGGGGAAAAAATAG	58	2.5	643	35 (30-30-30)		3' UTR

each primer, 0.2 mM of each dNTP, optimum concentration of MgCl₂, and 0.5 unit of *Taq polymerase* (Invitrogen, Carlsbad, California, USA) in a Thermocycler (GeneAmp-9700, PE Applied Biosystems, Foster City, CA, USA). 5 µl of the PCR products were analyzed by electrophoresis in either 6% polyacrylamide gel or 2% agarose gel and visualized under UV light after staining the gel in ethidium bromide solution (674).

3.2.2.3 Gel electrophoresis

Mainly two types of gel electrophoresis (i) polyacrylamide gel electrophoresis (PAGE) and (ii) agarose gel electrophoresis was used in this study. The different buffers and running conditions for these two types of electrophoresis are listed below in Table 18.

Agarose gel electrophoresis

Agarose gels were employed for electrophoresis of PCR & PCR-RFLP products. Agarose gels were prepared using TBE buffer (Table 18). Samples to be electrophoresed were mixed with 1/6th volume of 6X gel loading dye. Electrophoresis was carried out at 2-3 volts per cm of gel for 1-2 hours at room temperature depending on the size of the gel and run length. To visualize the DNA, the gels were prestained in ethidium bromide solution (0.5 µg/ml). Gel images were captured using a gel documentation system (Gel Doc 1000, BioRad, Hercules, CA, USA) and QuantityOne® software package (BioRad, USA). All images were processed through Adobe Photoshop CS2 (Adobe Systems, San Jose, USA).

Polyacrylamide gel electrophoresis (PAGE)

Polyacrylamide is a cross linked polymer of acrylamide and bis-acrylamide. Polyacrylamide gel has high resolving power for separating DNA fragments lower than 1 kb. For PAGE, the vertical gel apparatus was used. The samples were electrophoresed in 6% polyacrylamide gel. 5 µl of the samples were mixed with 1/6th volume of gel loading dye. Electrophoresis was carried out at 6-8 volts/cm of the gel for 1 to 1.5 hours at room temperature depending on the size of the gel and the fragment size. To visualize the DNA fragments, the gels were stained in ethidium bromide solution (0.5 µg/ml) for 10 minutes and then de-stained in water for 5 minutes. The gels were visualized and documented as mentioned above.

Table 18: List of Buffers and solutions used for gel electrophoresis.

Buffers / Solutions	Compositions
Stock Solutions for Electrophoresis:	
10X TBE buffer	0.89 M Tris base, 0.89 M borate, 0.02 M Na ₂ -EDTA (pH 8.2–8.4)
6X Gel Loading Dye	0.25% Bromophenol blue, 0.25% Xylene cyanol FF, 15% Ficoll (type 400) in water
Agarose gel electrophoresis buffer	Gel contained 1 to 2% agarose, 1X TAE buffer
Agarose gel running buffer	1X TAE buffer
Acrylamide stock for PAGE	38% (w/v) acrylamide and 2% (w/v) bis-acrylamide in water
Acrylamide gel electrophoresis buffer	1X TBE buffer
Acrylamide gel running buffer	1X TBE buffer
Gel staining solution	Ethidium bromide solution (10 mg/ml) in water.

3.2.2.4 DNA sequencing

In this study, DNA sequencing was performed using a BigDye Terminator v3.1 sequencing kit (Applied Biosystems, Foster City, CA, USA) based on Sanger sequencing chemistry (676). The sequencing was carried on 3130xl Genetic Analyser (Applied Biosystems, Foster City, CA, USA). All PCR amplicons were sequenced in both directions, using the respective PCR primer. The reaction mixture (Table 19) was incubated in a GeneAmp-9700 thermocycler (PE Applied Biosystems, Foster City, CA, USA) using the cycling conditions outlined in Table 20. The PCR products free of contaminating bands due to non-specific amplification were either column-purified using Qiagen PCR-purification kit (Qiagen, Hilden, Germany) or ExoSAP-IT® PCR product cleanup kit (Affymetrix Inc., USA), and bi-directional sequencing was performed. Nucleotide changes were promptly detected by identifying 'double peaks' in the chromatogram. Sequences were compared with reference sequences using the BLAST online software (<https://blast.ncbi.nlm.nih.gov/Blast.cgi>) (677). Sequencing files were visualized by Chromas Lite (Technelysum, Australia) software package.

Table 19: Sequencing reaction composition

Component	Volume
10 ng/μl PCR product	1.0 μl
BigDye Terminator Mix	0.5 μl
5x sequencing buffer [40 mM Tris-HCl (pH 9.0), 1 mM MgCl ₂	2.0 μl
2 μM primer	1 μl
RNase/DNase-free water	5.5 μl
Total volume	10 μl

Table 20: Thermocycler condition for DNA sequencing

Temperature	Time
96 °C	1 min
25 cycles of	
96 °C	10 s
55 °C	5 s
60 °C	4 min

Protocol for column purification of PCR products

The PCR products were column purified before the sequencing reaction to make the template DNA free from excess primers and dNTPs using manufacturer's instruction (Qiagen, Hilden, Germany). In brief, 75 µl of the PCR product was diluted by 375 µl (5 volumes) of binding buffer PB and mixed. To bind DNA, the mixture was applied to the QIAquick column and centrifuged for 30–60 s at 13000 rpm. Flow-through was discarded and the QIAquick column was placed back into the same tube. To wash, 0.75 ml of Buffer PE was added to the QIAquick column and centrifuged for 30–60 s at 13000 rpm. Flow-through was discarded and the QIAquick column was placed back into the same tube. The column was centrifuged for an additional 1 min for complete dry-up of the membrane. The QIAquick column was placed in a clean 1.5 ml microcentrifuge tube. To elute DNA, 30 µl Buffer EB (10 mM Tris-Cl, pH 8.5) was added to the center of the QIAquick membrane, waited for 1 min and centrifuged for 1 min at 13000 rpm. Eluted purified PCR product was then checked in to agarose gel electrophoresis.

Protocol for ExoSAP-IT® PCR product purification

Shrimp Alkaline Phosphatase (SAP), in combination with Exonuclease I (ExoI) offers the simplest, safest and most cost-effective method for removing nucleotides and

primers from PCR products prior to sequencing or genotyping. In principle, SAP dephosphorylates nucleotides and ExoI degrades single-stranded molecules (excess primers), which interfere with the primer extension reaction.

Briefly, 5 µl of post-PCR reaction product was mixed with 2 µl of ExoSAP-IT[®] reagent for a combined 7 µl reaction volume. The mixture was then incubated at 37 °C for 15 minutes to degrade remaining primers and nucleotides followed by incubation at 80 °C for 15 minutes to inactivate ExoSAP-IT[®] reagent. The PCR product was then ready for use in DNA sequencing. ExoSAP-IT[®] reagent was stored in -20 °C freezer and kept on ice throughout this procedure.

Protocol for post-sequencing purification

After the sequencing reaction the products were cleaned by EDTA/sodium acetate/ethanol precipitation before the electrophoresis. The protocol is described below.

- 1) To each tube containing 20 µl of sequencing product, 2 µl of 125 mM EDTA and 2 µl of 3 M sodium acetate (pH 4.6) was added and mixed well.
- 2) After that 50 µl of 95% ethanol was added to each tube and after a thorough mixing incubated for 30 minutes at room temperature in dark.
- 3) The tubes were spun at 13000 rpm for 20 minutes at room temperature.
- 4) The supernatant was discarded and 250 µl of 70% ethanol (at room temperature) was added for washing the residual salts.
- 5) The tubes were spun at 13000 rpm for 10 minutes and the supernatant was discarded.
- 6) Steps 5 & 6 were repeated once more.

- 7) The supernatant was aspirated and the pellets were air dried for 30-45 minutes.
- 8) To the pellet, 10 μ l of Hi-Di™ formamide was added and mixed well by mild vortexing followed by a quick spin.
- 9) Then the sample was denatured at 98 °C for 5 min and chilled in ice immediately to retain the single stranded conformation. The sample was then ready for sequencing in capillary electrophoresis.

3.2.2.5 Restriction fragment length polymorphism (RFLP)

Restriction fragment length polymorphism analysis was carried out to confirm the identified nucleotide variants or to genotype the targeted SNPs in patients, their family members and control population. Alteration of restriction enzyme recognition sites were checked by online tool NEB CUTTER (<http://nc2.neb.com/NEBcutter2/>). If the nucleotide variant alters restriction site, genotyping was done by RFLP analysis. The restriction enzyme digestion of PCR amplified products (50-70 ng) was carried out in a total reaction volume of 20 μ l with specific enzymes and compatible buffers under the conditions specified by the manufacturers. For genotyping of each SNP, the primers used for PCR, the restriction enzyme used and the digestion condition are provided in the Table 21. The DNA fragments in the digest were separated by PAGE as described earlier in this section. Alleles were scored based on the DNA band patterns in the gel.

3.2.3 Statistical and *in silico* analysis

In silico analysis was done for non-synonymous nucleotide variations by PolyPhen 2.0 (<http://genetics.bwh.harvard.edu/pph2/>) (678), SIFT (<http://sift.icvi.org/>) (679) and

Screening of *TOR1A* & *THAP1* genes in Indian primary dystonia patients

Table 21: PCR primers and restriction enzymes were used for genotyping.

	rs13300897	rs1801968	rs1182	rs3842225
Major/Minor allele	G/A	G/C	G/T	G/Δ
PCR amplicon size (bp)	502	390	386	321
Forward Primer (5' to 3')	GAGGGGACACAGTCTTGCTC	CAGGGCTAGGACATGATGGA	TCCTTCCCTGGAAGAGGAATC	GGCCACACTGTCAACATTTG
Reverse Primer (5' to 3')	CCACCCTGCTTGTTCTCGC	GTTACCTGGAGTTCATCAGC	CCAGTAAAGATACATCACAGTC	GCACATGCAAAAATTTTATTGTA
Enzyme for RFLP	MboII	AfIII	TaqI	CviKI-1

Mutation Taster (<http://www.mutationtaster.org>) (680). Functional annotation (MetaSVM and CADD score) for non-synonymous nucleotide variants were done by dbNSFP v2.0 software package (681). The case-control association study was done by 'JAVASTAT – 2 Way Contingency Table Analysis' with Fisher Exact Test (<http://statpages.org/ctab2x2.html>) (682). The secondary mRNA structures and thermodynamic parameters of wild type and mutant *THAP1* were predicted by 'the mfold web server' (<http://mfold.rna.albany.edu/?q=mfold>) (683). Haplotype analysis and LD calculation was done by Haploview software (684). Best predictive gene-gene interaction model was used for SNP-SNP interaction by MDRpt (Multifactor dimensionality reduction –permutation testing) software (685).

3.3 Results

3.3.1 Identification of nucleotide variants in *TOR1A* gene

Upon screening of the entire exon 4, exon 5 and 5' & 3' UTR region of *TOR1A* gene in 297 primary pure dystonia patients, two coding & four non coding nucleotide variants were identified (Table 22). Among two coding variants, the most common trinucleotide deletion mutation (c. 904-906/907-909 Δ GAG; p. 302/303 Δ E) was found in exon 5 in two generalized dystonia patients. The other coding variant (c.646 G>C; p. D216H) is a functional SNP (rs1801968) found in exon 4. The other variants were common SNPs found both in patient and control cohort.

3.3.2 Primary torsion dystonia due to the *TOR1A* Δ GAG in an Indian family

In this study, we found the *TOR1A* Δ GAG mutation in two juvenile onset generalized dystonia patients in the same family who are siblings and their asymptomatic mother (Table 23). Both the patients were diagnosed in movement disorder clinic at Bangur

Table 22: *TOR1A* nucleotide variants identified in primary dystonia patients.

Nucleotide variant	Amino acid change	Location	Patients Chromosome No.	Control Chromosome No.	Remarks
c. -104 G > A	NA	5' UTR	104/536	117/596	rs13300897
c.646 G > C	p. D216H	Exon 4	102/574	52/560	rs1801968
IVS4 + 113 C > G	NA	Intron 4	56/396	ND	rs13297609
c. 904-906/907-909 ΔGAG	p. 302/303 ΔE	Exon 5	1/580	0/554	Disease causing
c. *191 G > T	NA	3' UTR	116/594	130/664	rs1182
c. *824 ΔG	NA	3' UTR	97/540	133/574	rs3842225

IVS: Intervening sequence, NA: Not applicable, ND: Not determined, UTR: Untranslated region.

Table 23: Clinical parameters of individuals harbouring *TOR1A* ΔGAG mutation.

Subjects	II-1	II-2	I-2
Diagnosis	Generalized dystonia	Generalized dystonia	Asymptomatic
Sex/Age	Male/26 years	Male/21 years	Female/33 years
Age at Onset	10 years	10 years	-
Nucleotide Variation	c. 904-906/907-909 ΔGAG	c. 904-906/907-909 ΔGAG	c. 904-906/907-909 ΔGAG
Variant location	Exon 5	Exon 5	Exon 5
Protein change	p. 302/303 ΔE	p. 302/303 ΔE	p. 302/303 ΔE
Protein structure	Sensor 2 domain	Sensor 2 domain	Sensor 2 domain
SIFT prediction	Damaging	Damaging	Damaging
Polyphen 2	Damaging	Damaging	Damaging
MutationTaster	Disease causing	Disease causing	Disease causing
rs1801968 (c.646 G > C)	c.646 G	c.646 G	c.646 G
Clinical symptoms			
Site of onset	Both upper limbs	Both lower limbs	None
Disease Progression	Progressive	Progressive	-
Postural imbalance	Absent	Absent	Absent
Facial dystonia	Absent	Absent	Absent
Head movement	Normal	Normal	Normal
Neck dystonia	Present	Present	Absent
Upper limb dystonia	Present	Present	Absent
Lower limb dystonia	Present	Present	Absent
Truncal dystonia	Present	Absent	Absent
Tongue dystonia	Present	Present	Absent
Ocular movement	Broken saccadic	Normal	Normal
Dysphonia	Absent	Absent	Absent
Tremor	Action tremor in both upper limbs	Both postural & action tremor in whole body	Absent
Gait problem	Circumduction gait in both lower limbs	Circumduction gait only in right lower limb	Absent
Speech problem	Slurring of speech	Severe dysarthria	Absent
Associated Pain	Absent	Absent	Absent
Memory problem	Absent	Absent	Absent
Psychiatric problem	Absent	Absent	Absent

Institute of Neurosciences, Kolkata and have negative history of developmental complications, malignant diseases or any brain injury. EEG, NCV (nerve conduction

velocity) test with H-reflex, neuroimaging (CT, MRI, etc) studies for any brain lesions and other biochemical measurements (e.g. serum ceruloplasmin, uric acid, etc) were found to be normal. None of them have K-F ring as verified by routine slit-lamp eye examination.

Case I: A 26-year-old male (II-1; proband) diagnosed as primary generalized dystonia patient. Disease onset was at 10 years of age with writing problem and holding objects in both upper limbs. During writing abnormal sensation with cramps in right upper limb was felt and subsequently problem in holding an object was developed. Gradually, disease progressed to the lower limbs with abnormal posture during walking with a pattern of circumduction gait. Later on postural and action tremor was developed in both the upper limb along with a flex posture in right upper limb. The patient also developed truncal dystonia, an atypical dystonic feature for generalized dystonia with asymmetric distribution more towards the right side of the body (laterocorpus). The neck and shoulder position slightly tilted to left side. At that time patient was advised with levodopa-carbidopa (55 mg TDS), clonazepam (0.5 mg BDS), tetrabenazine (25 mg BDS) and trihexyphenidyl (4 mg BDS).

Case II: The sibling (II-2) of the proband is a 21-year-old male also affected with primary generalized dystonia. Problem starts at the age of 10 years with dragging and lifting of toe during walking. Gradually the disease progressed to upper body parts leading to generalized dystonia. Writer's cramp developed with overflow of muscle contraction and action tremor during writing on the right upper limb. Whole body postural and action tremor were also present. Asymmetric twisting posture of the right side of body was developed with stiffness. Circumduction in right toe was

found during walking though the tandem walking was normal. Tone and activation in both upper limbs were normal. The patient was under the following combination of medication consisting levodopa-carbidopa (110 mg TDS), clonazepam (0.5 mg BDS), trihexyphenidyl (2 mg TDS) and propranolol (40 mg OD).

Genetic screening for *TOR1A* and *THAP1* mutation

All the exons, promoter and 3' UTR of *TOR1A* and *THAP1* gene were screened and identified a heterozygous c.904-906/907-909 Δ GAG mutation of *TOR1A* gene was found (Figure 2) in the patients and their asymptomatic mother (I-2). For this penetrance issue, we also analyzed the presence and orientation of c. 646 C allele of rs1801968 (c.646 G>C, p. D216E), as presence of this allele in trans- orientation to the Δ GAG can greatly suppress the disease expression (113). But none of them does harbor the c.646 C allele in exon 4 of *TOR1A* gene.

3.3.3 Case control association study of identified *TOR1A* SNPs

Along with the coding mutation, four SNPs rs13300897 (*TOR1A* promoter SNP), rs1801968 (functional cSNP in exon 4), rs1182 & rs3842225 (3' UTR SNPs) in *TOR1A* gene were also identified both in patients and control individuals. Case control association study for rs1801968 was done in 287 index primary pure dystonia patients and 280 control individuals as some of the samples failed for genotypic assay quality (Figure 3). The two tailed Fisher exact test revealed the minor allele (C) and GC+CC genotype were significantly predisposed as a risk factor for primary dystonia pathogenesis (Table 24). It has been found that the minor allele of rs1801968, 216H forms perinuclear inclusion bodies like the p. 302/303 Δ E variant of

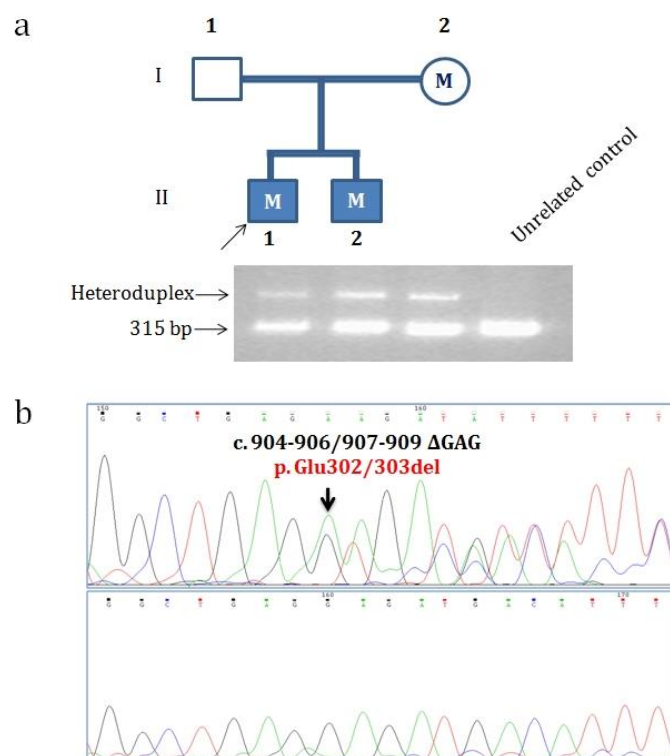


Figure 2: Identification of *TOR1A* Δ GAG mutation in an Indian family.

a) Pedigree of the small isolated Indian family affected with primary torsion dystonia. Visualization of the *TOR1A* exon 5 PCR product in 2% agarose gel forming heteroduplex due to the small in-frame deletion. b) Representative Sanger sequencing chromatogram of the *TOR1A* Δ GAG (heterozygous) mutation (upper panel) found in both the patients and their asymptomatic mother and the normal control individual (lower panel).

TOR1A in a cellular based experiment (118). So, the association data of rs1801968 in our study cohort reflects the pathobiology of primary dystonia reported in functional experimental evidences. Next, the genotyping of rs3842225 has been done among 270 primary dystonia patients and 287 healthy individuals and found that the minor allele (c. *824 Δ) of rs3842225 may acts as a protective factor (odds ratio = 0.726; $p = 0.038$) (Table 25). The genotyping for rs1182 and rs13300897 has been completed among 297 and 268 primary dystonia patients respectively followed by 332 and 298 control individuals. Case control association study concluded that, both the SNPs are not associated with primary dystonia in our cohort (Table 26 & Table 27).

Table 24: Allele and genotype frequency of rs1801968.

Test Group	Allele frequency		Genotype frequency			Odds ratios (95% Confidence Intervals)	p-value
	G	C	GG	GC	CC		
Cases (N = 287)	472 (82.22%)	102 (17.78%)	193 (67.24%)	86 (29.96%)	8 (2.78%)	G vs C : 0.474 (0.326 – 0.687)	0.0001
Controls (N = 280)	508 (90.71%)	52 (9.29%)	234 (83.57%)	40 (14.28%)	6 (2.14%)	C vs G : 2.111 (1.456 – 3.065)	0.0001
						GG vs GC + CC : 0.404 (0.265 – 0.614)	0.0001
						GC + CC vs GG : 2.478 (1.629 – 3.776)	0.0001
						GC vs GG+ CC : 2.567 (1.654 – 3.992)	0.0001

Table 25: Allele and genotype frequency of rs3842225.

Test Group	Allele frequency		Genotype frequency			Odds ratios (95% Confidence Intervals)	p-value
	G	Δ	GG	GΔ	ΔΔ		
Cases (N = 270)	443 (82.03%)	97 (17.97%)	188 (69.62%)	67 (24.81%)	15 (5.56%)	G vs Δ : 1.377 (1.017 – 1.866)	0.038
Controls (N = 287)	441 (76.82%)	133 (23.18%)	168 (58.53%)	105 (36.58%)	14 (4.88%)	Δ vs G: 0.726 (0.536 – 0.983)	0.038
						GG vs GΔ + ΔΔ : 1.624 (1.127 – 2.341)	0.008
						GΔ vs GG+ ΔΔ : 0.572 (0.39 – 0.838)	0.003

Screening of *TOR1A* & *THAP1* genes in Indian primary dystonia patients

Table 26: Allele and genotype frequency of rs1182.

Test Group	Allele frequency		Genotype frequency			Odds ratios (95% Confidence Intervals)	p value
	G	T	GG	GT	TT		
Cases (N = 297)	478 (80.47%)	116 (19.53%)	190 (63.97%)	98 (32.99%)	9 (3.04%)	G vs T : 1.003 (0.752 – 1.339)	1.000
Controls (N = 332)	534 (80.42%)	130 (19.58%)	214 (64.45%)	106 (31.92%)	12 (3.62%)	GG vs GT+TT: 0.934 (0.697 – 1.376)	0.934
						GT vs GG+ TT : 1.05 (0.741 – 1.487)	0.798

Table 27: Allele and genotype frequency of rs13300897.

Test Group	Allele frequency		Genotype frequency			Odds ratios (95% Confidence Intervals)	p value
	G	A	GG	GA	AA		
Cases (N = 268)	432 (80.59%)	104 (19.41%)	177 (66.04%)	78 (29.1%)	13 (4.86%)	G vs A: 1.015 (0.748 – 1.377)	0.94
Controls (N = 298)	479 (80.36%)	117 (19.64%)	190 (63.75%)	99 (33.22%)	9 (3.03%)	GG vs GA+ AA: 1.106 (0.771 – 1.586)	0.597
						GA vs GG+ AA: 0.825 (0.568 – 1.198)	0.318

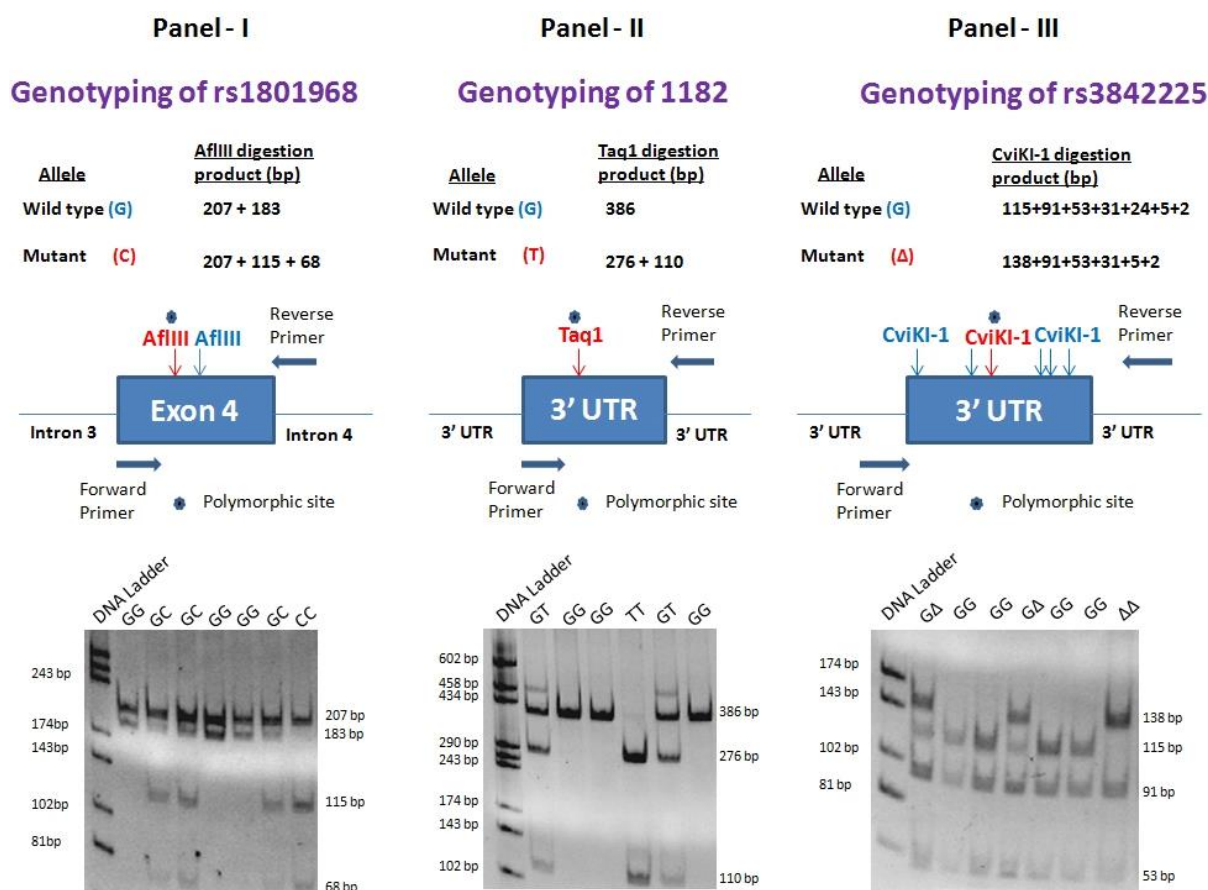


Figure 3: Genotyping of *TOR1A* SNPs for case-control association study. Schematic representation of RFLP design and representative gel pictures of rs1801968 (Panel-I), rs1182 (Panel-II) and rs3842225 (Panel-III) are shown here.

To further evaluate the contribution of the *TOR1A* SNPs towards the dystonia pathogenesis, a haplotype based association study has been conducted (Figure 4). When the haplotype analysis was done using rs1182 and rs3842225, it was found that two haplotypes GΔ ($p = 0.025$; OR = 1.826; 95% CI=1.072 – 3.123) & TG ($p = 0.0001$; OR = 5.594; 95% CI = 2.365–13.871) act as significant risk factors for primary dystonia (Table 28) while TΔ ($p = 0.002$; OR = 0.582; 95% CI = 0.408 – 0.83) haplotype may pose a protective effect against the disease. Another haplotype analysis was done using rs1801968, rs1182 and rs3842225 and evaluated the effect of rs1801968 over the significantly associated haplotypes of rs1182 and rs3842225 (Table 29). It has been found that, the CGG haplotype is significantly associated as

risk factor ($p = 0.002$; OR = 1.94; 95% CI = 1.305 – 2.889) for dystonia as the minor allele (C) of rs1801968 and major allele (G) of rs3842225 are individually associated with dystonia as a risk factor. The other two haplotypes, GGG ($p = 0.004$; OR = 0.685; 95% CI = 0.527 – 0.888) and GT Δ ($p = 0.001$; OR = 0.572; 95% CI = 0.397 – 0.824) were significantly associated as protective factor against dystonia pathogenesis.

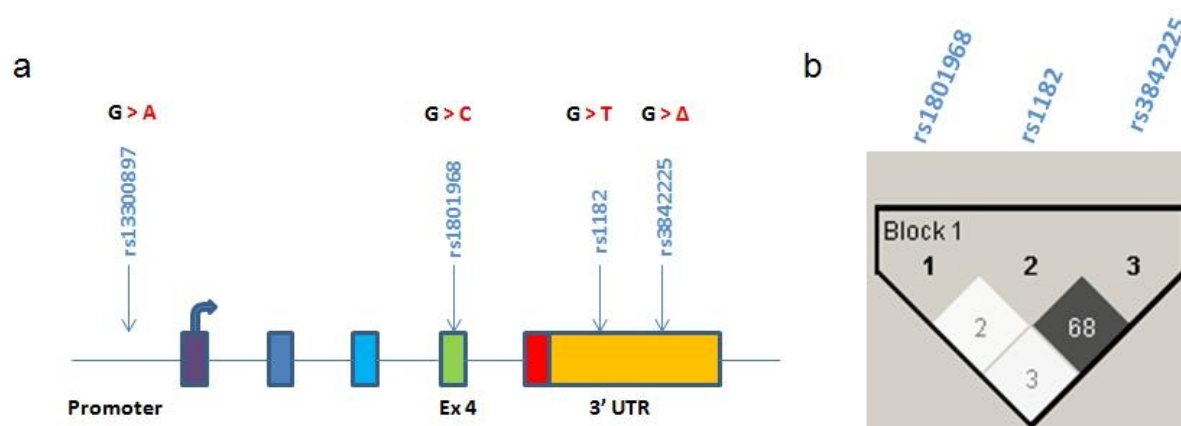


Figure 4: Haplotype analysis of common *TOR1A* gene variants. Schematics of a) The positions of the SNPs in *TOR1A* gene and b) The linkage disequilibrium (LD) block with the r^2 - value.

Table 28: rs1182-rs3842225 haplotypic association study.

Haplotype	Haplotype frequency		Odds ratio (95% CI)	p - value
	Patients (N = 270)	Controls (N = 285)		
GG	0.739	0.758	0.908 (0.686 – 1.203)	0.533
T Δ	0.114	0.182	0.582 (0.408 – 0.83)	0.002
G Δ	0.08	0.046	1.826 (1.072 – 3.123)	0.025
TG	0.067	0.013	5.594 (2.365 – 13.871)	0.0001

Table 29: rs1801968-rs1182-rs3842225 haplotypic association study.

Haplotype	Haplotype frequency		Odds ratio (95% CI)	p - value
	Patients (N = 269)	Controls (N = 258)		
GGG	0.573	0.663	0.685 (0.527 – 0.888)	0.004
CGG	0.162	0.092	1.94 (1.305 – 2.889)	0.002
GTA	0.115	0.185	0.572 (0.397 – 0.824)	0.001
GGA	0.065	0.047	1.446 (0.819 – 2.56)	0.224

3.3.4 Identification of nucleotide variants in *THAP1* gene

Sequence analysis of *THAP1* identified two heterozygous nucleotide variants in coding regions of two individuals and three nucleotide variants in non-coding region (Figure 5a). RFLP analysis (Figure 5c) for the variants in the coding region (c.427A>G) and the 3'-UTR (c.*157 T>C) was consistent with the sequence analysis. Among these variants, c.427A>G represents a *de novo* change in the patient since neither of his two parents harbor the change (Figure 5c). Among the coding variants a novel 2-bp heterozygous deletion mutation (c.208-209 Δ AA) in exon 2 leading to frame shift was identified in a primary early onset cervical dystonia patient. This mutation is predicted to result in a truncated protein (p.K70VfsX15) creating a premature stop codon at position 84. This would change the amino acid sequences from residue 70 of the highly conserved THAP domain leading to the loss of the entire proline-rich region and predicted NLS (nuclear localization signal). The second coding variant [c.427A>G (p.M143V)] in exon 3, a heterozygous *de novo* missense mutation was found in a patient affected with primary early-onset generalized dystonia. Neither of these two variants was found in controls. Multiple sequence alignment using ClustalW2 (<http://www.ebi.ac.uk/Tools/msa/clustalw2/>) showed that both the coding variants changed the amino acid residues, which were highly conserved throughout the mammals (Figure 5b) suggesting probable pathogenicity due to amino acid change. Also the predicted mRNA structure of mutant *THAP1* (c.427A>G) revealed a different folding pattern compared to the wild type with a decrease in free energy (ΔG^0) of the mutant resulting in decrease in RNA stability, which may affect the expression level (Figure 6).

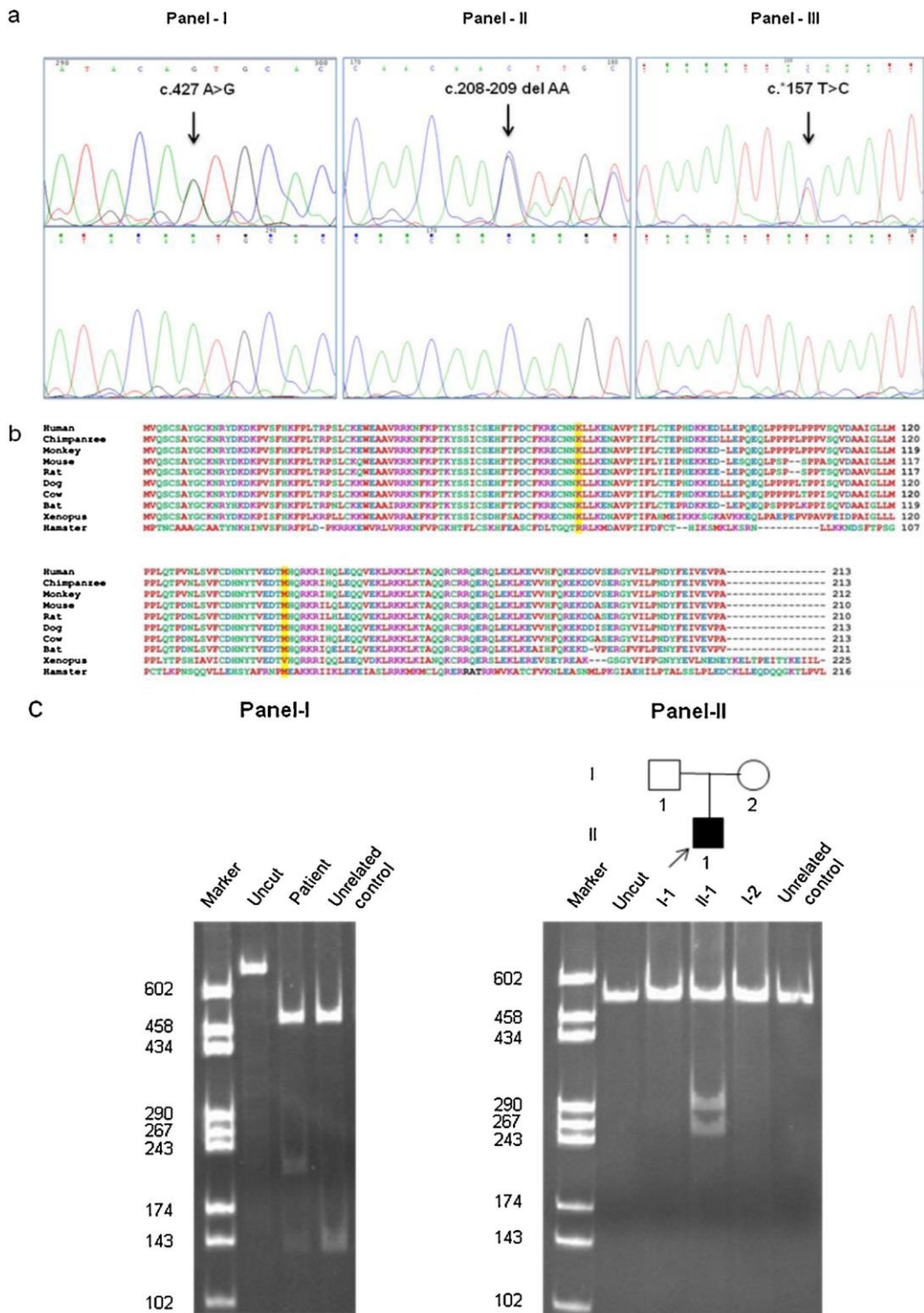


Figure 5: Identification of *THAP1* gene variants in Indian primary dystonia patients. (a) Chromatograms of DNA sequences demonstrating *THAP1* variations. *Upper Panel-I*, demonstrate heterozygous missense variant c.427 A > G in exon 3; *Upper Panel-II*, demonstrates heterozygous frame shift deletion mutation c.206-207 Δ AA in exon 2; and *Upper Panel-III*, demonstrates heterozygous nucleotide variant, c.*157 T>C in 3'-UTR. *Lower Panels*, demonstrate chromatograms of DNA

sequences from the corresponding areas of wild type *THAP1*. (b) Conservation Status of THAP1 protein. Multiple sequence alignment of THAP1 protein from human, chimpanzee, rhesus monkey, mouse, rat, dog, cow, bat, xenopus, and hamster are shown. The shaded residues indicate the site of variation. (c) The 6% polyacrylamide gel picture of RFLP experiments for two identified mutations. *Panel-I* shows the allelic difference between patient and control digested DNA fragments for c.*157 T > C, and *Panel-II* shows the allelic difference between digested DNA fragments of patient having c.427 A>G variant, relative and unrelated control.

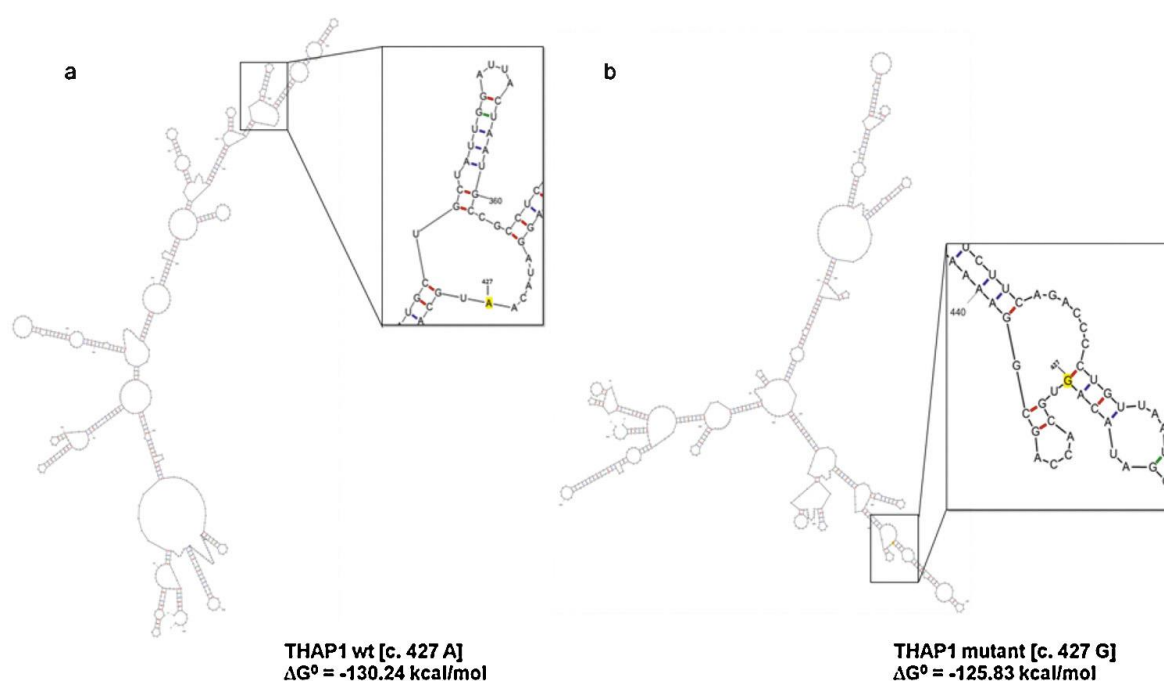


Figure 6: The secondary mRNA structure prediction of *THAP1*. The secondary mRNA structure of wild type (c.427A) and mutant (c.427G) *THAP1* mRNA as predicted by mfold software (simulated under standard parameters).

Among three non-coding nucleotide variants, two reported SNPs (rs71521601 & rs11989331) were found in both patients and controls. A novel rare-variant (c.*157 T>C) in 3' UTR was found in a primary adult onset focal dystonia patient affected with blepharospasm (Table 30). The family members of this patient were not available for genetic screening. Detailed clinical spectrums for all three patients are summarized in Table 31.

Table 30: *THAP1* Nucleotide Variants in Indian primary dystonia patients.

Nucleotide change	Location	Amino acid change	Number of chromosomes (allele frequency)		Remarks
			Patient n = 454 (%)	Control n = 508 (%)	
c.208-209 ΔAA	Exon 2	p.K70VfsX15	1 (0.22)	0	Novel
c.427 A > G	Exon 3	p.M143V	1 (0.22)	0	Reported
IVS1+126 T > C	Intron 1	NA	8 (1.76)	ND	rs71521601
IVS2-87 A > G	Intron 2	NA	41 (9.03)	86 (16.93)	rs11989331
c.*157 T > C	3' UTR	NA	1 (0.22)	0	Novel

The nucleotide number has been assigned using the first nucleotide of ATG (Translation start site) as +1; reference SNP (rs) no., taken from dbSNP (<http://www.ncbi.nlm.nih.gov/SNP/>). NA, not applicable; ND, not determined; UTR, untranslated region.

Table 31: Clinical characteristics of patients having *THAP1* genetic variants

Dystonia Subjects	Patient – I	Patient – II	Patient – III
Diagnosis	Generalized dystonia	Cervical dystonia	Blepharospasm
Sex/Age	Male/13 years	Male/34 years	Female/33 years
Age at Onset	5 years	9 years	4 years
Family History	Negative	Negative	Negative
Nucleotide Variation	c. 427 A>G	c. 208-209 Δ AA	c. *157 T>C
Variant location	Exon 3	Exon 2	3'UTR
Protein change	p. M143V	p. K70VfsX15	NA
Protein structure	Coiled-coil domain	L4-THAP domain	NA
SIFT prediction	Tolerated	NA	NA
Polyphen 2	Benign	NA	NA
MutationTaster	Polymorphism	Disease causing	Polymorphism
Clinical symptoms			
Site of onset	Both upper limbs	Neck	Both eye lids
Disease Progression	Progressive	Progressive	Progressive
Postural imbalance	Absent	Present	Absent
Facial dystonia	Present	Present	Absent
Head movement	Normal	Normal	Both "yes-yes" & predominantly "No-No" head movement
Neck dystonia	Present	Present	Absent
Upper limb dystonia	Present	Present	Absent
Lower limb dystonia	Present	Present	Absent
Truncal dystonia	Present	Present	Absent
Tongue dystonia	Present	Present	Present
Ocular movement	Broken saccadic movement	Normal	Normal
Dysphonia	Present	Absent	Absent
Tremor	Action tremor in both upper limbs	Both action & rest tremor in whole body	Present in both upper limbs
Gait problem	Dystonic gait in left lower limb	Scoliosis of the spine with flexed knee gait	Normal
Speech problem	Slurring of speech	Severe dysarthria	Absent
Associated Pain	Absent	Present	Present
Memory problem	Absent	Absent	Absent
Psychiatric problem	Absent	Absent	Absent

3.3.5 Clinical characterization of patients

The patient harboring *de novo* c.427 A>G variant developed juvenile onset generalized dystonia with negative family history. The patient developed abnormal posture unilaterally on left upper limb during any activity. As the disease was progressive in nature, it affected gradually the whole body including face and lower extremities. Patient developed unsteady dystonic gait with action tremor in both upper limbs. The lower half of the face including tongue developed irregular continuous movement. Abnormal neck movement was also present in the form of laterocollis with a hypertrophy of left sternomastoid muscle. Patient also developed dysphonia and slurring of speech.

The patient harboring the 2-bp deletion mutation (c.208-209 Δ AA; p.K70VfsX15) developed cervical dystonia. At the age of 9 years, the patient developed right torticollis. The rapid disease progression resulted in dystonic posture both in the upper & the lower extremities. Facial dystonia was also present as jaw tilted to the right side along with a protruding tongue. During physical activity, patients showed both rest and action tremor and developed speech problem. As the disease progressed, scoliosis of spine with knee flexion was observed as a marked gait difficulty. No abnormal head and ocular movements were observed.

A rare sequence variant in the 3'-UTR (c.*157 T>C) was found in an adult-onset (age of onset: 33 years) female primary dystonia patient affected with blepharospasm. The patient suffered from drooping eyelids with a foreign body sensation in both eyes. The symptoms progressed over time creating visual disturbance. She also suffered from migraine like symptoms without nausea, which was relieved by sleep.

Gradually, patient developed abnormal head movement (titubation) both ‘Yes-Yes’ and predominantly ‘No-No’ type. Mild tremor was present in both upper limbs.

3.3.6 Association study of rs11989331 (IVS2-87 A>G)

During screening for variants in *THAP1* exon 3, we found an intronic SNP (IVS2-87 A>G; rs11989331) with a minor allele frequency (MAF) of 0.13. As we checked, there was no deviation from Hardy-Weinberg equilibrium (HWE) for this SNP ($p > 0.05$). Then we conducted a case-control association study using this SNP and found that the major allele (A) and AA genotype are significantly over represented (Fischer Exact Test, $p < 0.05$) in the patients compared to controls (Table 32). The major allele might act as a risk factor towards the disease pathogenesis. However, the functionality of this intronic SNP, if any, is not yet known.

Table 32: Allele and genotype frequency of rs11989331.

Test Group	Allele frequency		Genotype frequency			Odds ratios (95% Confidence Intervals)	P value
	A (%)	G (%)	AA (%)	AG (%)	GG (%)		
Cases N = 227	413 (90.96)	41 (9.03)	190 (83.7)	33 (14.53)	4 (1.76)	A vs G : 2.053 (1.358 - 3.111)	0.0003
Controls N = 254	422 (83.07)	86 (16.92)	177 (69.68)	68 (26.77)	9 (3.54)	AA vs AG+GG : 2.234 (1.404–3.564) AG vs AA + GG : 0.465 (0.285–0.756)	0.0004 0.001

3.3.7 Gene-gene interaction for *TOR1A* and *THAP1* SNPs

As *THAP1* gene product may act as a transcriptional repressor for *TOR1A* transcription, both the genes are functionally related to each other. To evaluate the interaction between them, a best predictive gene-gene interaction model was used to

study the non-additive epistatic interaction by Multifactor dimensionality reduction – permutation testing (MDRpt). Genotype counts for rs1801968, rs1182 and rs3842225 of *TOR1A* and rs11989331 of *THAP1* was assembled for run through the MDRpt software. The genotypes for each SNP were coded like “0” for major-major, “1” for major-minor and “2” for minor-minor allelic combination. Two 2-factors (Model II & III) and one 3-factor (Model IV) gene-gene interaction models have been identified with an average cross-validation consistency (CVC) = 100% and P value < 0.05 using MDR permutation testing program (Table 33).

Table 33: Best predictive gene-gene interaction models identified by multifactor dimensionality reduction analysis.

Model	Best predictive interaction model ^a	Prediction error (1-TBA) ^b	1000 permutations p value*	CVC (in %) ^c
I	rs1182/rs11989331	0.4705	0.243	100
II	rs3842225/rs11989331	0.4485	0.042	100
III	rs1801968/rs11989331	0.4157	0.0001	100
IV	rs1182/rs3842225/rs11989331	0.4339	0.019	100

^aThe best model was selected as the one with the minimum prediction error and maximum CVC.

^bTBA corresponds to the testing balanced accuracy defined as the prediction error (PE) = 1-TBA.

^cCVC corresponds to cross validation consistency.

*p-values for gene-gene interaction models were calculated after 10,000 permutations in MDRpt software.

3.4 Discussion

The aim of this study was to evaluate the contribution of genetic variants of *TOR1A* and *THAP1* towards the primary dystonia pathogenesis in Indian primary dystonia patients. For this, the gene screening strategy was adopted using PCR-RFLP and Sanger sequencing techniques. The screening and targeted genotyping identified the most prevalent c. 904-906/907-909 Δ GAG mutation in *TOR1A* gene in two juvenile onset generalized dystonia patients, who are siblings, and in their asymptomatic mother. Moreover, four common genetic variants were also identified and analyzed for their individual contribution and /or in haplotypes. For *THAP1*, two coding variants and one non-coding rare variant were identified in three index primary dystonia patients.

In this study, we are reporting two generalized dystonia patients from a single family having marked variation in phenotype. Phenotypic variability of primary dystonia patients having Δ GAG deletion in *TOR1A* gene perhaps widespread, but two clinical features are relatively common: 1) early onset and 2) dystonia in a limb. Moreover, intrafamilial phenotypic variability of dystonia patients having Δ GAG deletion is rare (686). The site of disease onset was different as the proband (II-1) has onset at the upper limb, while case II (II-2) has onset at lower limb. As the disease nature was progressive, both of them gradually developed generalized dystonia, however, the direction of generalization was exactly opposite. The disease at the upper body parts and progressed to lower body parts for proband, while his sibling has lower limb onset and then generalized to upper body parts. In addition, as the disease progressed proband developed truncal dystonia unlike the sibling developed a tremor predominant generalized dystonia. There are only three individual reports till date, where generalized dystonia patients harboring *TOR1A*

Δ GAG have truncal involvement (657, 660, 687). Interestingly, the age of onset for both the patients was same at the age of 10 years. This could be governed by age related spatial expression of certain modifier genes in cerebellum or could be triggered by environmental factors. Genetic analysis concludes that the mutant allele is inherited from their asymptomatic mother. Thus in this family, disease penetrance as well as phenotypic variation could be governed by any other genetic or environmental factors.

The case-control association study has been done for a cSNP rs1801968 (c. 646G>C, p. D216H) in *TOR1A* gene, the minor allele (C) shows a very strong and significant association with the primary dystonia ($p = 0.0001$). Further analysis on genotype revealed that GC ($p = 0.0001$) and GC+CC ($p = 0.0001$) genotypes are also predisposed as a risk factor for isolated dystonia pathogenesis. This association study complements the finding in the Argentinean (688) and Dutch (689) population but this association was not found in Chinese (690), French (691) and the Caucasian (692) population. Though in another study from China demonstrated that rs1801968 is associated with writer's cramp (693), a subgroup of primary isolated dystonia. So it could be concluded that the p. 216H may influence the dystonia pathogenesis through population specific genetic and environmental modifiers. Association study also has been done for two 3' UTR SNPs, rs1182 and rs3842225 and one promoter SNP, rs13300897. Statistical analysis illustrated that rs13300897 and rs1182 were not associated with the disease, however, the major allele (G) of rs3842225 was significantly predisposed as a risk factor ($p = 0.03$) for primary isolated dystonia. This may be governed by miRNA binding site alteration due to the deletion, which actually been beneficial as the minor allele shows a protective effect towards the dystonia pathogenesis ($p = 0.038$, OR = 0.726; 95% CI = 0.536 – 0.983). Similar studies also

have been done previously in Chinese (694), Dutch (689), Icelandic (695) and Caucasian (696) with variable association status. Haplotype analysis for rs1182-rs384225 revealed that G Δ & TG haplotypes were significantly associated as risk factor whereas the T Δ haplotype predisposed as a protective haplotype. So it could be concluded that the *TOR1A* genetic variants are a major player for primary isolated dystonia pathogenesis.

THAP1 gene screening identified two non-synonymous variants, c.427A>G (p. M143V), a *de-novo* heterozygous missense variant in exon 3 of *THAP1* gene was found in a juvenile onset (5 year of age) generalized dystonia patient. This variant was also reported in a female German patient, who developed adult-onset (age of onset: 46 years) focal cervical dystonia without any other dystonic symptoms (353). While in German patient the affected body part is neck, our index patient started with upper limb dystonia progressed unilaterally to generalized dystonia. This observation is consistent with the genotype-phenotype correlation reported in 100 patients harboring 63 mutations in *THAP1* (329), where “no obvious, indisputable genotype-phenotype correlation” was shown. This variant (c.427 A>G) might also alter the *THAP1* mRNA structure, which may affect its thermodynamic stability by increasing ΔG^0 value ~ 5 kcal/mol as predicted *in-silico*. This particular variant (p. M143V) is located in the coiled-coil domain of *THAP1* protein, which is necessary for dimerization of *THAP1* to constitute a functional unit.

The second variant, a heterozygous 2-bp deletion (c.208-209 Δ AA; p. K70VfsX15) in exon 2 of *THAP1* was identified in a patient affected with generalized and prominent cervical dystonia. The truncated protein, having lost most of the important domains of *THAP1* and acquired 14 unrelated amino acids, might undergo nonsense mediated decay and any residual aberrant protein would be

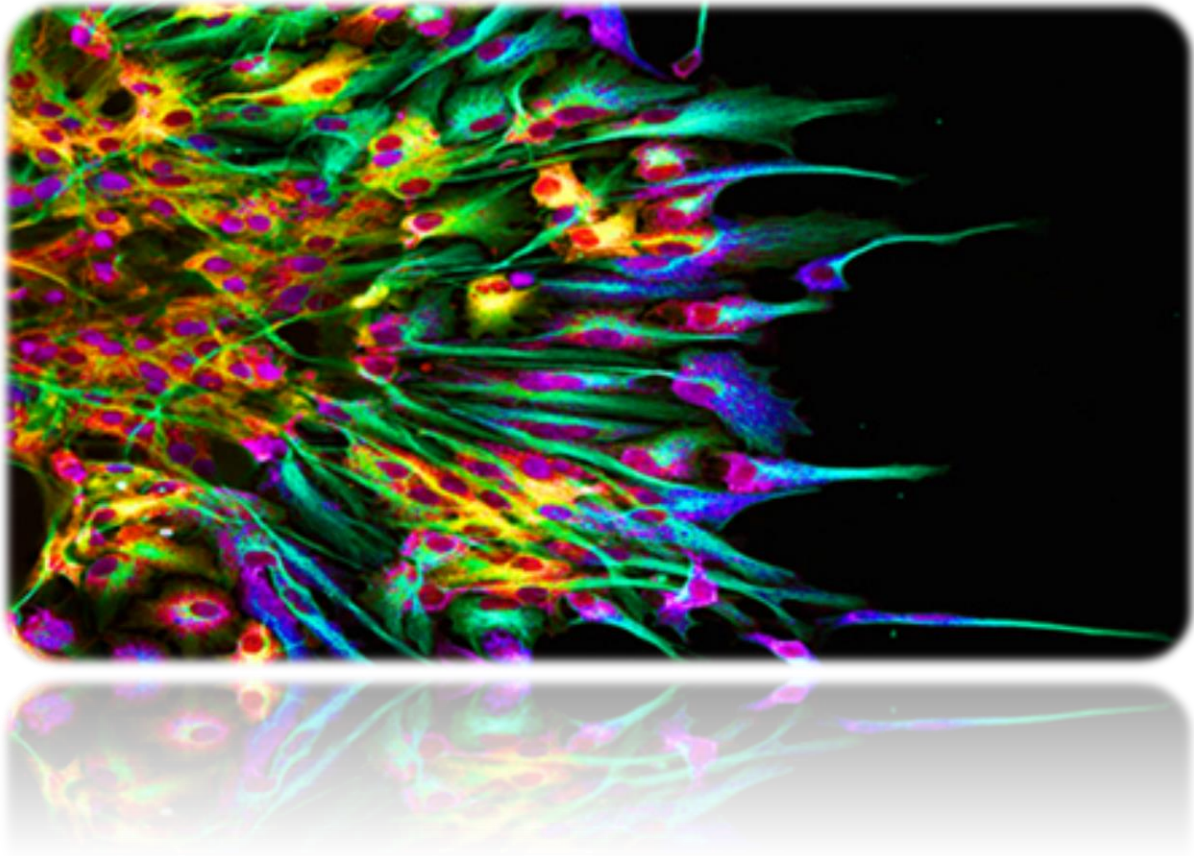
inconsequential with respect to biological function of THAP1. Thus this variant can be described as a mutation based on its compelling functional implication. Therefore, it is obvious that the truncated protein fragment would not be targeted for nuclear localization and also would fail to dimerize with the normal copy of THAP1 protein; thus may develop haploinsufficiency causing severe pathogenesis.

The patient having the *THAP1* 3'-UTR sequence variant (c.*157 T>C) was affected with blepharospasm. *THAP1* mutations are also found in focal blepharospasm patients in the Greek population (697). As this variation occurred in non-coding position of *THAP1* mRNA, it does not have a direct effect on protein sequence or structure. But the 3'-UTR contains regulatory region, which can influence polyadenylation, translation efficiency and stability of the mRNA. Moreover, 3'-UTR region also possess binding sites for various regulatory proteins and micro-RNAs, which can also decrease the gene expression by inhibiting translation process or by degradation of mRNA. So, it would be interesting to explore any potential effect of this c. *157 T>C nucleotide alteration on *THAP1* mRNA stability or the binding site alteration for regulatory proteins and miRNA.

An intronic SNP rs11989331 identified by *THAP1* screening was significantly overrepresented in primary dystonia patients compared to control cohort and suggested a risk factor for dystonia. Though the functional effect of this variant is not obvious yet. To envisage the single common variant association status, MDR was used to reduce the dimensionality of the multilocus genetic data pertaining to primary dystonia pathogenesis to identify the combination of SNPs associated with risk of dystonia disorder. In this study, MDR analysis identified the combination II, III & IV consisting of all 3 SNPs of *TOR1A* (rs1801968, rs1182 & rs3842225) and rs11989331 of *THAP1* are significantly associated with primary dystonia. Though all

the 4 SNPs are associated with dystonia either individually or in haplotype, MDR analysis further assessed the multigenic association status for better understanding of the complex nature of dystonia pathogenesis.

As THAP1 is a transcription factor, the mutant THAP1 protein may be responsible for differential expression of its downstream target genes. Another dystonia related gene *TOR1A* contains one THAP binding site TxxxGGCA and an inverted bipartite THAP-binding consensus motif TxxGGx(A/T) (698). Considering these facts, recently, two studies used electrophoretic mobility shift assay (EMSA) for protein/DNA binding, chromatin immunoprecipitation (ChIP) and luciferase reporter gene assay to show that normal THAP1 protein physically binds to the core promoter region of *TOR1A* gene and specifically represses its expression. *DYT6*-dystonia causing mutations diminish the repressor activity of THAP1 and an elevated expression of *TOR1A* (331, 332). It is evident from various studies that over expression of both wild type Torsin1A as well as mutant form (Glu302/303del Torsin1A, 216H Torsin1A) causes nuclear envelop disruption and formation of inclusion bodies (699). Additionally, the mutant THAP1 proteins are unable to repress the *TOR1A* expression leading to a high level of Torsin1A suggesting a gain of function of *TOR1A*, whereas most of the published studies on Torsin1A function demonstrate a loss of function for the only confirmed pathogenic *TOR1A* mutation (141). This may results in stoichiometric imbalance of Torsin1A/THAP1 protein levels leading to perturbation of the cellular homeostasis. This could be relevant to *DYT6* dystonia, which is currently thought to share strikingly similar phenotypic parameters to the *DYT1* dystonia.



CHAPTER 4

FUNCTIONAL CHARACTERIZATION OF *THAP1* MISSENSE VARIANTS

4.1 Introduction

Thanatos-associated [THAP] domain-containing apoptosis associated protein 1 (THAP1) is a DNA-binding protein that has been recently found to be associated with DYT6 dystonia (91). As mentioned previously, mutation in *THAP1* gene could lead to the primary pure dystonia which is emerged as a significant cause of familial dystonia irrespective of ethnic background. Substantial amount of population based genetic studies confirmed the occurrence of different kind of mutations like missense, nonsense, small in-frame insertion, small in-frame deletion, small out-of-frame insertion and small out-of-frame deletion, majority of which were found in heterozygous state. *In-silico* analysis was done for majority of the mutations to predict the pathogenicity. A number of efforts were made to determine the molecular mechanism and characterization of certain pathogenic mutations through cell culture and animal based model. Certain missense and frameshift mutations introduced in full length *hTHAP1* cDNA expression vector and were functionally characterized in cell culture based experiments. Those mutations are checked for its subcellular localization by immuno-cytochemistry followed by confocal microscopy, the THAP1 repressor activity is measured by luciferase reporter assay, *in-vivo* DNA binding ability by EMSA, *in-vitro* DNA binding ability by ChIP/qPCR and dimerization assay by co-immunoprecipitation. The mutations located in the DNA binding THAP domain were primarily investigated for its DNA binding ability and affinity, the transcriptional repressor activity and also for thermostability (Table 34). The mutations sited at coiled-coil domain, which is predicted to be involved in self dimerization, were

Functional characterization of *THAP1* missense variants

Table 34: Comparison of the different approach for functional characterization of *THAP1* gene variants reported in literature.

Mutation	Subcellular localization	THAP1 activity	Thermo stability	DNA binding affinity (ITC)	Dimerization	DNA binding ability (EMSA)	DNA binding ability (ChIP/qPCR)	Reference
p. S6F			Less than WT	Reduced				(330)
		40%						(349)
p. Y8C			Less than WT	Same as WT				(330)
p. G9C			Less than WT	Reduced				(330)
p. N12K			Less than WT	Same as WT				(330)
p. R13H		80%						(333)
		57%						(331)
p. K16E		60%						(333)
p. D17G			Less than WT	Increased				(330)
p. S21T	Nucleus					Abolish binding	Decreased	(332)
			Less than WT	Reduced				(330)
p. H23P		20%						(333)
		<10%						(349)
	Nucleus & Cytoplasm							(334)
		<10%						(331)
p. K24E		60%					(333)	
p. P26L		40%						(333)
		<10%						(349)
p. R29X	Cytoplasm							(334)
p. R29Q		50%						(349)
			Less than WT	Reduced				(330)
p. A39T			Less than WT	Reduced				(330)
p. C54Y						Abolish binding		(332)
	Perinuclear inclusion				Normal			(329)
p. C54F	Nucleus							(323)
p. I80V		100%						(333)

Functional characterization of *THAP1* missense variants

Mutation	Subcellular localization	THAP1 activity	Thermo stability	DNA binding affinity (ITC)	Dimerization	DNA binding affinity (EMSA)	DNA binding affinity (ChIP/qPCR)	Reference
p. F81L	Nucleus							(334)
						Abolish binding		(332)
			Less than WT	Same as WT				(330)
	Nucleus				Normal			(329)
p. F132Δ	Nucleus				Normal			(329)
p. T142A	Nucleus				Normal			(329)
p. I149T	Nucleus				Normal			(329)
p. A166T	Nucleus				Normal			(329)
p. L180S	Nucleus							(323)
p. F22fsX71	Nucleus & Cytoplasm							(323)
p. F25fsX53	Nucleus & Cytoplasm							(323)
p. F45fsX73	Nucleus & Cytoplasm							(334)
p. V131fsX133	Nucleus & Cytoplasm							(334)
p. Q154fsX180	Nucleus & Cytoplasm						Decreased	(332)
	Cytoplasm				Failed			(329)
p. L159fsX180	Nucleus & Cytoplasm							(334)
p. D191TfsX9	Nucleus & Cytoplasm							(333)

analyzed for its ability for dimerization (329). Determination of subcellular localization was done for almost all the mutations listed in Table 34 irrespective of its location in protein. DNA binding affinity measurement by isothermal titration calorimetry (ITC) and thermostability determination by differential scanning fluorimetry (DSF) were done for the mutations in THAP domain, where only the THAP domain was expressed (330). Till now, 29 distinct mutations out of 88 total identified mutations in *THAP1* gene have been studied for functional characterization to determine the pathogenicity of respective mutant THAP1 protein. Therefore, a lot of mutations yet to be characterized to unravel the molecular mechanism involved in developing primary dystonia. This could also be beneficial to develop the genotype phenotype correlation on the basis of impaired protein function of THAP1.

Thus in this functional characterization study, apart from the identified variant (p. M143V), another four missense variants have been selected from literature based on the following criteria 1) the nature of change in amino acid residues, 2) mutations are in the functionally important structural motifs, 3) the conservation pattern and pathogenicity values, 4) none of the mutations are functionally characterized previously. The mutations are listed in Table 35 along with pathogenicity scores and predictions. All the mutations were introduced in episomal expression vector and expressed into HEK293T cells to evaluate the subcellular localization, mRNA & protein stability and transcriptional activity of mutant THAP1 protein.

Functional characterization of *THAP1* missense variants

Table 35: *In-silico* prediction for pathogenicity of the selected *THAP1* variants for functional characterization.

Nucleotide Variant	Amino acid change	Exon No	Protein Structure affected	Domain Function	fathmm-score	fathmm-pred	MetaSVM_score	MetaSVM_pred	CADD	
									RawScore	PHRED
c. 86 G > C	p. R29P	2	L2-THAP domain	DNA binding	0.99344	D	0.9902	D	6.967026	33
c. 95 T>A	p. L32H	2	L2-THAP domain		0.99708	D	1.0597	D	5.669159	26.7
c.169 C>A	p. H57N	2	THAP domain	C2CH motif	0.99718	D	0.9364	D	5.824175	27.2
c.215 T>G	p. L72R	2	L4-THAP domain	DNA binding	0.99318	D	1.0924	D	3.691608	23.3
c.427A>G	p. M143V	3	Coiled-coil domain	Dimerization	0.75855	D	-0.3844	T	-0.24029	0.901

FATHMM: Functional Analysis Through Hidden Markov Models, Pathogenic threshold value > 0.5; **MetaSVM:** Ensemble score by Support Vector Machine (SVM), Pathogenic threshold value > 0.2; **CADD:** Combined Annotation Dependent Depletion, Pathogenic PHRED > 15

4.2 Materials and methods

4.2.1 Generation of *THAP1* mutant constructs by site-directed mutagenesis

For functional characterization of the selected *THAP1* mutations in cell culture based experiments, first different mutant constructs were introduced in pcDNA3.1-nV5-*hTHAP1* expression vector (a kind gift from Dr. Laurie Ozelius). Site directed mutagenesis was carried out using Q5[®] Site-Directed Mutagenesis Kit (New England Biolabs, USA) following the manufacturer's protocol. The primers used for each SDM reaction are listed in Table 36 along with their sequences and melting temperature. The graphical representation of the SDM strategy is depicted in Figure 7.

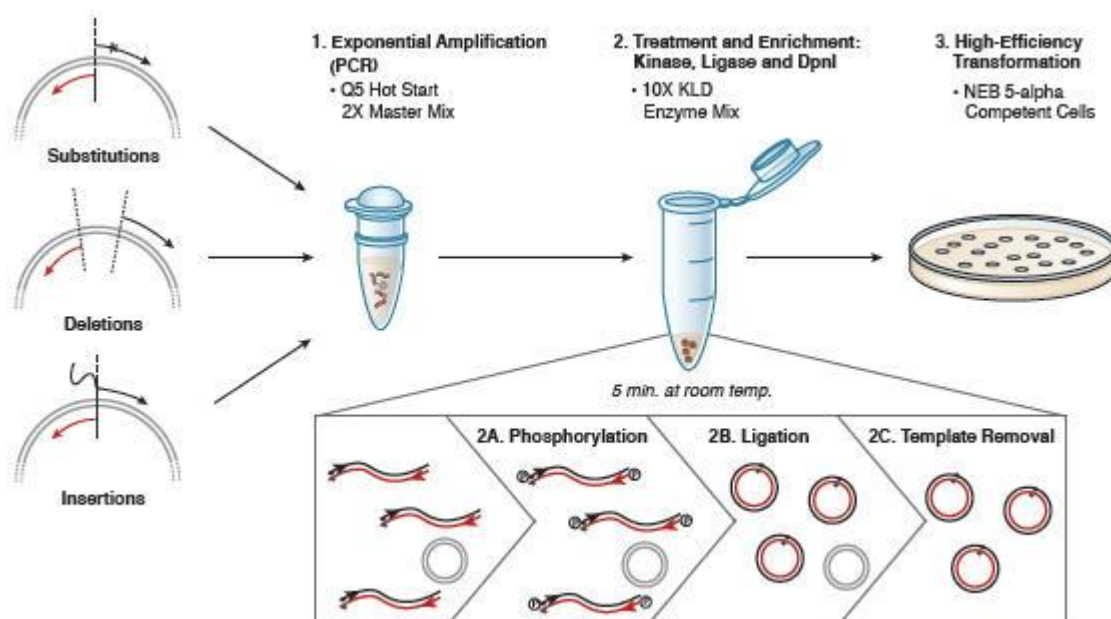


Figure 7: NEB Q5 Site-Directed Mutagenesis kit overview. The first step is an exponential amplification using standard primers and a master mix formulation of Q5 Hot Start High-Fidelity DNA Polymerase. The second step involves incubation with a unique enzyme mix containing a kinase, a ligase and DpnI. Together, these enzymes allow for rapid circularization of the PCR product and removal of the template DNA. The last step is a high-efficiency transformation into chemically competent cells.

Functional characterization of *THAP1* missense variants

Table 36: Primer sequences used for site-directed mutagenesis to generate different *THAP1* mutant constructs.

Primer Name	Sequence (5' to 3')	Length (bp)	%GC content	Tm Value (°C)	5' flanking region (bp)	3' flanking region (bp)
THAP1-G86C-F	CCACAAGTTTCCTCTTACTC C ACCCAGTCTTTGTAAAGAATG	42	42.86	74	20	21
THAP1-G86C-R	CATTCTTTACAAAGACTGGGT G GAGTAAGAGGAAACTTGTGG	42	42.86	74	21	20
THAP1-T95A-F	CTCTTACTCGACCCAGTC A TTGTAAAGAATGGGAGG	36	47.22	73	18	17
THAP1-T95A-R	CCTCCATTCTTTACAA T GACTGGGTCGAGTAAGAG	36	47.22	73	17	18
THAP1-C169A-F	GCAGTATTTGTTCCAGAG A ACTTTACTCCAGACTGC	35	42.86	71	17	17
THAP1-C169A-R	GCAGTCTGGAGTAAAGT T CTCTGAACAAATACTGC	35	42.86	71	17	17
THAP1-T215G-F	GTGCAACAACAAGTTAC G GAAAGAGAATGCTGTGCC	36	47.22	75	17	18
THAP1-T215G-R	GGCACAGCATTCTCTTT C GTAACTTGTTGTTGCAC	36	47.22	75	18	17
THAP1-A427G-F	CTATACTGTGGAGGATACA G TGCACCAGCGGAAAAGG	37	51.35	76	19	17
THAP1- A427G-R	CCTTTTCCGCTGGTGCA C TGTATCCTCCACAGTATAG	37	51.35	76	17	19

In brief, a PCR step was done using pcDNA3.1-*nV5-hTHAP1* as DNA template and the designed SDM primers along with the other reagents as listed in Table 37. The PCR condition is elaborated below (Table 38). The PCR products was then subjected to one step Kinase, Ligase & Dpn I (KLD) treatment for degradation of parental methylated plasmid and isolation of new synthetic plasmid incorporating the desired nucleotide variant in *THAP1* coding sequence. 1 μ l of the PCR product was treated with the reagents depicted in Table 39 and incubated at room temperature (25 °C) for 5 minutes. 5 μ l of the KLD product was transformed into XL-10 Gold *E. coli* competent cells.

Table 37: SDM reaction composition

Component	Volume used (For 25 μ l reaction)
Q5 Hot start High-Fidelity 2x master mix	12.5 μ l
10 μ M forward primer	1.25 μ l
10 μ M reverse primer	1.25 μ l
Template DNA (20 ng/ μ l)	1 μ l
Nuclease free water	9 μ l
Total volume	25 μ l

Table 38: Thermocycler condition for SDM

Step	Temperature	Time
Initial denaturation	98 °C	30s
25 cycles	98 °C	10s
	60 °C	30s
	72 °C	4 min
Final extension	72 °C	2 min
Hold	4 °C	Hold

Table 39: KLD reaction composition

Component	Volume used
PCR product	1 μ l
2X KLD reaction buffer	5 μ l
10X KLD enzyme mix	1 μ l
Nuclease free water	9 μ l
Total volume	16 μ l

The procedure for transformation, plasmid purification and plasmid sequencing protocol is elaborated below.

Transformation of plasmid DNA in chemically competent *E. coli* cells

1. *E. coli* XL-10 Gold (endA1 glnV44 recA1 thi-1 gyrA96 relA1 lac Hte Δ (mcrA)183 Δ (mcrCB-hsdSMR-mrr)173 tet^R F'[proAB lacI^qZ Δ M15 Tn10(Tet^R Amy Cm^R)] cells were grown in 5 ml of Luria broth (LB) overnight at 37 °C.
2. Next morning, 200 μ l of overnight culture was added to 10 ml of fresh LB aseptically and grown for 2 to 3 hours or until turbidity to have log phase cells.
3. Total of 3 ml of culture was precipitated down in 1.5 ml eppendorf tube at 6000 rpm for 3 minutes. This could be done in two step manner.
4. Cells were precipitated down as pellet and the supernatant was discarded.
5. 1 ml of chilled 100 mM CaCl₂ was added to the tube containing the bacterial pellet and mixed by tapping gently.
6. The mixture was then centrifuged at 6000 rpm for 2 minutes to precipitate down the bacterial cells.
7. The supernatant was then discarded and 200 μ l of chilled 100 mM CaCl₂ was added and mixed by tapping gently.
8. The tube was then kept in ice for at least 3 hours and continues tapping to mix occasionally.
9. Then 10-20 ng of plasmid DNA was added in the tube and mixed by gentle tapping.
10. The tube was kept in ice for another 30 minutes.
11. The cells were then set for heat shock at 42 °C in water bath for 1.5 minute.
12. Immediately the tube is kept in ice to chill it down.

13. Then 1 ml of LB was added to the tube and kept in 37 °C for at least 1 hour.
14. After 1 hour, the tube was centrifuged at 6000 rpm for 1-2 minutes to pellet the cells down.
15. 1 ml of supernatant was discarded and 200 µl of remaining supernatant was kept for mixing the bacterial pellet.
16. The cells were then plated aseptically in Luria Agar (LA) plate containing 100 µg/ml of Ampicillin (as the plasmid DNA contained ampicillin resistant gene).
17. The cells were allowed to grow on plate overnight at 37 °C.
18. Bacterial colonies were visualized on next day to confirm the successful transformation.

Plasmid purification from ampicillin resistant colonies

From the LA_{amp} plate, several ampicillin resistant positively selected bacteria colonies were selected and individually grown in 5 ml of LB overnight at 37 °C. Then plasmid DNA from each culture was isolated and purified as follows:

1. 3 ml of competent *E. coli* culture was precipitated down in 1.5 ml eppendorf tube at 13000 rpm for 1 minute in two step manner.
2. Supernatant was discarded and dried by inverting the tube on a tissue paper.
3. Then 300 µl of buffer P1 (Qiagen, Germany) containing 100 µg/ml of RNaseA was added to the tube.
4. The pellet was mixed by vigorous shaking in a vortex ensuring there is no clump remaining.
5. Then 300 µl of chilled buffer P2 (Qiagen, Germany) was added to the tube and mixed well by inverting it several time.

6. Within 3 minute, chilled buffer P3 (Qiagen, Germany) was added to the same tube and mixed well by inverting it 20 times. The solution turned cloudy white.
7. The tubes were then kept in -20 °C for 5 minutes to chill it down.
8. Then the tubes were centrifuged at 13000 rpm for 15 minutes.
9. About 800 µl of the supernatant was collected very carefully and transferred to a fresh 2 ml eppendorf tube.
10. Then 800 µl of chloroform was added to it and mixed by shaking vigorously.
11. The mixture was then centrifuged at 10000 rpm for 10 minutes.
12. Carefully the upper aqueous layer (700 µl) was transferred to another fresh 2 ml eppendorf tube.
13. 700 µl of chloroform was added to the tube containing the aqueous layer and mixed by shaking it again.
14. Then the mixture was centrifuged at 10000 rpm for 10 minutes.
15. About 600 µl of aqueous layer was transferred into a 1.5 ml eppendorf tube and same volume of Isopropanol (Merck, Germany) was added. The mixture was then kept at room temperature for 10 minutes.
16. Then it was centrifuged at 13000 rpm for 15 minutes to pellet the plasmid DNA down.
17. Supernatant was discarded and 1 ml of chilled 70% ethanol was added and shaken well.
18. Then the tubes were centrifuged again at 13000 rpm for 10 minutes.
19. The supernatant was discarded by inverting the tube against a piece of tissue paper and allowed to dry in open air until air-dried.
20. Then 20 µl of TE buffer was added to dissolve it down.

21. The plasmid DNA samples were then checked for concentration (ng/μl) and quality by UV/Vis- spectroscopy or Nanodrop spectrophotometer ($A_{260/280}$).

Confirmation of SDM product by plasmid Sanger sequencing

The plasmid sequencing strategy is similar to that of Sanger sequencing for PCR products described in section 3.2.2.4. The reaction component and the cycling parameters were somewhat different, which are tabulated in Table 40 and Table 41. The post sequencing purification was done according to the protocol described earlier in section 3.2.2.4. The bidirectional sequencing was done with T7-forward and BGH-reverse primers. The insertion of the variants was confirmed by visualization of the nucleotide sequence through Chromas Lite (Technelysum, Australia) software.

Table 40: Sanger sequencing reaction composition for plasmid sequencing

Component	Volume
10 ng/μl plasmid DNA	1.0 μl
BigDye Terminator Mix	4.0 μl
5x sequencing buffer [40 mM Tris-HCl (pH 9.0), 1 mM MgCl ₂	2.0 μl
2 μM primer	1.6 μl
RNase/DNase-free water	11.4 μl
Total volume	20 μl

Table 41: Thermocycler condition for plasmid DNA sequencing

Temperature	Time
96 °C	10 min
25 cycles of	
96 °C	10 s
55 °C	10 s
60 °C	4 min

4.2.2 Immunocytochemistry and confocal microscopy

Subcellular localization of mutant THAP1 protein was done by immunofluorescence confocal imaging. HEK293T cells were cultured and maintained in Dulbecco's Modified Eagle Medium (DMEM) supplemented with 10% Fetal Bovine Serum (FBS) and 1X Penicillin/ Streptomycin. Wild type THAP1 construct along with other mutant constructs were transfected into 80% confluent cells grown over poly D lysine coated cover slip in 35 mm culture dish with TurboFect transfection reagent (Thermo Scientific, USA) following the manufacturer's instruction. One day before transfection, at least 2.4×10^5 number of cells was seeded in a 6-well plate or 35 mm culture dish (Corning, Sigma-Aldrich) with 2 ml of complete media. Next day before transfection, the media was changed with fresh complete media. For transfection, 2 μ g of DNA was diluted in 200 μ L of serum-free DMEM. The transfection reagent was briefly vortexed and 4 μ L was added to the diluted DNA. It was mixed immediately by pipetting it up and down and incubated for 15-20 minutes at room temperature. Then the 200 μ L of transfection reagent/DNA mixture was added drop-wise to each well. The plate was gently rocked to achieve even distribution of the complexes immediately after adding the transfection reagent. The plates were incubated at 37 °C in a CO₂ incubator for 48 hours. For confocal microscopy, cells were grown on cover slip and it was washed with phosphate buffered saline (PBS) and fixed with 4% buffered formalin after 48 hours of post-transfection. The cells were then permeabilized with 0.2% Tween 20 (Sigma Aldrich, USA) in 1X PBS and blocked with 10% BSA (Sigma Aldrich, USA) in PBS. After subsequent washing, 1:500 dilution of mouse anti-V5 antibody (Thermo Scientific; R960-25) diluted in 0.1% BSA in PBS and incubated at 4 °C for overnight. Next day, after washing thrice with PBS, 1:100 dilution of Cy™2 AffiniPure Goat Anti-Mouse IgG (Jackson laboratory; 115-225-146)

was added for secondary antibody treatment and incubated 1 hour at room temperature in dark. DAPI was used for nuclear staining. Cells were mounted on glass slide with ProLong® Gold Antifade Mounting solution (Thermo Scientific, USA). Images were taken by Zeiss LSM 710 confocal microscope (Carl Zeiss, Germany) using 40X objective.

Preparation of Phosphate buffer saline

In 800 ml of distilled water, 8 g of NaCl, 0.2 g of KCl, 1.44 g of Na₂HPO₄ and 0.24 g of KH₂PO₄ were added and dissolved well by magnetic stirrer. The pH was adjusted to 7.4 with HCl. Volume was made up to 1 liter with distilled water.

4.2.3 Cycloheximide chase assay/western blot

The effect of nucleotide variation on THAP1 protein stability was evaluated by Cycloheximide treatment followed by immunoblotting in a time course manner. Cycloheximide (4-[(2R)-2-[(1S,3S,5S)-3,5-Dimethyl-2-oxocyclohexyl]-2-hydroxyethyl]piperidine-2,6-dione) is an eukaryotic protein synthesis inhibitor that interfere movement of two tRNA molecules and mRNA in relation to the ribosome thus blocking translation elongation. It is generally used in cell culture to inhibit further protein synthesis, thus enable to measure the protein degradation rate by western blotting and subsequently the protein half life.

So in this experiment, HEK293T cells were grown in 6-well plate (Corning, Sigma-Aldrich) and transfected with six different *THAP1* constructs including wild type as described in section 4.2.2. After 24 hour of transfection, cells were treated with 50 µg/ml Cycloheximide (Sigma-Aldrich) and cells were harvested on a time course manner like 0h, 6h, 12h, 24h, 32h and 48h for each constructs. Whole cell

lysates were prepared using CellLytic™ M (C2978, Sigma-Aldrich, USA) as per manufacture's instruction and protein concentrations were measured by *NanoDrop* ND-100 spectrophotometer (*NanoDrop* Technologies LLC, Wilmington, DE). 30 µg of protein from each samples were then loaded on 4-12% Criterion™ XT Bis-Tris gel (BioRad) and run for 2.5 h at 30 mA. The resolved protein bands were then transferred to PVDF membrane (BioRad) by wet transfer method. The blots were then blocked by 5% BSA and incubated with 1:5000 dilution of mouse anti-V5 antibody (Thermo Scientific; R960-25) at 4 °C overnight. Next day, the blots were washed with PBST (0.05% Tween-20 in PBS) thrice and incubated in secondary antibody HRP conjugated goat anti-mouse secondary antibody (Jackson ImmunoResearch Laboratories, West Grove, PA) in room temperature for 1 hour. The blots were then washed five times with PBST and then developed with ECL Prime kit (Amersham, GE Healthcare) as per manufacturer's instructions. For internal control, rabbit anti β-tubulin antibody (1:20000, ab6046, Abcam) was used to develop β-tubulin protein band. The densitometric band intensity measurement was done and normalized with β-tubulin bands by ImageJ software. The plot was drawn on GraphPad prism software (GraphPad, San Diego).

Cell lysate preparation by lysis buffer CellLytic™ M

The volume of CellLytic M lysis/extraction reagent to be added to the cells varies according to cell size and protein concentration required. In general, 125 µl of CellLytic M is recommended for $10^6 - 10^7$ cells. In this particular experiment for 35 mm dish, 300 µl of CellLytic™ M was used. Halt™ Protease and Phosphatase Inhibitor Cocktail (78442, Thermo Scientific, USA) was added in lysis buffer at a final concentration of 1X. The detailed protocol is given below.

1. Growth media was removed and cells were rinsed by 1X Dulbecco's phosphate buffer saline (DPBS) without dislodging the cells and the wash material was discarded.
2. 300 µl of CelLytic™ M was added to plate and incubated for 15 minute in a shaker at 4 °C.
3. The cell lysate was collected by scraping the cells from plate.
4. The lysate was centrifuged at 13000 rpm for 15 minute at 4 °C to pellet down the cellular debris.
5. The protein containing clear supernatant was then collected to a pre-chilled eppendorf tube and continued to quantify for concentration.

4.2.4 Actinomycin D chase assay/qRT-PCR

The wild type and mutant *THAP1* mRNA expression and stability assay were done by transcription inhibition by Actinomycin D treatment followed by quantitative real time PCR by TaqMan assay. Actinomycin D (2-Amino- 4,6-dimethyl- 3-oxo- 3H-phenoxazine- 1,9-dicarboxylic acid bis- [(5,12-diisopropyl- 9,13,16-trimethyl- 4,7,11,14,17-pentaoxo-hexadecahydro-10-oxa-3a,6,13,16-tetraaza-cyclopenta-cyclohexadecen - 8-yl)- amide]) is a class of antibiotic having the ability to inhibit transcription by binding DNA at the transcription initiation complex and preventing elongation of RNA chain by RNA polymerase. It could be used in cell culture to inhibit transcription for further RNA production and subsequently quantification of intrinsic RNA level by quantitative real time PCR (qPCR) in time course based analysis.

HEK293T cells were grown to 80% confluency and transfected with different *THAP1* constructs by TurboFect transfection reagent (Thermo Scientific, USA)

following the manufacturer's instruction as described in the section 4.2.3. Cells were treated with 15 μ M of Actinomycin D (A1410-2MG, Sigma-Aldrich, USA) and the cells were harvested at different time points like 0h, 2h, 4h, 6h and 8h. Total RNA was isolated from harvested cells by adding Ambion™ TRI® reagent (AM9738, Thermo Scientific, USA) and then following the manufacturer's instruction. The isolated RNA samples were then treated with DNase I (RNase-Free DNase Set, Qiagen) and purified by RNeasy MinElute Cleanup Kit (74204, Qiagen, Germany). Then the concentration and purity of RNA samples were measured by NanoDrop ND-100 spectrophotometer (NanoDrop Technologies LLC, Wilmington, DE) and RNA integrity was determined by Agilent 2100 Bioanalyzer using the Agilent RNA 6000 Nano kit. 1 μ g of purified total RNA from each sample was then reverse transcribed to cDNA by High Capacity cDNA Reverse Transcription Kit (4368814, Applied Biosystems, Thermo Scientific, USA). 10 ng of cDNA samples were used as template for TaqMan based real time PCR in a LightCycler® 480 System (Roche). The signal intensity of *THAP1* amplification was normalized with amplification signal intensity of β -actin as an internal control. $\Delta\Delta C_p$ values were calculated for each sample and fold changes were calculated with respect to wild type *THAP1* expression. The primer sequences and qPCR information is provided in Table 42. The reaction components used for qPCR is given in Table 43.

Table 42: Primer sequences used for TaqMan based qRT-PCR

Primer	Sequence (5'→3')	Transcript	Location	Purpose	Probe used	Product (bp)
THAP1_p16F	ctgctatacttggtgggttaaagt	NM_018105.2	Exon 2	qPCR	16	78
THAP1_p16R	tcttactcgaccagtccttggtaa	NM_018105.2	Exon 2			
ACTB_p11F	attggcaatgagcgggttc	NM_001101.3	Exon 4	qPCR	11	79
ACTB_p11R	agtcctgtggcatccacg	NM_001101.3	Exon 5			

Table 43: qPCR reaction component

Component	Volume used (For 25 µl reaction)
LightCycler® 480 Probes 2X master mix	5 µl
10 µM forward primer	0.2 µl
10 µM reverse primer	0.2 µl
Template cDNA (10ng/ µl)	2 µl
Probe	0.1 µl
Nuclease free water	2.5 µl
Total volume	10 µl

Preparation of Actinomycin D stock solution

As Actinomycin D (AD) is partially soluble in water, Dimethyl sulfoxide (DMSO) could be used to dissolve it properly. Thus, 50 µl of DMSO was added per 1 mg of AD powder and dissolved it properly. Then 950 µl of 1X PBS was added to make the concentration 1 mg/ml of Actinomycin D stock solution.

Protocol for total RNA extraction by Ambion™ TRI® reagent

Reagent preparation: 75% ethanol was prepared by mixing 250 µL nuclease-free water (AM9932, Thermo Scientific, USA) with 750 µL 100% ethanol (BP2818500, Fischer Scientific, USA) per mL of TRI Reagent solution to be used. An average of 10% was prepared to ensure a sufficient volume.

Protocol:

1. The growth media was poured off and cells were washed once with 1X DPBS. The washed solution was discarded.
2. Then 1 mL TRI Reagent solution was added and homogenized by pipetting the cell lysate several times to homogenize it properly.
3. The homogenate was incubated for 5 minute at room temperature.

4. Then 100 μ L of 1-bromo-3-chloropropane (BCP) (BP151, MRC Inc., USA) was added per 1 mL of TRI Reagent solution and mixed well by shaking and incubated at room temperature for 5–15 minutes.
5. Centrifuged at 13000 rpm for 10–15 minutes at 4°C, then the aqueous phase was transferred to a fresh tube.
6. To the collected aqueous phase, 500 μ L of isopropanol was added per 1 mL of TRI Reagent solution, vortexed for 5–10 sec, and incubated at room temperature for 5–10 minutes.
7. Then centrifuged at 13000 rpm for 8 min at 4–25 °C, and the supernatant was discarded.
8. 1 mL of 75% ethanol was added to the tube containing a small white pellet of total RNA. The pellet was washed with 75% ethanol.
9. Then centrifuged at 8000 rpm for 5 minute, the ethanol was removed, and the RNA pellet was allowed to air-dry briefly.
10. Then 50 μ l of nuclease-free water was added to dissolve the RNA sample and kept at 4 °C for quantification in NanoDrop ND-100 spectrophotometer.

DNase I digestion of RNA samples

RNase free DNase I (79254, Qiagen, Germany) stock solution was prepared by adding 550 μ l of nuclease free water to the solid DNase I powder (1500 Kunitz units). It was mixed gently inverting the tube.

1. To nuclease free eppendorf tube \leq 87.5 μ l of RNA sample, 10 μ l of buffer RDD and 2.5 μ l of DNase I stock solution were added. The volume was made up to 100 μ l by nuclease free water whenever applicable.
2. The mixture was incubated for 10 minute at room temperature.

3. Then continued for RNeasy MinElute Cleanup protocol.

RNeasy MinElute Cleanup protocol

Things to do before start:

1. A maximum of 45 µg RNA in a maximum starting volume of 200 µl can be used. This amount corresponds to the binding capacity of the RNeasy MinElute Spin Columns.
2. Buffer RPE is supplied as a concentrate. So, 4 volumes of 100% ethanol was added to obtain a working solution.
3. Adding β-mercaptoethanol (β-ME) to buffer RLT may be helpful when cleaning up crude preps of RNA (e.g., after salting-out methods) or samples that contain large amounts of RNases. 10 µl of β-ME was added per 1 ml of Buffer RLT.

Protocol for column based RNA cleanup

1. RNA sample volume was adjusted to 100 µl by adding nuclease free water. 350 µl of buffer RLT was added and mixed thoroughly.
2. Then 250 µl of 100% ethanol was added to the diluted RNA and mixed thoroughly by pipetting.
3. 700 µl of the mixture was applied to an RNeasy MinElute spin column in a supplied 2 ml collection tube. The tube was closed gently and centrifuged for 15 sec at ≥10000 rpm. The flow through was discarded.
4. If there is more than 700 µl of RNA sample in mixture, the step 3 can be repeated on the same MinElute spin column.
5. The spin column was placed into a new 2 ml collection tube. 500 µl buffer RPE was added onto the spin column. The tube was closed gently, and

centrifuged for 15 s at $\geq 10,000$ rpm to wash the column. The flow-through was discarded.

6. 500 μ l of 80% ethanol was added to the RNeasy MinElute Spin Column. The tube was closed gently, and centrifuged for 2 min at $\geq 10,000$ rpm to dry the silica-gel membrane. The flow-through and collection tube was discarded.
7. The RNeasy MinElute Spin Column was transferred into a new 2 ml collection tube (supplied). Centrifuged in a microcentrifuge at 13000 for 5 min with open cap of the tube. The flow-through and collection tube was discarded.
8. To elute, the spin column was transferred to a new 1.5 ml collection tube (supplied). Then 14 μ l of RNase-free water was directly added onto the center of the silica-gel membrane. Tube has been closed, and centrifuged for 1 min at 13000 rpm to elute.
9. The elute was kept in ice and proceed to quality and quantity check in NanoDrop ND-100 spectrophotometer.

Protocol for High Capacity cDNA Reverse Transcription Kit

1. All the kit components were allowed to thaw on ice.
2. The reverse transcription reaction components were mixed referring to the Table 44.
3. 10 μ L of 2 X RT master mixes was pipetted into each well of a 96-well reaction plate or individual tube.
4. Then 10 μ L of RNA sample (2 μ g) was pipetted into into each well, pipetting up and down twice for mixing.
5. The plates or tubes were sealed.

6. The plate or tubes were briefly centrifuged to spin down the contents and to eliminate any air bubbles.
7. The plate or tubes were placed on ice until to load the thermal cycler.
8. The reaction condition of PCR is tabulated in Table 45.
9. After conversion to cDNA, it could be directly used for qPCR or stored at -20 °C.

Table 44: Reaction components for single reverse transcription reaction.

Component	Volume/Reaction (μL)
10× RT Buffer	2.0
25× dNTP Mix (100 mM)	0.8
10× RT Random Primers	2.0
MultiScribe™ Reverse Transcriptase	1.0
RNase Inhibitor	1.0
Nuclease-free H ₂ O	3.2
Total per Reaction	10

Table 45: Reaction condition of thermal cycler for cDNA conversion.

Temperature	Time
25 °C	10 min
37 °C	60 min
37 °C	60 min
85 °C	5 sec
4 °C	∞

4.2.5 Dual - Luciferase assay

The core promoter sequence of *TOR1A* gene was amplified from genomic DNA sample using forward and reverse primers having restriction enzyme specific sequence of NheI-HF® (R3131S, NEB, Ipswich, MA, USA) and HindIII-HF® (R3104S,

NEB, Ipswich, MA, USA). Then the amplified sequence and pGL4.10 (E665A, Promega, Madison, WI, USA) were double digested with these two enzymes following the NEB double digest protocol. The digested PCR product and plasmid were then ligated by T4 DNA ligase (M0202S, NEB, Ipswich, MA, USA). The ligated construct was then validated by Sanger sequencing. The reporter construct (1 μ g) was transfected in HEK293T cells with nV5-pcDNA3.1-wtTHAP1 and other mutant constructs (1 μ g each individually) along with pRL-TK renilla luciferase reporter vector (E2241, Promega, Madison, WI, USA) as an internal transfection control. Cell lysates were collected after 48h of post-transfection by passive lysis buffer (Promega, Madison, WI, USA) and luminescence was measured in a GloMax® 20/20 Luminometer (Promega, Madison, WI, USA) using a dual luciferase assay kit (E1910, Promega, Madison, WI, USA) following the manufacturer's instruction. Firefly luciferase luminescence values were normalized with renilla luminescence. Luminescence value of wild type THAP1 was set to 100% and relative luminescence of other mutant constructs were calculated.

Protocol for directional cloning

The reporter construct was generated by introducing the core promoter sequence of *TOR1A* gene in pGL4.10 Firefly luciferase vector. The introduction process was done by directional cloning. The detailed protocol is described as follows.

1. The restriction sites were selected by searching the available sites in multiple cloning sequences (MCS) of pGL4.10 vector with more similar double digestion parameters. The selected sites are for Nhe I and Hind III restriction enzymes.

- Then cloning primers were designed to amplify the core promoter sequence of *TOR1A*. The forward primer contains the cutting site sequence for Nhe I and reverse primer contains the site for Hind III. This has been done following the rule of landing pad. The sequences for the primers are given in Table 46.

Table 46: Primer sequences for amplification of *TOR1A* core promoter.

Primer	Sequence (5'- 3')*	T _m (°C)	RE site
DYT1 5' F1	CTAG <u>GCTAGCG</u> AGGGGACACAGTCTTGCTC	67.7	NheI
DYT1 5' R1	CCCA <u>AAGCTT</u> CCACCCTGCTTGTTCTCGC	70.0	HindIII

*Underlined sequences are restriction enzyme cut site.

- The *TOR1A* core promoter sequence was amplified from a control human genomic DNA sample previously screened for any potential pathogenic nucleotide variation.
- The PCR product was purified by column purification protocol already described in section 3.2.2.4.
- Then the purified PCR product (at least 10 times of the plasmid vector used) and pGL4.10 vector was set for double digestion separately with NheI-HF[®] and HindIII- HF[®] enzymes and CutSmart[®] Buffer. The reaction was done at 37 °C for a maximum 30 minutes.
- Both the digested products were then purified by column purification protocol described in section 3.2.2.4.
- Then ligation reaction was done using T4 DNA ligase (NEB, USA). The amount of insert and vector was calculated in NEB ligation calculator (<https://nebiocalculator.neb.com/#!/ligation>) considering the required amount of insert to vector = 3:1.
- The ligation reaction was set according to the Table 47.

Table 47: Reaction component for ligation reaction by T4 DNA ligation.

Component	20 μ l reaction
T4 DNA Ligase Buffer (10X)	2 μ l
Vector DNA	100 ng
Insert DNA	35.5 ng
Nuclease-free water	Up to 20 μ l
T4 DNA Ligase	1 μ l

9. The reaction components were gently mixed by pipetting up and down and microfuged briefly.
10. The reaction was incubated for 2 hours in room temperature.
11. Then it was heat inactivated at 65 °C for 10 minutes.
12. Chilled in ice immediately and proceed for bacterial transformation.
13. The transformation protocol is described in the section 4.2.1.
14. The positively inserted colonies were selected by colony PCR where the whole bacterial colony was replicated through replica plate method and instead of DNA; bacterial cells of individual colonies were used for colony PCR.
15. Bacterial colonies were picked by toothpick and dissolved in 10 μ l of PCR grade water. Then the PCR components were added as used to amplify the *TOR1A* core promoter sequence. Those bacterial colonies were selected as positively inserted, gave a specific amplified product similar size to the insert length as visualized in agarose gel.
16. Then the plasmid DNA from positively inserted bacterial colony was purified as described in section 4.2.1.
17. The cloned construct was then ready to transform in cell.

Protocol for dual luciferase reaction

Preparation of reagents before start the experiment

Passive lysis buffer (PLB) was provided as 5X concentrate. 1X PLB was made by diluting it with autoclaved distilled water just before using it. 1X PLB could be stored at 4 °C for up to 1 month. Luciferase Assay Reagent II (LAR II) was prepared by resuspending the provided lyophilized Luciferase Assay Substrate in 10ml of the supplied Luciferase Assay Buffer II. LAR II is stable for one month at –20 °C or for one year when stored at –70 °C. Stop & Glo® Substrate was supplied at a 50X concentration. To prepare the working stock, 1 volume of 50X Stop & Glo® Substrate was added to 50 volumes of Stop & Glo® Buffer in a glass or siliconized polypropylene tube. Stop & Glo® Reagent may be stored at –20 °C for 15 days with no decrease in activity. The whole experimental steps are illustrated in Figure 8.

Protocol for experiment

1. Growth medium was removed from cell culture dish 48 hours of post transfection and rinsed carefully with 1X DPBS.
2. 500 µl of 1X chilled PLB was added to each 35 mm dish and kept in a rocker for 15 minute at room temperature.
3. Cellular debris was pelleted down by centrifugation at 13000 rpm for 5 minute in 4 °C temperature.
4. Clear protein containing supernatant was transferred to a new vial.
5. LARII and Stop & Glo® reagents were thawed in a water bath at room temperature and mixed well by inverting the tubes several times prior to use.

6. The assays for Firefly luciferase activity and Renilla luciferase activity were performed sequentially using one reaction tube.
7. 100 µl of LAR II was predispensed into the appropriate number of luminometer tubes to complete the desired number of DLR™ Assays.
8. The luminometer was programmed to perform a 2-second premeasurement delay, followed by a 10-second measurement period for each reporter assay.
9. Up to 20 µl of cell lysate was transferred carefully into the luminometer tube containing LAR II; mixed by pipetting 2 or 3 times. The tube was placed in the luminometer and initiate reading. As it was a manual luminometer, the reading was recorded manually.
10. Then the sample tube was removed from the luminometer, 100 µl of Stop & Glo® reagent was added and mixed by tapping several times. The tube was placed in luminometer and initiated for second reading. The reading and the ratio of firefly to renilla activity was recorded.
11. The reaction tube was discarded, and continued to the next DLR™ Assay.
12. Then all the readings for firefly luciferase activity were normalized against renilla activity. The bar diagram was generated for all mutant THAP1 activity and compared with that of wild type THAP1.

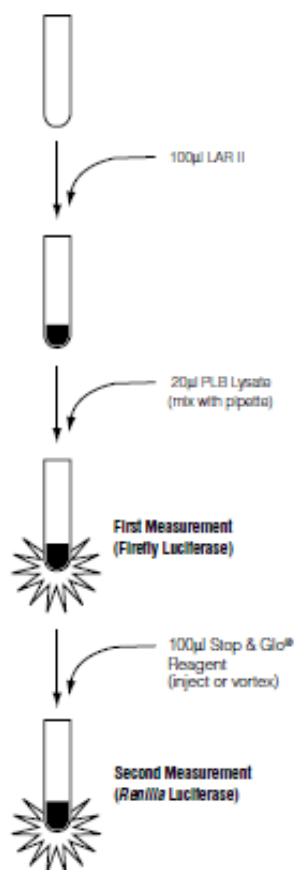


Figure 8: Format of the DLR™ Assay using a luminometer.

4.3 Results

4.3.1 Generation of different *THAP1* mutant constructs

The generation of different *THAP1* mutant constructs were successfully completed by site directed mutagenesis as confirmed by direct Sanger sequencing. The sequencing chromatograms are illustrated in Figure 9. The plasmid sequence also checked for introduction of any other unwanted nucleotide variant(s) throughout the *THAP1* ORF and also for the N-terminal V5 sequence. It was found that, apart from desired variant there was no other undesired variant(s) present.

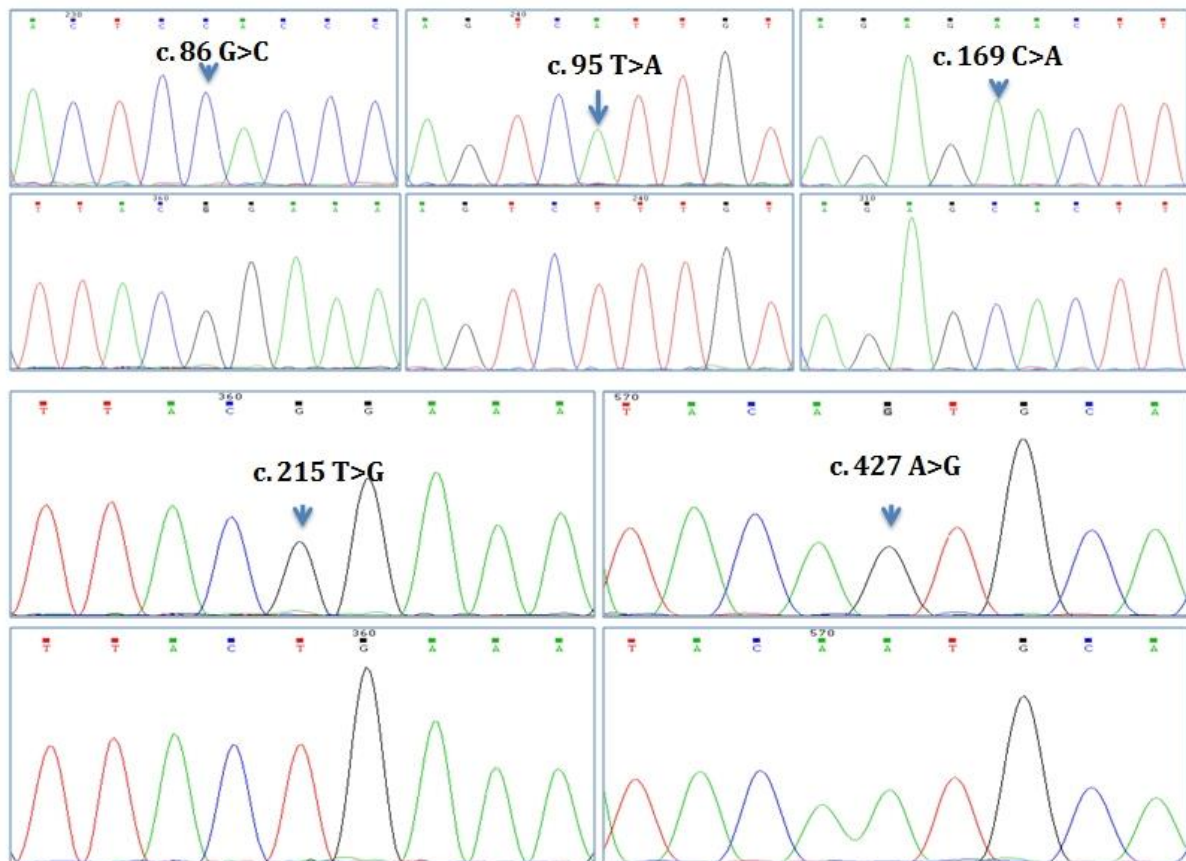


Figure 9: Representative chromatogram of *THAP1* SDM reaction products. Representative chromatogram for confirmation of successful introduction of specific nucleotide variants to generate different *THAP1* mutant constructs through site directed mutagenesis.

4.3.2 Subcellular localization of mutant THAP1 protein

In cells expressing V5-wtTHAP1 (Fig. 10, panel a-c), showing specific strong immunostaining specific to nucleus, which is normal localization of a transcription factor. The L32H (Fig. 10, panel g-i), H57N (Fig. 10, panel j-l) and L72R (Fig. 10, panel m-o) mutants all produced similar staining patterns which did not differ significantly from that of V5-wtTHAP1. Whereas R29P (Fig. 10, panel d-f) and M143V (Fig. 10, panel p-r), these two mutant form of THAP1 protein produced an perinuclear immunostaining suggesting formation of perinuclear inclusion bodies. The R29P mutation is in L2-THAP domain and M143V occurs in the coiled-coil domain of THAP1 protein, both of which does not fall under the nuclear localization signal (aa: 146-162). Though there is no gross alteration in nuclear transport, the mutant THAP1 protein gets trapped in the perinuclear space, which could be governed by interaction with some other perinuclear proteins.

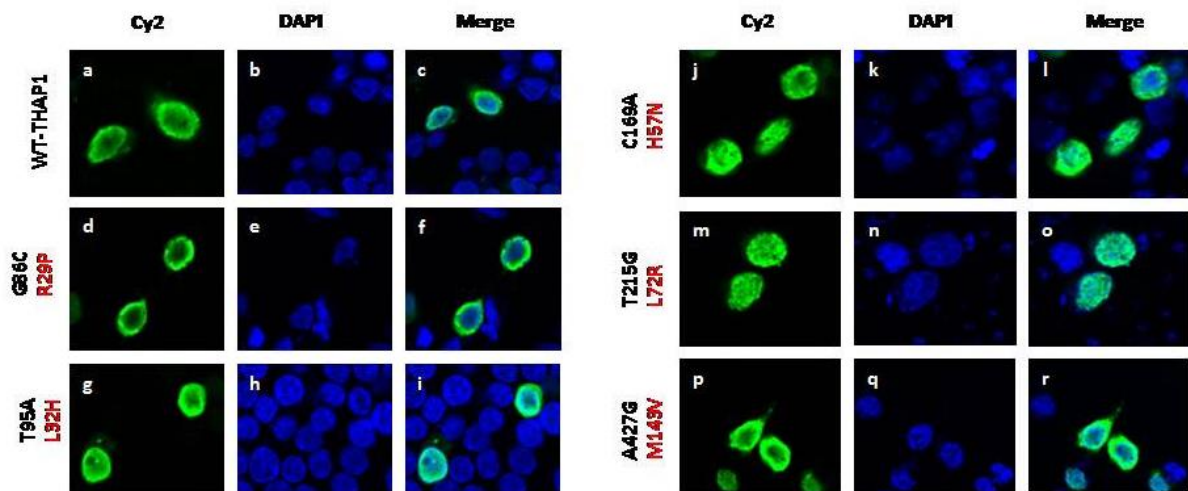


Figure 10: Subcellular localization of wild type & mutant THAP1 protein. HEK293T cells are transfected with wild type nV5-pcDNA3.1-*THAP1* or mutant constructs and after 48 h of transfection cells are fixed by paraformaldehyde and treated with 1:500 dilution of mouse anti-V5 antibody (Thermo Scientific; R960-25) and 1:100 dilution of CyTM2 AffiniPure Goat Anti-Mouse IgG (Jackson laboratory; 115-225-146). DAPI was used for nuclear staining. Images were taken by Zeiss LSM 710 confocal microscope under 40X objective.

4.3.3 Mutant THAP1 protein stability determination

Mutant THAP1 protein stability was determined by Cycloheximide chase/immunoblotting assay (Fig. 11a). Cycloheximide used as a eukaryotic translational elongation blocker. Here it was found that, at time $t = 0$ h the protein abundance of R29P is relatively higher (expression fold ≈ 1.3), while M143V is relatively lower (expression fold ≈ 0.55) than the wild type THAP1 protein (Fig. 11c).

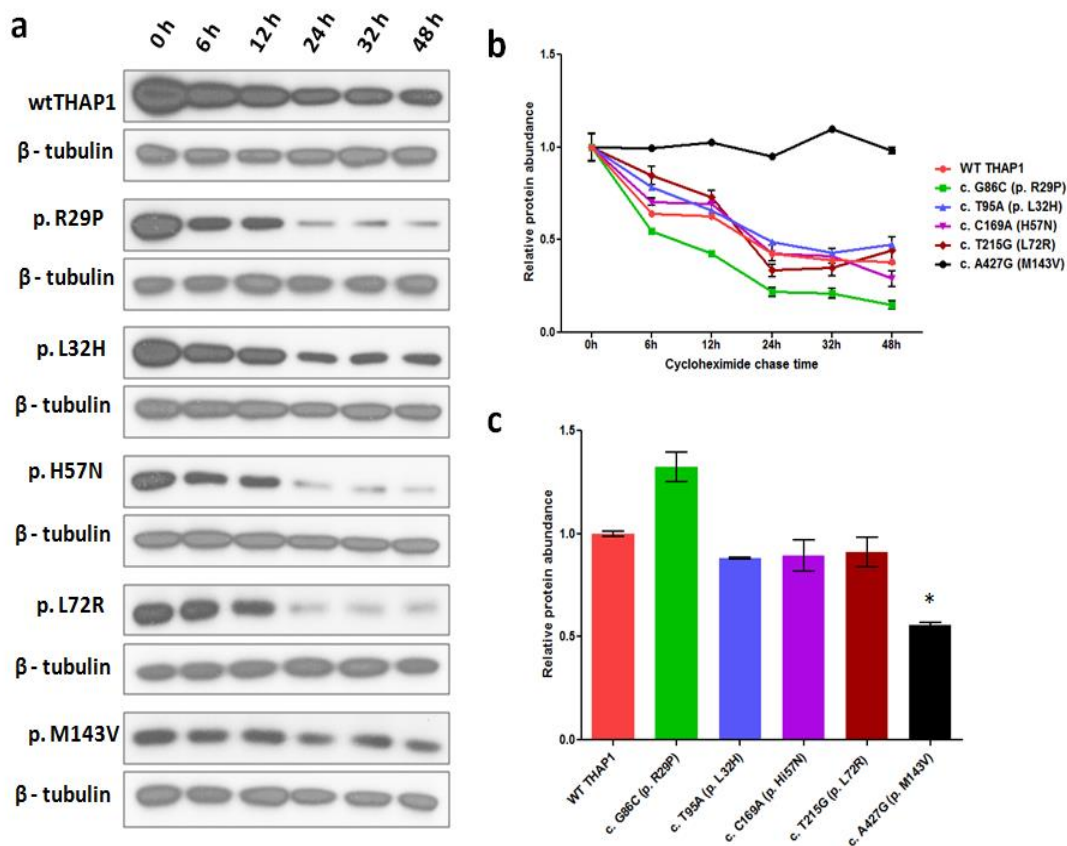


Figure 11: THAP1 mutant protein stability determination by cycloheximide chase/ western blot assay. a) Representative western blot images of wild type and mutant THAP1 proteins harvested in different time points after cycloheximide treatment. 30ug whole cell protein was loaded in each lane and β – tubulin was developed as internal control. b) Quantification of cycloheximide-chase/immunoblot assay monitoring mutant THAP1 stability compared to wild type one. Protein expression at $t = 0$ h of cycloheximide treatment was set as 1 (100%) and quatitation was done as time course analysis. c) Relative protein expression at time $t = 0$ h of wild type and mutant THAP1 proteins as determined by western blot. * $p < 0.05$ as calculated by student t-test.

The protein expression of other mutant form of THAP1 protein is comparable to the expression of wild type one (Fig. 11c). But when the protein abundances at different time point of Cycloheximide treatment were plotted, it was found that the R29P is less stable than wild type THAP1 protein, whereas the mutant M143V is much more stable than wild type one and apparently have a steady state expression during the time course (Fig. 11b). The stability of other mutant form of THAP1 is equivalent to that of wild type THAP1 protein (Fig. 11b). This time course plot was generated considering the protein expression of different THAP1 proteins at time $t = 0$ h as 100% expression (Expression fold = 1).

4.3.4 Mutant *THAP1* mRNA stability assay

To understand the differential protein expression of mutant THAP1, the *THAP1* gene expression and the respective mRNA stability assay was done by actinomycin D treatment followed by TaqMan based qRT-PCR. Actinomycin D is able to block eukaryotic transcription by binding DNA at the transcription initiation complex and preventing elongation of RNA chain by RNA polymerase (700). *THAP1* gene expression was determined by respective *THAP1* mRNA quantification at time $t = 0$ h of actinomycin D treatment by two step qRT-PCR followed by calculation of $\Delta\Delta C_p$ values. THAP1 transcript expression was normalized with that of β -actin as internal control. Considering the mRNA expression of wild type *THAP1* as 100% (expression fold = 1), the relative fold change of mutant *THAP1* mRNA were depicted in Figure 12a. It has been found that, the relative expression of T95A mutant *THAP1* mRNA is significantly down-regulated to 35% with respect to that of wild type *THAP1* mRNA. Whereas the expression of other mutant forms including G86C (p. R29P) and A427G (p. M143V) were comparable to wild type expression.

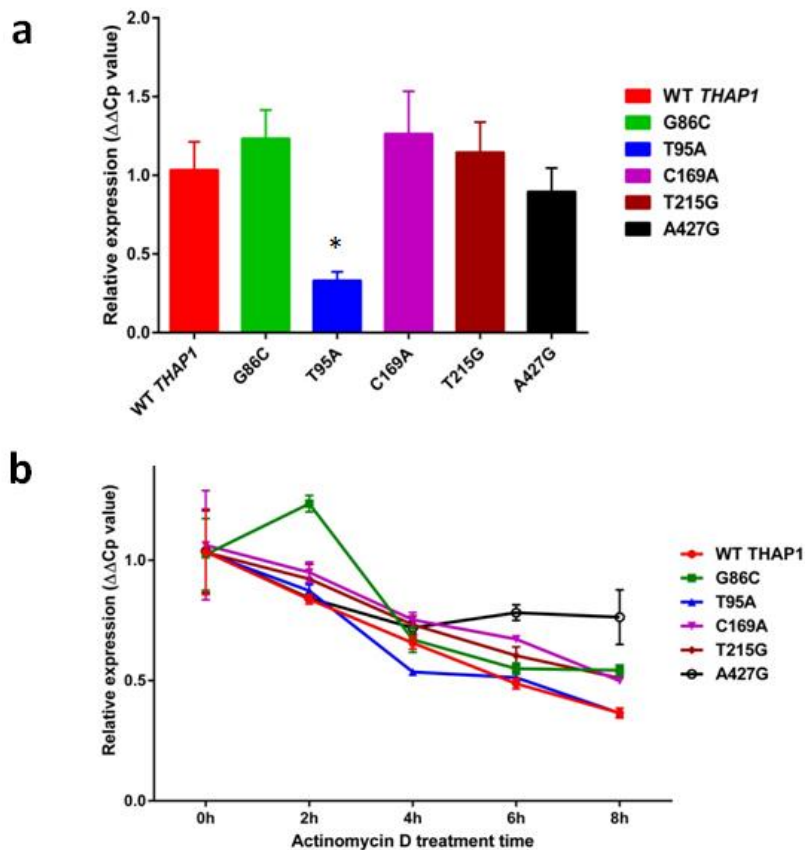


Figure 12: *THAP1* mutant mRNA stability assay by actinomycin D treatment followed by TaqMan based qRT-PCR. a) Relative expression of wild type and mutant *THAP1* transcripts normalized with β -actin expression as internal control. * $p < 0.05$ as calculated by student t-test. b) Mutant *THAP1* mRNA stability determination compared to wild type *THAP1* mRNA at different time points. The expression values at time $t = 0$ h was set to 100% (expression fold = 1) and quantitation was done as time course analysis.

THAP1 mRNA quantification at different time point of actinomycin D treatment was done to assess the effect of nucleotide variation to the relative mRNA stability, which revealed that all the mutant *THAP1* mRNA have the comparable stability with respect to that of wild type one (Fig. 12b). So, this experiment suggests that, none of the mutation have any effect on the *THAP1* mRNA stability, while the T95A variant has a significant role in down regulation of *THAP1* mRNA expression. This time course plot was generated considering the mRNA expression of different *THAP1* variants at time $t = 0$ h as 100% expression (Expression fold = 1).

4.3.5 Effect of *THAP1* mutation over *TOR1A* transcription

Dual luciferase assay was done to assess the mutant THAP1 protein activity over *TOR1A* gene expression. The experimental results showed decreased luciferase signal intensity for THAP1 R29P, H57N, L72R and M143V, whereas an increased luciferase signal for L32H compared to that of wild type THAP1 protein (Figure 13). As THAP1 protein acts as transcriptional repressor, the L32H mutation disrupts the THAP1 repressor activity, whereas other mutations enhance the repressor activity, thereby decreasing luciferase signal intensity.

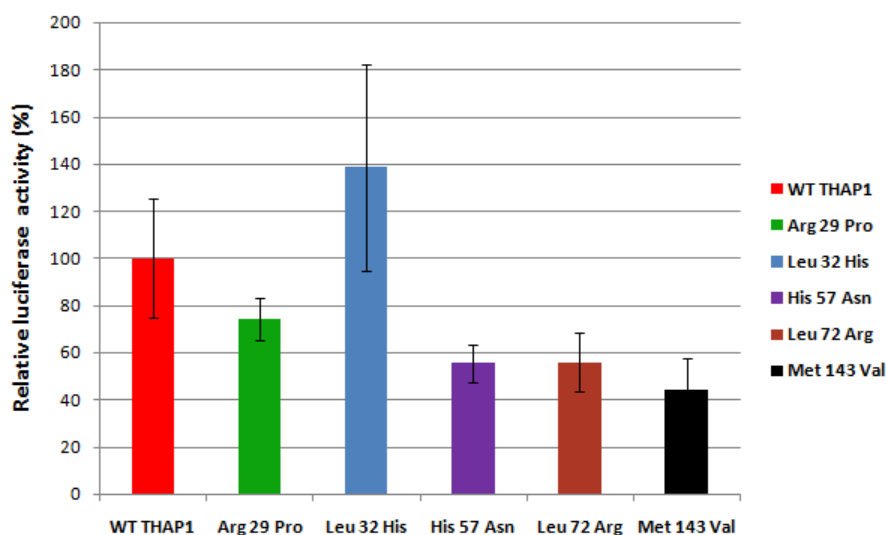


Figure 13: Effect of *THAP1* missense changes on *TOR1A* repression as measured by dual luciferase assay. Activity of THAP1 was measured by repression of the *TOR1A* promoter in a luciferase reporter gene assay. Wild type THAP1-mediated repression of the *TOR1A* core promoter activity was set as 100%. The luciferase intensity of Leu32His was higher than the wild type protein. All other missense changes resulted in lower luciferase activity of 40 to 75%. Bars indicate standard error.

4.4 Discussion

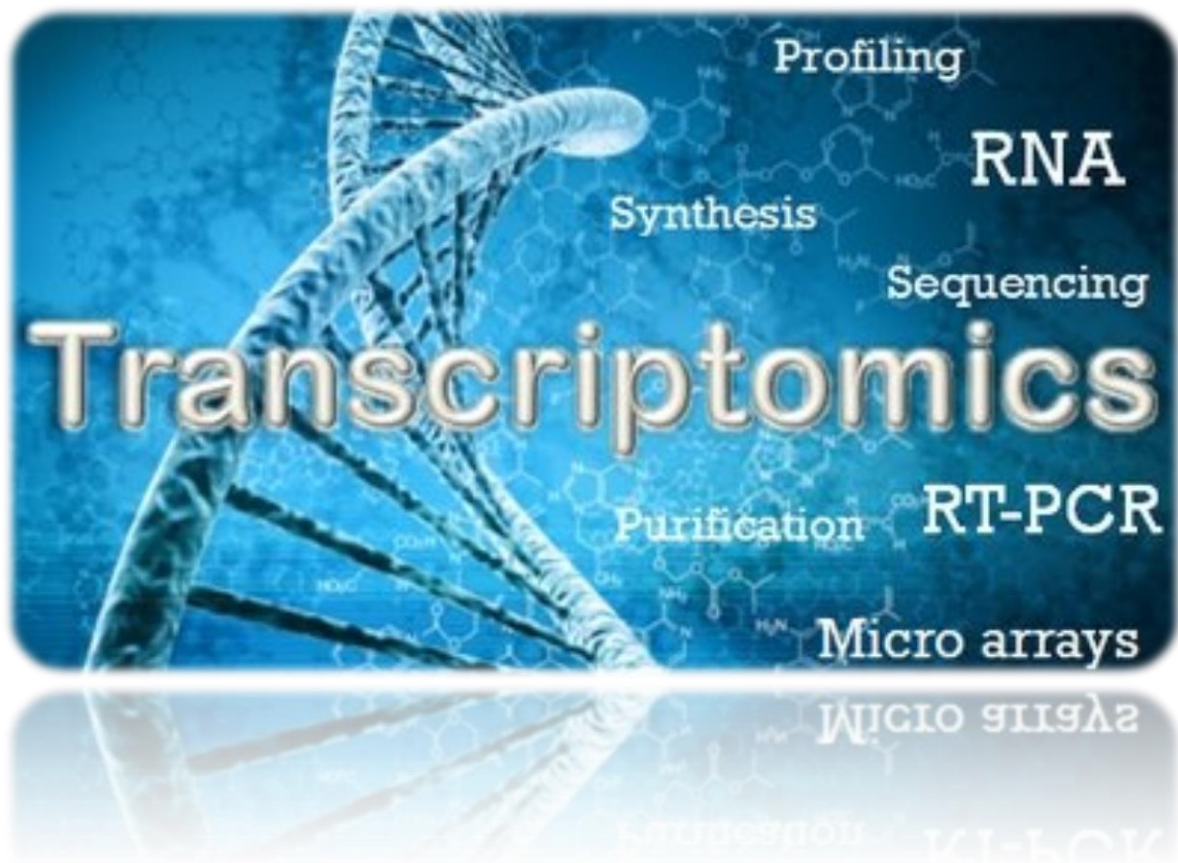
To understand the underlying molecular mechanism of primary isolated dystonia, a total of five missense pathogenic nucleotide variants were selected [c. 86 G>C (THAP domain), c. 95 T>A (THAP domain), c. 169 C>A (THAP domain), c. 215 T>G (THAP domain) and c. 427 A>G (Coiled-coil domain)] for functional characterization. The first experiment done was determination of subcellular localization of mutant THAP1 protein by confocal immunofluorescence microscopy. It has been found that c. 86 G>C (p. R29P) and c. 427 A>G (p. M143V) mutant THAP1 localized in the perinuclear space, where other mutants have a normal localization in nucleus as that of wild type THAP1. Though the R29P mutant falls in the DNA binding THAP domain, it shows a similar effect as reported for another mutation C54Y (329). It is uncertain whether the perinuclear inclusions formed by R29P mutant are relevant to DYT6 pathogenesis, or if they bear any relationship to the abnormal membrane structures induced by torsinA Δ E. Nuclear envelop (NE) dysfunction has been implicated as a mechanism underlying DYT1 dystonia (148), this observation may propose that there could be interactions between THAP1 and the NE that require further analysis. On the other hand, M143V mutation occurs in the NLS (aa146-162) linker region, it could affect the nuclear localization as some mutations within NLS linkers have been shown to disrupt nuclear trafficking (701).

The next experiment was the assessment of mutant THAP1 protein stability by Cycloheximide chase followed by western blot. Cycloheximide was used as a translation inhibitor and the mutant THAP1 proteins are subjected to cellular internal quality control mechanism. Here it was found that the initial protein abundances (at time $t = 0$ h) for THAP1-R29P was 30% higher while the abundance of THAP1-M143V was \approx 45% lower than that of wild type THAP1. Further time course analysis

surprisingly revealed that though the initial protein abundance of THAP1-R29P was quite high, but it is unstable and degrades in a much faster rate than wild type THAP1 protein. On the contrary, THAP1-M143V initial protein abundance was lower but much more stable than the wild type THAP1 during the course of Cycloheximide chase. The initial protein abundances and stability for other mutants were comparable to wild type THAP1. For THAP1-R29P, the lower stability could be explained by the fact that cell possess different strategies to get rid of pathogenic misfolded mutant proteins (702-704). In the case of THAP1-M143V, though the protein expression was lowered, a compensatory higher protein stability was observed (705, 706) suggesting a nontoxic effect of this mutation.

To corroborate this protein abundances and stability in the transcription level, mutant *THAP1* mRNA expression and stability were investigated by actinomycin D treatment followed by TaqMan based qRT-PCR. This experiment demonstrated the comparable transcript expression of all the mutants compared to wild type *THAP1* transcript except for c. 95 T>A, which was significantly downregulated by 70%. However, this downregulation of transcription was not reflected in the protein level, where p.L32H protein abundance and stability was identical to that of wild type THAP1. This may be due to enhanced translation efficiency by slowing down the translational elongation (707). Time course analysis for all the mutant *THAP1* mRNA stability did not identify any aberrant stability. To further characterize the effect *THAP1* mutations upon the *TOR1A* transcription, reporter gene assay was done by dual luciferase assay. For this instance, it was found that only THAP1-L32H partially abolished the THAP1 repressor activity, while the other mutant forms enhanced the repressor activity followed by decrease transcriptional level of *TOR1A* as identified

by luciferase signal intensity. This could cause a stoichiometric imbalance of cellular torsinA, which could in turn trigger the primary dystonia pathogenesis.



CHAPTER 5

WHOLE GENOME GENE EXPRESSION
ANALYSIS OF PRIMARY DYSTONIA
PATIENTS HAVING *THAP1* MUTATION
BY RNA-SEQUENCING

5.1 Introduction

THAP1 protein is well characterized as a transcription factor, which contain an N-terminal DNA binding THAP domain (327) followed by a proline rich region and a nuclear localization signal. The protein exclusively localized in the nucleus, where it co-localizes with DAXX (Death domain associated protein), a well-characterized protein that is expressed in promyelocytic leukemia (PML) nuclear bodies (NBs). It has been previously found that ectopic expression of THAP1 could specifically target the pivotal genes involved in cell cycle progression with a special emphasis with pRb-E2F pathway (336). Through the same study, it has been found that siRNA based *THAP1* gene silencing lead to the inhibition of G1/S cell cycle progression and down regulation of certain genes involved in pRB-E2F pathway and S-phase DNA synthesis (336). In another study, using patient's lymphoblastoid cells having THAP1 gene variant, it has been found that the THAP1 variant could enhance the apoptosis by demonstrating fewer cells in G2 phase than the control lymphoblastoid cells (335). Microarray based differentially expressed gene expression analysis revealed that the mutant *THAP1* affect the genes involved in DNA synthesis, cell growth and proliferation, cell survival and cytotoxicity (335). So, based on these experimental evidences, it is absolutely essential to identify the global differentially expressed genes due to the *THAP1* mutation(s). This could be a potential approach to recognize the common molecular mechanism of primary dystonia pathogenesis, which develops due to mutation in *THAP1* gene.

In this experimental chapter, I have performed a whole genome gene expression experiment based on RNA-seq approach by using total RNA samples extracted from patient's fibroblast samples having different pathogenic *THAP1* mutations and age-gender matched control fibroblast samples.

5.2 Materials & Methods

5.2.1 Selection of patient and control subjects

For the transcriptome analysis, the selection of patient samples and control subjects is critical. The patient samples having the *THAP1* variants, should be pathogenic as predicted by different algorithm based on pathogenicity scoring and degree of conservation. Here in this study, we have collected fore arm skin fibroblast tissue from primary dystonia patients having different *THAP1* missense variants (Table 48). Among them six patient fibroblast samples were selected, as the *THAP1* variants for them were predicted as potential pathogenic through analysis in dbNSFP v2.0 algorithm. The age and gender matched control fibroblast samples were collected from Coriell Biorepository (Coriell Institute for Medical Research, Camden, NJ, USA) through database searching. All the patient and control individuals were Caucasian in ethnicity. All the fibroblast samples were checked for mycoplasma contamination prior to *in-vitro* culture by MycoFluor™ Mycoplasma detection kit (M7006, Thermo Scientific, USA).

RNA sequencing based gene expression analysis

Table 48: *THAP1* genotype and pathogenicity values of patient and control fibroblast samples.

Patient ID	Gender	Age of onset	Age of investigation	Family History	Nucleotide Variant	Amino acid change	fathmm-score	fathmm-pred	MetaSVM_score	MetaSVM_pred	CADD		Control ID	Gender	Age
											RawScore	PHRED			
ML10	M	6	43	Positive	c.46 A>G	K16E	0.94215	D	1.2071	D	6.18	28.6	ML9	M	44
ML8	M	6	20	Negative	c.161 G>A	C54Y	0.99236	D	0.8793	D	5.87	27.30	ML7	M	24
ML11	M	53	62	Positive	c.446 T>C	I149T	0.98367	D	0.7269	D	5.56	26.40	ML12	M	55
ML1	F	43	56	Negative	c.50 A>G	D17G	0.94215	D	0.389	D	3.02	22.30	ML4	F	48
ML2	F	51	58	Negative	c.395 T>C	F132S	0.93716	D	0.3156	D	1.81	15.05	ML6	F	50
ML3	F	Unknown	70	Positive	c.153C>G	S51R	0.98841	D	1.0373	D	5.82	27.20	ML5	F	71

FATHMM: *Functional Analysis Through Hidden Markov Models*, pathogenic threshold value > 0.5; **MetaSVM:** Ensemble score (Meta) using Support Vector Machine, pathogenic threshold value > 0.2; **CADD:** Combined annotation dependent depletion, pathogenic PHRED > 15. **D:** Deleterious, **T:** Tolerated.

5.2.2 Fibroblast cell culture

The fibroblast samples of patients preserved in liquid nitrogen in a 2 ml cryovial (Corning, Sigma, USA) containing complete growth medium with 5% DMSO were taken out and thawed immediately in a 37 °C water bath prior to set it for *in-vitro* culture. The whole content of the vial was transferred to a 15 ml centrifuge tube (Corning, Sigma, USA) prefilled with 5 ml of complete growth media, the cells were pelleted down by centrifugation at 3000 rpm for 3 minute. The washed supernatant was discarded and the cell pellet was reconstituted with 2 ml of complete growth media. It was then transferred to a 75 cm² culture flask and filled with 14 ml of complete growth media. The flask was placed in 37 °C incubator with 5% CO₂ and grown for 90-95% confluency. The culture media was changed in an interval of 4-5 days. The whole procedure has been done aseptically under the BL-2 grade laminar flow cabinet equipped with HEPA filter. The complete growth media contained DMEM (Gibco, Thermo Scientific, USA) supplemented with 10% FBS (Corning, Sigma, USA) and 1X Penicillin/ Streptomycin (15140122, Gibco, Thermo Scientific, USA). The confluency percentage was checked under the light microscope. The control fibroblast samples were delivered in completely filled T25 (25 cm²) culture flask by Coriell Biorepository. The quality of cell was verified by integrity of cell-sheet and presence of any contamination. Then the media was discarded and rinsed once with 1X DBPS. The cell sheet was dislodged by trypsin digestion as described below.

Trypsinization of cultured cells

1. To the already rinsed cell sheet, 3 ml of 0.05% Trypsin/EDTA (25300054, Gibco, Thermo Scientific, USA) was added.

2. The cells were incubated at 37⁰C for 7-8 minutes, till the complete dissociation under light microscope.
3. 5 ml of complete growth media was added to stop the reaction. The cells were suspended by mild pipetting up and down.
4. The whole content was then transferred to a 15 ml centrifuge tube and cells were pelleted down by centrifuge it at 3000 rpm for 3 minute.
5. The cell pellet was resuspended and set for culture as described previously.

The genotype of THAP1 for each patient was identified through population based genetic screening study and again confirmed by extracting the genomic DNA from fibroblast cells followed by direct Sanger sequencing of all the exons of *THAP1*.

Extraction of genomic DNA from fibroblast cells

To isolate the genomic DNA from fibroblast cells, DNA isolation kit for cells (Roche, USA) was used. At least 1 X 10⁷ cells were collected from cell culture flask by trypsinizing as described above. The detailed protocol is as follows.

1. 3 ml of cellular lysis buffer was added to the cell kept in 15 ml centrifuge tube.
2. Homogenize until the cells are in fine suspension by brief vortexing.
3. Then 2 μ l of Proteinase K solution was added and mixed well by brief vortex.
4. Then the tube was kept at 65 ⁰C for at least 2 hours.
5. 100 μ l of 10mg/ml RNaseA solution was added and mixed well by brief vortexing.
6. The sample was then kept in 37 ⁰C for at least 30 minutes.
7. Then 1.2 ml of protein precipitation solution was added to each sample and vortexed thoroughly for 10 seconds and placed in ice.

8. The sample was then centrifuged at 14000 rpm for 20 minutes at room temperature.
9. The supernatant containing DNA was then transferred very carefully to a new centrifuge tube without disturbing the pellet.
10. To the supernatant, 0.7 volume of isopropanol was added and mixed by inverting the tube several times to precipitate DNA, centrifuged at 2500 rpm for 10 minutes to pellet down the DNA sample.
11. After centrifugation, the supernatant was discarded and 2 ml of 70% ethanol was added and shook to wash the DNA pellet.
12. Then the tube was centrifuged at 2500 rpm for 10 minutes to pellet the DNA again.
13. The wash solution was then discarded and the DNA pellet was allowed to air-dry briefly.
14. To resuspend the DNA, 1 ml of TE buffer (pH 8.0) was added and kept at 4 °C overnight to dissolve it properly.

5.2.3 Isolation and purification of total RNA from fibroblast samples

The total RNA including small RNA were isolated and purified from fibroblast samples using miRNeasy mini kit (217004, Qiagen, Germany) following manufacturer's instruction.

Preparation of reagents

Buffers RWT and RPE were supplied as concentrates. Required volumes of ethanol (96%–100%) was added as indicated on the bottle, to obtain a working solution.

Protocol

1. Fibroblast cells were grown in a T-75 culture flask up to 95% confluency to attain a cell number 1×10^7 .
2. The cell culture media was removed and rinsed once with 1X DPBS.
3. For direct lysis of cells grown in a monolayer, 700 μ l QIAzol Lysis Reagent was added to the cell-culture dish. The lysate was collected with a rubber policeman.
4. The lysate was pipetted into a microcentrifuge tube and mixed thoroughly by vortexing or pipeting to ensure that no cell clumps are visible.
5. To homogenize the cells, QIAshredder homogenizer was used. Homogenized cell lysates could be stored at -70°C for several months.
6. The tube containing the homogenate was placed at room temperature (15–25 $^\circ\text{C}$) for 5 min.
7. 140 μ l chloroform was added to the homogenate and mixed by shaking vigorously for 15 second.
8. The homogenate was placed at room temperature for 2–3 minute, then centrifuged for 15 minute at 13000 rpm at 4 $^\circ\text{C}$.
9. About 350 μ l of the aqueous phase (upper layer) was transferred to a new collection tube. Then 1.5 volumes (525 μ l) of 100% ethanol was added and mixed thoroughly by pipetting up and down several times. Continued without delay with step 10.
10. Up to 700 μ l of the sample was loaded into an RNeasy Mini spin column in a 2 ml collection tube. The lid was closed gently and centrifuged at $\geq 10,000$ rpm for 15 seconds at room temperature. The flow-through was discarded.

11. Step 11 was repeated using the remainder of the sample. The flow-through was discarded.
12. 700 μ l Buffer RWT was added to the RNeasy Mini spin column. The lid was closed gently and centrifuged at $\geq 10,000$ rpm for 15 seconds at room temperature to wash the column. The flow-through was discarded.
13. Up to 500 μ l Buffer RPE was added onto the RNeasy Mini spin column. The lid was closed gently and centrifuged at $\geq 10,000$ rpm for 15 seconds at room temperature to wash the column. The flow-through was discarded.
14. Another 500 μ l Buffer RPE was added to the RNeasy Mini spin column. The lid was closed gently and centrifuged at $\geq 10,000$ rpm for 2 minutes to dry the RNeasy Mini spin column membrane.
15. The RNeasy Mini spin column was placed into a new 2 ml collection tube and the old collection tube was discarded with the flow-through. Centrifuged in a microcentrifuge at 13000 rpm for 1 min.
16. The RNeasy Mini spin column was transferred to a new 1.5 ml nuclease free collection tube. 50 μ l RNase-free water was added directly onto the RNeasy Mini spin column membrane. The lid was closed gently and centrifuged at $\geq 10,000$ rpm for 1 min to elute the RNA.
17. The eluted RNA sample was then kept in ice and continued with determination of quantity and quality by NanoDrop ND-100 spectrophotometer. The RNA Integrity Number (RIN) was determined by Agilent Bioanalyzer 2100 (Agilent Technologies, USA) using Agilent RNA 6000 Nano Kit (Agilent Technologies, USA).

5.2.4 Sequencing library preparation for RNA-seq

The purified total RNA samples were used to generate the 100 bp RNA-seq library using TruSeq RNA Sample Prep Kit v2 (Illumina, USA) following the manufacturer's protocol. The general workflow is given in Figure 14 and the detailed protocol is described below.

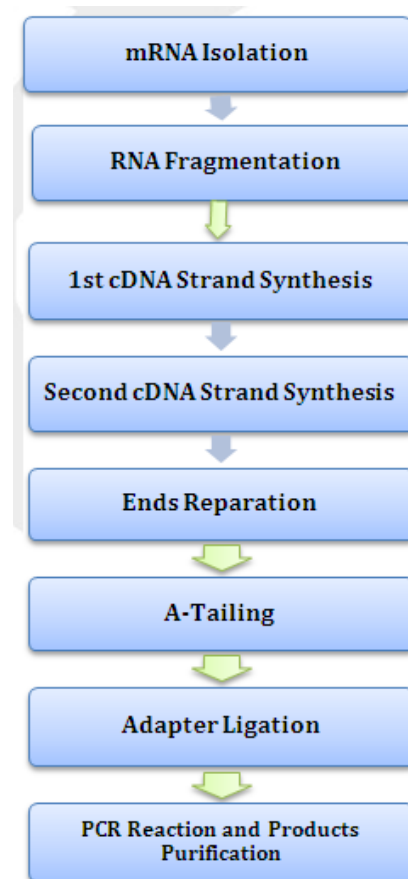


Figure 14: TruSeq RNA sample preparation v2 workflow for eukaryote transcriptome library construction.

5.2.4.1 Purify and fragment mRNA

This process purifies the polyA containing mRNA molecules using oligo-dT attached magnetic beads using two rounds of purification. During the second elution of the polyA RNA, the RNA is also fragmented and primed for cDNA synthesis (Figure 15).

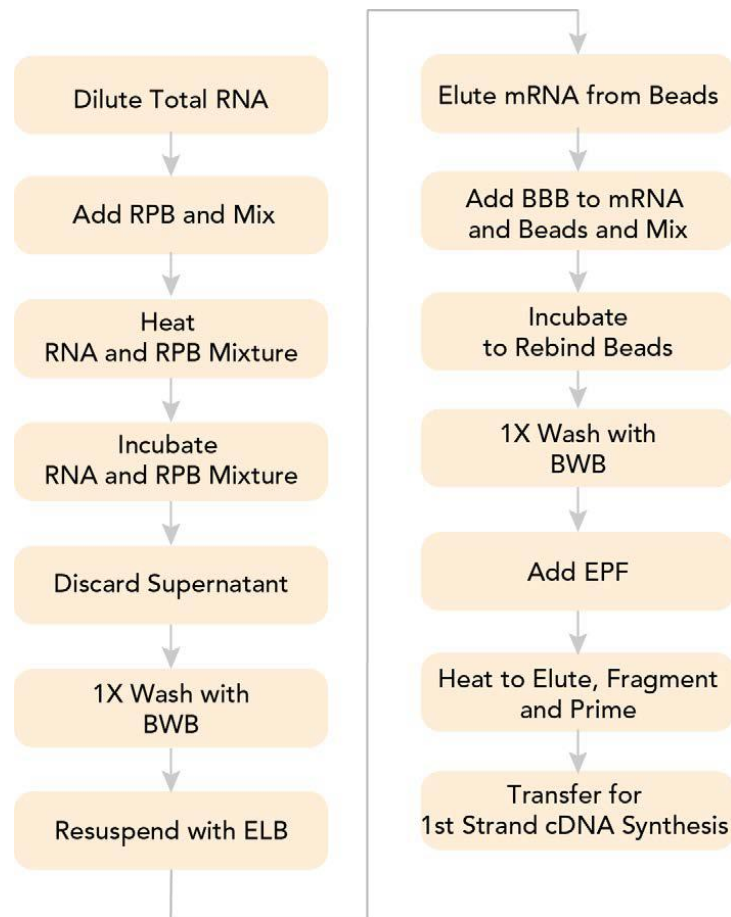


Figure 15: TruSeq RNA sample preparation v2 mRNA purification and fragmentation workflow.

Reagents preparation

The following items were removed from -25°C to -15°C storage and thawed at room temperature: 1. Bead Binding Buffer (BBB), Bead Washing Buffer (BWB), Elution Buffer (ELB), Elute, Prime, Fragment Mix (EPF), Resuspension Buffer (RSB).

The RNA Purification Beads (RPB) tube was removed from 4°C storage and let stand to bring to room temperature. The Resuspension Buffer (RSB) can be stored at 4°C after the initial thaw. After use in this procedure, the Bead Binding Buffer, Bead Washing Buffer and Elution Buffer were stored at 4°C for subsequent experiments.

Programming the thermal cycler

The thermal cycler was pre-programmed with the following programs:

- Choose the pre-heat lid option and set to 100 °C
- 65 °C for 5 minutes, 4 °C hold—saved as **mRNA Denaturation**
- 80 °C for 2 minutes, 25 °C hold—saved as **mRNA Elution 1**
- 94 °C for 8 minutes, 4 °C hold—saved as **Elution 2 - Frag - Prime**

RBP preparation

1. The total RNA was diluted with nuclease-free ultra pure water to a final volume of 50 µl in the new 96-well 0.3 ml PCR plate labeled with the RBP barcode.
2. RNA Purification Beads were vortexed vigorously at room temperature to resuspend the oligo-dT beads.
3. 50 µl RNA Purification Beads were added to each well of the RBP plate to bind the polyA RNA to the oligo-dT beads. Gently pipetted the entire volume up and down 6 times to mix thoroughly.
4. The RBP plate was sealed with a Microseal 'B' adhesive seal.

Incubation 1 RBP

1. The sealed RBP plate was placed on the pre-programmed thermal cycler. Close the lid and select **mRNA Denaturation step** (65 °C for 5 minutes, 4 °C hold) to denature the RNA and facilitate binding of the polyA RNA to the beads.

2. The RBP plate was removed from the thermal cycler when it reaches 4 °C and then incubated at room temperature for 5 minutes to allow the RNA to bind to the beads.

Wash RBP

1. The adhesive seal was removed from the RBP plate and then placed on the magnetic stand at room temperature for 5 minutes to separate the polyA RNA bound beads from the solution.
2. All of the supernatant from each well of the RBP plate was removed and discarded.
3. The RBP plate was removed from the magnetic stand.
4. The beads were washed by adding 200 µl Bead Washing Buffer in each well of the RBP plate to remove unbound RNA. Gently pipetted the entire volume up and down 6 times to mix thoroughly.
5. The RBP plate was placed on the magnetic stand at room temperature for 5 minutes.
6. The thawed Elution Buffer was centrifuged at 600 × g for 5 seconds.
7. All of the supernatant from each well of the RBP plate was removed and discarded. The supernatant contains most of the ribosomal and other non-messenger RNA.
8. The RBP plate was removed from the magnetic stand.
9. 50 µl Elution Buffer was added in each well of the RBP plate. Gently pipetted the entire volume up and down 6 times to mix thoroughly.
10. The RBP plate was sealed with a Microseal 'B' adhesive seal.
11. The Elution Buffer tube was stored at 4 °C.

Incubation 2 RBP

1. The sealed RBP plate was placed on the pre-programmed thermal cycler. Closed the lid and **mRNA Elution 1** (80 °C for 2 minutes, 25 °C hold) was selected to elute the mRNA from the beads. Both the mRNA and any contaminant rRNA that have bound the beads nonspecifically are released.
2. The RBP plate was removed from the thermal cycler when it reaches 25 °C was placed at room temperature.
3. Then the adhesive seal was removed from the RBP plate.

RFP preparation

1. The Bead Binding Buffer thawed and then centrifuged at 600 × g for 5 seconds.
2. 50 µl Bead Binding Buffer was added to each well of the RBP plate. This allows mRNA to specifically rebind the beads, while reducing the amount of rRNA that non-specifically binds. Gently pipetted the entire volume up and down 6 times to mix thoroughly.
3. The RBP plate was incubated at room temperature for 5 minutes and the Bead Binding Buffer tube was stored at 4 °C.
4. The RBP plate was placed on the magnetic stand at room temperature for 5 minutes.
5. All of the supernatant was removed and discarded from each well of the RBP plate.
6. Then the RBP plate was removed from the magnetic stand.

7. The beads were washed by adding 200 μ l Bead Washing Buffer in each well of the RBP plate. Gently pipetted the entire volume up and down 6 times to mix thoroughly.
8. The Bead Washing Buffer tube was stored at 4 $^{\circ}$ C.
9. The RBP plate was placed on the magnetic stand at room temperature for 5 minutes.
10. All of the supernatant was removed and discarded from each well of the RBP plate. The supernatant contains residual rRNA and other contaminants that were released in the first elution and did not rebind the beads.
11. The RBP plate was removed from the magnetic stand.
12. Then 19.5 μ l Elute, Prime, Fragment Mix was added to each well of the RBP plate. Gently pipetted the entire volume up and down 6 times to mix thoroughly. The Elute, Prime, Fragment Mix contains random hexamers for RT priming and serves as the first strand cDNA synthesis reaction buffer.
13. The RBP plate was sealed with a Microseal 'B' adhesive seal.
14. The Elute, Prime, Fragment Mix tube was stored at -20 $^{\circ}$ C.

Incubate RFP

1. The sealed RBP plate was placed on the pre-programmed thermal cycler. The lid was closed and **Elution 2 - Frag - Prime** (94 $^{\circ}$ C for 8 minutes, 4 $^{\circ}$ C hold) step was selected to elute, fragment, and prime the RNA.
2. The RBP plate was removed from the thermal cycler when it reached 4 $^{\circ}$ C and centrifuged briefly.
3. Immediately carried on to *Synthesize First Strand cDNA*.

5.2.4.2 Synthesis of first strand cDNA

This process reverse transcribes the cleaved RNA fragments primed with random hexamers into first strand cDNA using reverse transcriptase and random primers.

Reagent preparation

One tube of First Strand Master Mix was removed from -20 °C storage and thawed it at room temperature. In note, the First Strand Master Mix with SuperScript II added is stable to additional freeze-thaw cycles and can be used for subsequent experiments. If more than six freeze-thaw cycles are anticipated, divide the First Strand Master Mix into smaller aliquots and store at -25 °C to -15 °C. A CDP barcode label was added to a new 96-well 0.3 ml PCR plate.

Programming the thermal cycler

The thermal cycler was pre-programmed with the following program and saved as

1st Strand:

- Choose the pre-heat lid option and set to 100°C
- 25 °C for 10 minutes
- 42 °C for 50 minutes
- 70 °C for 15 minutes
- Hold at 4 °C.

cDNA Plate (CDP) preparation

1. The RBP plate was placed on the magnetic stand at room temperature for 5 minutes. The plate was kept on the magnetic stand.
2. The adhesive seal was removed from the RBP plate.

3. Then 17 μ l of the supernatant (fragmented and primed mRNA) was transferred from each well of the RBP plate to the corresponding well of the new 0.3 ml PCR plate labeled with the CDP barcode.
4. The thawed First Strand Master Mix tube was centrifuged at 600 \times g for 5 seconds.
5. Then 50 μ l SuperScript II was added to the First Strand Master Mix tube. As the entire contents of the First Strand Master Mix tube was not used, SuperScript II was added at a ratio of 1 μ l SuperScript II for each 9 μ l First Strand Master Mix. Mixed gently and thoroughly, and centrifuged briefly. The First Strand Master Mix tube was labelled to indicate that the SuperScript II has been added.
6. 8 μ l First Strand Master Mix and SuperScript II mix was added to each well of the CDP plate. Gently pipetted the entire volume up and down 6 times to mix thoroughly.
7. The CDP plate was sealed with a Microseal 'B' adhesive seal and centrifuged briefly.
8. The First Strand Master Mix tube was kept to -20 $^{\circ}$ C storage immediately after use.

Incubation 1 CDP

1. The sealed CDP plate was placed on the pre-programmed thermal cycler. Closed the lid, and then the **1st Strand** program was selected for run.
 - a. Choose the pre-heat lid option and set to 100 $^{\circ}$ C
 - b. 25 $^{\circ}$ C for 10 minutes
 - c. 42 $^{\circ}$ C for 50 minutes
 - d. 70 $^{\circ}$ C for 15 minutes

- e. Hold at 4 °C
2. When the thermal cycler reached at 4 °C, the CDP plate was removed from the thermal cycler and continued immediately to *Synthesize Second Strand cDNA*.

5.2.4.3 Synthesis of Second Strand cDNA

This process removes the RNA template and synthesizes a replacement strand to generate ds cDNA. AMPure XP beads are used to separate the ds cDNA from the second strand reaction mix.

Reagent preparation

The Second Strand Master Mix (SSM) was removed from -20 °C storage and thawed at room temperature. The Resuspension Buffer was removed from 4 °C and brought it to room temperature. The AMPure XP beads was removed from storage and let stand for at least 30 minutes to bring them to room temperature. The thermal cycler was pre-heated to 16 °C. An IMP barcode label was applied to a new 96-well 0.3 ml PCR plate.

Addition of SSM

1. The thawed Second Strand Master Mix was centrifuged at 600 × g for 5 seconds.
2. The adhesive seal was removed from the CDP plate.
3. 25 µl thawed Second Strand Master Mix was added to each well of the CDP plate. Gently pipetted the entire volume up and down 6 times to mix thoroughly.
4. The CDP plate was sealed with a Microseal 'B' adhesive seal.

Incubation 2 CDP

1. The sealed CDP plate was placed on the pre-heated thermal cycler. Closed the lid and incubated at 16 °C for 1 hour.
2. The CDP plate was removed from the thermal cycler and placed on the bench.
3. The adhesive seal was removed from the CDP plate.
4. The CDP plate was then cooled to room temperature.

Purification of CDP

1. The AMPure XP beads were vortexed until they are well dispersed.
2. Then 90 µl well-mixed AMPure XP beads were added to each well of the CDP plate containing 50 µl ds cDNA. Gently pipetted the entire volume up and down 10 times to mix thoroughly.
3. The CDP plate was incubated at room temperature for 15 minutes.
4. The CDP plate was then placed on the magnetic stand at room temperature, for 5 minutes to make sure that all of the beads are bound to the side of the wells.
5. About 135 µl of the supernatant was remove and discarded from each well of the CDP plate. The CDP plate was left on the magnetic stand while performing the following 80% EtOH wash steps (6–8).
6. With the CDP plate on the magnetic stand, 200 µl freshly prepared 80% EtOH was added to each well without disturbing the beads.
7. The CDP plate was incubated at room temperature for 30 seconds, and then all of the supernatant removed and discarded from each well.

8. The steps 6 and 7 were repeated one time for a total of two 80% EtOH washes.
9. The CDP plate was left to stand at room temperature for 15 minutes to dry, and then removed from the magnetic stand.
10. The thawed, room temperature Resuspension Buffer was centrifuged at 600 × g for 5 seconds.
11. Then 52.5 µl Resuspension Buffer was added to each well of the CDP plate. Gently pipetted the entire volume up and down 10 times to mix thoroughly.
12. The CDP plate was incubated at room temperature for 2 minutes.
13. The CDP plate was then placed on the magnetic stand at room temperature for 5 minutes.
14. 50 µl supernatant (ds cDNA) was transferred from the CDP plate to the new 96-well 0.3 ml PCR plate labeled with the IMP barcode.
15. The library preparation was carried on for *End Repair*. The process could be stopped here by sealing the IMP plate with a Microseal 'B' adhesive seal and stored at -20 °C for up to seven days.

5.2.4.4 Perform End Repair

This process converts the overhangs resulting from fragmentation into blunt ends using an End Repair Mix. The 3' to 5' exonuclease activity of this mix removes the 3' overhangs and the polymerase activity fills in the 5' overhangs.

Reagent preparation

End Repair Control (CTE) and End Repair Mix (ERP) were removed from -20 °C storage and thawed them at room temperature. The Resuspension Buffer was removed from 4 °C storage and brought to room temperature. The AMPure XP

beads were also removed from storage and let stand for at least 30 minutes to brought them to room temperature. The thermal cycler was pre-heated to 30 °C. An ALP barcode label was applied to a new 96-well 0.3 ml PCR plate.

Preparation of IMP

1. As the in-line control reagent was used the thawed End Repair Control tube was centrifuged at 600 × g for 5 seconds. The End Repair Control was diluted to 1/100 in Resuspension Buffer (1 µl End Repair Control + 99 µl Resuspension Buffer) before use. The diluted End Repair Control was discarded after use. Then 10 µl of diluted End Repair Control was added to each well of the IMP plate that contained 50 µl ds cDNA.
2. 40 µl End Repair Mix was added to each well of the IMP plate containing the ds cDNA. Gently pipetted the entire volume up and down 10 times to mix thoroughly.
3. The IMP plate was sealed with a Microseal 'B' adhesive seal.

Incubation of IMP

1. The sealed IMP plate was placed on the pre-heated thermal cycler. Closed the lid and incubated at 30 °C for 30 minutes.
2. The IMP plate was removed from the thermal cycler.

Clean Up of IMP

1. The adhesive seal was removed from the IMP plate.
2. The AMPure XP beads were vortexed to mix until they are well dispersed.
3. Then 160 µl well-mixed AMPure XP beads were added to each well of the IMP plate containing 100 µl End Repair Mix. Gently pipetted the entire volume up and down 10 times to mix thoroughly.

4. The IMP plate was incubated at room temperature for 15 minutes.
5. The IMP plate was placed on the magnetic stand at room temperature for 5 minutes or until the liquid is clear.
6. Using a 200 μ l single channel, 127.5 μ l of supernatant was removed and discarded from each well of the IMP plate.
7. Step 6 was repeated one time. The IMP plate was left on the magnetic stand while performing the following 80% EtOH wash steps (8–10).
8. With the IMP plate on the magnetic stand, 200 μ l freshly prepared 80% EtOH was added to each well without disturbing the beads.
9. The IMP plate was then incubated at room temperature for 30 seconds, and then removed and discarded all of the supernatant from each well. Care was taken for not to disturb the beads.
10. Steps 8 and 9 were repeated one more time for a total of two 80% EtOH washes.
11. The IMP plate left stand at room temperature for 15 minutes to dry, and then the plate was removed from the magnetic stand.
12. 17.5 μ l Resuspension Buffer was added to each well of the IMP plate. Gently pipetted the entire volume up and down 10 times to mix thoroughly.
13. The IMP plate was incubated at room temperature for 2 minutes.
14. Then the IMP plate was placed on the magnetic stand at room temperature for 5 minutes or until the liquid is clear.
15. 15 μ l of supernatant was transferred from each well of the IMP plate to the corresponding well of the new 0.3 ml PCR plate labeled with the ALP plate barcode.

16. Then continued to the step *Adenylate 3' Ends* or it can safely stopped here by sealing the ALP plate with a Microseal 'B' adhesive seal and store at -20°C for up to 7 days.

Adenylate 3' Ends

A single 'A' nucleotide is added to the 3' ends of the blunt fragments to prevent them from ligating to one another during the adapter ligation reaction. A corresponding single 'T' nucleotide on the 3' end of the adapter provides a complementary overhang for ligating the adapter to the fragment. This strategy ensures a low rate of chimera (concatenated template) formation.

Preparation of reagents

A-Tailing Control and A-Tailing Mix were Removed the following from -20 °C storage and thawed them at room temperature and then place them on ice. The Resuspension Buffer was removed from 4 °C storage and brought to room temperature.

Programming of thermal cycler

The thermal cycler was pre-programmed with the following parameters and saved as

ATAIL70:

- Choose the pre-heat lid option and set to 100 °C
- 37 °C for 30 minutes
- 70 °C for 5 minutes
- Hold at 4 °C

Addition of ATL

1. As the in-line control reagent was used, the thawed A-Tailing Control tube was centrifuged at 600 × g for 5 seconds. Then the A-Tailing Control was diluted to 1/100 in Resuspension Buffer (For example, 1 µl A-Tailing Control + 99 µl Resuspension Buffer) before use. A-Tailing Control was discarded after use. Then 2.5 µl diluted A-Tailing Control was added to each well of the ALP plate.
2. 12.5 µl thawed A-Tailing Mix was added to each well of the ALP plate. Gently pipetted the entire volume up and down 10 times to mix thoroughly.
3. The ALP plate was sealed with a Microseal 'B' adhesive seal.

Incubation 1 ALP

1. The sealed ALP plate was placed on the pre-programmed thermal cycler. Closed the lid, then the **ATAIL70** program was selected for run.
 - a. The pre-heat lid option was selected and set to 100°C
 - b. 37 °C for 30 minutes
 - c. 70 °C for 5 minutes
 - d. Hold at 4 °C
2. When the thermal cycler temperature is 4 °C, the ALP plate was removed from the thermal cycler, and then continued immediately to *Ligate Adapters* step.

5.2.4.5 Ligate Adapters

This process ligates multiple indexing adapters to the ends of the ds cDNA, preparing them for hybridization onto a flow cell.

Reagent preparation

Ligation Control, RNA Adapter Index tubes and Stop Ligation Buffer removed from -20 °C and thawed at room temperature. The Resuspension Buffer was removed from 4 °C storage and brought to room temperature. The AMPure XP beads were removed from storage and let stand for at least 30 minutes to brought them to room temperature. A CAP barcode label and a PCR barcode label were applied to a new 96-well 0.3 ml PCR plate.

Addition of LIG

1. Centrifuge the thawed RNA Adapter Index tubes, Ligation Control (if using Ligation Control), and Stop Ligation Buffer tubes at 600 × g for 5 seconds.
2. Immediately before use, remove the Ligation Mix tube from -25 °C to -15 °C storage.
3. Remove the adhesive seal from the ALP plate.
4. As the in-line control reagent was used, the Ligation Control was diluted to 1/100 in Resuspension Buffer (1 µl Ligation Control + 99 µl Resuspension Buffer) before use. The diluted Ligation Control was discarded after use. Then 2.5 µl diluted Ligation Control was added to each well of the ALP plate.
5. 2.5 µl Ligation Mix was added to each well of the ALP plate.
6. The Ligation Mix tube was returned back to -20 °C storage immediately after use.
7. 2.5 µl thawed RNA Adapter Index was added to each well of the ALP plate. Gently pipette the entire volume up and down 10 times to mix thoroughly.
8. The ALP plate was sealed with a Microseal 'B' adhesive seal.

Incubation 2 of ALP

1. The sealed ALP plate was placed on the pre-heated thermal cycler. Closed the lid and incubated at 30 °C for 10 minutes.
2. The ALP plate from the thermal cycler was removed.

Addition of STL

1. The adhesive seal was removed from the ALP plate.
2. 5 µl Stop Ligation Buffer was added to each well of the ALP plate to inactivate the ligation. Gently pipetted the entire volume up and down 10 times to mix thoroughly.

Cleaning Up ALP

1. The AMPure XP beads were vortexed for at least 1 minute or until they are well dispersed.
2. 42 µl mixed AMPure XP beads were added to each well of the ALP plate. Gently pipetted the entire volume up and down 10 times to mix thoroughly.
3. The ALP plate was incubated at room temperature for 15 minutes.
4. The ALP plate was placed on the magnetic stand at room temperature for 5 minutes or until the liquid is clear.
5. 79.5 µl of supernatant from each well of the ALP plate was removed and discarded. Care was taken for not to disturb the beads. The ALP plate was left on the magnetic stand while performing the following 80% EtOH wash steps (6–8).
6. With the ALP plate on the magnetic stand, 200 µl freshly prepared 80% EtOH was added to each well without disturbing the beads.

7. The ALP plate was incubated at room temperature for 30 seconds, and then removed and discarded all of the supernatant from each well. Care was taken for not to disturb the beads.
8. Steps 6 and 7 were repeated one time for a total of two 80% EtOH washes.
9. With the ALP plate on the magnetic stand, the samples were allowed to air-dry at room temperature for 15 minutes.
10. The ALP plate was removed from the magnetic stand.
11. The Resuspension Buffer, 52.5 μ l was added to each well of the ALP plate. Gently pipetted the entire volume up and down 10 times to mix thoroughly or until the beads are fully resuspended.
12. The ALP plate was incubated at room temperature for 2 minutes.
13. The ALP plate was placed on the magnetic stand at room temperature for 5 minutes or until the liquid is clear.
14. 50 μ l of supernatant was transferred from each well of the ALP plate to the corresponding well of the new 0.3 ml PCR plate labeled with the CAP barcode. Care was taken for not to disturb the beads.
15. The AMPure XP beads were vortexed until they are well dispersed.
16. 50 μ l mixed AMPure XP beads were added to each well of the CAP plate for a second cleanup. Gently pipetted the entire volume up and down 10 times to mix thoroughly.
17. The CAP plate was incubated at room temperature for 15 minutes.
18. The CAP plate was then placed on the magnetic stand at room temperature for 5 minutes or until the liquid is clear.
19. 95 μ l of supernatant from each well of the CAP plate was removed and discarded. Care was taken for not to disturb the beads. The CAP plate was

- left on the magnetic stand while performing the following 80% EtOH wash steps (20–22).
20. With the CAP plate on the magnetic stand, 200 μ l freshly prepared 80% EtOH was added to each well. Care was taken for not to disturb the beads.
 21. The CAP plate was incubated at room temperature for 30 seconds, and then all of the supernatant from each well was removed and discarded. Care was taken for not to disturb the beads.
 22. The steps 20 and 21 were repeated one time for a total of two 80% EtOH washes.
 23. With the CAP plate on the magnetic stand, the samples left for air-dry at room temperature for 15 minutes, and then the plate was removed from the magnetic stand.
 24. 22.5 μ l Resuspension Buffer was added to each well of the CAP plate. Gently pipetted the entire volume up and down 10 times to mix thoroughly until the beads are fully resuspended.
 25. The CAP plate was incubated at room temperature for 2 minutes.
 26. The CAP plate was placed on the magnetic stand at room temperature for 5 minutes until the liquid is clear.
 27. 20 μ l of supernatant from each well of the CAP plate was transferred to the corresponding well of the new 0.3 ml PCR plate labeled with the PCR barcode. Care was taken for not to disturb the beads.
 28. Continued to the step *Enrich DNA Fragments*. Otherwise the PCR plate was sealed with a Microseal 'B' adhesive seal and stored at -20 $^{\circ}$ C for up to 7 days.

5.2.4.6 Enrich DNA Fragments

This process uses PCR to selectively enrich those DNA fragments that have adapter molecules on both ends and to amplify the amount of DNA in the library. The PCR is performed with a PCR Primer Cocktail that anneals to the ends of the adapters. Minimize the number of PCR cycles to avoid skewing the representation of the library. PCR enriches for fragments that have adapters ligated on both ends. Fragments with only one or no adapters on their ends are by-products of inefficiencies in the ligation reaction. Neither species can be used to make clusters. Fragments without any adapters cannot hybridize to surface-bound primers in the flow cell. Fragments with an adapter on only one end can hybridize to surface bound primers, but cannot form clusters.

Reagent preparation

The PCR Master Mix (PMM) and PCR Primer Cocktail (PPC) were removed from -20°C storage and thawed them at room temperature and then place them on ice. The thawed PCR Master Mix and PCR Primer Cocktail tubes were centrifuged at 600 × g for 5 seconds. The Resuspension Buffer was removed from 4 °C storage and brought it to room temperature. The AMPure XP beads were removed from 4 °C storage and let stand for at least 30 minutes to bring them to room temperature. A TSP1 barcode label was applied to a new 96-well 0.3 ml PCR plate.

Programming of thermal cycler

The thermal cycler was pre-programmed with the following program and save as

PCR:

- Choose the pre-heat lid option and set to 100 °C

- 98 °C for 30 seconds
- 15 cycles of:
 - 98 °C for 10 seconds
 - 60 °C for 30 seconds
 - 72 °C for 30 seconds
- 72 °C for 5 minutes
- Hold at 10 °C

Preparation for PCR

1. 5 µl of thawed PCR Primer Cocktail was added to each well of the PCR plate.
2. Then 25 µl of thawed PCR Master Mix was added to each well of the PCR plate. Gently pipetted the entire volume up and down 10 times to mix thoroughly.
3. The PCR plate was sealed with a Microseal 'B' adhesive seal.

Amplification by PCR

1. The sealed PCR plate was placed on the pre-programmed thermal cycler. Closed the lid, then **PCR** programme was selected and set for run to amplify the plate.
 - a. Choose the pre-heat lid option and set to 100 °C
 - b. 98 °C for 30 seconds
 - c. 15 cycles of:
 - 98 °C for 10 seconds
 - 60 °C for 30 seconds
 - 72 °C for 30 seconds
 - d. 72 °C for 5 minutes

- e. Hold at 10 °C

Clean Up PCR

1. The adhesive seal was removed from the PCR plate.
2. The AMPure XP Beads were vortexed until they are well dispersed.
3. 50 µl mixed AMPure XP Beads were added to each well of the PCR plate containing 50 µl of PCR amplified library. Gently pipetted the entire volume up and down 10 times to mix thoroughly.
4. The PCR plate was incubated at room temperature for 15 minutes.
5. The PCR plate was placed on the magnetic stand at room temperature for 5 minutes or until the liquid is clear.
6. 95 µl of supernatant was removed and discarded from each well of the PCR plate. The PCR plate was left on the magnetic stand while performing the following 80% EtOH wash steps (7–9).
7. With the PCR plate on the magnetic stand, 200 µl freshly prepared 80% EtOH was added to each well without disturbing the beads.
8. The PCR plate was incubated at room temperature for 30 seconds, and then removed and discarded all of the supernatant from each well.
9. The steps 7 and 8 were repeated one time for a total of two 80% EtOH washes.
10. With the PCR plate on the magnetic stand, the samples were left to air-dry at room temperature for 15 minutes and then the plate was removed from the magnetic stand.

11. The dried pellet was resuspended in each well with 32.5 µl Resuspension Buffer. Gently pipetted the entire volume up and down 10 times to mix thoroughly.
12. The PCR plate was incubated at room temperature for 2 minutes.
13. Then the PCR plate was placed on the magnetic stand at room temperature for 5 minutes or until the liquid is clear.
14. 30 µl of clear supernatant was transferred from each well of the PCR plate to the corresponding well of the new 0.3 ml PCR plate labeled with the TSP1 barcode.
15. Then continued to *Validate Library* step. Otherwise the TSP1 plate was sealed with a Microseal 'B' adhesive seal and stored at -20°C for up to seven days.

5.2.4.7 Validate Library

Quality control analysis is important for sample library and quantification of the DNA library templates.

Quantify Libraries

To achieve the highest-quality data on Illumina sequencing platforms, it is important to create optimum cluster densities across every lane of the flow cell. Optimizing cluster densities requires accurate quantitation of DNA library templates. It was quantified using qPCR according to the Illumina *Sequencing Library qPCR Quantification Guide (part # 11322363)*.

Quality Control

Quality of library was done on an Agilent Technologies 2100 Bioanalyzer. To do it, 1 µl of resuspended construct was loaded on an Agilent Technologies 2100 Bioanalyzer using a DNA-specific chip Agilent DNA 1000.

The validated libraries were then normalized and pooled as per the standard guidelines provided in the *TruSeq Sample Preparation Pooling Guide (part # 15042173)*. Then for sequencing purpose, cluster generation was done and the libraries were set for sequencing in a HiSeq 2000 (Illumina, USA) instrument following the standard protocol. This whole process was outsourced to Beijing Genomics Institute (BGI, Beijing, China).

5.2.5 RNA-seq data analysis

The sequencing raw data files for each sample were extracted from server connected to HiSeq 2000. The sequencing files were in .fq format. Then the quality of sequencing was evaluated through Galaxy/SlipStream server of University of Tennessee Health Science Center, Memphis, USA (<https://galaxy.uthsc.edu>). The quality of 100 bp paired end sequencing (Forward and reverse sequencing) was evaluated on the 1. Quality score across all bases, 2. Quality score distribution over all sequences, 3. GC distribution over all sequences, 4. N content across all bases, 5. Sequence length distribution. The sequence alignment and normalized read counts were done through STAR online software following the STAR manual 2.3.0.1(708) considering hg38 as reference sequence. The normalized read counts for both the patients and controls were counted and fold change were calculated based on average read counts for both the patient and control groups. The significance (p value) was calculated based on two-tailed heteroscedastic student t-test and the p value ≤ 0.05 was taken as a significant one. The false discovery rate (FDR) was calculated by Benjamini–Hochberg (BH) procedure and ≤ 0.05 value was considered as significant one. Ingenuity Pathway Analysis was done on IPA[®] software (IPA, Qiagen, USA) for network analysis and molecular annotation.

5.3 Results

5.3.1 Quality and quantity determination of isolated total RNA samples

The total RNA samples isolated from patient and control fibroblast samples were evaluated for concentration (A_{260}) and purity ($A_{260/280}$). The $A_{260/280}$ cut off value was set to 1.9 where any RNA samples have $A_{260/280}$ value lower than that was not selected for further processing. Then the RNA samples were checked for its RIN (RNA integrity number) value which is pivotal for RNA-seq library preparation. All the samples were selected which have the RIN value at least 9 out of 10. The RNA quality and yield data is depicted below (Table 49). The electropherogram of these 12 samples were shown in Figure 16 & 17.

Table 49: The quality and concentration determined for total RNA samples.

Sample No	Concentration (ng/ μ l)	$A_{260/280}$	RIN value	28S/18S
ML1	88	1.96	9.7	1.7
ML2	93	1.98	10.0	1.9
ML3	163	2.00	9.7	1.7
ML4	114	1.98	9.6	1.6
ML5	73	1.97	9.7	1.7
ML6	118	2.1	9.8	1.8
ML7	43	2.06	10.0	1.9
ML8	56	2.02	10.0	2.0
ML9	41	1.98	10.0	2.0
ML10	60	2.02	10.0	1.9
ML11	41	2.00	10.0	1.9
ML12	43	1.96	10.0	2.0

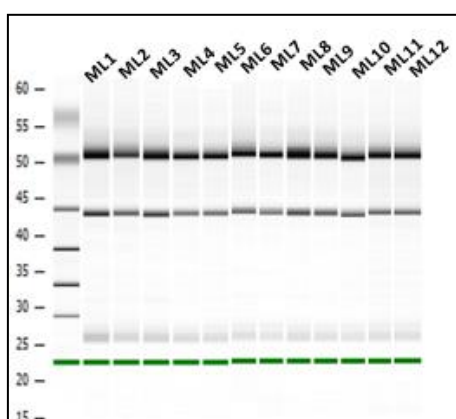
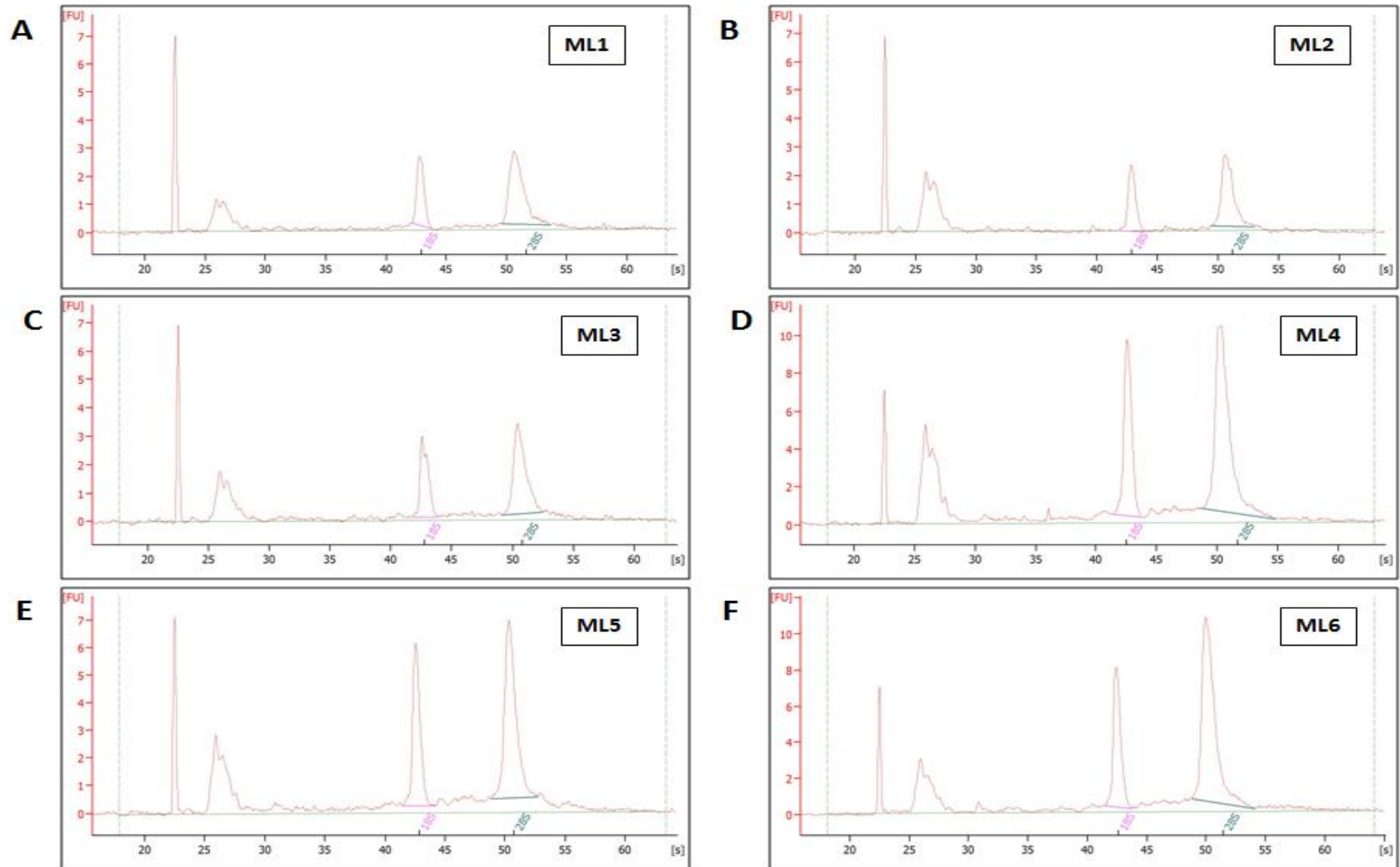


Figure 16: Representative electropherogram of the RNA samples from fibroblast samples.



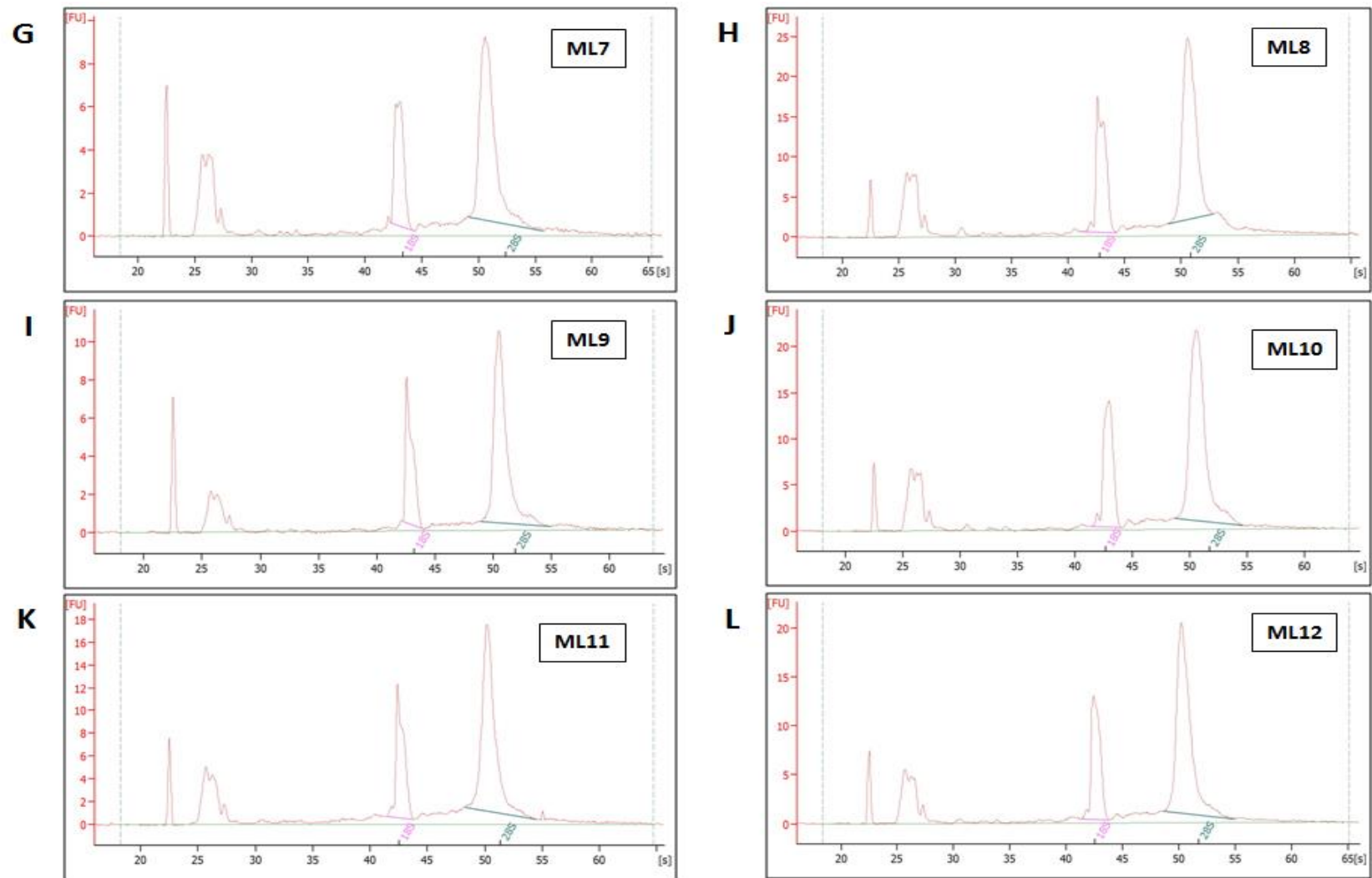


Figure 17: The representative chromatograms of RNA electrophoresis in Agilent 2000 Bio-analyzer for individual RNA samples.

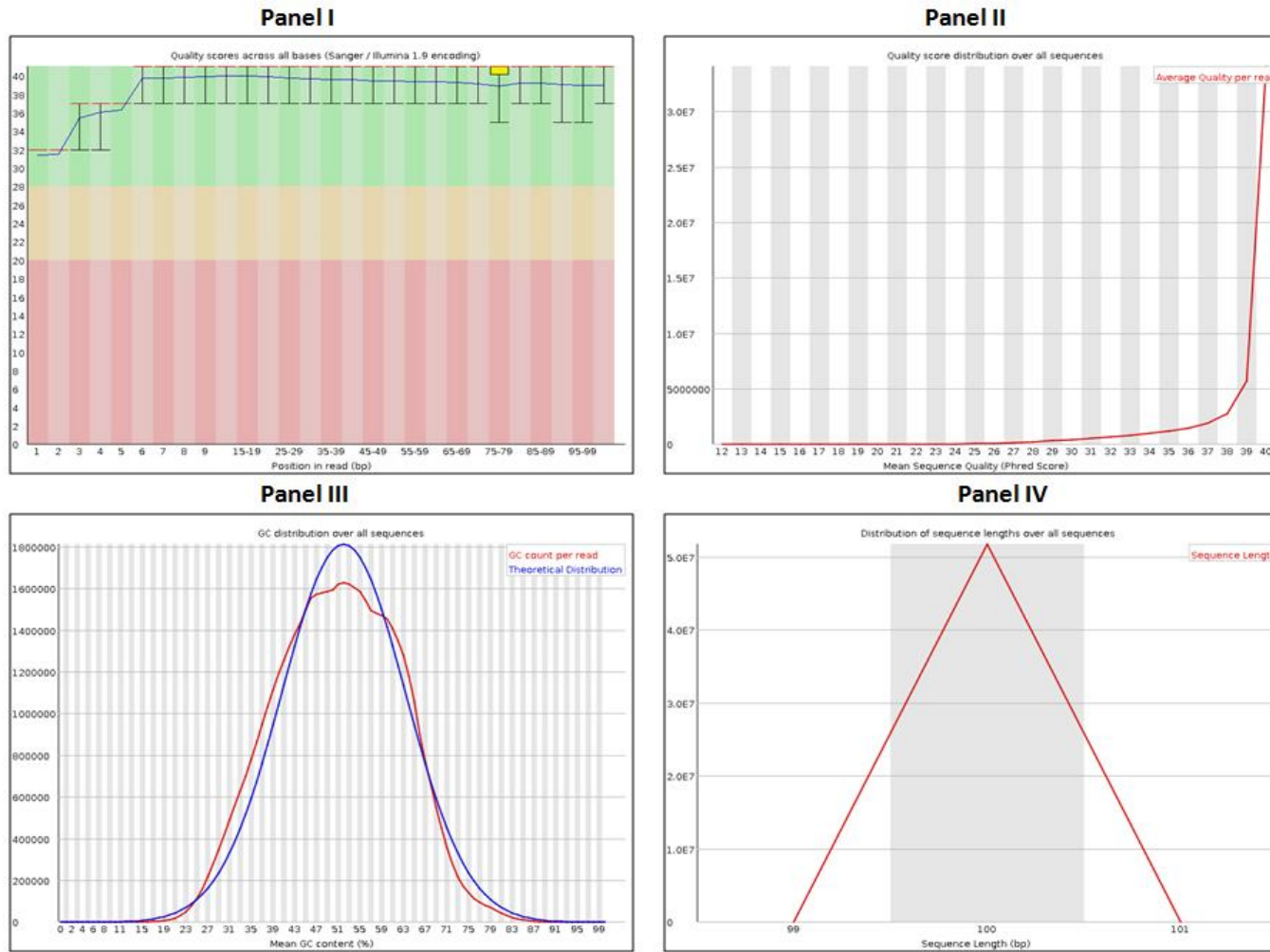
5.3.2 The sequencing quality determination

The individual sequencing files were extracted from the HiSeq 2000 (Illumina, USA) sequencing machine for each sample. There were forward sequencing and reverse sequencing files for each sample, so in total 24 sequencing files were collected in .fq file format. Then each .fq file was uploaded in Galaxy SlipStream server and converted to FASTQ format by FASTQ Groomer. Subsequently, the sequencing files were analysed in FASTQC to evaluate the overall quality of the sequences. It has been found that, 'per base sequencing quality' for all the files have a Phred score close to 40 which means the accuracy of base calling in each position of a 100 bp short read was more than 99.99%. So, the 'Quality score across all bases (Sanger /Illumina 1.9 encoding)' was in well accepted range. The 'Per sequence quality score' for all sample also have a Phred score close to 40 for maximum number of reads. The sequences also evaluated for 'Per sequence GC content' and found to be well accepted as the experimental GC content was lower than the theoretical distribution. It was also found that, none of sequences have any spurious base call other than A, T, G and C. So the N (spurious base) content for all sequences was found to be nonexistent. 'Sequence length distribution' was also checked for consistent sequencing throughout the 100 bp and it has been found that the distribution of sequence lengths over all sequences was 100 for all the samples. The 'per base sequencing quality' plots, the 'quality score distribution over all sequences' plots, 'GC distribution over all sequences' plots and 'sequence length distribution' plots for all the samples are depicted in Figure 18-29. So, overall the quality of all the sequencing reactions was found to be excellent enough for further processing to identify the differentially expressed genes. The variant calling and visualization was done by NextGENe® software (SoftGenetics, USA) to confirm each

THAP1 variant genotypes (Figure 30-35). This has been done using the raw sequencing .fq files (raw read).

RNA sequencing based gene expression analysis

A.



(Continued...)

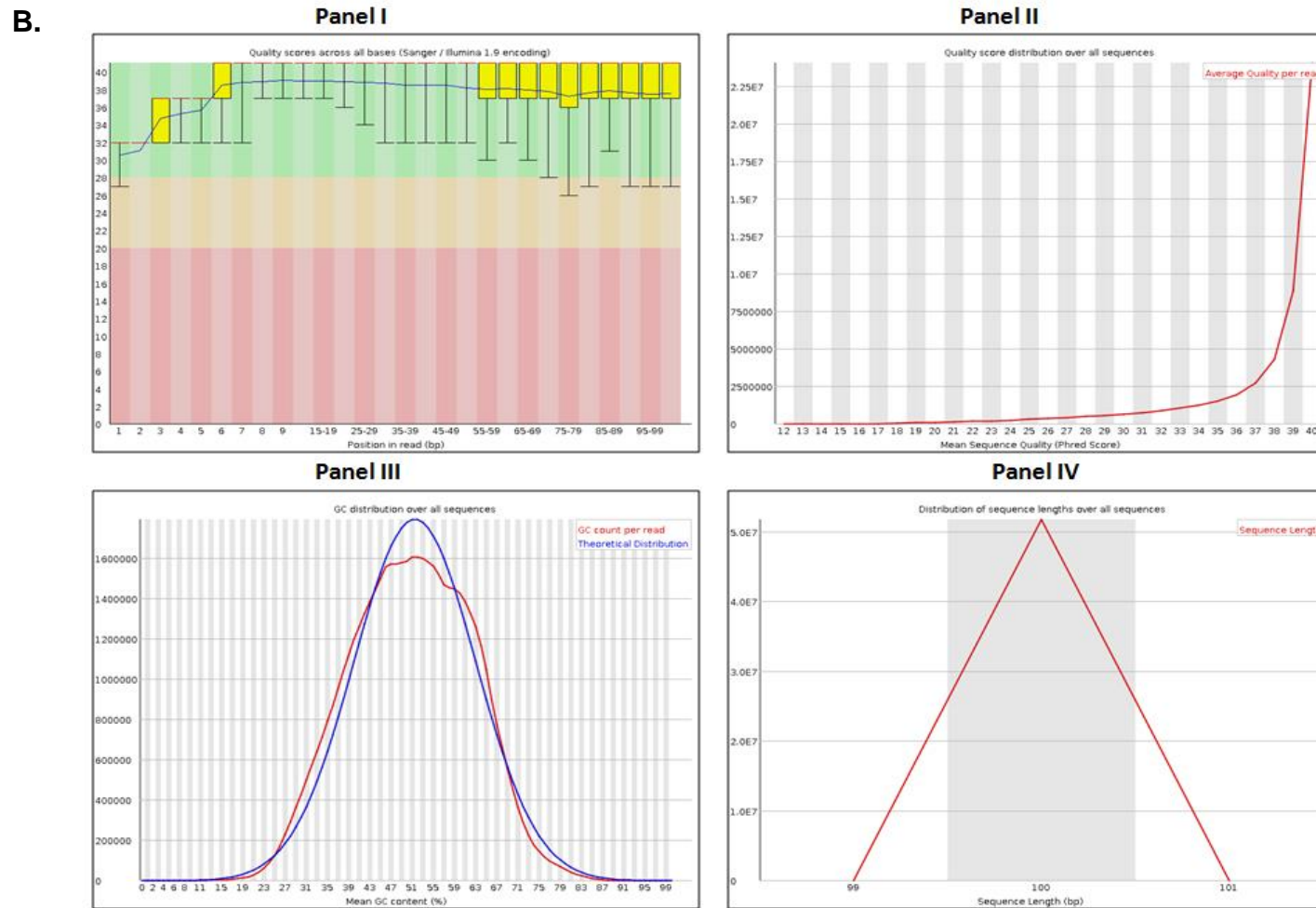
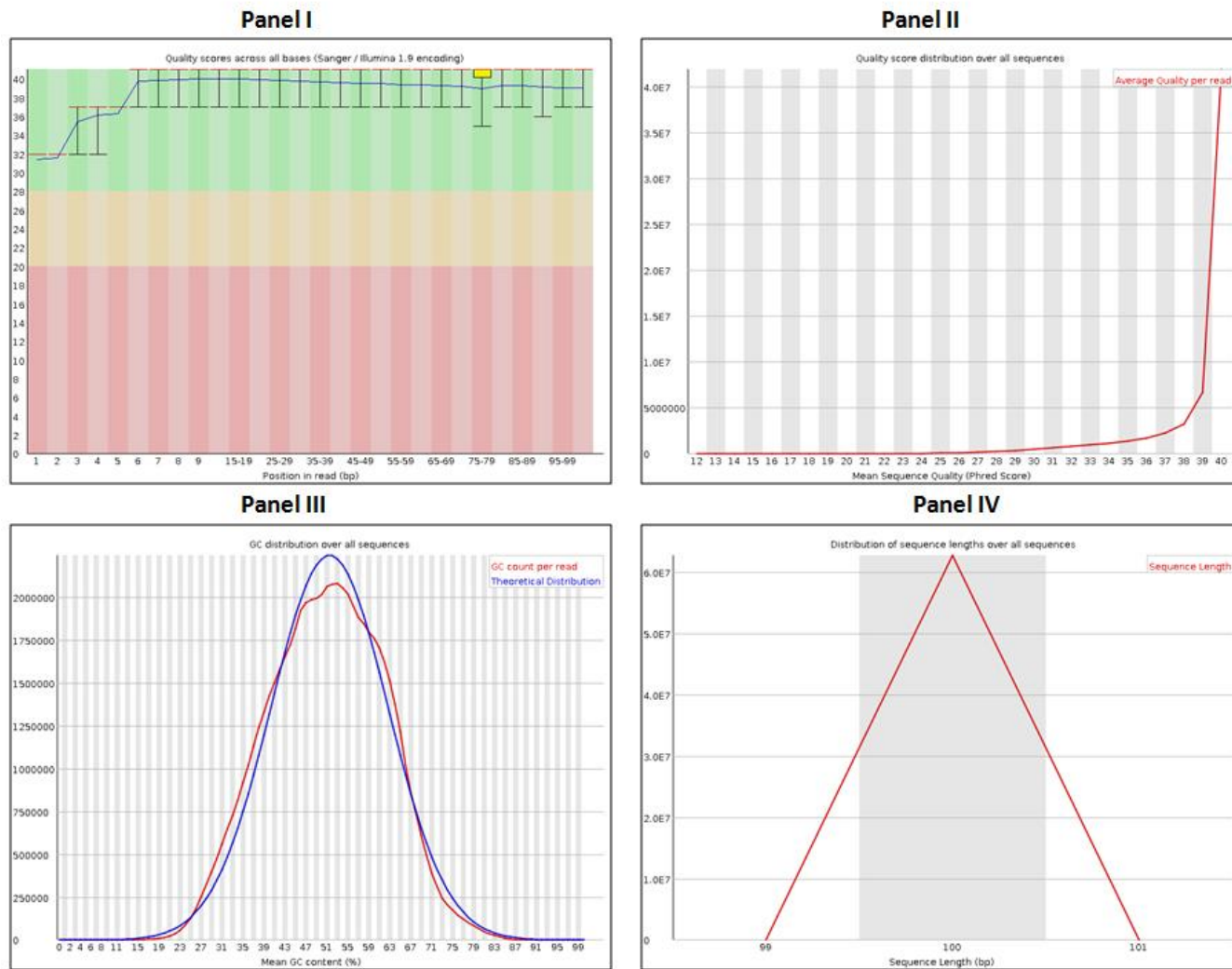


Figure 18: Representative figures of RNA sequencing quality of sample ML-1. A) The forward sequencing and B) The reverse sequencing quality plots are depicted in Panel I: per base sequencing quality, Panel II: quality score distribution over all sequences, Panel III: GC distribution over all sequences and Panel IV: sequence length distribution.

RNA sequencing based gene expression analysis

A.



(Continued....)

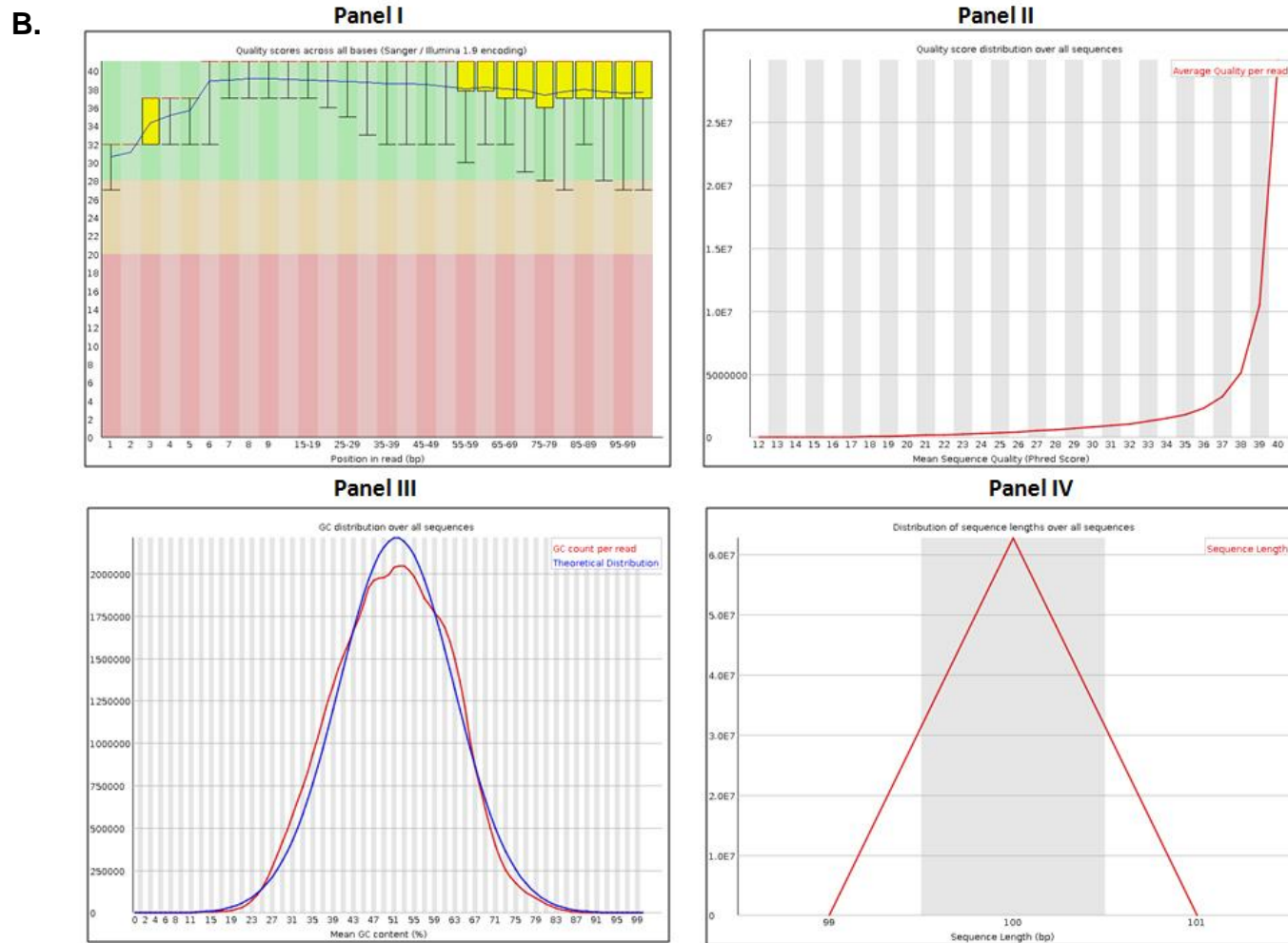
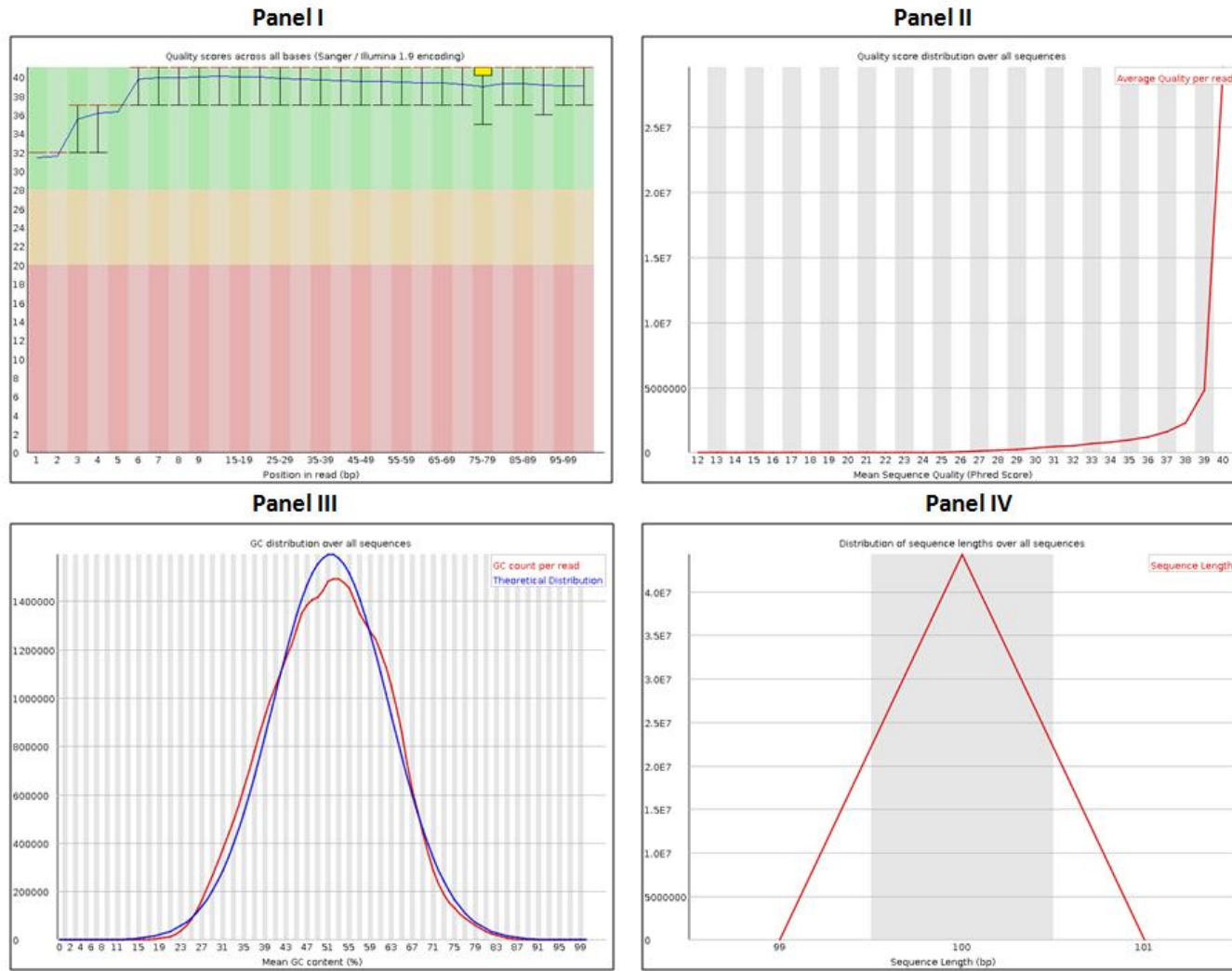


Figure 19: Representative figures of RNA sequencing quality of sample ML-2. A) The forward sequencing and B) The reverse sequencing quality plots are depicted in Panel I: per base sequencing quality, Panel II: quality score distribution over all sequences, Panel III: GC distribution over all sequences and Panel IV: sequence length distribution.

RNA sequencing based gene expression analysis

A.



(Continued.....)

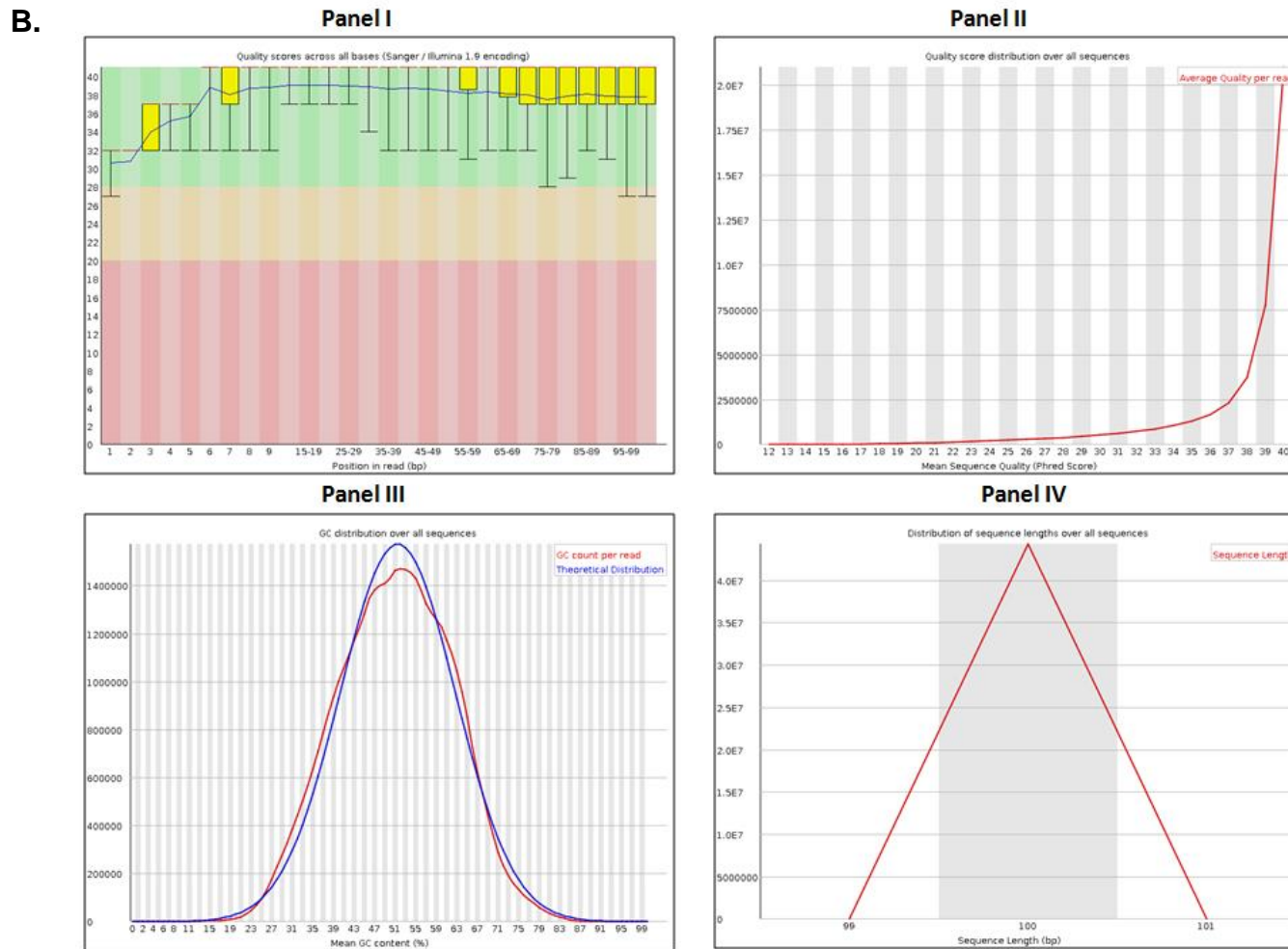
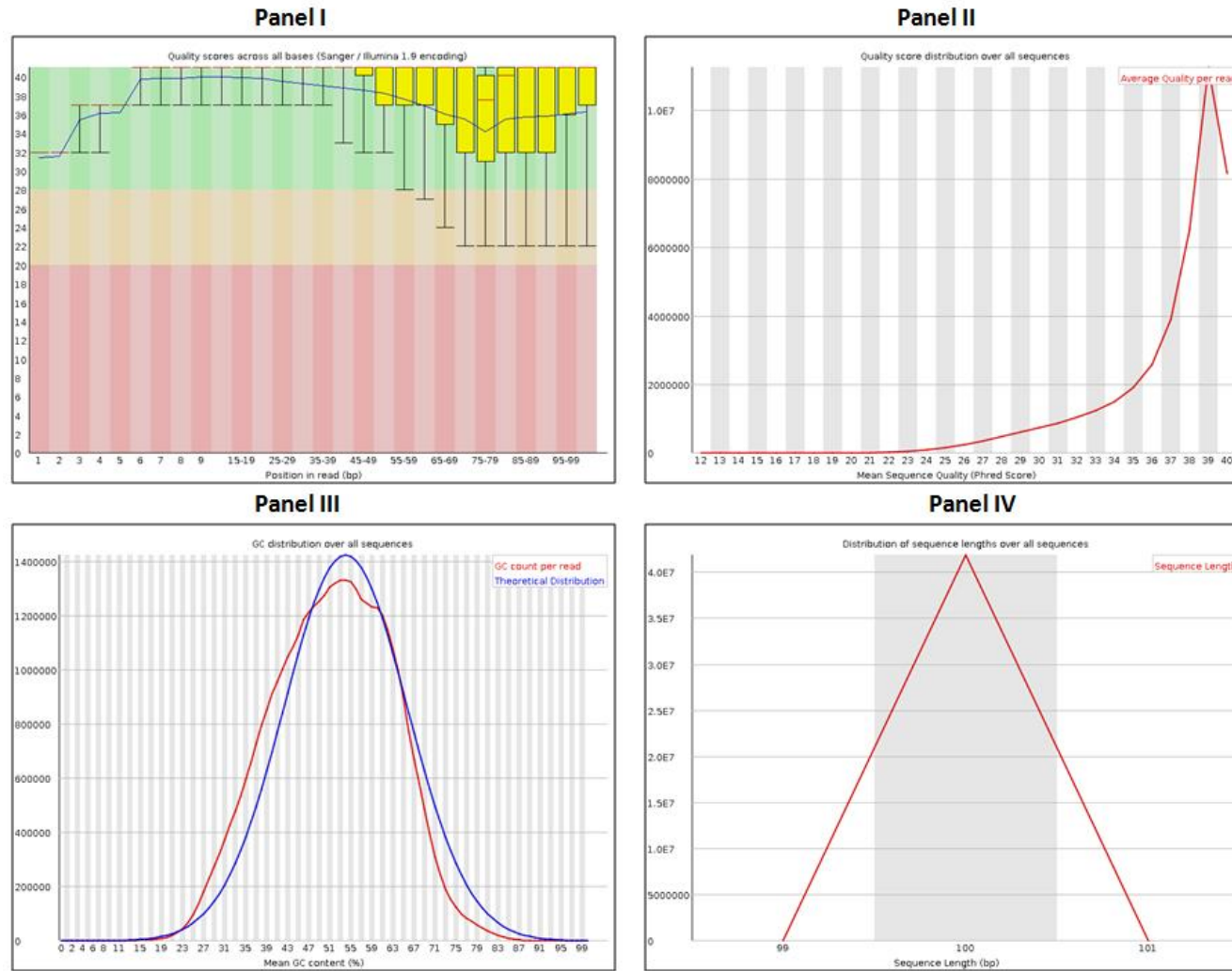


Figure 20: Representative figures of RNA sequencing quality of sample ML-3. A) The forward sequencing and B) The reverse sequencing quality plots are depicted in Panel I: per base sequencing quality, Panel II: quality score distribution over all sequences, Panel III: GC distribution over all sequences and Panel IV: sequence length distribution.

RNA sequencing based gene expression analysis

A.



(Continued.....)

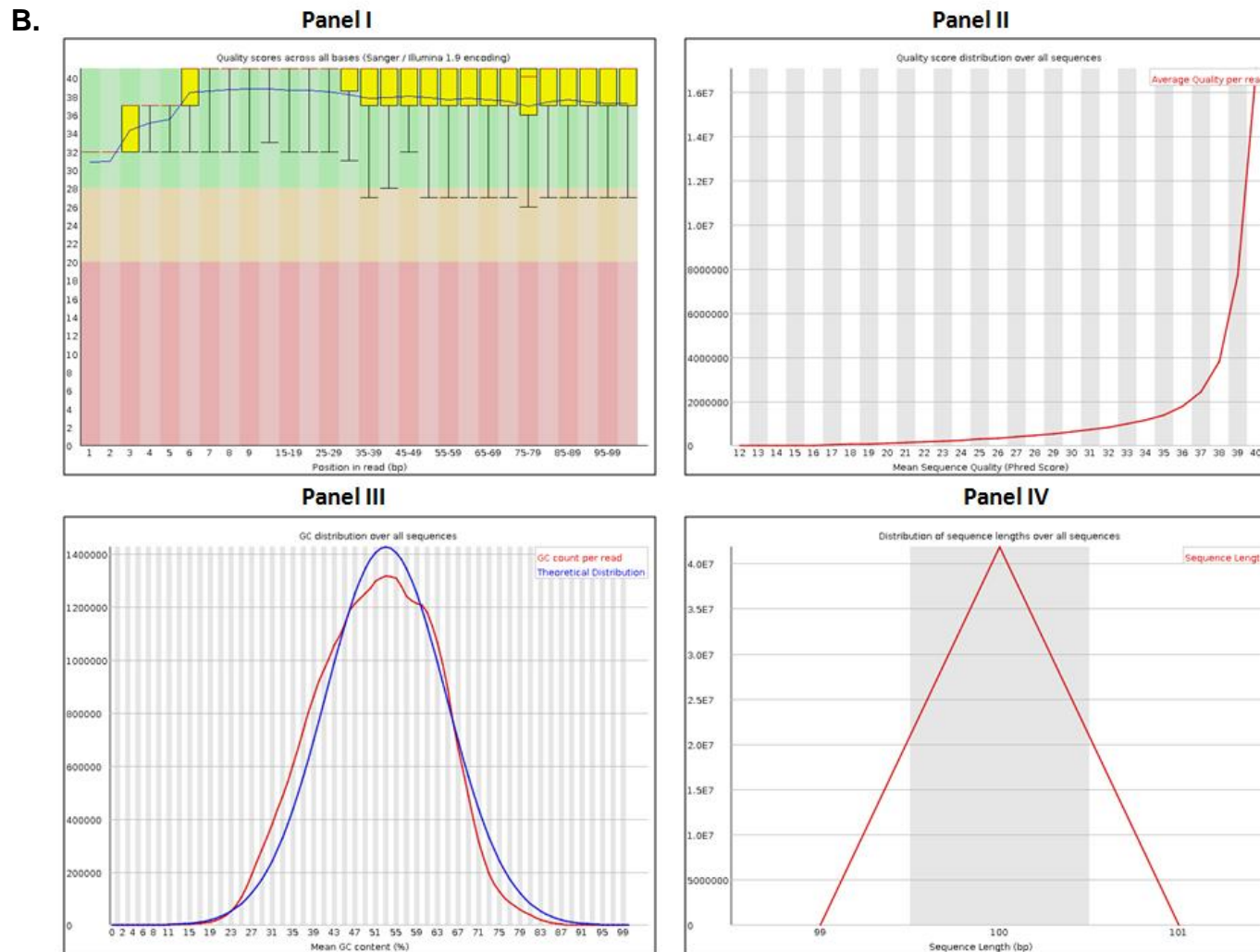
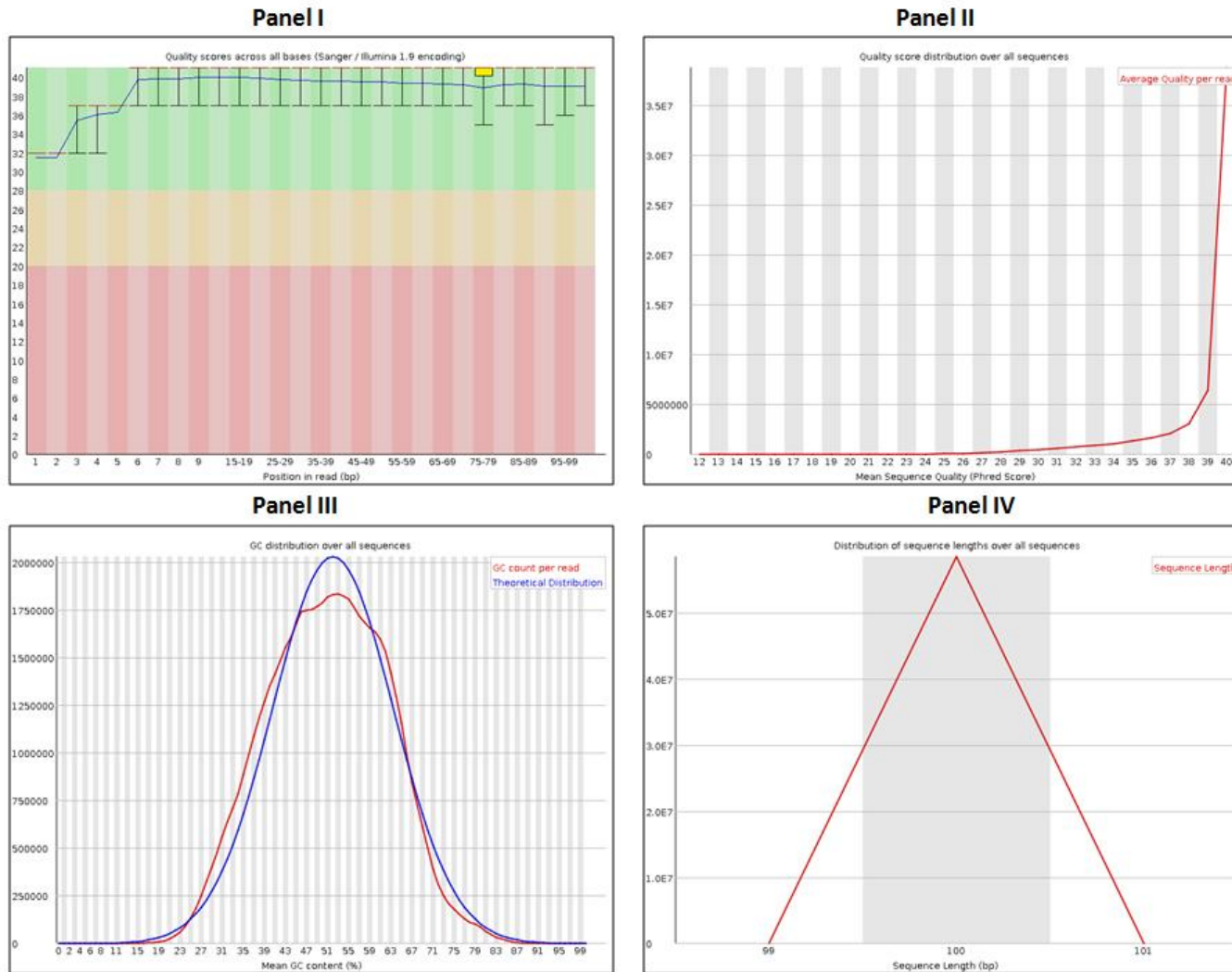


Figure 21: Representative figures of RNA sequencing quality of sample ML-4. A) The forward sequencing and B) The reverse sequencing quality plots are depicted in Panel I: per base sequencing quality, Panel II: quality score distribution over all sequences, Panel III: GC distribution over all sequences and Panel IV: sequence length distribution.

RNA sequencing based gene expression analysis

A.



(Continued.....)

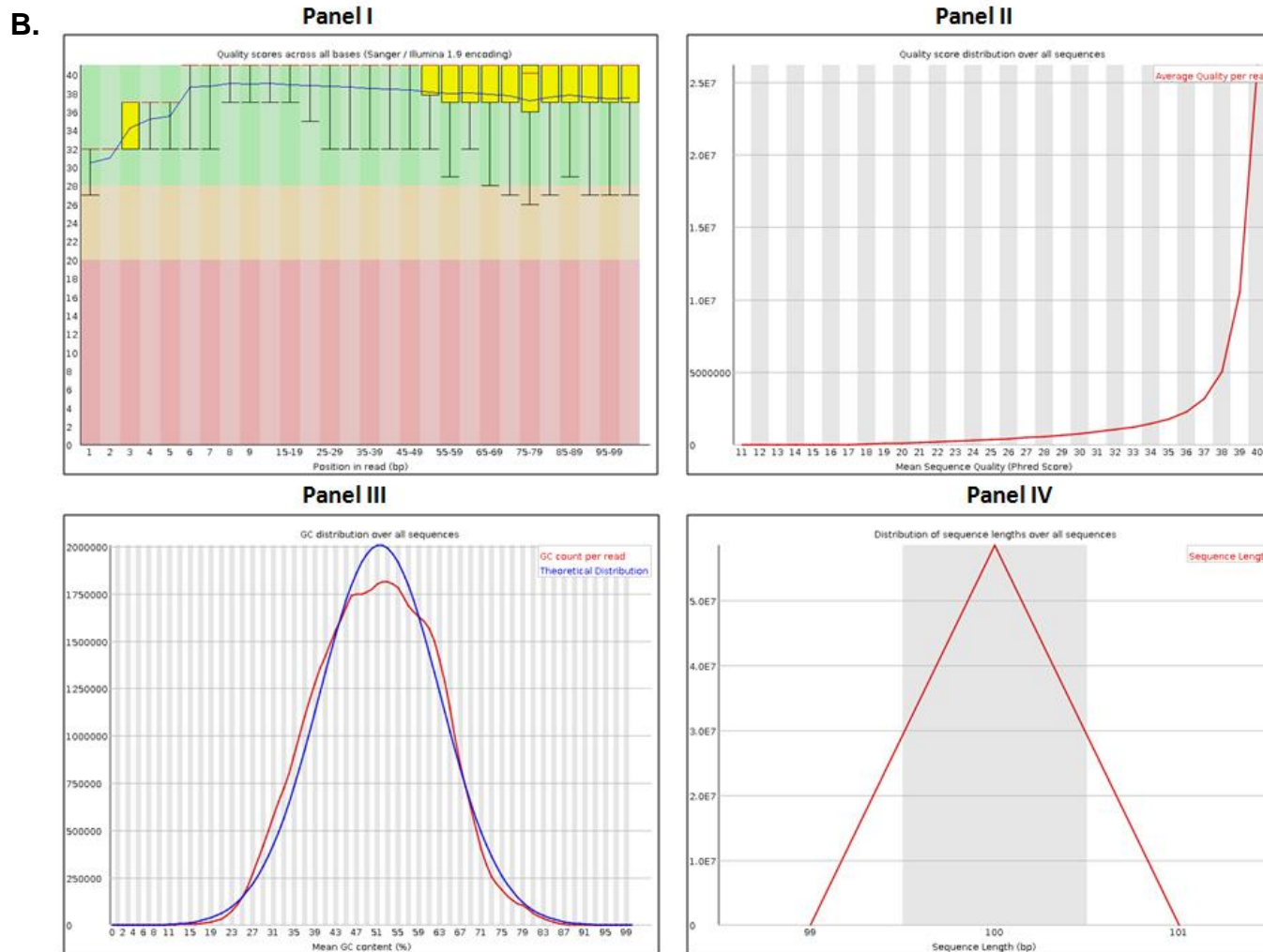
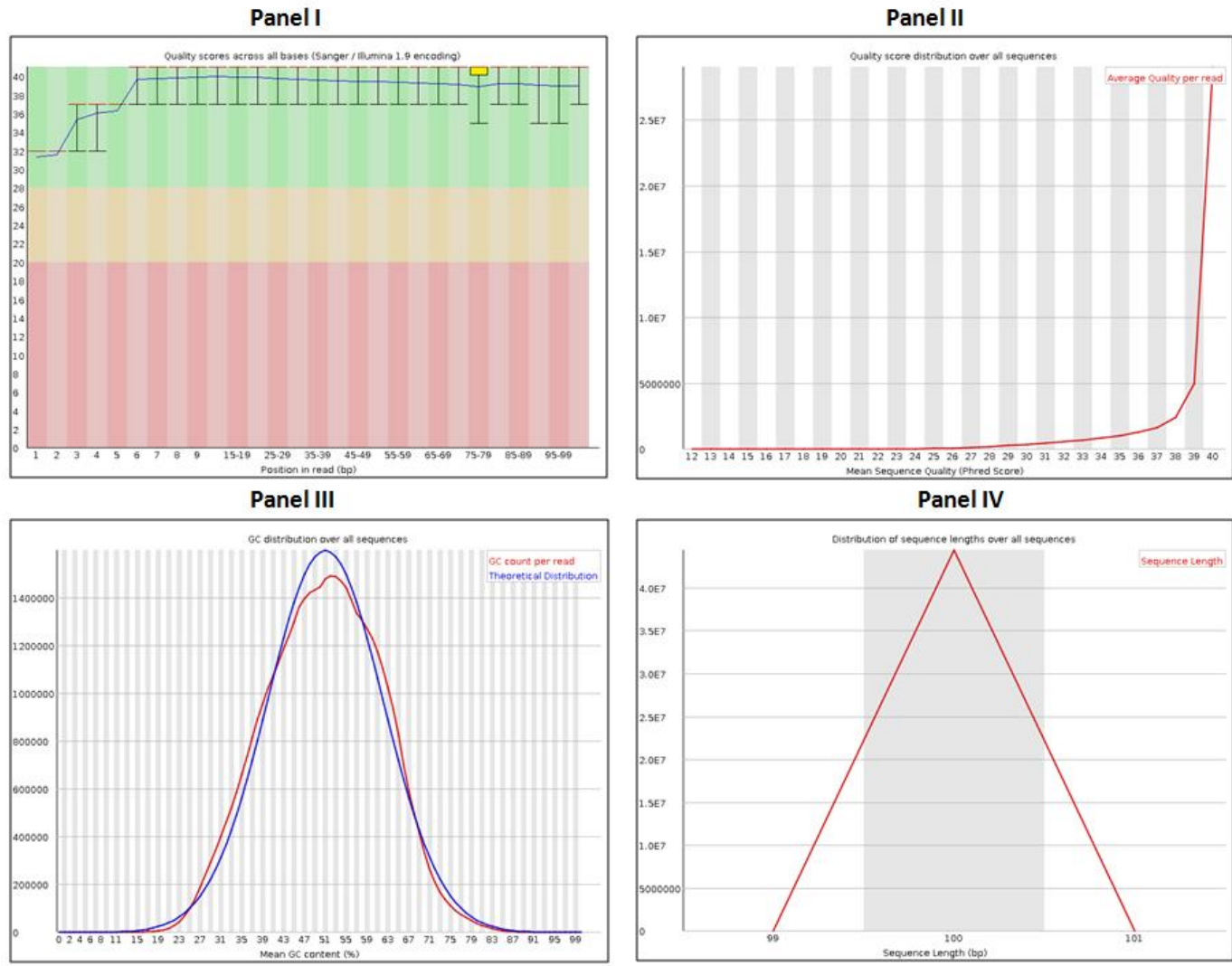


Figure 22: Representative figures of RNA sequencing quality of sample ML-5. A) The forward sequencing and B) The reverse sequencing quality plots are depicted in Panel I: per base sequencing quality, Panel II: quality score distribution over all sequences, Panel III: GC distribution over all sequences and Panel IV: sequence length distribution.

A.



(Continued.....)

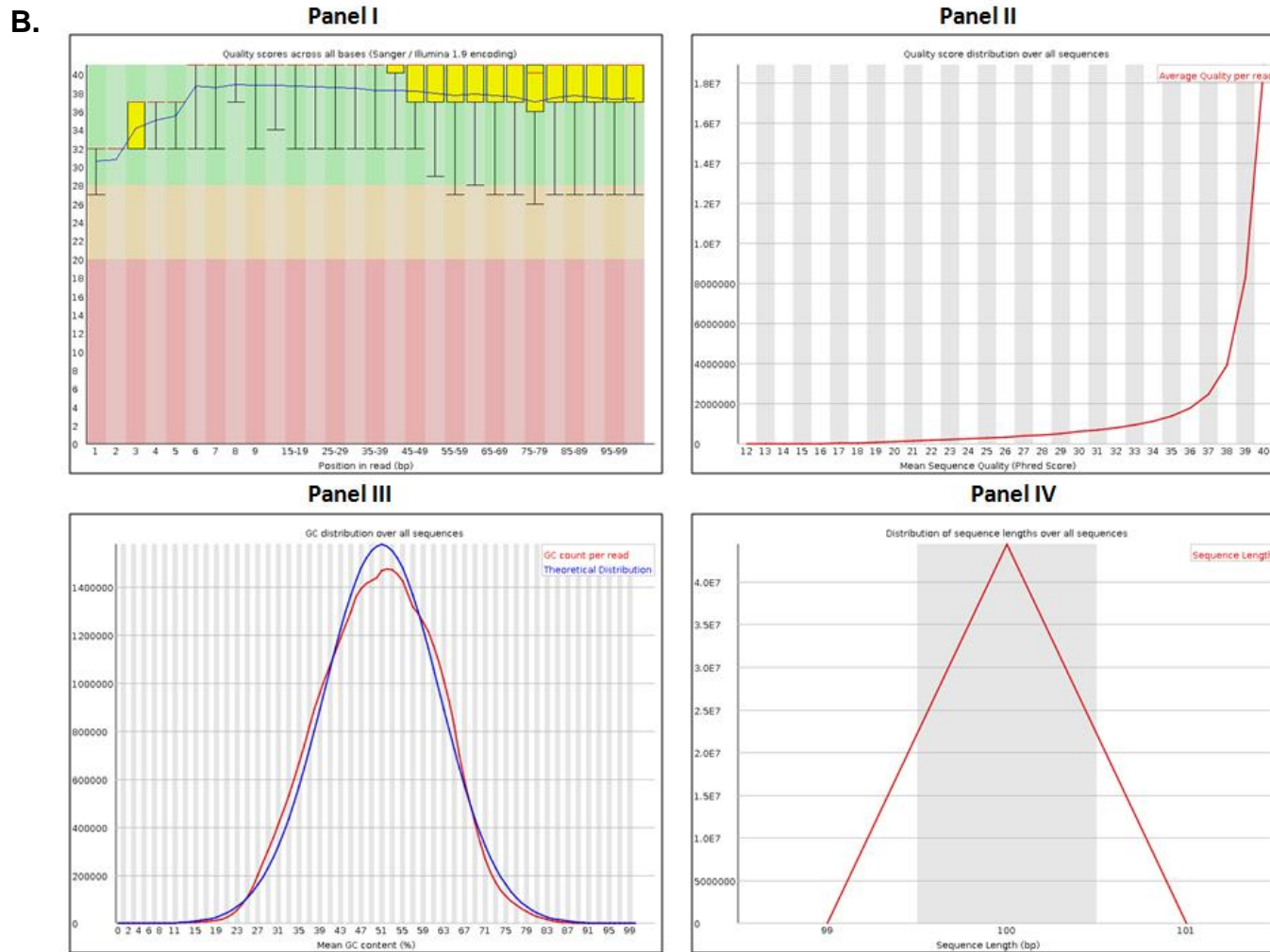
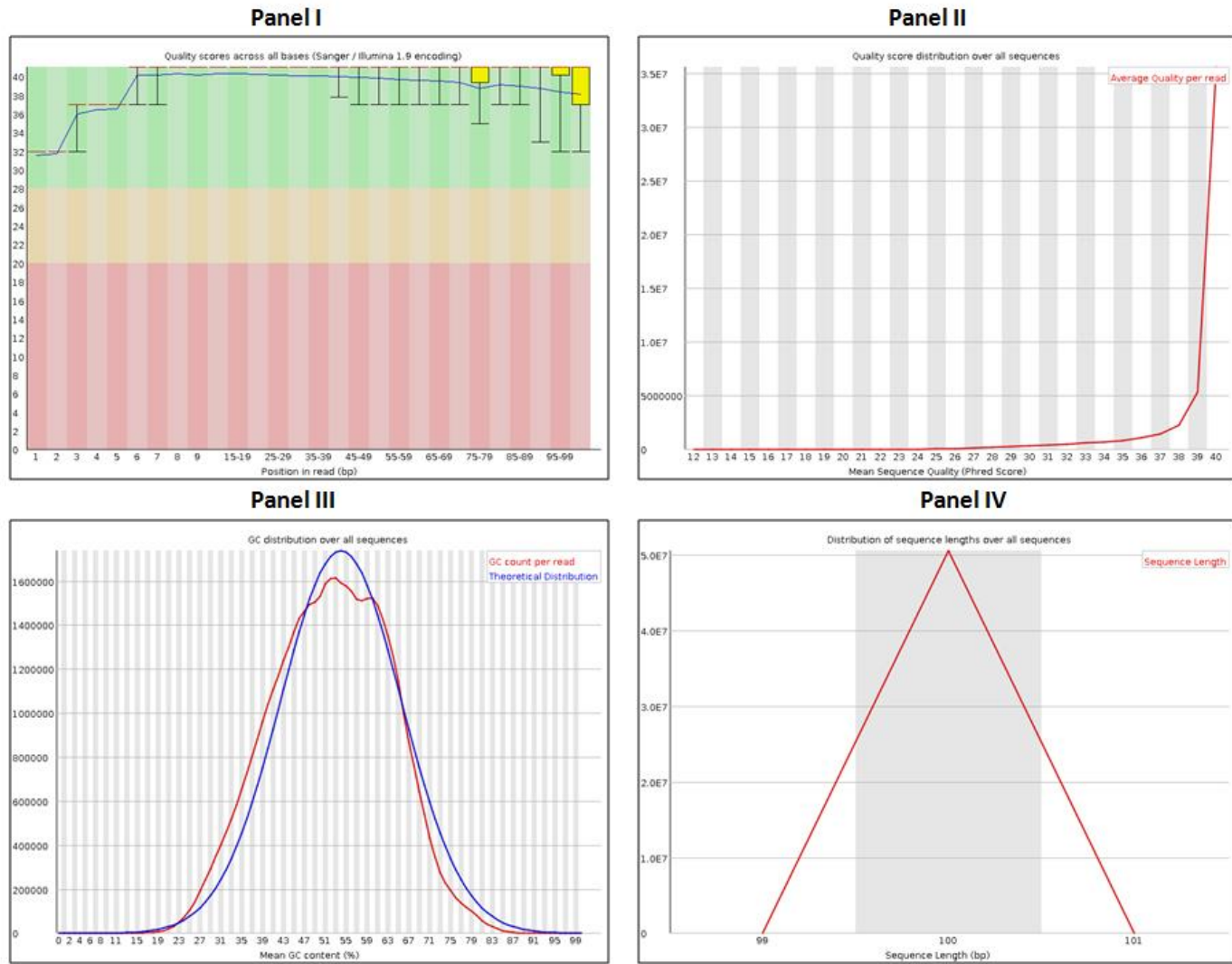


Figure 23: Representative figures of RNA sequencing quality of sample ML-6. A) The forward sequencing and B) The reverse sequencing quality plots are depicted in Panel I: per base sequencing quality, Panel II: quality score distribution over all sequences, Panel III: GC distribution over all sequences and Panel IV: sequence length distribution.

RNA sequencing based gene expression analysis

A.



(Continued.....)

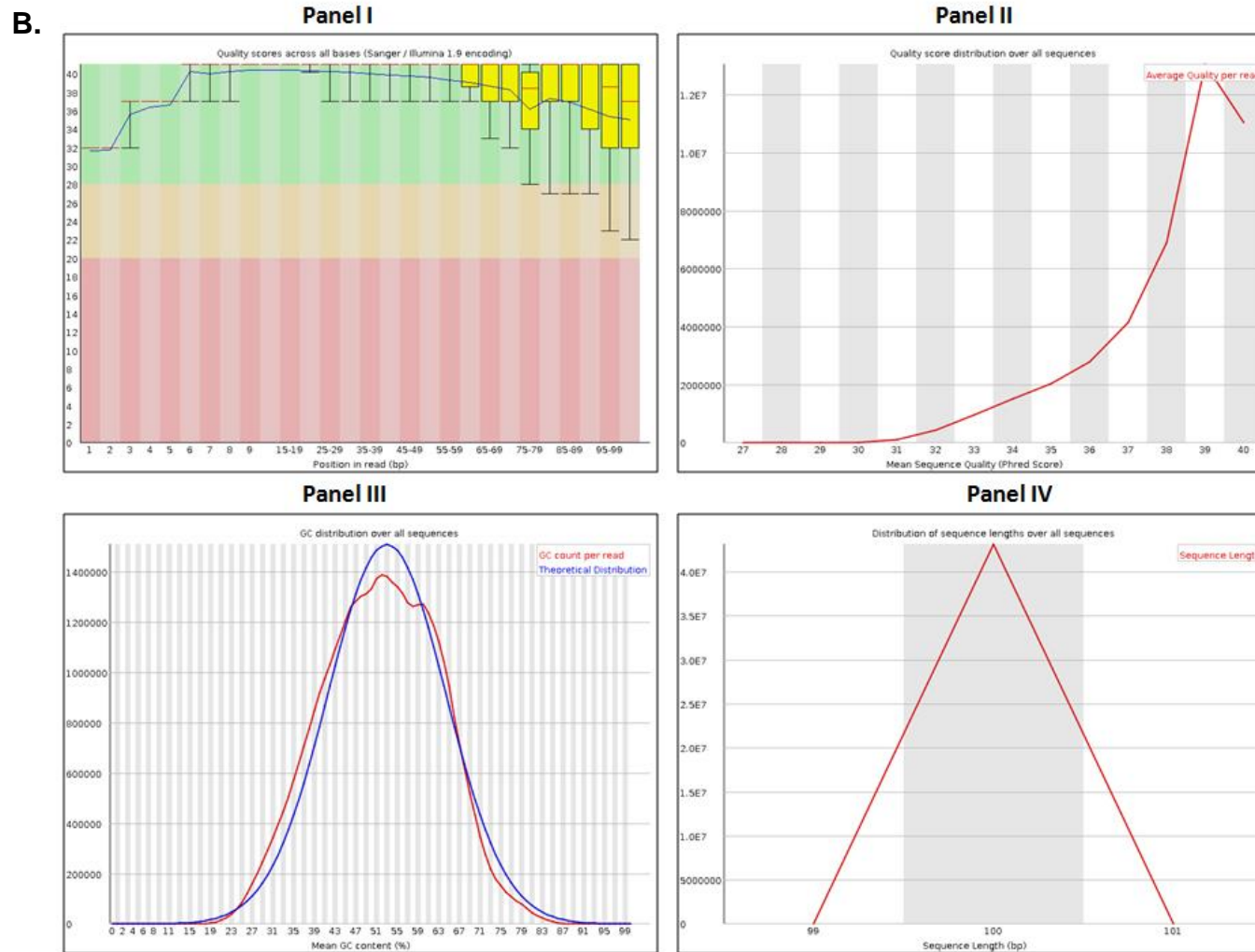
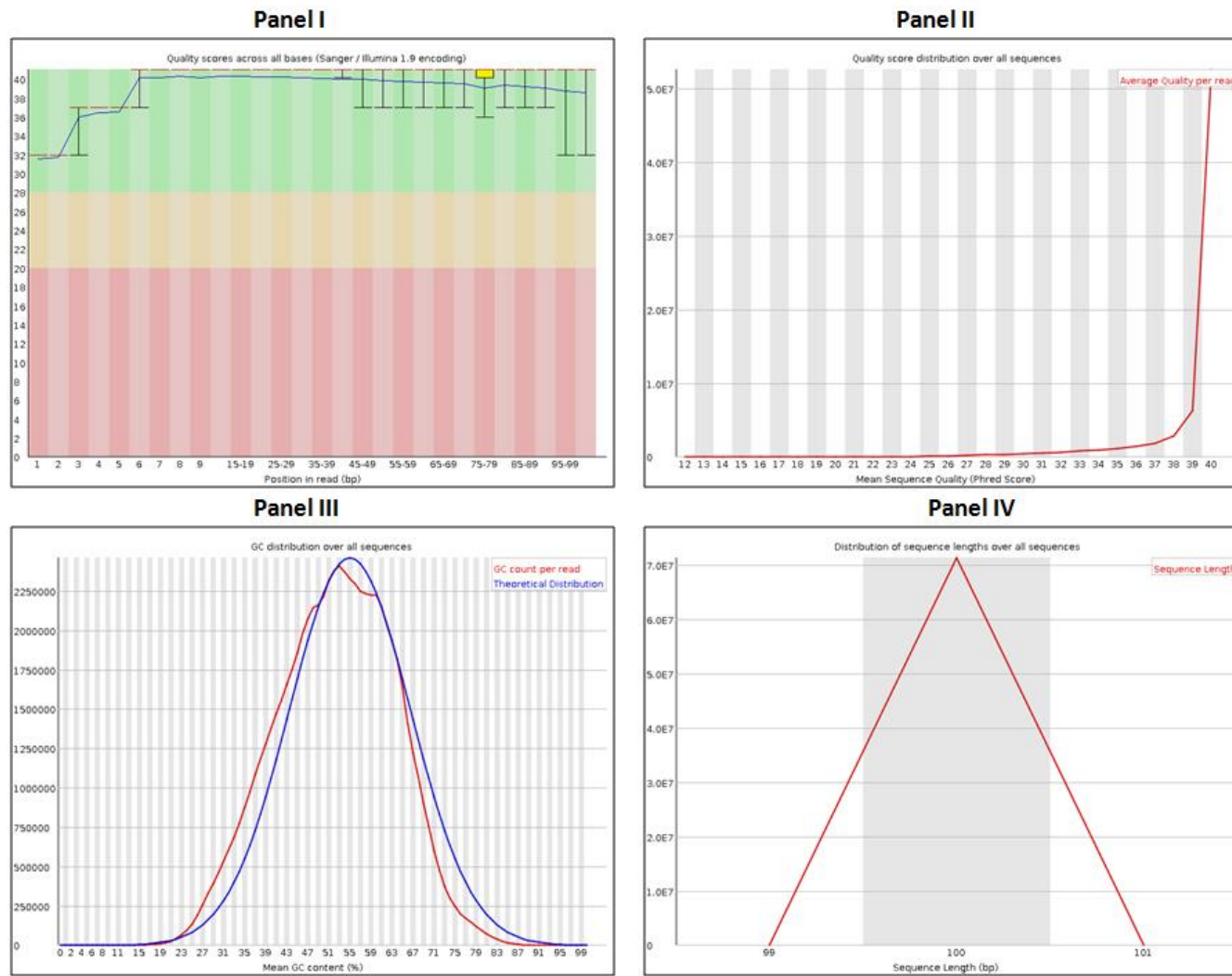


Figure 24: Representative figures of RNA sequencing quality of sample ML-7. A) The forward sequencing and B) The reverse sequencing quality plots are depicted in Panel I: per base sequencing quality, Panel II: quality score distribution over all sequences, Panel III: GC distribution over all sequences and Panel IV: sequence length distribution.

RNA sequencing based gene expression analysis

A.



(Continued.....)

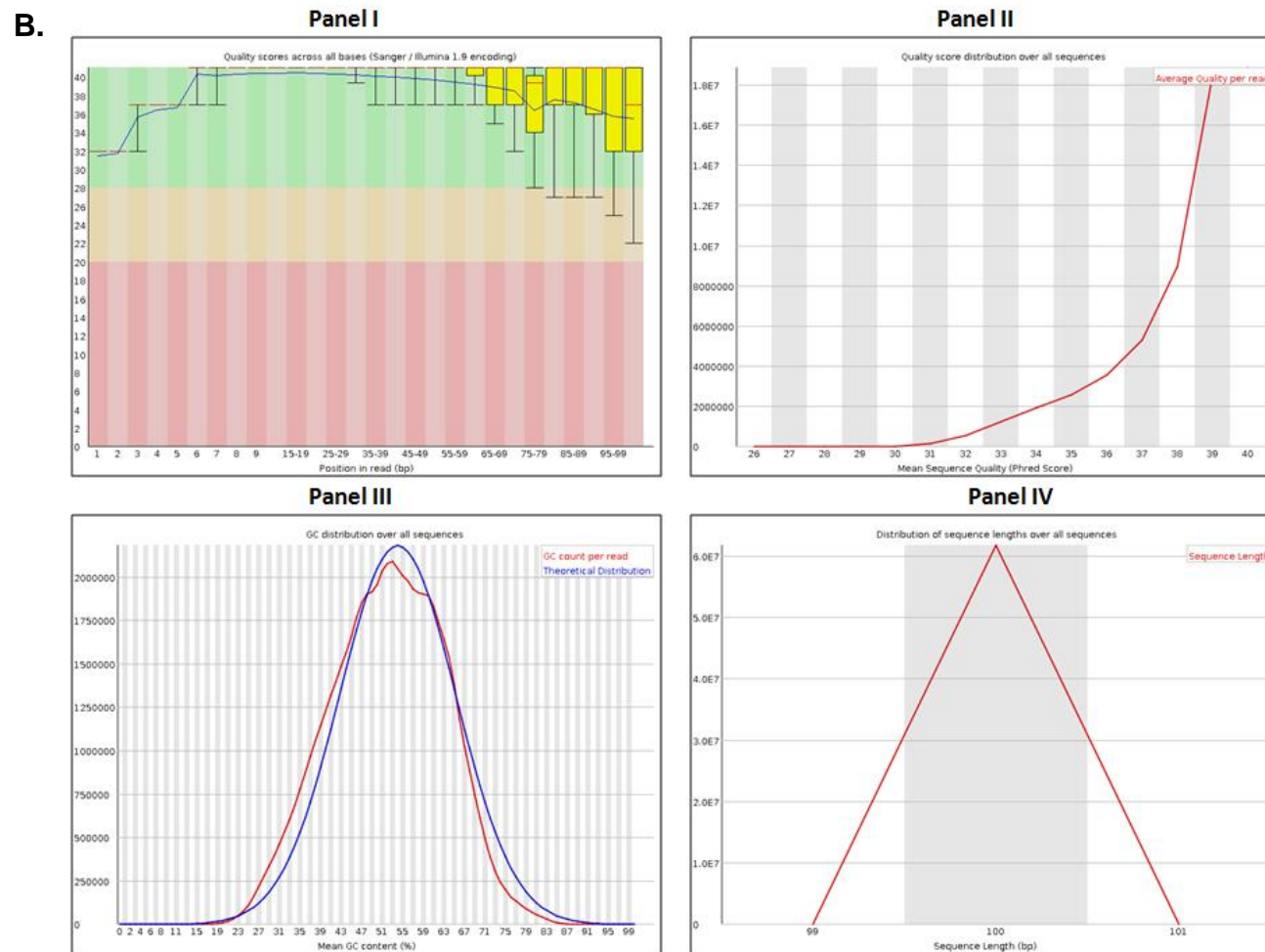
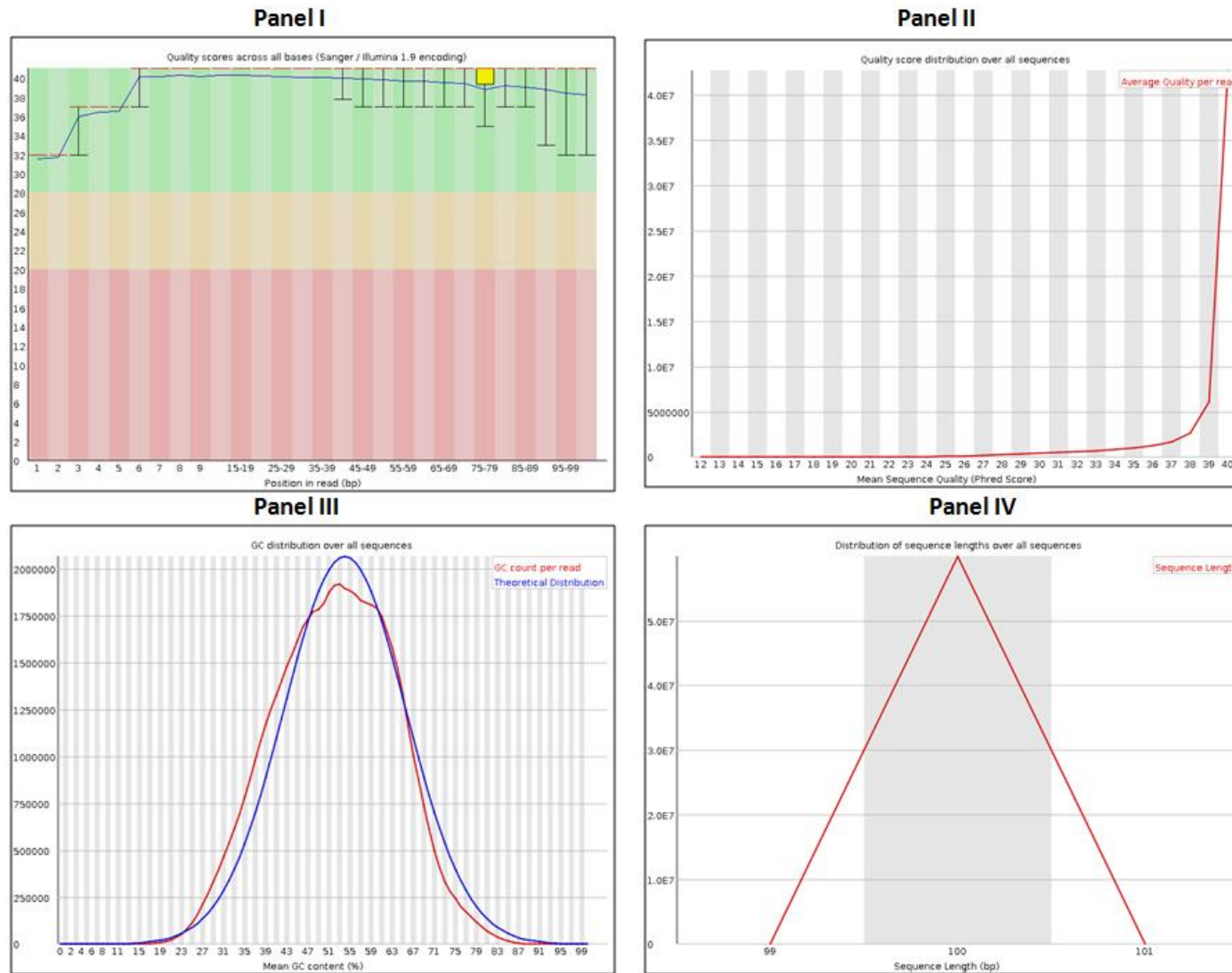


Figure 25: Representative figures of RNA sequencing quality of sample ML-8. A) The forward sequencing and B) The reverse sequencing quality plots are depicted in Panel I: per base sequencing quality, Panel II: quality score distribution over all sequences, Panel III: GC distribution over all sequences and Panel IV: sequence length distribution.

RNA sequencing based gene expression analysis

A.



(Continued.....)

RNA sequencing based gene expression analysis

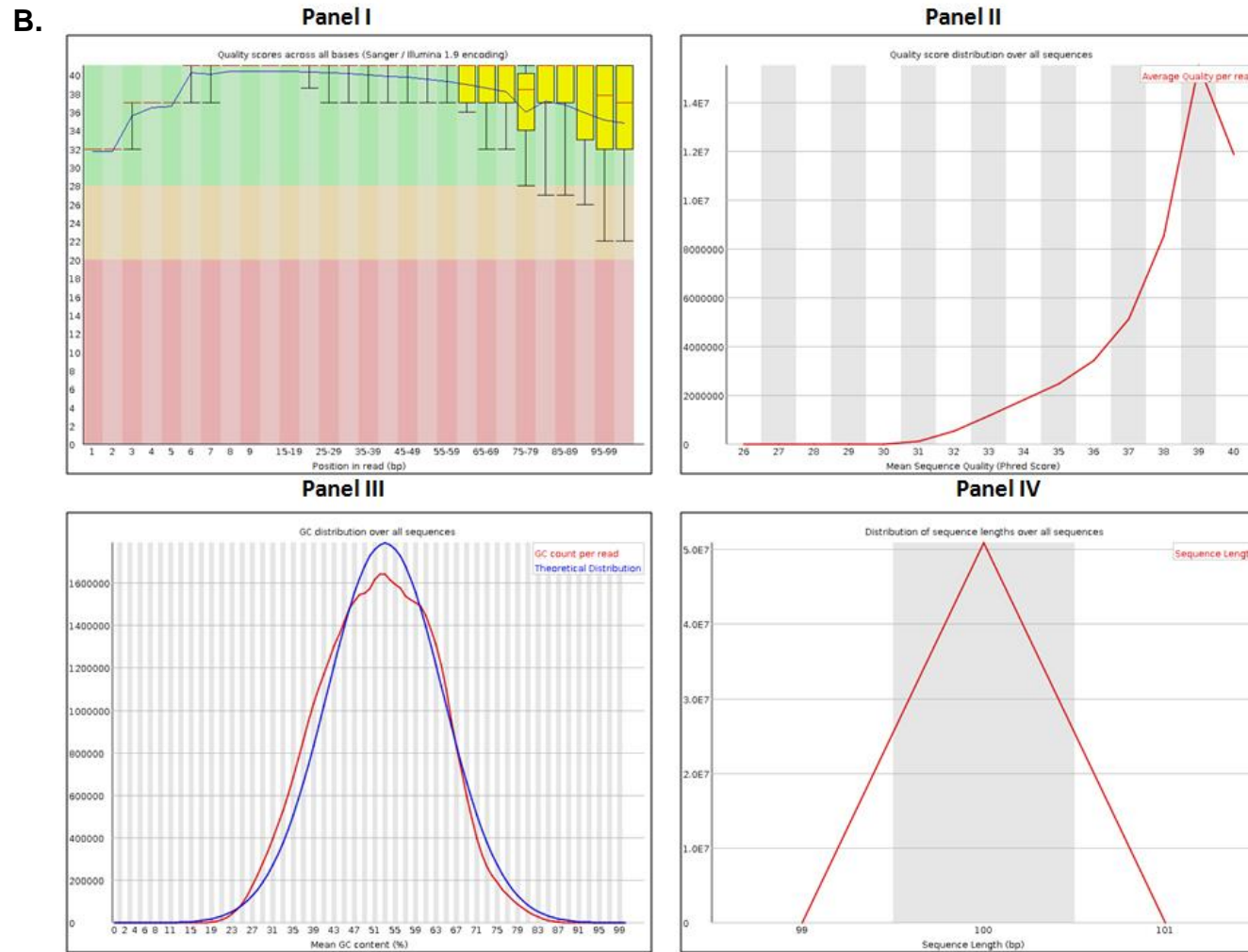
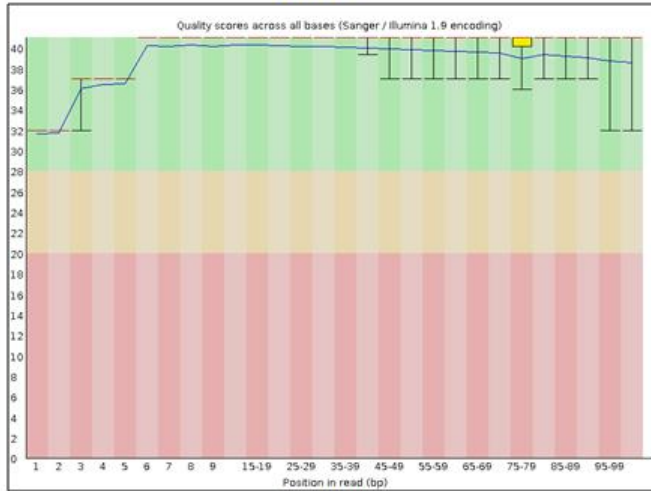


Figure 26: Representative figures of RNA sequencing quality of sample ML-9. A) The forward sequencing and B) The reverse sequencing quality plots are depicted in Panel I: per base sequencing quality, Panel II: quality score distribution over all sequences, Panel III: GC distribution over all sequences and Panel IV: sequence length distribution.

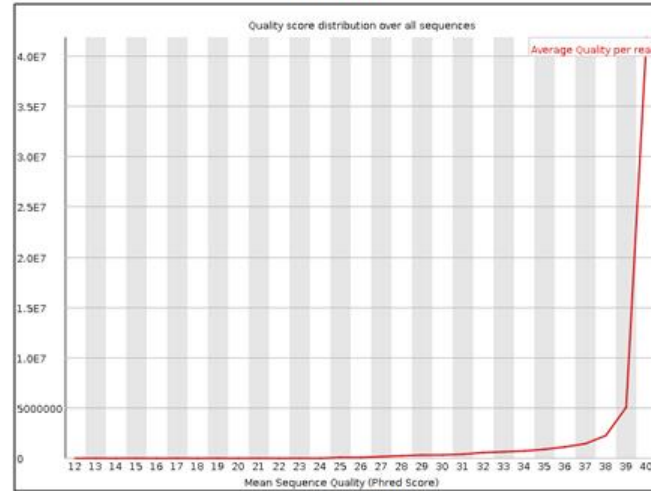
RNA sequencing based gene expression analysis

A.

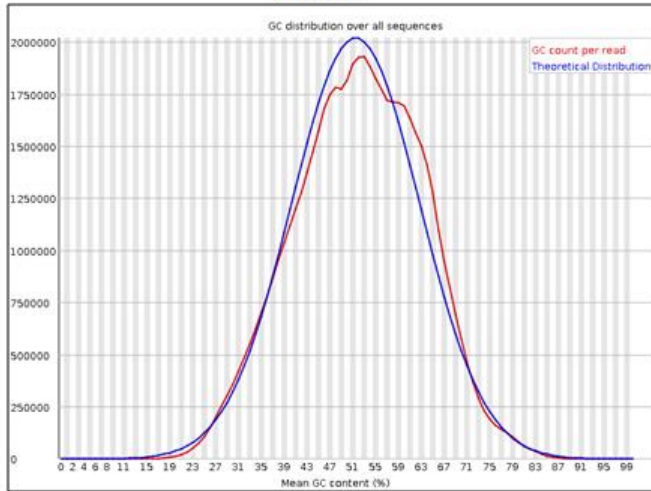
Panel I



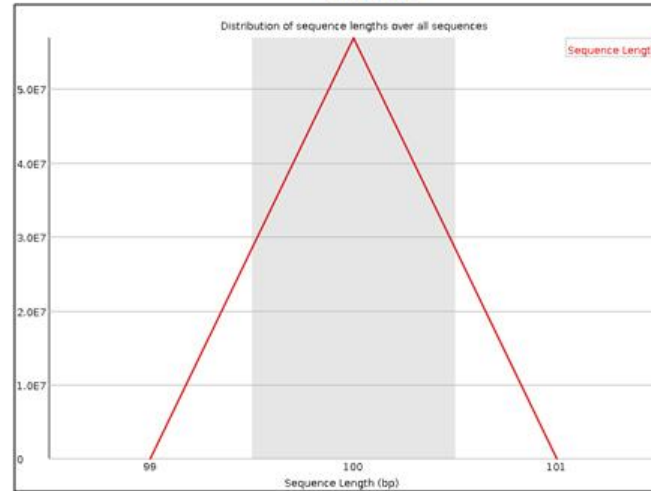
Panel II



Panel III



Panel IV



(Continued.....)

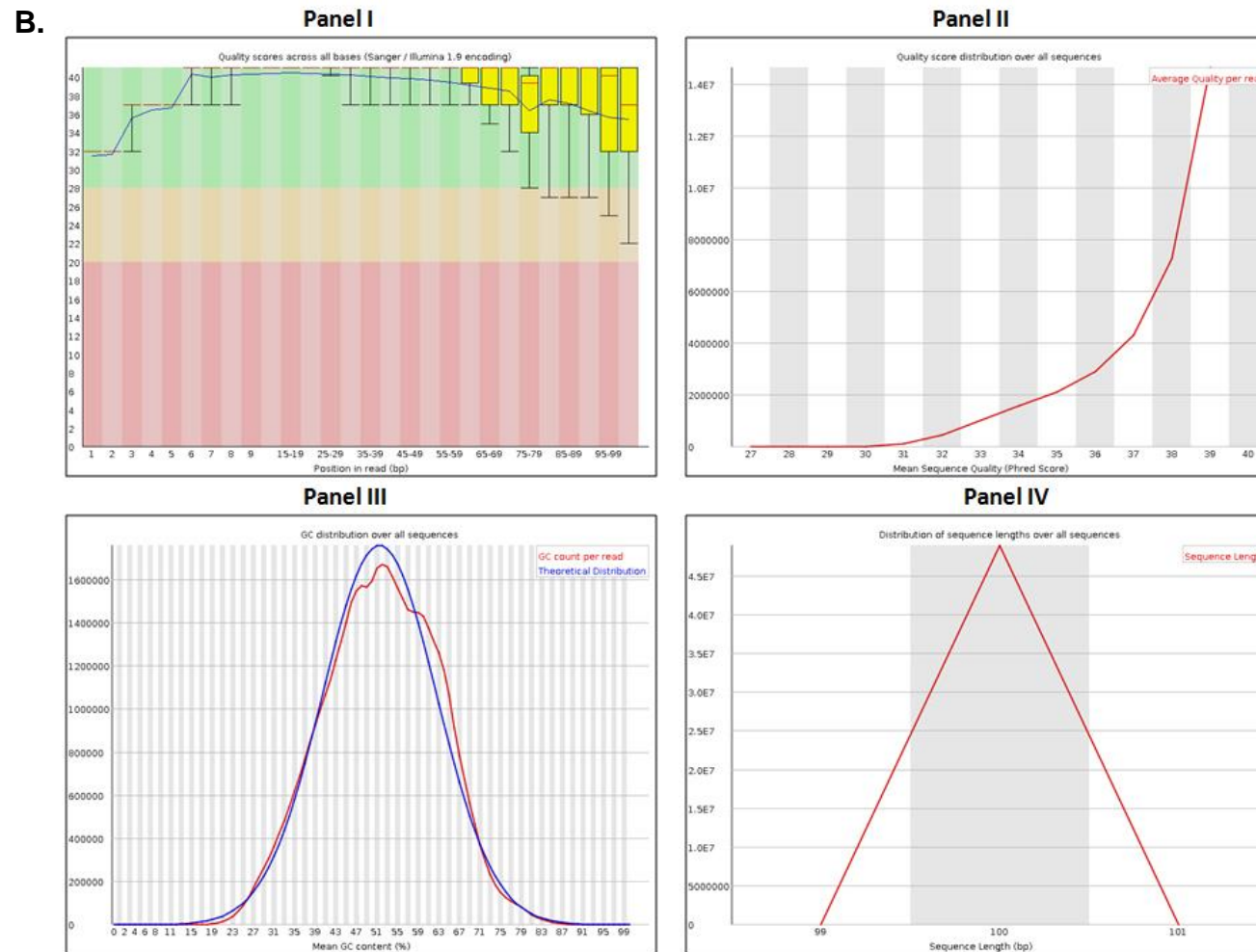
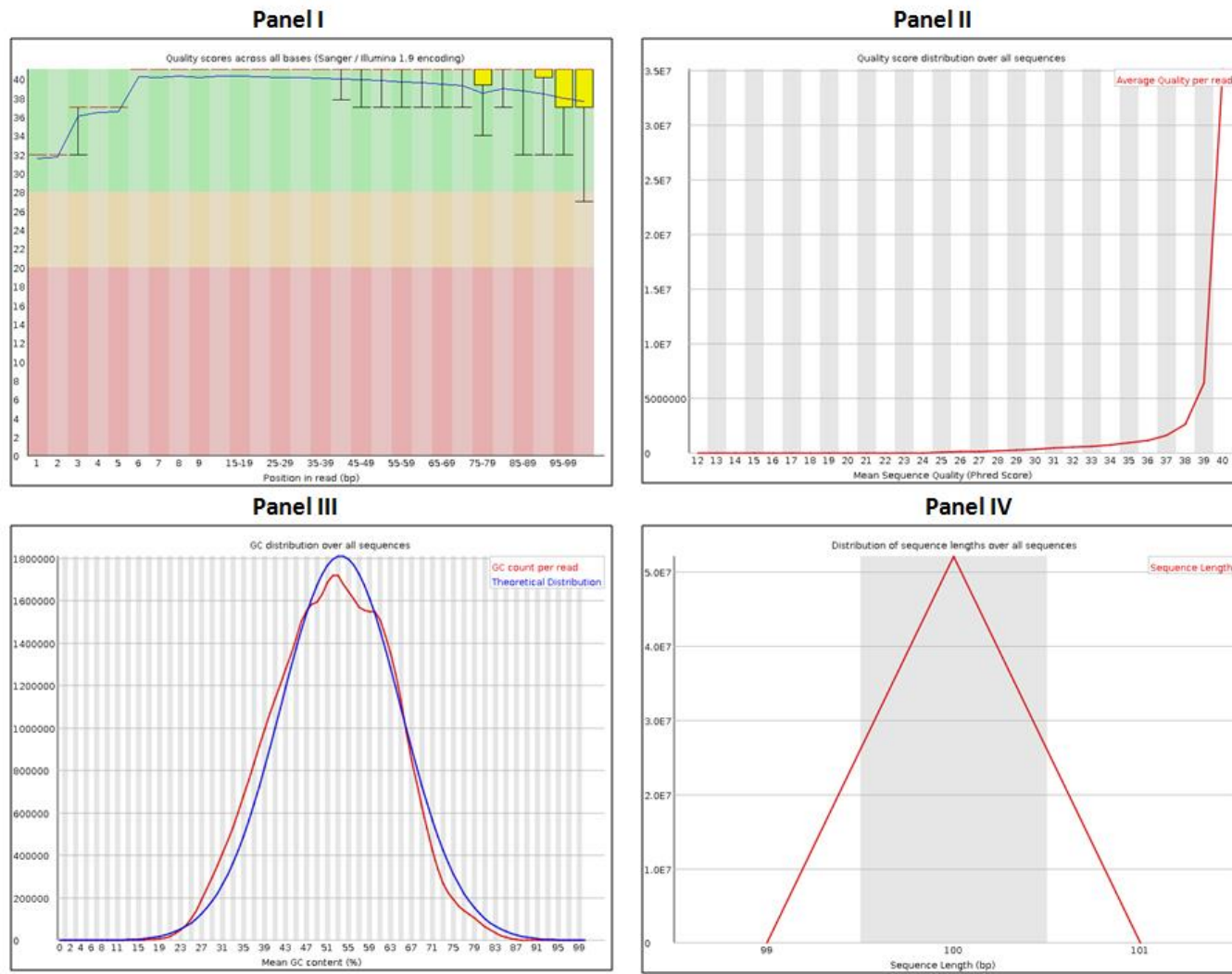


Figure 27: Representative figures of RNA sequencing quality of sample ML-10. A) The forward sequencing and B) The reverse sequencing quality plots are depicted in Panel I: per base sequencing quality, Panel II: quality score distribution over all sequences, Panel III: GC distribution over all sequences and Panel IV: sequence length distribution.

RNA sequencing based gene expression analysis

A.



(Continued.....)

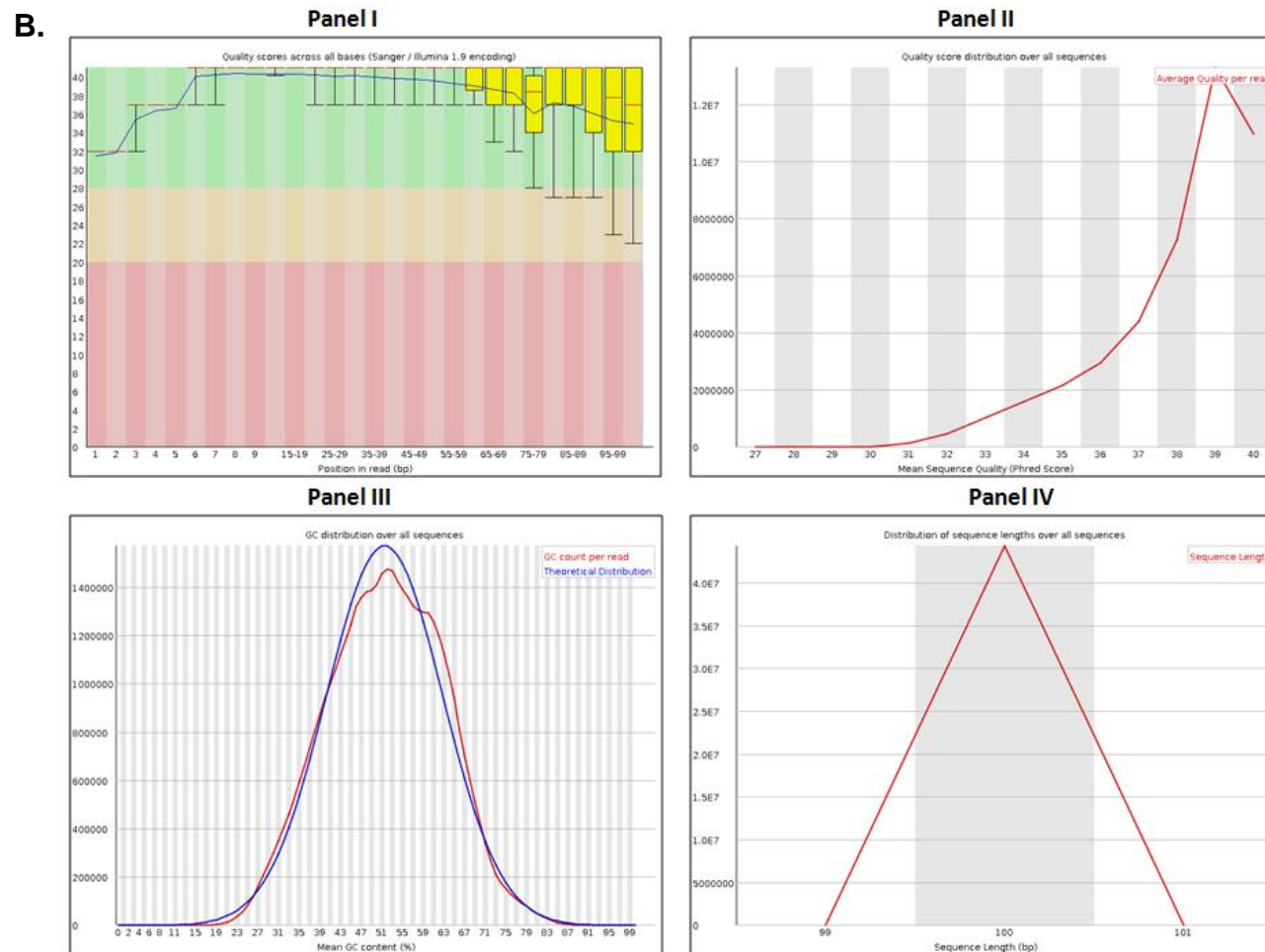
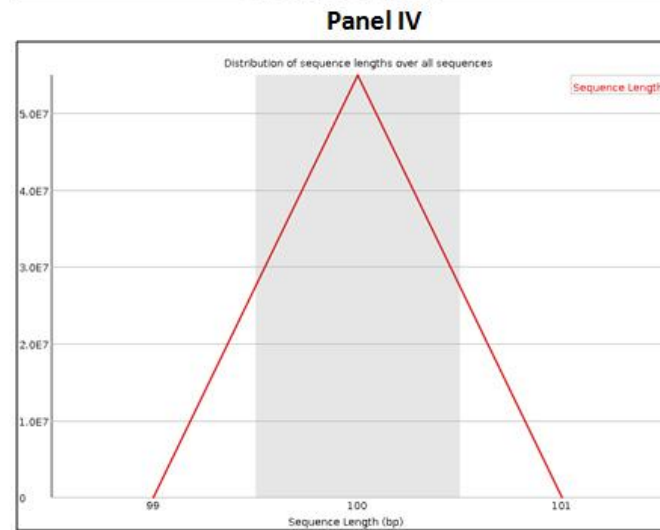
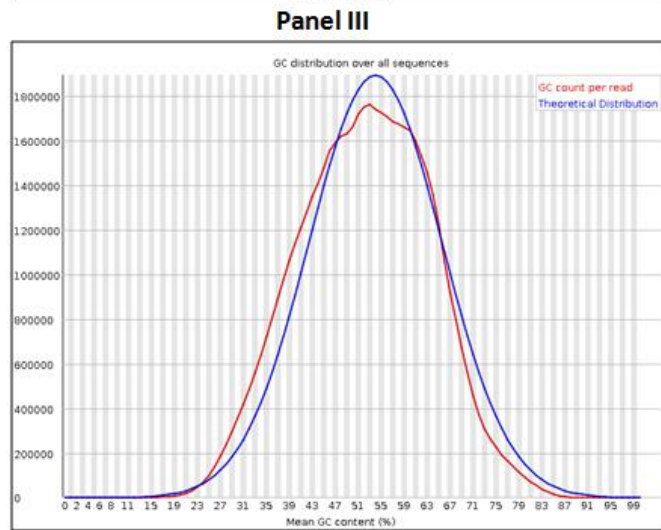
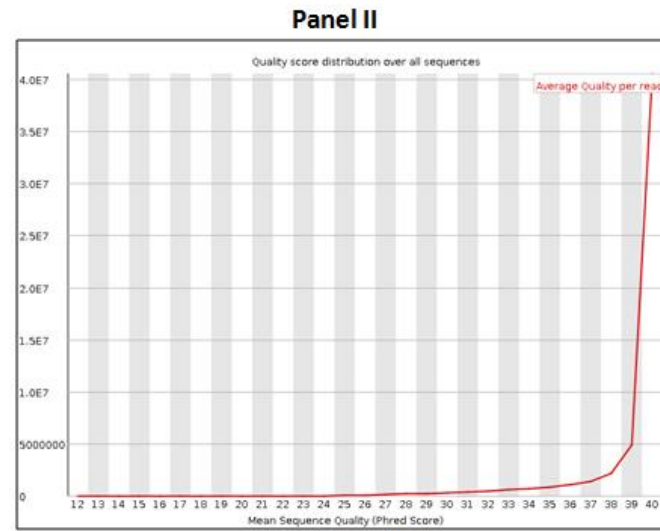
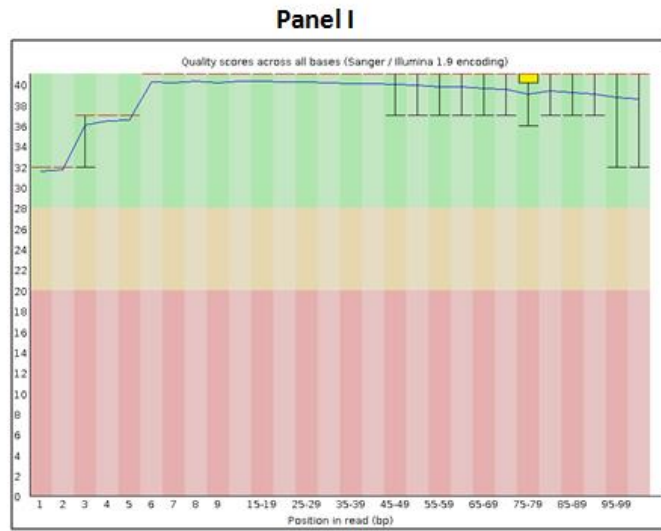


Figure 28: Representative figures of RNA sequencing quality of sample ML-11. A) The forward sequencing and B) The reverse sequencing quality plots are depicted in Panel I: per base sequencing quality, Panel II: quality score distribution over all sequences, Panel III: GC distribution over all sequences and Panel IV: sequence length distribution.

RNA sequencing based gene expression analysis

A.



(Continued.....)

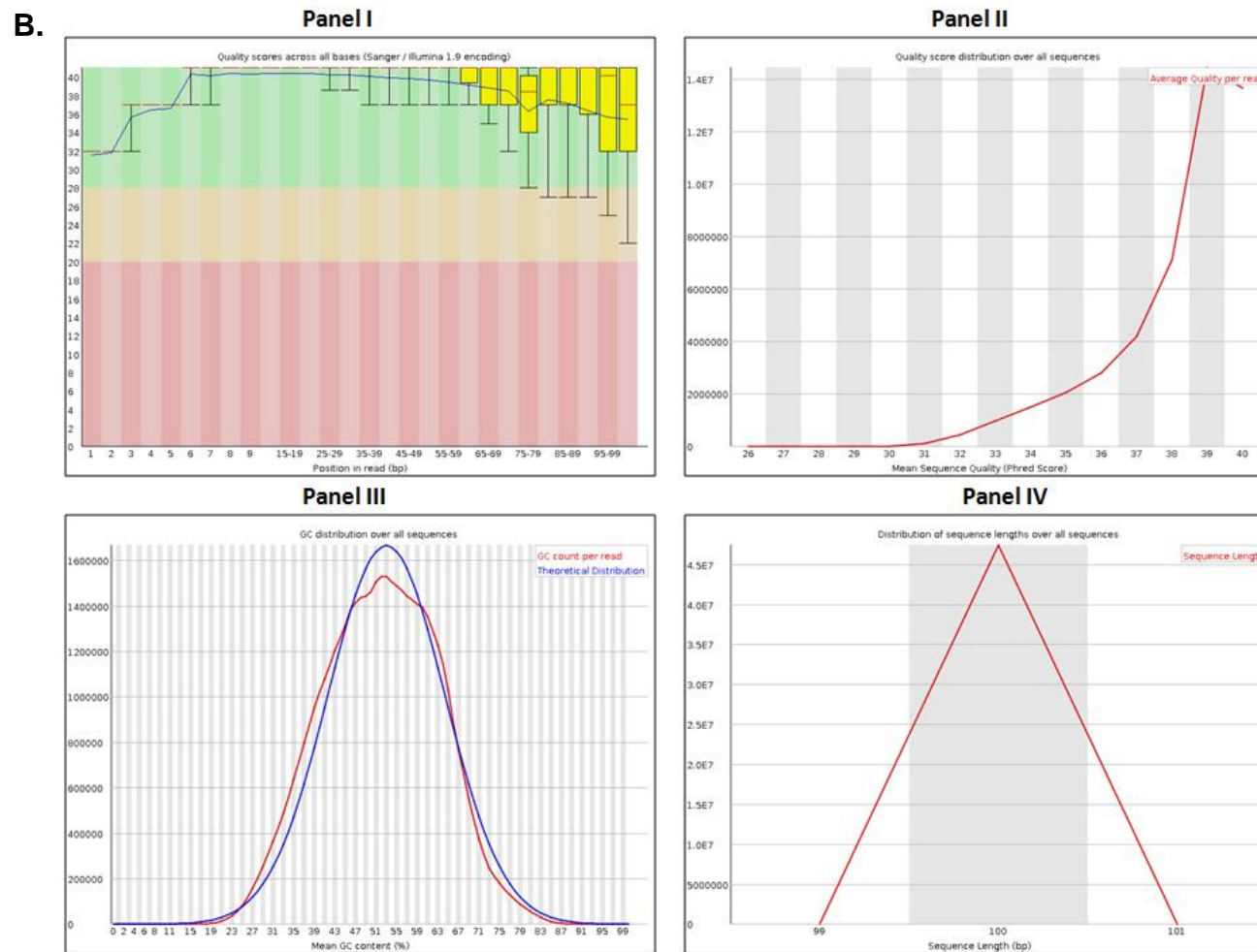


Figure 29: Representative figures of RNA sequencing quality of sample ML-12. A) The forward sequencing and B) The reverse sequencing quality plots are depicted in Panel I: per base sequencing quality, Panel II: quality score distribution over all sequences, Panel III: GC distribution over all sequences and Panel IV: sequence length distribution.

RNA sequencing based gene expression analysis

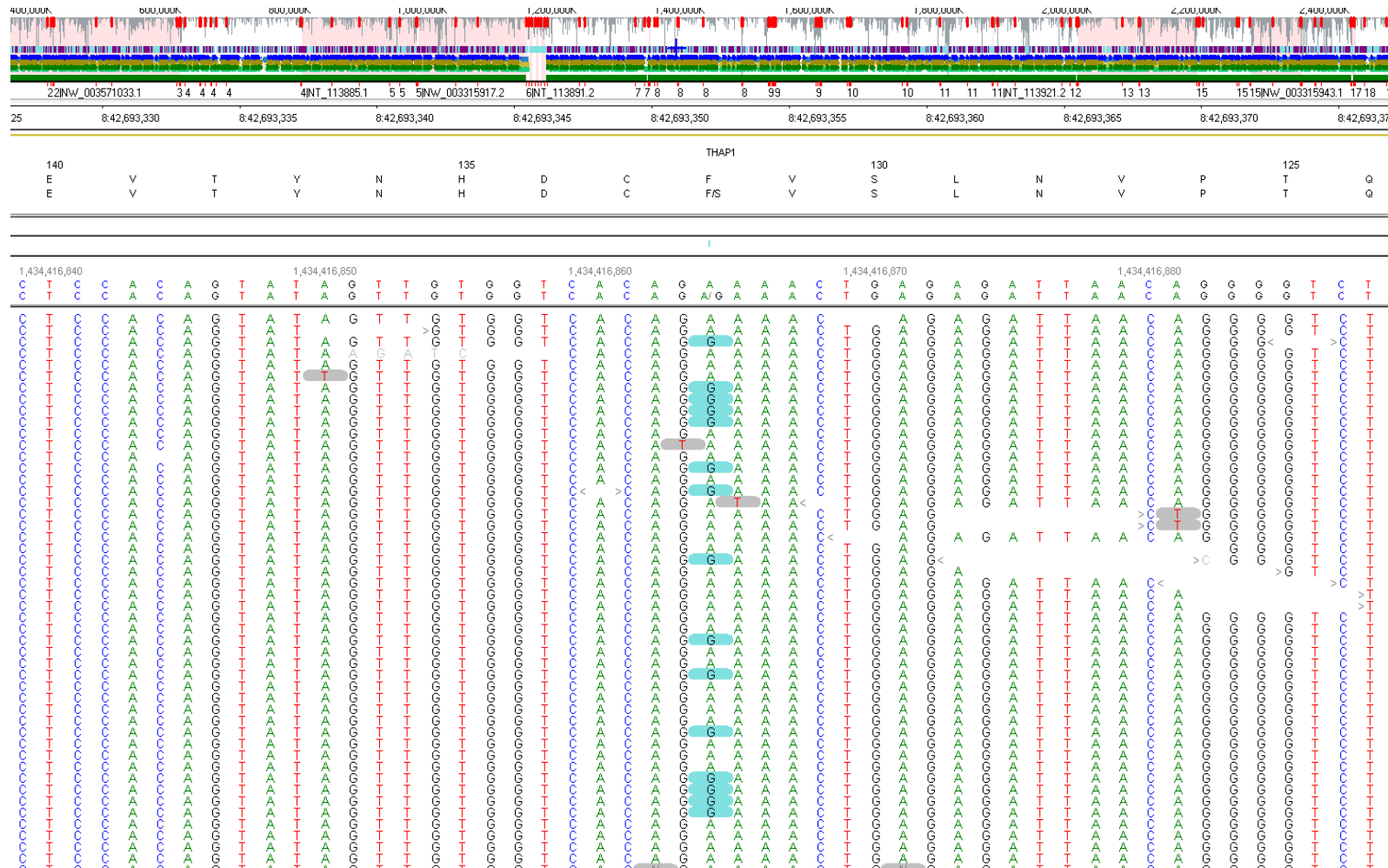


Figure 31: The alignment of raw RNA-seq reads of ML2 and visualization of mutant allele of *THAP1* (c.395 T>C) through NextGENE® software.

RNA sequencing based gene expression analysis

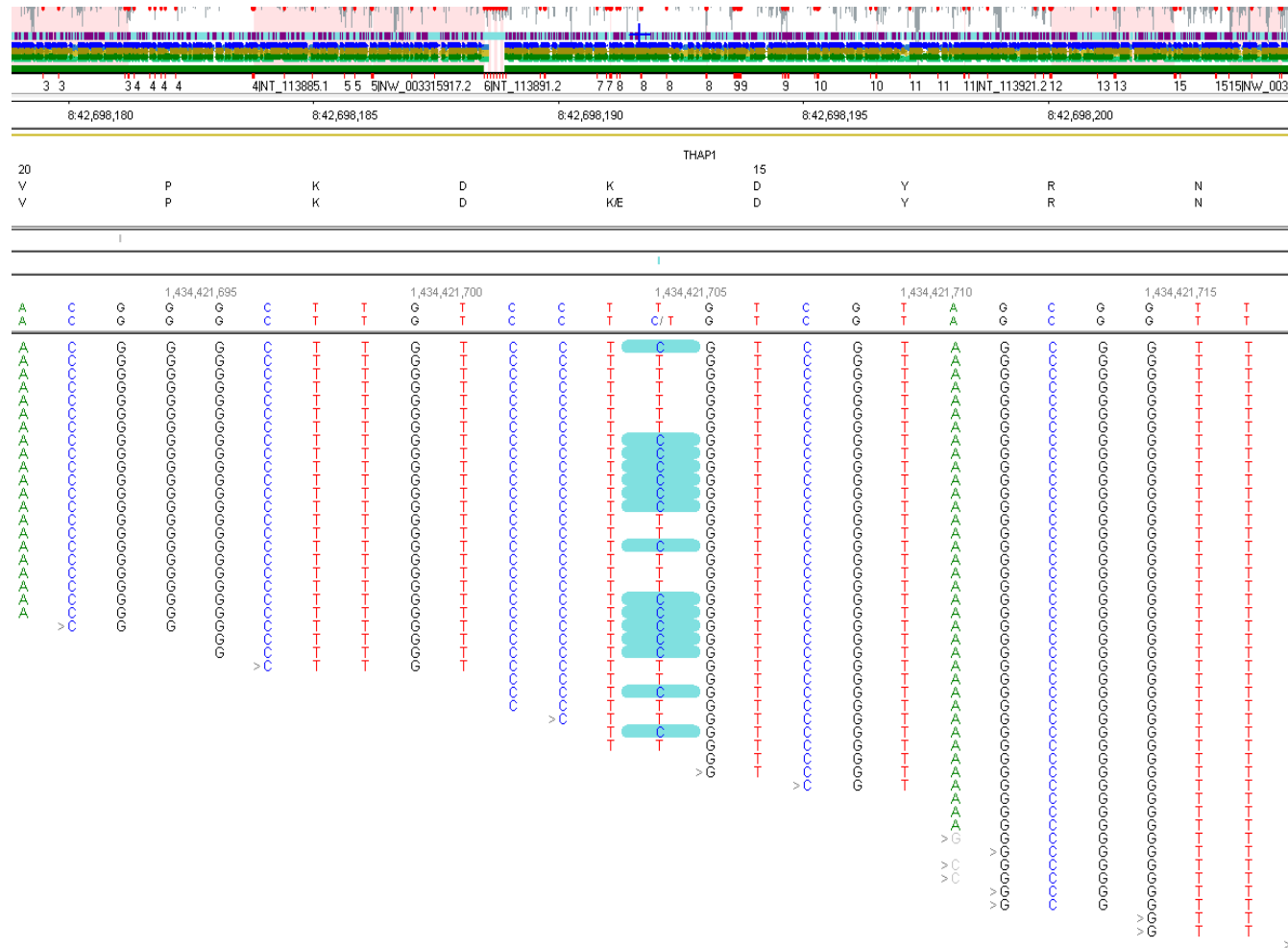


Figure 34: The alignment of raw RNA-seq reads of ML10 and visualization of mutant allele of *THAP1* (c.46 A>G) through NextGENe® software.

RNA sequencing based gene expression analysis

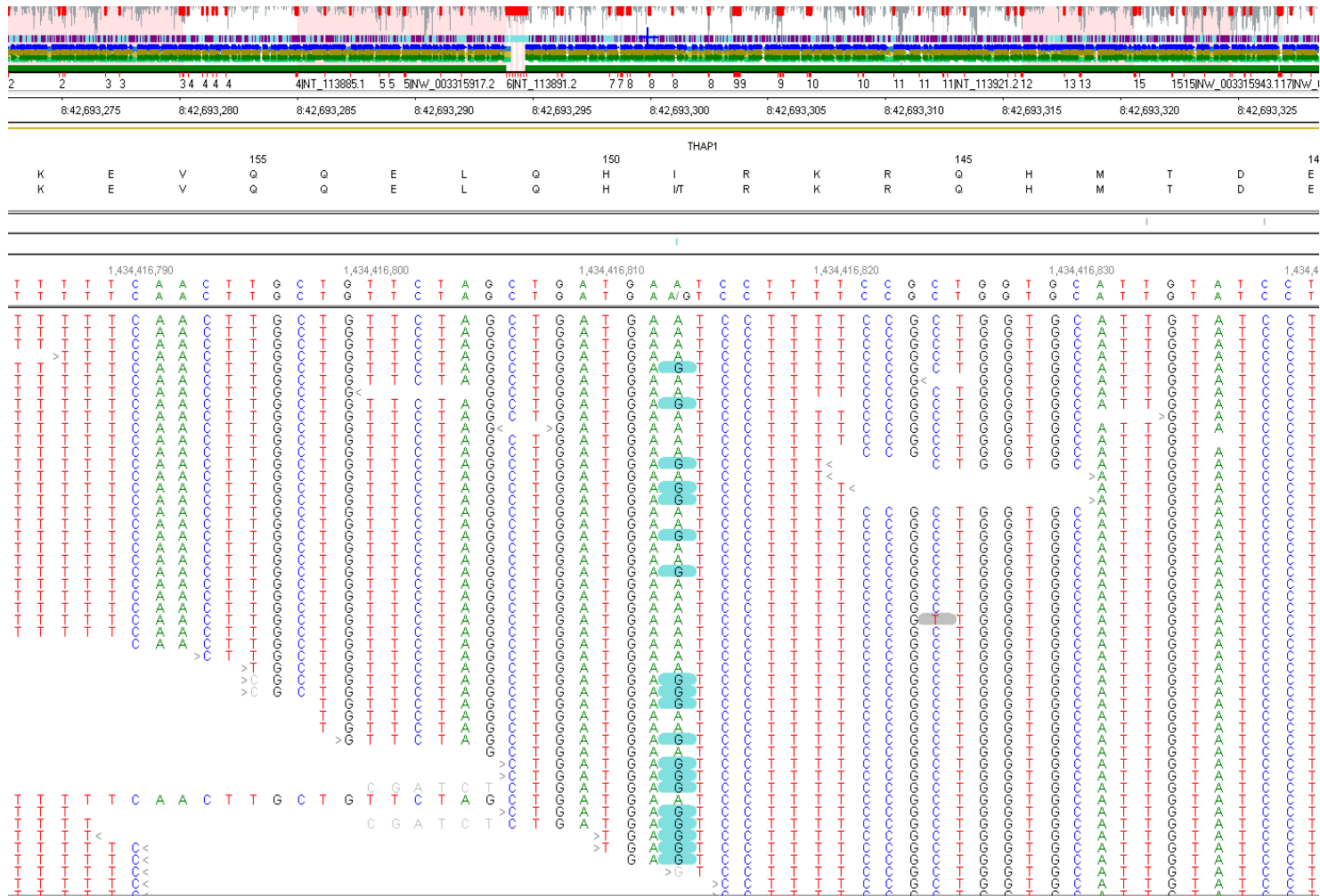


Figure 35: The alignment of raw RNA-seq reads of ML11 and visualization of mutant allele of *THAP1* (c.446 T>C) through NextGENe® software.

5.3.3 Identification of differentially expressed genes in *THAP1* mutant dystonia patients compared to controls

Given the diverse role of THAP1 in regulating the gene expression as a transcription factor, whole genome gene expression studies were performed to identify the possible dysregulated pathways by mutant THAP1 proteins. These experiments employed total RNA isolation from fibroblast cell lines derived from six isolated dystonia patients (three male and three female) harbouring *THAP1* mutations and six age and gender matched control individuals. Gene expression analysis by RNA-seq revealed significant upregulation of 17 genes (Table 50) and down regulation of 38 genes (Table 51). The significance level was set for Benjamini-Hochberg False discovery rate (FDR) < 0.05, p-value < 0.05 and fold change ≥ 1.5 . The heat map of differentially expressed genes is illustrated in Figure 36. The scatter plot (Figure 37) and the volcano plot (Figure 38) is also generated for DEG. The gene set enrichment analysis by Ingenuity Pathway Analysis (IPA) recognized five major dysregulated networks (Table 52) which are involved in tissue development, cellular development, cell signalling, vitamin and mineral metabolism, cell death and survival. Disease and function annotation of significant up and down regulated genes enriched for neurological disease (*CTSB*, *KCNK1*, *NTF3*, *PACSIN3*, *PDE5A*, *SYT1*), psychological disorders (*CTSB*, *KCNK1*, *NTF3*, *PACSIN3*, *PDE5A*, *PML*, *SYT1*), cell cycle progression (*CDKL1*, *LTBP1*, *NEDD1*, *NTF3*, *PLA2G16*, *PML*, *SPDYA*), abnormal morphology of cells (*BPNT1*, *CREB5*, *CTSB*, *DSTN*, *F11R*, *KALRN*, *LMO7*, *NEDD1*, *NTF3*, *PML*, *POSTN*, *PPP1R13L*, *PTGFRN*), quantity of cells (*CTSB*, *FAAH*, *KALRN*, *NEO1*, *NTF3*, *PML*, *POSTN*, *PPP1R13L*, *SPDYA*) and cell death of motor neurons (*FAAH*, *NTF3*) (Table 53). IPA interactome analysis identified NF- κ B (complex), Creb, ERK & ERK-1/2 as a major hub for network 1

(Figure 39). The interactome of other two major networks (network 2 & 3) are illustrated in Figure 40 and Figure 41 respectively. Further analysis based on the normalized read counts revealed that none of the other dystonia related genes were dysregulated in terms of expression (Table 54).

RNA sequencing based gene expression analysis

Table 50: Significant up-regulated genes in primary dystonia patients having *THAP1* mutation compared to controls.

HGNC Gene Symbol	Gene Name	Control average read count	Patient average read	Fold Change*	T-Test**	FDR***
<i>SYT1</i>	Synaptotagmin 1	20.67	62.5	3.02	0.04	0.04
<i>KCNK1</i>	Potassium channel, two pore domain subfamily K,	43.5	109.5	2.51	0.03	0.04
<i>CREB5</i>	cAMP responsive element binding protein 5	70	166.16	2.37	0.04	0.04
<i>LOC101927751</i>	E3 Ubiquitin-Protein Ligase RING1-Like	50.5	114.33	2.26	0.04	0.04
<i>PLBD1</i>	Phospholipase B domain containing 1	8.16	16.33	2	0.03	0.04
<i>FAAH</i>	Fatty acid amide hydrolase	8.83	16.83	1.9	0.04	0.04
<i>TEKT4P2</i>	Tektin 4 Pseudogene 2	11	19.5	1.77	0.04	0.04
<i>EPB41L4A</i>	Erythrocyte membrane protein band 4.1 like 4A	50.33	89	1.76	0.04	0.04
<i>PTGFRN</i>	Prostaglandin F2 receptor inhibitor	1007.66	1763.5	1.75	0.03	0.04
<i>INSIG2-v4</i>	Insulin Induced Gene 2 transcript variant 4	8.33	14.16	1.7	0.04	0.04
<i>MAGOHB</i>	Mago homolog B, exon junction complex core	8.5	14.33	1.68	0.04	0.04
<i>SPDYA</i>	Speedy/RINGO cell cycle regulator family member A	10.33	17.33	1.67	0.04	0.04
<i>FRG1CP</i>	FSHD Region Gene 1 Family Member C, Pseudogene	83.66	131.5	1.57	0.04	0.04
<i>CTSB</i>	Cathepsin B	17.83	27.83	1.56	0.03	0.04
<i>ZNF431-v1</i>	Zinc Finger Protein 431 transcript variant 1	11.66	17.83	1.52	0.04	0.04
<i>CDKL1</i>	Cyclin dependent kinase like 1	63.83	97.5	1.52	0.04	0.04
<i>LINC01410</i>	Long Intergenic Non-Protein Coding RNA 1410	38.66	58.16	1.5	0.04	0.04

HGNC: *HUGO Gene Nomenclature Committee*, *Fold change ≥ 1.5 , Fold change calculated as patient average read counts/control average read counts, **T-Test: Two tailed heteroscedastic student t-test (significant level, p-value < 0.05), ***FDR: Benjamini Hochberg false discovery rate (significance level: q-value < 0.05).

RNA sequencing based gene expression analysis

Table 51: Significant down-regulated genes in primary dystonia patients having *THAP1* mutation compared to controls

HGNC Gene Symbol	Gene Name	Control average read counts	Patient average read counts	Fold Change*	T-Test**	FDR***
<i>ShRNA-MAN2A2</i>	Mannosidase alpha class 2A member 2 (MAN2A2), transcript variant 4, non-coding RNA.	28.5	19	1.5	0.043	0.048
<i>NEDD1</i>	Neural precursor cell expressed, developmentally down-regulated 1	42.83	28.5	1.5	0.044	0.048
<i>BPNT1</i>	3'(2'), 5'-bisphosphate nucleotidase 1	17	11.16	1.52	0.036	0.049
<i>MCM3AP-AS1</i>	MCM3AP Antisense RNA 1	23.5	15.33	1.53	0.044	0.048
<i>PACSLIN3</i>	Protein kinase C and casein kinase substrate in neurons 3	312.66	200.67	1.55	0.043	0.048
<i>LOC100129461</i>	LYRM4 antisense RNA 1	10.67	6.83	1.56	0.042	0.049
<i>BCL7A</i>	B-cell CLL/lymphoma 7A	166.83	106.67	1.56	0.002	0.044
<i>ZGPAT</i>	Zinc finger, CCCH-type with G-patch domain	10.17	6.5	1.56	0.04	0.049
<i>LMO7</i>	LIM domain 7	10228.5	6525.67	1.56	0.046	0.048
<i>PLEKHG4</i>	Pleckstrin homology and RhoGEF domain containing G4	73.33	46.67	1.57	0.042	0.049
<i>PML</i>	Promyelocytic leukemia	23.16	14.67	1.57	0.002	0.045
<i>ZNF674</i>	Zinc Finger Protein 674	14	8.83	1.58	0.042	0.049
<i>LTN1</i>	listerin E3 ubiquitin protein ligase 1	23	14.5	1.58	0.0006	0.04
<i>SP110</i>	SP110 nuclear body protein	9.33	5.83	1.6	0.035	0.049
<i>DSTN</i>	destrin (actin depolymerizing factor)	116	71.83	1.61	0.044	0.048
<i>HSPB2-C11orf52</i>	Homo sapiens HSPB2-C11orf52 readthrough	8.66	5.33	1.62	0.041	0.049
<i>NEO1</i>	neogenin 1	1210.33	734.83	1.64	0.04	0.049
<i>VPS29</i>	VPS29 retromer complex component	8.83	5.33	1.65	0.041	0.049

RNA sequencing based gene expression analysis

HGNC Gene Symbol	Gene Name	Control average read counts	Patient average read counts	Fold Change*	T-Test**	FDR***
<i>TMEM134</i>	transmembrane protein 134	8.33	5	1.67	0.043	0.048
<i>TXNDC11-7</i>	Homo sapiens thioredoxin domain containing 11, transcript variant 7	10.33	6.16	1.67	0.043	0.048
<i>GBP3-v4</i>	Homo sapiens guanylate binding protein 3 (GBP3), transcript variant 4	57	32.33	1.76	0.001	0.046
<i>SLC7A5</i>	solute carrier family 7 (amino acid transporter light chain, L system),	4123.83	2294	1.79	0.039	0.049
<i>METTL15</i>	methyltransferase like 15	8.5	4.67	1.82	0.049	0.049
<i>SPT6-homolog</i>	SPT6 homolog, histone chaperone (SUPT6H), transcript variant 1	12.83	7	1.83	0.049	0.049
<i>HHIPL1</i>	HHIP-like 1	178.83	96.83	1.84	0.0009	0.049
<i>NKIRAS2</i>	NFKB inhibitor interacting Ras-like 2	6.83	3.67	1.86	0.043	0.048
<i>DCLK2</i>	doublecortin like kinase 2	34.16	17.33	1.97	0.047	0.048
<i>PPP1R13L</i>	protein phosphatase 1 regulatory subunit 13 like	25.66	12.83	2	0.045	0.048
<i>LTBP1</i>	latent transforming growth factor beta binding protein 1	69.83	34.5	2.02	0.048	0.049
<i>MOK</i>	MOK protein kinase	30.33	14.83	2.04	0.001	0.045
<i>MIR137HG</i>	MIR137 Host Gene	20.33	9.33	2.17	0.03	0.049
<i>PDE5A</i>	phosphodiesterase 5A	485.67	211.16	2.29	0.044	0.048
<i>POSTN</i>	periostin, osteoblast specific factor	11.16	4.67	2.39	0.04	0.049
<i>KALRN</i>	kalirin, RhoGEF kinase	10.5	4.33	2.42	0.002	0.049
<i>PLA2G16</i>	phospholipase A2 group XVI	12.33	5	2.46	0.042	0.049
<i>TSPAN18</i>	tetraspanin 18	406.67	135.83	2.99	0.041	0.049
<i>F11R</i>	F11 receptor	33.33	9.33	3.57	0.04	0.049
<i>NTF3</i>	neurotrophin 3	78.5	18	4.36	0.004	0.049

HGNC: *HUGO Gene Nomenclature Committee*, *Fold change ≥ 1.5 , Fold change calculated as control average read counts/patient average read counts. **T-Test: Two tailed heteroscedastic student t-test (significant level: p-value < 0.05), ***FDR: Benjamini Hochberg false discovery rate (significance level: q-value < 0.05).

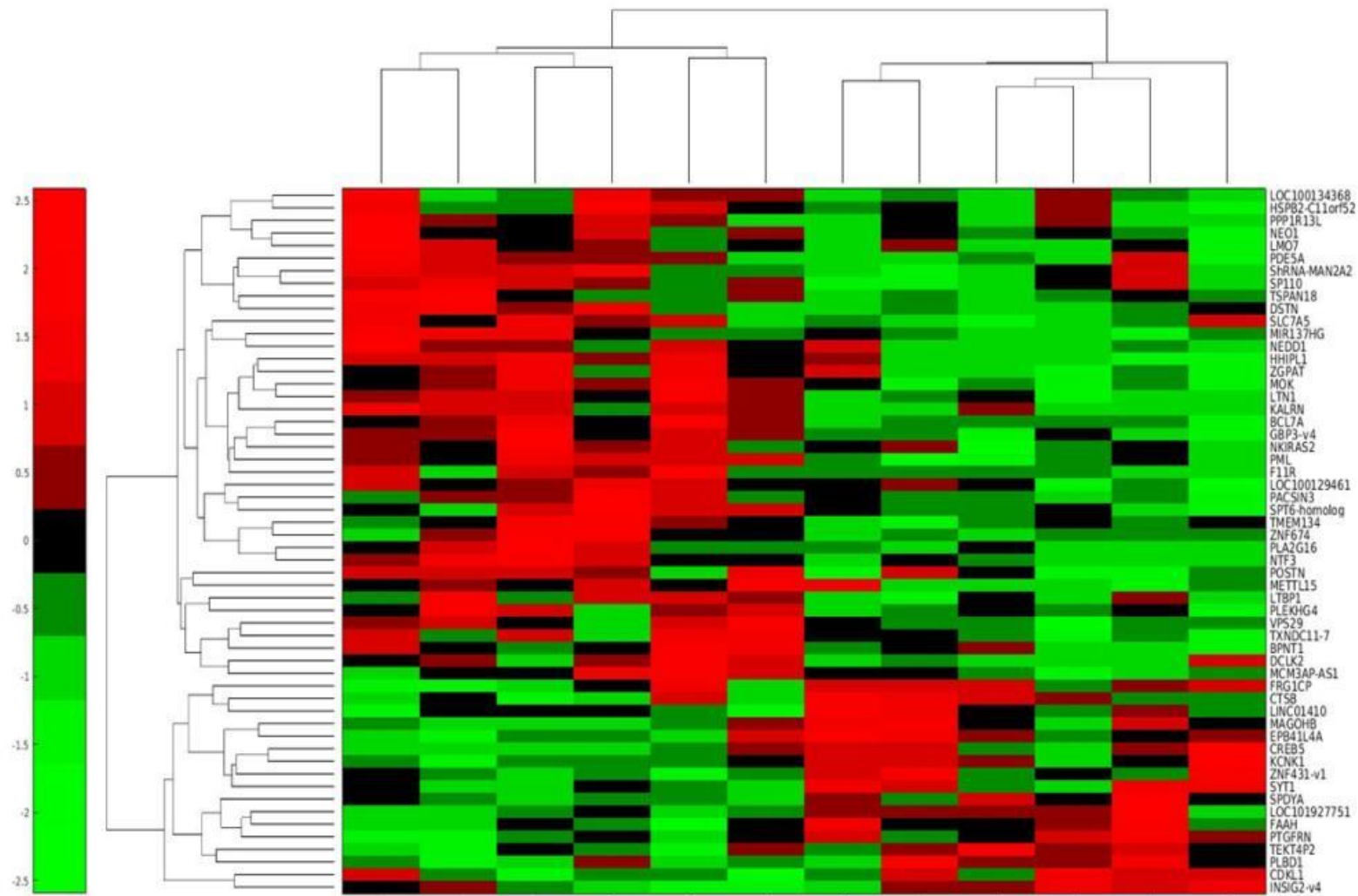


Figure 36: Heat map of differentially expressed genes (DEG).

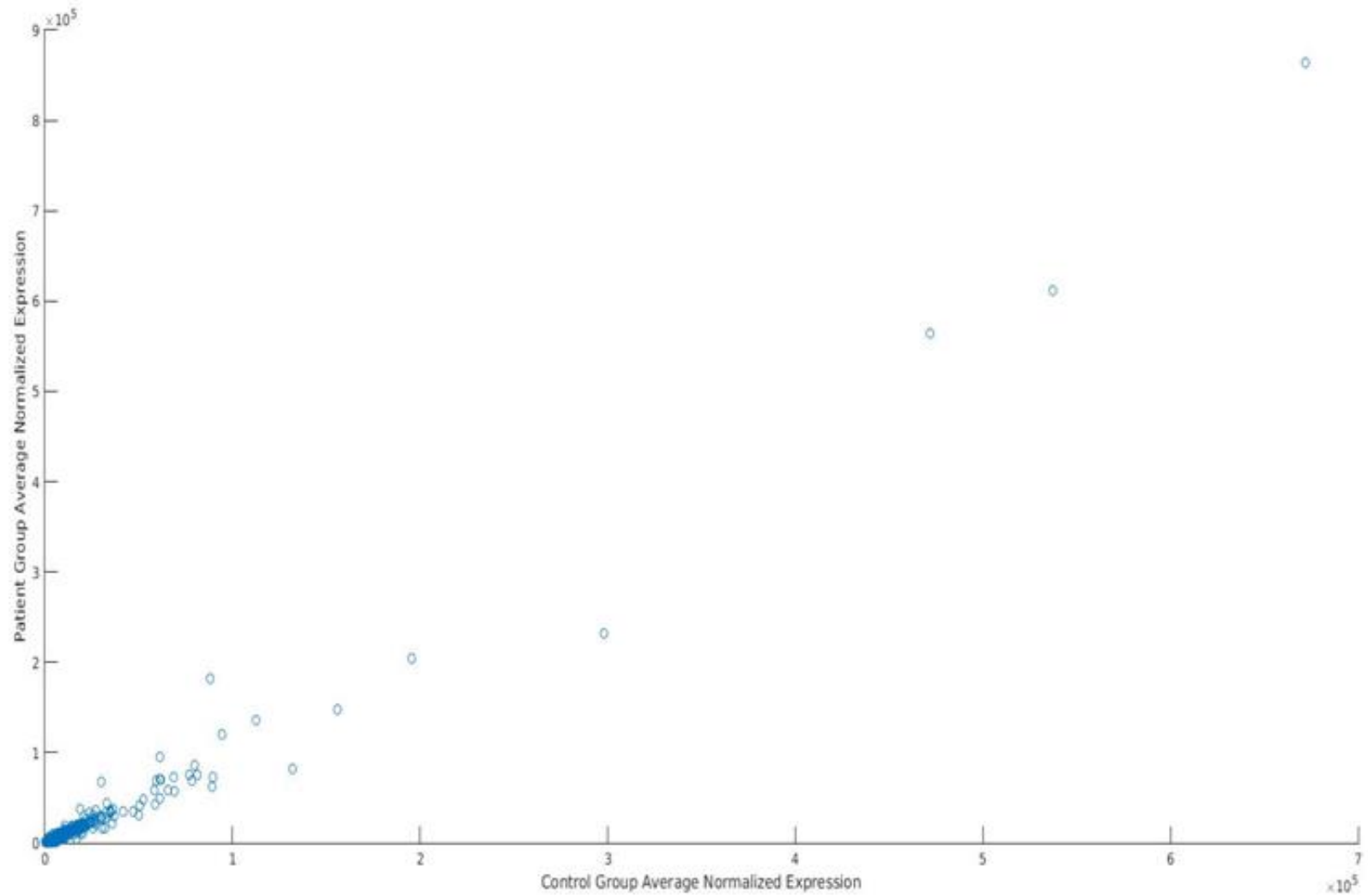


Figure 37: Scatter plot of differentially expressed genes (DEG).

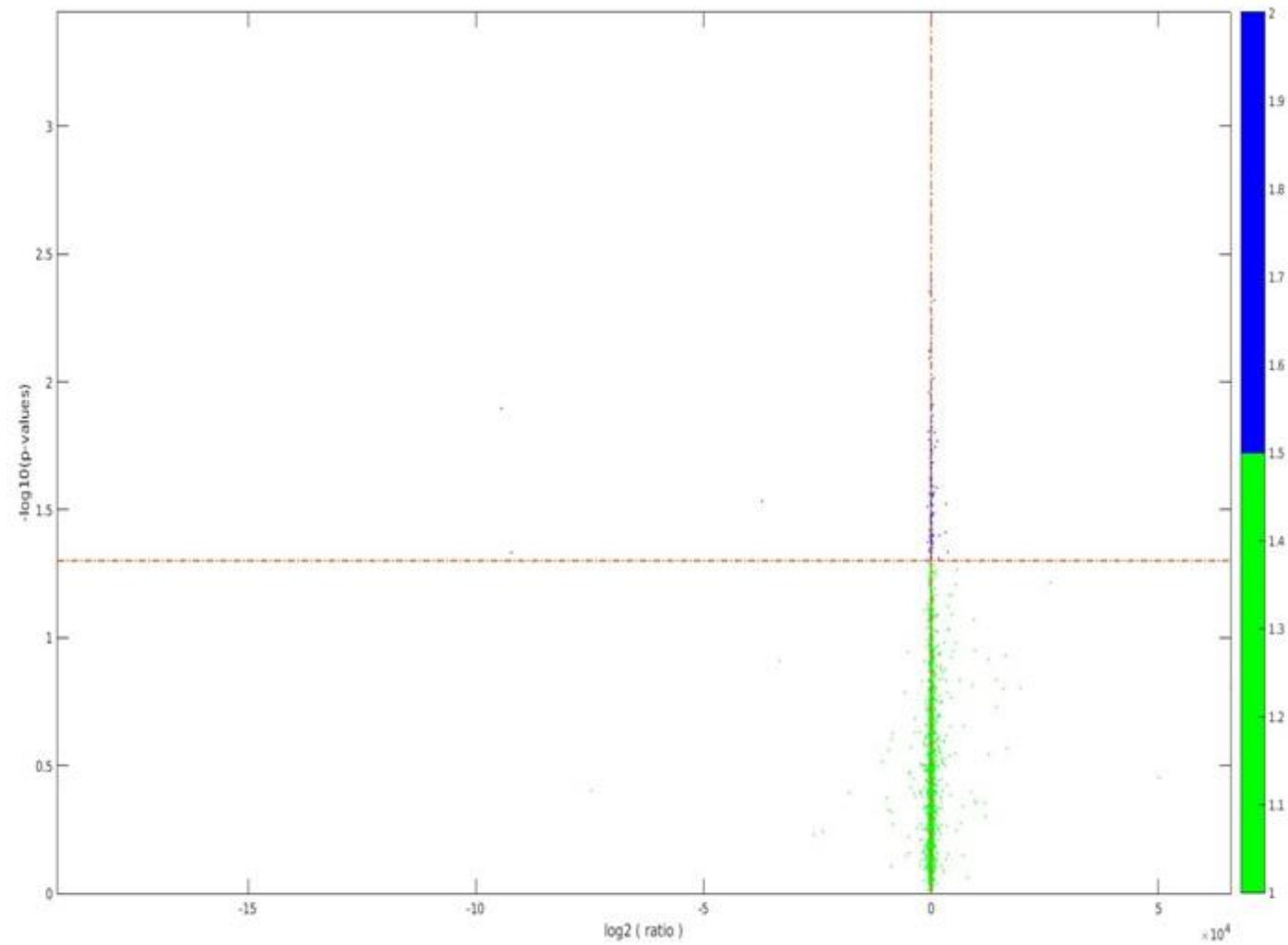


Figure 38: Volcano plot of differentially expressed genes (DEG).

RNA sequencing based gene expression analysis

Table 52: Ingenuity pathway analysis (IPA) to identify top affected disease network.

ID	Molecules in Network	Score	Focus Molecules	Top Diseases and Functions
1	26s Proteasome, Akt,CBP-CREB-CRTC2, Cbp/p300 Creb, CD3, Collagen(s), Creb, CREB5 , CREB-NFkB, CTSB , ERK, ERK1/2, F11R , Foxn3, glucose oxidase, IL1, LTBP1 , LTN1 , MOK , NFkB (complex), NKIRAS2 , NTF3 , P38 MAPK, Pad4, PDE5A , PML , POSTN , PPP1R13L , Ras, SLC39A12, SLC7A5 , SPDYA , SYT1 , TMEM184C, Vegf	35	15	Tissue Development, Cardiovascular Disease, Congenital Heart Anomaly
2	Actin, AGBL2, BCL7A , Ca2+, CCNJ, CDK2, CTIF, CUL3, DSTN , ELAVL1, FAAH , dihydrotestosterone, KALRN , KCNK1 , LMO7 , MAGOHB , METTL15, mir-638, miR-638 (miRNAs w/seed GGGAU CG), MPV17L, MTMR11, MYNN, NEDD1 , NEO1 , PAC SIN3 , fPCNXL2, PLA2G16 , RAF1, S100PBP, SPATA18, TMEM127, TMEM134 , TP53, TP63, TRMT11.	28	13	Cancer, Cellular Development, Organismal Injury and Abnormalities
3	AIMP2, APP, ATCAY, BPNT1 , C11orf53, CDKL1, CDKL4, DCLK2 , DNAJB7, DNAJB14, DNAJC4, EPB41L4A , FAM160B2, FBXO27, FKBP5, FKBP51-TEBP-GR-HSP90-HSP70, GTPBP8, Hsp84-2, HSP90AA1, MAPK3, OLFM3, PLBD1 , PLEKHG4 , PRL, PSKH2, PTGFRN , RAB26, RXFP3, SP110 , STUB1, TBX22, THAP4, TRAF6, VPS29 , ZGPAT	20	10	Cell Signaling, Vitamin and Mineral Metabolism, Behavior
4	HHIPL1 , ING4	3	1	Cell Death and Survival, Cellular Development,
5	RNF130, TSPAN18	3	1	Metabolic Disease

RNA sequencing based gene expression analysis

Table 53: Disease and function annotation of significant up and down regulated genes.

Genes/Molecules		Categories	Disease and Function annotation	p-value*
Up regulated	Down regulated			
<i>CTSB, KCN1, SYT1</i>	<i>NTF3, PACSIN3, PDE5A</i>	Neurological Disease, Psychological Disorders	Schizophrenia	5.95E-04
<i>CTSB, KCN1, SYT1</i>	<i>NTF3, PACSIN3, PDE5A, PML</i>	Psychological Disorders	Schizophrenia spectrum disorder	1.08E-04
<i>CDKL1, SPDYA</i>	<i>LTBP1, NEDD1, NTF3, PLA2G16, PML,</i>	Cell Cycle	Cell cycle progression	1.67E-02
<i>CTSB, PTGFRN</i>	<i>BPNT1, CREB5, DSTN, F11R, KALRN, LMO7, NEDD1, NTF3, PML, POSTN, PPP1R13L</i>	Cell Morphology	Morphology of cells	1.14E-03
<i>CTSB, FAAH, SPDYA</i>	<i>KALRN, NEO1, NTF3, PML, POSTN, PPP1R13L</i>	Tissue Morphology	Quantity of cells	3.78E-02
<i>FAAH</i>	<i>NTF3</i>	Cell Death and Survival	Cell death of motor neurons	7.19E-03
<i>SYT1</i>	<i>KALRN, NTF3</i>	Cell-To-Cell Signaling and Interaction, Nervous System Development and Function	Excitatory postsynaptic potential	2.09E-03
-	<i>KALRN, NTF3</i>	Nervous System Development and Function	Growth of dendrites, branching of axons	8.25E-03

*p-value: Significance level of overlap of molecules to be associated in particular molecular pathway as predicted in IPA.

RNA sequencing based gene expression analysis

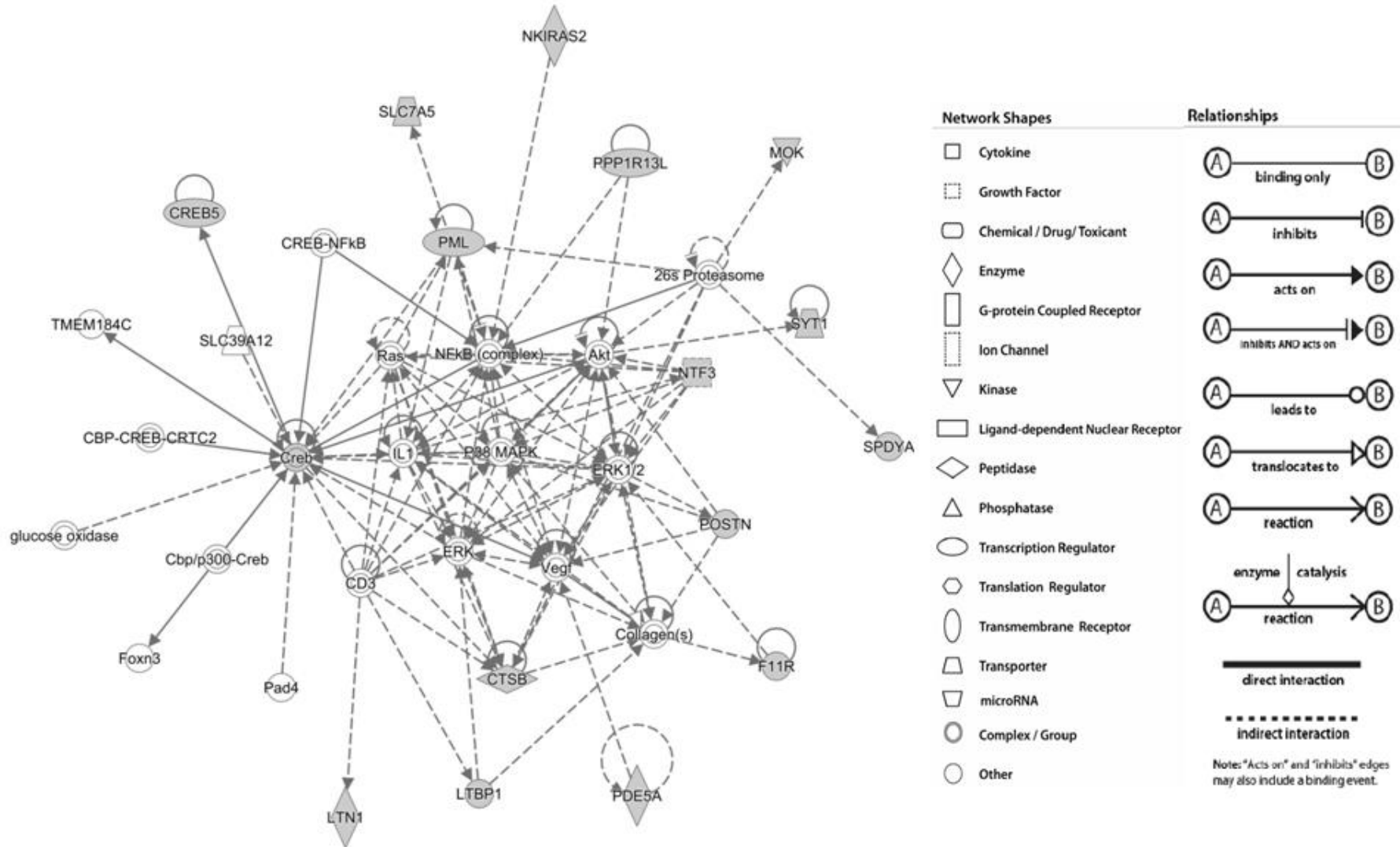


Figure 39: Ingenuity interactome analysis of up and down regulated genes enriched in disease network 1. NF-κB complex, Creb, ERK1/2 & Akt were found as the major hub of this interactome.

RNA sequencing based gene expression analysis

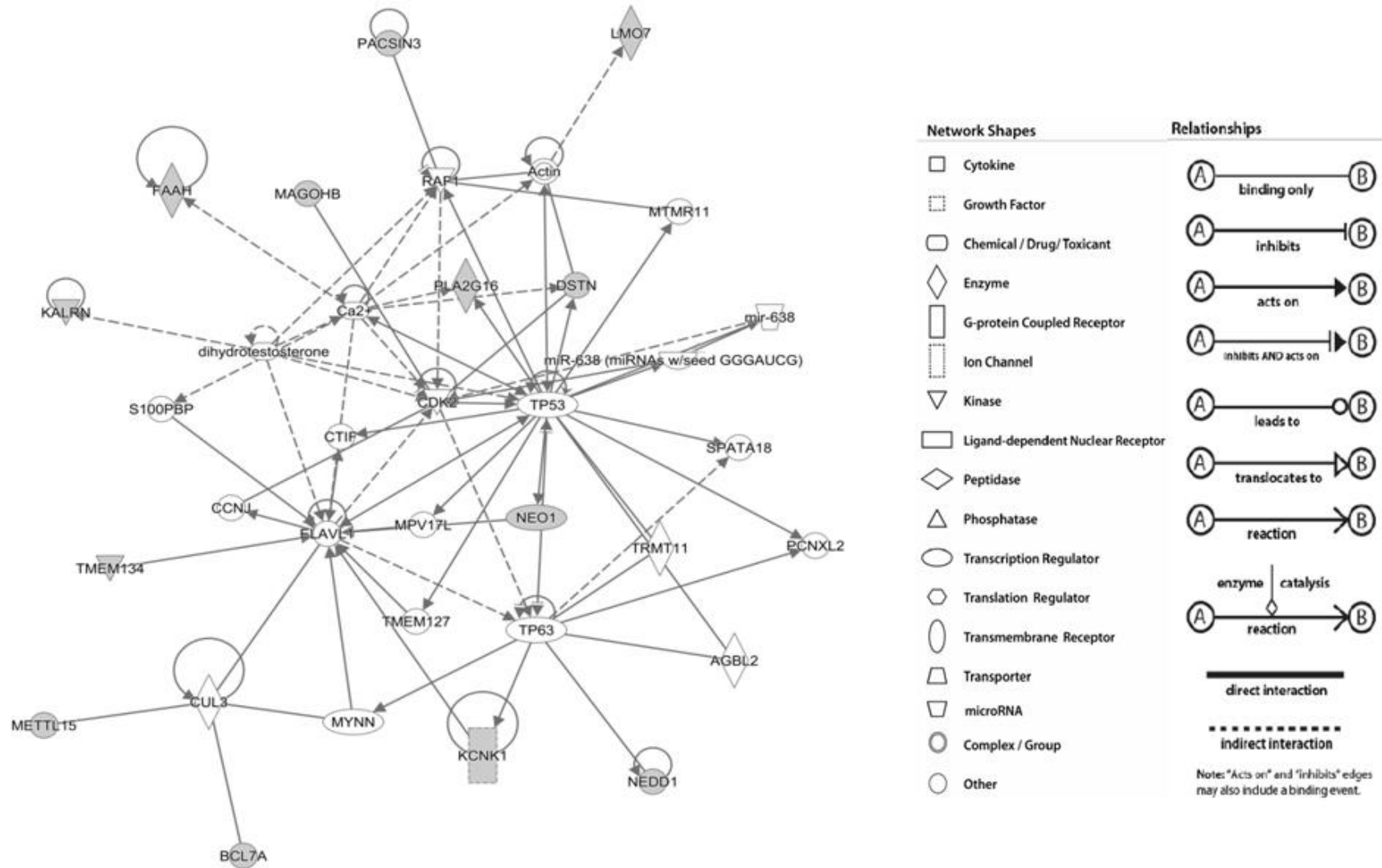


Figure 40: Ingenuity interactome analysis of up and down regulated genes enriched in disease network 2.

RNA sequencing based gene expression analysis

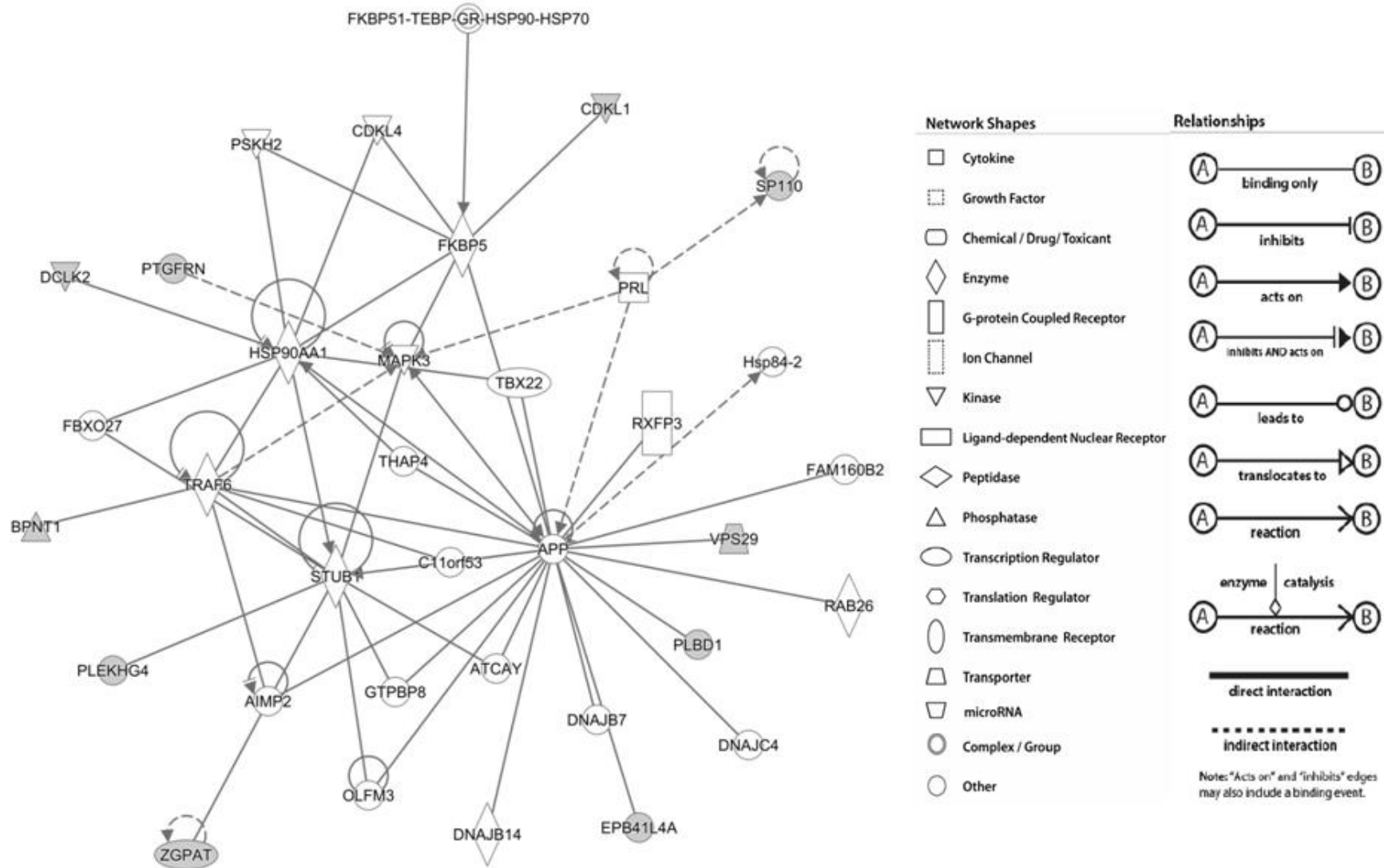


Figure 41: Ingenuity interactome analysis of up and down regulated genes enriched in disease network 3.

RNA sequencing based gene expression analysis

Table 54: Expression level of dystonia related genes in the *THAP1* mutant dystonia patients & control fibroblast samples

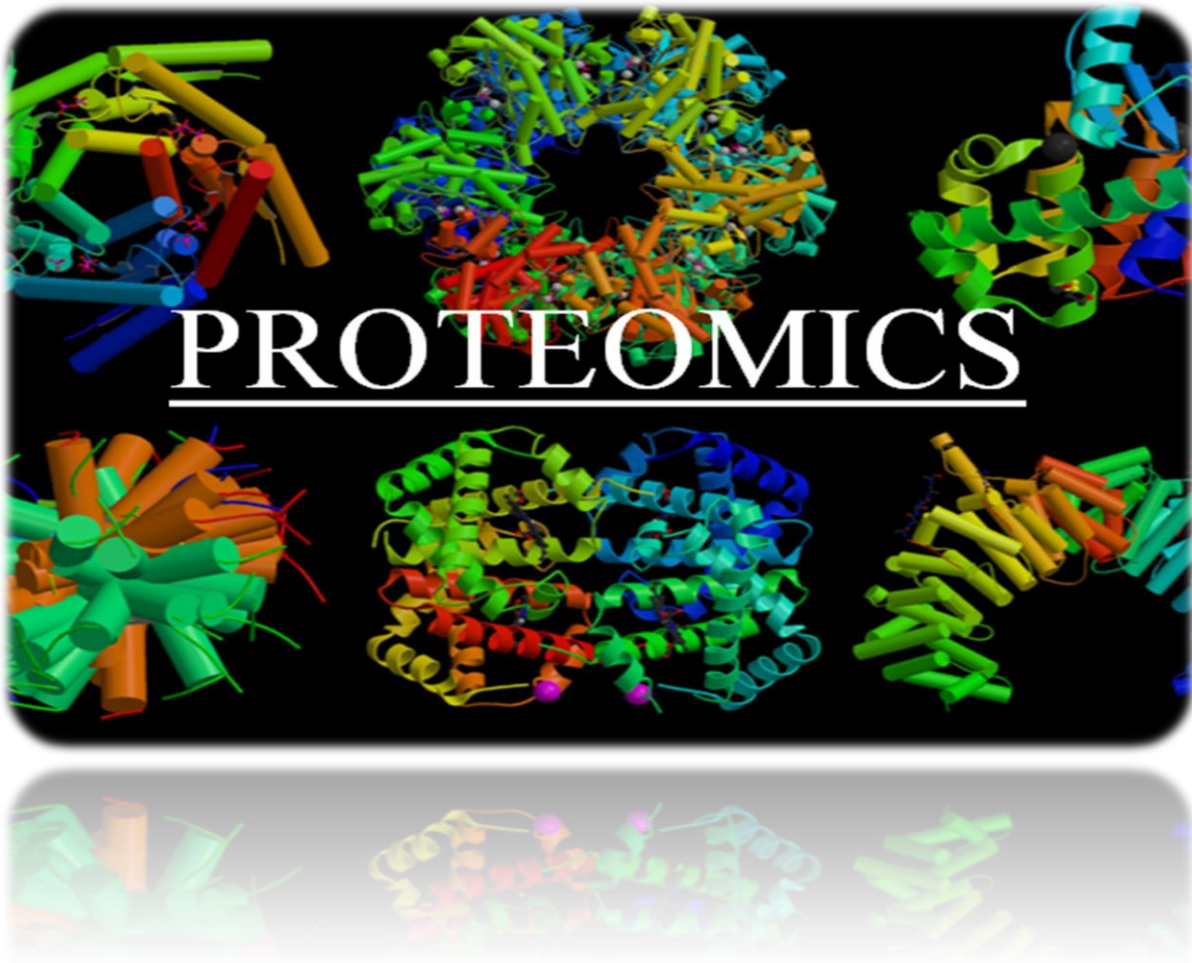
Gene Name	Transcript ID	Control average read counts	Patient average read counts	Control SEM	Patient SEM	Fold Change	T-Test*
<i>TOR1A</i>	NM_000113	962.33	992.83	46.70	45.32	0.97	0.65
<i>THAP1</i>	NM_018105	49.33	45.00	5.50	4.35	1.10	0.55
<i>TAF1</i>	NM_138923	194.00	199.50	6.36	10.65	0.97	0.67
<i>GNAL</i>	NM_182978	24.50	18.50	5.53	1.23	1.32	0.33
<i>CIZ1</i>	NM_001131015	22.67	20.17	4.42	3.28	1.12	0.66
<i>PRRT2</i>	NM_001256443	36.17	28.50	6.58	5.47	1.27	0.39
<i>GCH1</i>	NM_000161	29.00	29.83	6.23	5.90	0.97	0.92
<i>ANO3</i>	NM_031418	40.33	31.83	10.90	20.16	1.27	0.72
<i>PNKD</i>	NM_015488	6.33	6.50	1.05	0.76	0.97	0.90
<i>MR-1</i>	NM_001195000	118.00	107.50	10.41	14.07	1.10	0.56
<i>SGCE</i>	NM_001099401	170.17	161.33	36.42	32.30	1.05	0.86
	NM_001301139	168.83	154.67	31.37	19.66	1.09	0.71
	NM_001099400	508.83	496.67	90.23	82.78	1.02	0.92
<i>ATP1A3</i>	NM_152296	14.17	5.17	6.50	2.01	2.74	0.23
<i>PRKRA</i>	NM_003690	428.33	434.33	20.28	21.74	0.99	0.84
<i>SLC2A1</i>	NM_006516	1215.33	1109.33	117.04	357.94	1.10	0.79

SEM: Standard error of mean; *T-TEST: Two tailed heteroscedastic student t-test (significant level: p-value < 0.05)

5.4 Discussion

To investigate the molecular mechanism of primary dystonia caused by *THAP1* mutation in a broad aspect, whole genome gene expression analysis was performed to identify the differentially expressed genes (DEG). For this analysis, six patients' fibroblast samples were collected, who possess six different missense mutations in *THAP1* gene along with the six age and gender matched control fibroblast samples, then cultured and total RNA was isolated for RNA-seq library preparation followed by RNA sequencing in a HiSeq2500 instrument (Illumina). Data analysis for DEG revealed significant upregulation of 17 genes and down regulation of 38 genes. The upregulated genes include some of the important genes viz. *SYT1* (Synaptotagmin 1), *CREB5* (cAMP responsive element binding protein 5), *SPDYA* (Speedy/RINGO cell cycle regulator family member A), *CDKL1* (Cyclin dependent kinase like 1), which are involved in cell cycle progression and cell proliferation, nervous system development and function. The downregulated genes includes *PML* (Promyelocytic leukemia), *TMEM134* (Transmembrane protein 134), *NKIRAS2* (NFkB inhibitor interacting Ras-like 2), *PLA2G16* (phospholipase A2 group XVI), *NTF3* (neurotrophin 3) which are either direct interacting partner of *THAP1* (Roussigne et al., 2003) or involved in neurological problems. IPA of up and down regulated genes identified top affected cellular pathways including cell cycle progression (*CDKL1*, *LTBP1*, *NEDD1*, *NTF3*, *PLA2G16*, *PML*, *SPDYA*), abnormal morphology of cells (*BPNT1*, *CREB5*, *CTSB*, *DSTN*, *F11R*, *KALRN*, *LMO7*, *NEDD1*, *NTF3*, *PML*, *POSTN*, *PPP1R13L*, *PTGFRN*), quantity of cells (*CTSB*, *FAAH*, *KALRN*, *NEO1*, *NTF3*, *PML*, *POSTN*, *PPP1R13L*, *SPDYA*) and cell death of motor neurons (*FAAH*, *NTF3*). *THAP1* is reported to be a regulator of genes involved in G1/S phase of cell cycle progression through pRb-E2F pathway (336). It was also shown in two transgenic mouse model

(heterozygous null mutant THAP1^{+/-} & knock-in THAP1^{C54Y/+}), that deprivation of cellular THAP1 protein could cause abnormal cellular morphology and hypocellularity in dentate nucleus of the cerebellum (DNC) (322). So the primary dystonia could arise from differential gene expression, which could affect the normal development and function of specific brain region responsible for movement.



CHAPTER 6

MASS SPECTROMETRY BASED WHOLE CELL PROTEOMIC ANALYSIS OF PRIMARY DYSTONIA PATIENTS HAVING *THAP1* MUTATION

6.1 Introduction

With the advancement of cutting edge molecular techniques, whole cell proteomic profiling provides a detailed insight into the molecular mechanism of disease perspective (709, 710). It plays an important role for molecular diagnostics and biomarker development (711). Proteomic analysis also helps to identify the expression and abundances of novel disease specific protein, which in turn helps to identify the specific molecular mechanism associated with the protein expression. To understand the primary dystonia pathogenesis, no such proteomic approach was taken to dissect the differentially expressed proteins except for one cellular model. In that HEK293 based cellular model, the differentially expressed proteins were identified by 2D-DIGE for DYT1 Δ GAG mutation (712). In this study, the patients' fibroblast samples having mutation in *THAP1* were used for quantitative whole cell proteomic analysis based on liquid chromatography-tandem mass spectrometry (LC-MS/MS) to identify the differentially expressed proteins compared to the control fibroblast samples having wild type *THAP1*. The mass spectrometry was done by *in-vitro* labelling of cellular total proteins by tandem mass tags (713, 714). The labelled peptide samples were then sequenced quantitatively through a high-throughput mass spectrometer (715). This would generate the first experimental data to suggest the possible mechanism of primary dystonia associated with *THAP1* mutation.

Along with the transcriptome data, the proteogenomic analysis is the possible best method to discover the disease pathogenesis (716). In this chapter, the quantitative whole cell proteomic profiling of primary dystonia patients has been described with experimental methodologies and results.

6.2 Materials & Methods

6.2.1 Selection of patient and control subjects

The proteomic profiling of primary dystonia patient and control fibroblast samples was intended to identify the significant up and down regulated proteins. The same patients and control fibroblast samples were used for transcriptome analysis. The purpose of this selection was to determine the downstream effect of transcriptomic alteration in the protein level, which may direct the molecular mechanism of DYT6 dystonia caused by *THAP1* mutation.

6.2.2 Fibroblast cell culture

The same protocol was used which is described in the section 5.2.2.

6.2.3 Whole cell lysate preparation from fibroblast samples

The whole cell lysate were prepared for all the fibroblast samples using RIPA lysis buffer (89900, Thermo Scientific, USA). Halt™ Protease and Phosphatase Inhibitor Cocktail (78442, Thermo Scientific, USA) was added in lysis buffer at a final concentration of 1X. The detailed protocol is given below.

1. Growth media was removed and cells were rinsed by cold 1X DPBS without dislodging the cells and the wash material was discarded.
2. 0.5 ml of cold RIPA lysis buffer was added to the T75 flask containing about 1×10^7 fibroblast cells.
3. The flask was kept on ice for 5 minutes, swirling the plate occasionally for uniform spreading.

4. The lysate was gathered to one side using a cell scraper, collected and transferred to a microcentrifuge tube. The samples were then centrifuged at 13000 rpm for 15 minutes to pellet the cell debris.
5. The supernatant containing protein was transferred to a new tube and continued to protein concentration determination.

6.2.4 Protein concentration determination

The protein concentration of the extracted cell lysate was evaluated which was done by Pierce™ BCA assay kit (23227, Thermo Scientific, USA). The Thermo Scientific™ Pierce™ BCA Protein Assay is a detergent-compatible formulation based on bicinchoninic acid (BCA) for the colorimetric detection and quantitation of total protein. This method combines the well-known reduction of Cu^{+2} to Cu^{+1} by protein in an alkaline medium (the biuret reaction) with the highly sensitive and selective colorimetric detection of the cuprous cation (Cu^{+1}) using a unique reagent containing bicinchoninic acid (717). The purple-colored reaction product of this assay is formed by the chelation of two molecules of BCA with one cuprous ion. This water-soluble complex exhibits a strong absorbance at 562nm that is nearly linear with increasing protein concentrations over a broad working range (20-2000 $\mu\text{g}/\text{mL}$). The BCA method is not a true end-point method; that is, the final colour continues to develop. However, following incubation, the rate of continued color development is sufficiently slow to allow large numbers of samples to be assayed together. The macromolecular structure of protein, the number of peptide bonds and the presence of four particular amino acids (cysteine, cystine, tryptophan and tyrosine) are reported to be responsible for color formation with BCA (718). Studies with di-, tri- and tetrapeptides suggest that the extent of color formation caused by more than the

mere sum of individual color producing functional groups (718). Accordingly, protein concentrations generally are determined and reported with reference to standards of a common protein, such as, bovine serum albumin (BSA). A series of dilutions of known concentration are prepared from the protein and assayed alongside the unknown(s) before the concentration of each unknown is determined based on the standard curve.

Preparation of Standards and Working Reagent

A. Preparation of Diluted Albumin (BSA) Standards

Table 1 was used as a guide to prepare a set of protein standards. The contents of one Albumin Standard (BSA) ampule was diluted into several clean vials using the same diluents, water. Each 1mL ampule of 2mg/mL Albumin Standard was sufficient to prepare a set of diluted standards for either working range suggested in Table 1. There was sufficient volume for three replications of each diluted standard.

B. Preparation of the BCA Working Reagent (WR)

1. Use the following formula to determine the total volume of **WR** required:

$(\# \text{ standards} + \# \text{ unknowns}) \times (\# \text{ replicates}) \times (\text{volume of WR per sample}) = \text{total volume WR required.}$

For this instance, the standard test-tube procedure with 12 unknowns and 2 replicates of each sample:

$(9 \text{ standards} + 12 \text{ unknowns}) \times (2 \text{ replicates}) \times (2\text{mL}) = 84\text{mL WR required.}$

As the test tube procedure was followed in this study, only 2mL of WR reagent is required for each sample.

2. WR was prepared by mixing 50 parts of BCA Reagent A with 1 part of BCA Reagent B (50:1, Reagent A: B). For this experiment, 84 mL of Reagent A was combined with 1.68 mL of Reagent B.

Test-tube Procedure (Sample to WR ratio = 1:20)

1. 0.1 mL of each standard and unknown sample replicate was pipetted into an appropriately labeled test tube.
2. 2.0 mL of the WR was added to each tube and mixed well.
3. Tubes were covered and incubated at 37 °C for 30 minutes.
4. All tubes were cooled to RT.
5. The spectrophotometer was set to zero with water at 562 nm. The absorbances of all the samples were measured within 10 minutes. Because the BCA assay does not reach a true end point, colour development will continue even after cooling to RT. However, because the rate of colour development is low at RT, no significant error will be introduced if the 562 nm absorbance measurements of all tubes are made within 10 minutes of each other.
6. Subtracted the absorbance of the Blank from individual standards and unknown sample replicates.
7. A standard curve was prepared by plotting the average Blank-corrected BSA standard vs. its concentration in µg/mL. The standard curve was used to determine the protein concentration of each unknown sample.

6.2.5 Sample preparation with TMT™ Isobaric Mass Tagging

In this study, the extracted protein samples were subjected to Liquid chromatography - Tandem mass spectrometry (LC-MS/MS) by *in-vitro* labelling of

the peptide fractions. The *in-vitro* labelling was done using Thermo Scientific™ TMT™ sixplex reagents. The Thermo Scientific™ TMT™ Isobaric Mass Tagging kits and reagents enable multiplex relative quantitation by mass spectrometry (MS). Each mass-tagging reagent within a set has the same nominal mass (i.e., isobaric) and chemical structure composed of an amine-reactive NHS-ester group, a spacer arm and an MS/MS reporter (Figure 42).

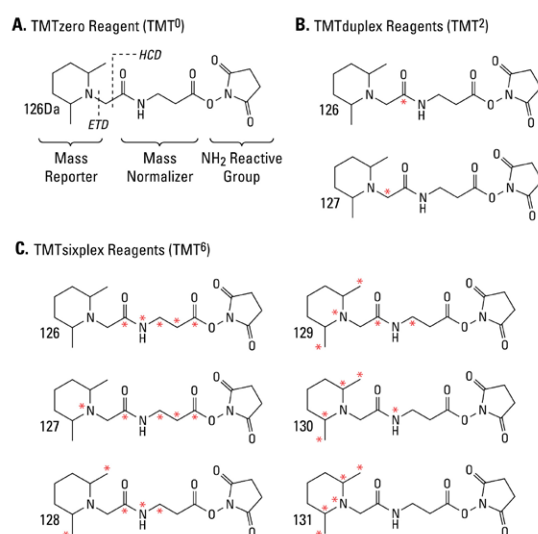


Figure 42: Chemical structure of the TMT Label Reagents. **A.** Functional regions of the reagent structure, including MS/MS fragmentation sites by higher energy collision dissociation (HCD) and electron transfer dissociation (ETD). **B.** TMTduplex Reagent structures and isotope positions (*); only HCD differentiates between these two reporters. **C.** TMTsixplex Reagent structures and isotope positions (*).

The reagent sets can be used to label two or six peptide samples prepared from cells or tissues. For each sample, a unique reporter in the low mass region of the MS/MS spectrum (i.e., 126-127Da for TMT² and 126-131Da for TMT⁶ Isobaric Label Reagents) is used to measure relative protein expression levels during peptide fragmentation. The TMTduplex™ Isotopic Label Reagent Set contains TMTzero™ and one of the TMTsixplex™ Reagents (TMT⁶ -127) to be used as “light” and “heavy” tags for MS-level peptide quantitation similar to duplex isotopic metabolic

labeling (e.g., SILAC) or isotopic dimethylation labeling. These isotopic pairs can also be used in targeted quantitation strategies, including selective reaction monitoring (SRM). Advantages of the TMTsixplex Isobaric Label Reagents include increased sample multiplexing for relative quantitation, increased sample throughput and fewer missing quantitative channels among samples.

Reagent preparation

100 mM TEAB (Triethyl ammonium bicarbonate): 500 μ L of the 1M TEAB (90114, Thermo Scientific, USA) added to 4.5 mL of LC-MS grade ultrapure water (51140, Thermo Scientific, USA).

200 mM TCEP: 70 μ L of the 0.5 M TCEP (77720, Thermo Scientific, USA) was added to 70 μ L of ultrapure water. Then 35 μ L of the Dissolution Buffer (1M TEAB) was added.

5% Hydroxylamine: 50 μ L of the 50% hydroxylamine (90115, Thermo Scientific, USA) was added to 450 μ L of 100 mM TEAB.

Reduction & alkylation of protein sample

1. 100 μ g of protein per sample (six for the TMTsixplex Label Reagents) was transferred into a fresh low protein binding collection tube (88379, Thermo Scientific, USA) and adjusted to a final volume of 100 μ L with 100 mM TEAB.
2. 5 μ L of the 200 mM TCEP was added and incubated at 55 $^{\circ}$ C for 1 hour.
3. Immediately before use, one tube of 9 mg iodoacetamide (90034, Thermo Scientific, USA) was dissolved with 132 μ L of 100 mM TEAB to make 375 mM iodoacetamide. Solution was protected from light.

4. 5 μ L of the 375 mM iodoacetamide was added to the sample and incubated for 30 minutes protected from light at room temperature.
5. About six volumes (~660 μ L) of pre-chilled (-20 $^{\circ}$ C) acetone (A929-1, Fischer Scientific, USA) was added and kept at -20 $^{\circ}$ C. It was allowed to precipitate for overnight.
6. The sample was centrifuged at 10000 rpm for 10 minutes at 4 $^{\circ}$ C. Then carefully inverted the tubes to decant the acetone without disturbing the white pellet. The pellet was allowed to air-dry for 2-3 minutes.

Protein digestion

The acetone precipitated protein pellet was resuspended in 100 μ l of 50 mM TEAB. Then 2.5 μ g of Trypsin/Lys-C mix, mass spec grade (V5071, Promega, Madison, USA) was added to each protein sample and incubated for digestion for overnight at 37 $^{\circ}$ C.

Protein labelling

1. Immediately before use, the TMT label reagents were equilibrated to room temperature. For the 0.8 mg vials, 41 μ L of anhydrous acetonitrile (400060, Thermo Scientific, USA) was added to each tube.
2. Carefully 41 μ L of the TMT Label Reagent (90061, Thermo Scientific, USA) was added to each 100 μ L of digested peptide sample and incubated the reaction for 1 hour at room temperature.
3. Then 8 μ L of 5% hydroxylamine (90115, Thermo Scientific, USA) was added to the sample and incubated for 15 minutes to quench the reaction.

4. Six samples were combined at equal amounts each (100 µg) in new micro-centrifuge tube. From this combined homogeneous sample 100 µg was aliquoted and proceed to speed-vac for dryness.
5. Then 100 µg of combined protein sample was taken in duplicate. Then it was continued to fractionate in to several fractions with different solubility.

Fractionation of combined labelled samples

The dried peptide combination was resuspended in 300 µL of 0.1% TFA (28904, Thermo Scientific, USA) solution. Then the fractionation was done using the Pierce High pH Reversed-Phase Peptide Fractionation Kit (84868, Thermo Scientific, USA) following the manufacturer protocol (Figure 43). High-pH reversed-phase chromatography is a robust method of peptide fractionation that separates peptides by hydrophobicity and provides excellent orthogonality to low-pH reversed-phase LC-MS gradients. In contrast to strong cation exchange (SCX) fractionation, high-pH reversed-phase fractions do not require an additional desalting step before LC-MS analysis. Each reversed-phase fractionation spin column enables fractionation of 10-100 µg of peptide sample using a microcentrifuge. Proteolytic digests of proteins extracted from cells or tissues are loaded onto an equilibrated, high-pH, reversed-phase fractionation spin column. Peptides are bound to the hydrophobic resin under aqueous conditions and desalted by washing the column with water by low-speed centrifugation. A step gradient of increasing acetonitrile concentrations in a volatile high pH elution solution is then applied to the columns to elute bound peptides into eight different fractions collected by centrifugation. Each fraction is then dried in a vacuum centrifuge and stored until analysis by mass spectrometry. During LC-MS analysis, peptides in each high-pH fraction are further separated using a low-pH

gradient, thus reducing the overall sample complexity and improving the ability to identify low-abundant peptides.

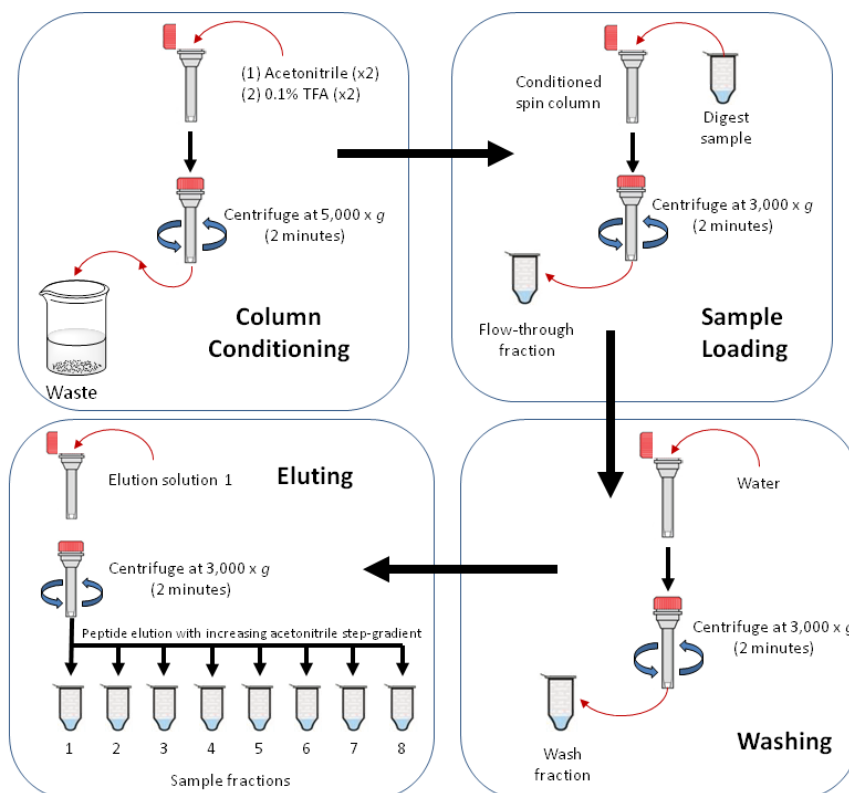


Figure 43: Spin column conditioning and sample fractionation workflow.

Reagent preparation

0.1% Trifluoroacetic acid (TFA): 10 mL of equilibration solution was prepared by adding 10 μ L of TFA to 10 mL of water. Volume was sufficient for equilibration of 12 columns.

High-pH step-elution solutions: Solutions were prepared in 2 mL tubes according to Table 55. Different sets of elution solutions were used for TMT-labeled samples due to different peptide retention behavior. 300 μ L of each solution was required per sample. Calculated volumes in Tables 1 were enough for fractionation of up to three samples.

Table 55: Preparation of elution solutions for TMT-labeled peptides.

Fraction No.	Acetonitrile (%)	Acetonitrile (μ L)	1% Triethylamine (μ L)
Wash	5.0	50	950
1	10.0	100	900
2	12.5	125	875
3	15.0	150	850
4	17.5	175	825
5	20.0	200	800
6	22.5	225	775
7	25.0	250	750
8	50.0	500	500

Fractionation of Proteolytic Digests

A. Conditioning of the Spin Columns

1. The protective white tip was removed from the bottom of the column and discarded. The column was placed into a 2.0 mL sample tube.
2. Centrifuge at $5000 \times g$ for 2 minutes to remove the solution and pack the resin material. Discard the liquid.
3. The top screw cap was removed and 300 μ L of acetonitrile was added into the column. The cap was removed; the spin column was placed back into a 2.0 mL sample tube and centrifuged at $5000 \times g$ for 2 minutes. Acetonitrile was discarded and the wash step repeated.
4. The spin column was washed twice with 0.1% TFA solution, as described in Step 3. The column is then conditioned and ready for use.

B. Fractionation of Digest Samples

1. Elution solutions were prepared according to Table 1.
2. 10-100 μ g of digested sample was dissolved in 300 μ L of 0.1% TFA solution.
3. The spin column was placed into a new 2.0 mL sample tube. 300 μ L of the sample solution was loaded onto the column; the top cap was replaced and

centrifuged at $3000 \times g$ for 2 minutes. Elute was retained as “flow-through” fraction.

4. The column was placed into a new 2.0 mL sample tube. 300 μ L of water was loaded onto the column and centrifuged again to collect the wash. Elute was retained as “wash” fraction.
5. The step 4 was repeated once to with 300 μ L of 5% ACN, 0.1% TEA to remove un-reacted TMT reagent.
6. The column was placed into a new 2.0 mL sample tube. 300 μ L of the appropriate elution solution was loaded (e.g., 5% ACN, 0.1% TEA) and centrifuged at $3000 \times g$ for 2 minutes to collect the fraction.
7. The liquid content of each sample was evaporated to dryness using Savant™ SpeedVac™ Concentrator (SPD131DDA, Thermo Scientific, USA).
8. Dry samples were then resuspended in an appropriate volume of 0.5% TFA before LC-MS analysis.
9. The peptide concentration was determined with a peptide quantitation assay, so equivalent sample amounts can be analyzed by LC-MS.

Peptide concentration determination Pierce Quantitative Colorimetric Peptide Assay

The Thermo Scientific™ Pierce™ Quantitative Colorimetric Peptide Assay provides modified BCA reagents along with a proprietary chelator and uses the biuret reduction of Cu^{+2} to Cu^{+1} to analyze peptide mixtures. In the reaction, copper is first reduced by the amide backbone of peptides under alkaline conditions (the biuret reaction), followed by the proprietary chelator coupling with the reduced copper to form a bright red complex at 480 nm absorbance. The kit also contains a

high quality peptide digest reference standard to generate linear standard curves and calibration controls. This colorimetric peptide assay requires a small amount of sample (20 µL) and has a working peptide concentration range of 25-1,000 µg/mL.

Preparation of Standards

According to Table 56, the dilution series was prepared for the Peptide Digest Assay Standard to generate a standard curve. The Peptide Digest Assay Standard was diluted into clean vials, using the same diluent as the sample(s). This was sufficient volume to run an 8-point standard curve (from 0-1000 µg/mL) in triplicate.

Table 56: Preparation of diluted peptide digests assay standards.

Centrifuge tubes	Volume of Water (µl)	Volume of Digest (µl)	Final Concentration of Digest (µg/mL)
A	0	150 of Stock	1000
B	75	75 of Vial A	500
C	75	75 of Vial B dilution	250
D	75	75 of Vial C dilution	125
E	75	75 of Vial D dilution	62.5
F	75	75 of Vial E dilution	31.3
G	75	75 of Vial F dilution	15.6
Blank	75	Use water for blank	0

Preparation of Working Reagent

1. Use the following formula to determine the total volume of Working Reagent (WR) required:

$$[(\# \text{ of standards}) + (\# \text{ of unknowns})] \times (\# \text{ of replicates}) \times (0.18\text{mL of WR per sample}) = \text{total volume WR required}$$

For this instance, an 8-point standard curve and 44 unknowns in triplicate: (8 standards + 44 unknowns) × (3 replicates) × (0.18 mL) = 28.08 (~ 30 ml) of WR was prepared.

2. WR was prepared by mixing:
 - 50 parts of Colorimetric Peptide Assay Reagent A

- 48 parts of Colorimetric Peptide Assay Reagent B
- 2 parts of Colorimetric Peptide Assay Reagent C

For the above experiment, 15 mL of Peptide Assay Reagent A, 14.4 mL of Peptide Assay Reagent B and 0.6 mL of Peptide Assay Reagent C was combined.

Procedure

1. Samples and standards were prepared. Total number of samples were 44 (Two individual sixplex reactions in duplicate, each have 11 fractions i.e. for each fractionation, there were 1 flow-through, 2 wash fractions and 8 elute fractions).
2. 20 μ L of each standard or unknown sample replicate were pipetted into a well of a 96-well micro plate.
3. 180 μ L of the WR was added to each well and mixed thoroughly on a plate shaker for 30 seconds to 1 minute.
4. Plate was covered and incubated at room temperature for 30 minutes.
5. The measurement was done on a spectrophotometer using blank-corrected 480 nm measurement. Following the standard curve, the concentration of the each fraction was measured.

6.2.6 Protein sequencing through Orbitrap FusionTM LumosTM TribidTM Mass Spectrometer

1. Each fraction were dried in a speed-vac and resuspended in 0.5% TFA in such a manner that final concentration will be 0.4 μ g / μ L.

2. Then 5 μ L (Total 2 μ g) of each fraction was injected in Orbitrap Fusion™ Lumos™ Tribid™ Mass Spectrometer (Thermo Scientific) using auto sampler.
3. Each fraction was run through the column of an HPLC integrated with the MS system for 150 minute gradient using all other parameters set to the standard.
4. Raw data was processed using Thermo Scientific™ Proteome Discoverer™ software version 2.1.0.8.
5. Protein identification was done by reporter ion quantification for TMT-labelled mode. MS2 spectra were searched with the SEQUEST® HT search engine.

6.2.7 Statistical analysis

The extracted data from SEQUEST® HT was analyzed for significant up and down regulated proteins in patient samples compared to control samples. The protein abundances were grouped into two classes as patients and controls. Protein abundance was averaged for its duplicate run for each fraction. The significant difference level (p value) was calculated as two tailed heteroscedastic student t-test and $p \leq 0.05$ was considered as significance cut-off value. The false discover rate (FDR) was calculated based on Benjamini–Hochberg (BH) procedure and $q \leq 0.05$ value was considered as significant one. For equal peptide abundances, the accepted grouped abundances counts were at least 9 for both the patient and control groups. Ingenuity Pathway Analysis was done on IPA® software (IPA, Qiagen, USA) for network analysis and molecular annotation.

6.3 Results

To complement the gene expression analysis, whole cell quantitative proteomic profiling was done followed by comparative quantification for up and down regulated proteins of the dystonia patient's fibroblast samples. These experiments were completed by isolation of whole cell protein samples, TMT-labelling and sample preparation mass spectrometry and finally the LC-MS/MS run. Subsequent data analysis identified significant up-regulation of 302 proteins (Table 57) and down-regulation of 152 proteins (Table 58). The significance level was set for Benjamini-Hochberg False discovery rate (FDR) < 0.05 , p-value < 0.05 and fold change $\geq 50\%$. The protein set enrichment analysis by Ingenuity Pathway Analysis (IPA) recognized sixteen major dysregulated networks (Table 59) including cell death and survival, RNA post transcriptional modification, cancer, gene expression, cellular function and maintenance, cell cycle, nervous system development. Disease and function annotation of significant up and down regulated protein were enriched for RNA post-transcriptional modification, protein synthesis, cellular growth and proliferation, gene expression, cell death and survival, neurological disease and gene expression (Table 60). Top affected canonical pathways are EIF2 signalling, mitochondrial dysfunction, mTOR signalling, oxidative phosphorylation, regulation of eIF4 and p70S6K signalling (Figure 44).

Whole cell proteomic analysis of primary dystonia patients having *THAP1* mutation

Table 57: Significant up-regulated proteins in primary dystonia patients having *THAP1* mutation compared to controls

Serial No	Accession	Description	Abundance Ratio: (Patient) / (Control)	Abundances (Grouped): Control	Abundances (Grouped): Patient	FDR adjusted p value
1	Q99880	Histone H2B type 1-L	7.065	24.8	175.2	0.004866
2	P22626	heterogeneous nuclear ribonucleoproteins A2/B1	5.118	32.7	167.3	0.003756
3	P07910-2	Isoform C1 of Heterogeneous nuclear ribonucleoproteins C1/C2	4.763	34.7	165.3	0.004547
4	P62805	histone H4	4.39	37.1	162.9	0.006932
5	Q71DI3	histone H3.2	4.328	42.4	183.5	0.00643
6	O00479	High mobility group nucleosome-binding domain-containing protein 4	4.306	37.7	162.3	0.000483
7	Q07666	KH domain-containing, RNA-binding, signal transduction-associated protein 1	4.276	37.9	162.1	0.004811
8	Q99715-1	Collagen alpha-1(XII) chain	4.234	38.2	161.8	0.001373
9	P52272	Heterogeneous nuclear ribonucleoprotein M	4.213	38.4	161.6	0.006258
10	Q8N6L1-2	Isoform 2 of Keratinocyte-associated protein 2	4.207	39.7	166.9	4.3E-05
11	P38159-1	RNA-binding motif protein, X chromosome	4.093	39.3	160.7	0.001877
12	P16401	Histone H1.5	4.056	41.6	168.8	0.019963
13	P21796	voltage-dependent anion-selective channel protein 1	3.956	40.4	159.6	0.001363
14	P02545	Prelamin-A/C	3.944	40.5	159.5	0.015923
15	Q5SSJ5-1	Heterochromatin protein 1-binding protein 3	3.907	40.8	159.2	0.000367
16	P06748	Nucleophosmin	3.693	42.6	157.4	0.001811
17	Q86V81	THO complex subunit 4	3.682	43.5	160.1	0.002449
18	P09651-1	Heterogeneous nuclear ribonucleoprotein A1	3.599	43.5	156.5	0.007677
19	P14866	Heterogeneous nuclear ribonucleoprotein L	3.58	43.7	156.3	0.010758
20	P16402	Histone H1.3	3.575	43.7	156.3	0.004017
21	Q16891-2	Isoform 2 of MICOS complex subunit MIC60	3.473	44.7	155.3	0.00078
22	P0C0S5	Histone H2A.Z	3.459	46.6	161.2	0.004637
23	P12236	ADP/ATP translocase 3	3.436	45.1	154.9	0.002388
24	P07305	Histone H1.0	3.408	45.4	154.6	0.000348
25	Q8WU90	Zinc finger CCCH domain-containing protein 15	3.298	48.4	159.7	1.18E-05
26	P51991-1	Heterogeneous nuclear ribonucleoprotein A3	3.293	46.6	153.4	0.001149
27	Q07065	Cytoskeleton-associated protein 4	3.264	46.9	153.1	0.000626
28	O60869-1	Endothelial differentiation-related factor 1	3.246	53.7	174.3	0.000203
29	Q9UKM9-1	RNA-binding protein Raly	3.219	47.4	152.6	0.022694
30	Q16666-1	gamma-interferon-inducible protein 16	3.214	48.4	155.6	0.000845
31	Q00341-1	Vigilin	3.212	47.5	152.5	0.000798
32	P61803	Dolichyl-diphosphooligosaccharide--protein glycosyltransferase subunit DAD1	3.161	51.1	161.6	0.000142
33	Q9P2E9-1	Ribosome-binding protein 1	3.137	48.3	151.7	0.000481
34	Q53EP0	Fibronectin type III domain-containing protein 3B	3.134	48.4	151.6	0.000147
35	Q08211	Atp-dependent rna helicase a	3.109	48.7	151.3	0.002326

Whole cell proteomic analysis of primary dystonia patients having *THAP1* mutation

Serial No	Accession	Description	Abundance Ratio: (Patient) / (Control)	Abundances (Grouped): Control	Abundances (Grouped): Patient	FDR adjusted p value
36	Q9BQG0-2	Isoform 2 of Myb-binding protein 1A	3.106	59.9	186.1	0.0283
37	P45880-1	Isoform 1 of Voltage-dependent anion-selective channel protein 2	3.076	49.1	150.9	0.004766
38	P35659-1	Protein DEK	3.046	49.4	150.6	0.002244
39	O43390-1	heterogeneous nuclear ribonucleoprotein r	3.043	49.5	150.5	0.001956
40	Q9Y277	Voltage-dependent anion-selective channel protein 3	3.038	49.5	150.5	0.001271
41	Q6NUQ4	Transmembrane protein 214	3.015	53.1	160.2	2.52E-09
42	Q13151	Heterogeneous nuclear ribonucleoprotein A0	3.012	50.9	153.3	0.005834
43	Q15717-2	Isoform 2 of ELAV-like protein 1	2.993	50.1	149.9	0.000883
44	P78527	DNA-dependent protein kinase catalytic subunit	2.989	50.1	149.9	0.000899
45	O14979-2	Isoform 2 of Heterogeneous nuclear ribonucleoprotein D-like	2.908	52.3	152.1	0.001925
46	Q14444-1	Caprin-1	2.86	57.9	165.6	0.006447
47	Q14978-2	Isoform Beta of Nucleolar and coiled-body phosphoprotein 1	2.812	52.5	147.5	0.01112
48	Q15233	Non-POU domain-containing octamer-binding protein	2.81	52.5	147.5	0.000314
49	P05141	ADP/ATP translocase 2	2.766	53.1	146.9	0.001006
50	Q99623	Prohibitin-2	2.76	53.2	146.8	0.000222
51	P16403	Histone H1.2	2.744	53.4	146.6	0.004959
52	Q13435	Splicing factor 3b subunit 2	2.723	53.7	146.3	0.007146
53	O14880	Microsomal glutathione S-transferase 3	2.722	56.2	153.1	0.003809
54	P09874	Poly [ADP-ribose] polymerase 1	2.716	56.3	153	0.002215
55	O00483	Cytochrome c oxidase subunit NDUFA4	2.71	53.9	146.1	0.000387
56	P09669	Cytochrome c oxidase subunit 6C	2.708	55.2	149.4	0.00121
57	P10620	Microsomal glutathione S-transferase 1	2.696	54.1	145.9	4.92E-06
58	P60903	Protein S100-A10	2.672	54.5	145.5	1.93E-05
59	P46977	Dolichyl-diphosphooligosaccharide--protein glycosyltransferase subunit STT3A	2.632	55.1	144.9	3.32E-05
60	Q96AG4	Leucine-rich repeat-containing protein 59	2.621	55.2	144.8	0.000322
61	Q99729-3	Isoform 3 of Heterogeneous nuclear ribonucleoprotein A/B	2.611	55.4	144.6	0.003169
62	Q86UE4	protein LYRIC	2.601	55.5	144.5	4.06E-06
63	Q92841-3	Isoform 4 of Probable ATP-dependent RNA helicase DDX17	2.571	56	144	0.000415
64	P17302	Gap junction alpha-1 protein	2.537	56.5	143.5	0.001489
65	P52948-1	nuclear pore complex protein Nup98-Nup96	2.535	56.6	143.4	0.003431
66	Q1KMD3	heterogeneous nuclear ribonucleoprotein U-like protein 2	2.517	56.9	143.1	0.003442
67	P12111	Collagen alpha-3(VI) chain	2.501	57.1	142.9	0.003298
68	P30536	translocator protein	2.479	61.9	153.6	0.000179
69	Q9UHB6	LIM domain and actin-binding protein 1	2.469	57.6	142.4	0.000207

(Continued....)

Whole cell proteomic analysis of primary dystonia patients having *THAP1* mutation

Serial No	Accession	Description	Abundance Ratio: (Patient) / (Control)	Abundances (Grouped): Control	Abundances (Grouped): Patient	FDR adjusted p-value
70	P17844	probable ATP-dependent RNA helicase DDX5	2.467	57.7	142.3	0.002272
71	P14678-3	Isoform SM-B1 of Small nuclear ribonucleoprotein-associated proteins B and B'	2.446	59.5	145.5	0.002136
72	P13073	Cytochrome c oxidase subunit 4 isoform 1, mitochondrial	2.443	58.1	141.9	0.002502
73	Q70UQ0	Inhibitor of nuclear factor kappa-B kinase-interacting protein	2.443	58.1	141.9	0.000424
74	Q86U42-1	polyadenylate-binding protein 2	2.397	61.9	148.4	5.98E-06
75	P31930	Cytochrome b-c1 complex subunit 1, mitochondrial	2.384	60.6	144.5	0.00083
76	P63220	40S ribosomal protein S21	2.376	62.3	148.1	0.000154
77	P61619	Protein transport protein Sec61 subunit alpha isoform 1	2.373	59.3	140.7	8.83E-07
78	P20674	Cytochrome c oxidase subunit 5A, mitochondrial	2.367	59.4	140.6	0.003437
79	O75533-1	splicing factor 3B subunit 1	2.36	67.4	159.1	0.017974
80	Q9NR99	Matrix-remodeling-associated protein 5	2.356	59.6	140.4	0.010864
81	P49207	60S ribosomal protein L34	2.343	59.8	140.2	0.000201
82	P35637-1	RNA-binding protein FUS	2.319	61.8	143.3	0.000913
83	Q5XKP0	MICOS complex subunit MIC13	2.314	60.3	139.7	0.000144
84	P43307	Translocon-associated protein subunit alpha	2.295	60.7	139.3	0.000447
85	P62318	small nuclear ribonucleoprotein sm d3	2.289	64.1	146.6	0.001222
86	Q6NUK1	Calcium-binding mitochondrial carrier protein SCaMC-1	2.271	61.1	138.9	5.26E-05
87	Q03135	Caveolin-1	2.269	61.2	138.8	0.000757
88	P14927	Cytochrome b-c1 complex subunit 7	2.243	63.3	142	0.005526
89	P04844-1	Dolichyl-diphosphooligosaccharide--protein glycosyltransferase subunit 2	2.235	61.8	138.2	0.000124
90	P25398	40S ribosomal protein S12	2.229	61.9	138.1	5.4E-05
91	P02751	fibronectin	2.218	62.1	137.9	0.00227
92	Q9BWM7	Sideroflexin-3	2.217	63.8	141.5	0.001062
93	P35232	Prohibitin	2.211	62.3	137.7	0.001166
94	Q00839	Heterogeneous nuclear ribonucleoprotein U	2.207	62.4	137.6	0.000485
95	P62899	60S ribosomal protein L31	2.197	62.6	137.4	2.52E-06
96	P51571	translocon-associated protein subunit delta	2.182	62.9	137.1	0.002857
97	Q14554	Protein disulfide-isomerase A5	2.18	62.9	137.1	0.000334
98	Q00688	peptidyl-prolyl cis-trans isomerase FKBP3	2.169	63.1	136.9	6.93E-05
99	P62701	40S ribosomal protein S4, X isoform	2.163	63.2	136.8	0.00029
100	Q14980-1	nuclear mitotic apparatus protein 1	2.161	75.9	164.1	0.034105
101	Q8N163-1	Cell cycle and apoptosis regulator protein 2	2.149	65.2	140.2	0.001254
102	P19367-3	Isoform 3 of Hexokinase-1	2.13	63.9	136.1	0.00489
103	P09661	U2 small nuclear ribonucleoprotein A'	2.127	64	136	0.000262
104	Q96A72	protein mago nashi homolog 2	2.125	65.8	139.7	1.91E-06

(Continued....)

Whole cell proteomic analysis of primary dystonia patients having *THAP1* mutation

Serial No	Accession	Description	Abundance Ratio: (Patient) / (Control)	Abundances (Grouped): Control	Abundances (Grouped): Patient	FDR adjusted p value
105	P26373-1	60S ribosomal protein L13	2.124	64	136	3.47E-06
106	P53007	Tricarboxylate transport protein, mitochondrial	2.121	64.1	135.9	0.000233
107	P50914	60S ribosomal protein L14	2.118	64.2	135.8	0.000177
108	Q9NYL4	Peptidyl-prolyl cis-trans isomerase FKBP11	2.116	67.8	143.5	0.000372
109	P40429	60S ribosomal protein L13a	2.115	64.2	135.8	8.97E-06
110	Q12905	Interleukin enhancer-binding factor 2	2.11	64.3	135.7	0.00167
111	Q5JTV8	Torsin-1A-interacting protein 1	2.097	64.6	135.4	0.000156
112	P35268	60S ribosomal protein L22	2.093	64.7	135.3	2.02E-06
113	Q9NYF8-1	Bcl-2-associated transcription factor 1	2.089	70.6	147.5	0.006888
114	Q96HY6-1	DDR GK domain-containing protein 1	2.086	64.8	135.2	4.46E-05
115	O00300	Tumor necrosis factor receptor superfamily member 11B	2.082	75.2	156.6	0.013683
116	P05386	60S acidic ribosomal protein P1	2.08	68.6	142.8	0.002825
117	Q9Y4P3	Transducin beta-like protein 2	2.08	70.7	147	0.00059
118	P36578	60S ribosomal protein L4	2.075	65	135	3.04E-05
119	P84090	Enhancer of rudimentary homolog	2.072	65.1	134.9	6.2E-05
120	P43243	Matrin-3	2.069	65.2	134.8	0.012771
121	Q9UMS4	Pre-mRNA-processing factor 19	2.063	71.1	146.7	0.012812
122	Q12906-7	Isoform 7 of Interleukin enhancer-binding factor 3	2.059	65.4	134.6	0.001266
123	P02452	Collagen alpha-1(I) chain	2.055	65.5	134.5	2.98E-05
124	O96000	NADH dehydrogenase [ubiquinone] 1 beta subcomplex subunit 10	2.041	65.8	134.2	0.005825
125	Q07020	60S ribosomal protein L18	2.041	65.8	134.2	0.000689
126	Q9UN86	Ras GTPase-activating protein-binding protein 2	2.04	65.8	134.2	0.013181
127	Q07955-1	Serine/arginine-rich splicing factor 1	2.04	65.8	134.2	0.00116
128	P46779	60S ribosomal protein L28	2.038	65.8	134.2	7.41E-05
129	P05997	Collagen alpha-2(V) chain	2.035	65.9	134.1	0.000146
130	P62917	60S ribosomal protein L8	2.035	65.9	134.1	7.74E-05
131	P62995	transformer-2 protein homolog beta	2.031	67.8	137.8	0.000464
132	O14495	lipid phosphate phosphohydrolase 3	2.024	66.1	133.9	0.002491
133	P30050-1	60S ribosomal protein L12	2.02	66.2	133.8	3.48E-06
134	Q13423	NAD(P) transhydrogenase, mitochondrial	2.007	68.4	137.3	0.010234
135	Q70UQ0-4	Isoform 4 of Inhibitor of nuclear factor kappa-B kinase-interacting protein	2.005	66.6	133.4	0.000673
136	Q06787	fragile X mental retardation protein 1	2.001	66.7	133.3	0.011479
137	Q2TAY7	WD40 repeat-containing protein SMU1	1.993	75.2	149.8	0.00996
138	Q92504	Zinc transporter SLC39A7	1.991	66.9	133.1	2.44E-06
139	Q13283	Ras GTPase-activating protein-binding protein 1	1.985	67	133	0.004291

(Continued....)

Whole cell proteomic analysis of primary dystonia patients having *THAP1* mutation

Serial No	Accession	Description	Abundance Ratio: (Patient) / (Control)	Abundances (Grouped): Control	Abundances (Grouped): Patient	FDR adjusted p value
140	P14174	Macrophage Migration inhibitory factor	1.984	67	133	0.004761
141	Q13724-1	Mannosyl-oligosaccharide glucosidase	1.982	69	136.8	0.00453
142	Q9BWS9-1	Chitinase domain-containing protein 1	1.976	67.2	132.8	0.000375
143	P99999	cytochrome c	1.959	69.6	136.2	0.000621
144	P62857	40S ribosomal protein S28	1.948	69.8	136	5.79E-05
145	P39023	60S ribosomal protein L3	1.942	68	132	7.19E-06
146	P84098	60S ribosomal protein L19	1.938	68.1	131.9	0.000107
147	P52895	Aldo-keto reductase family 1 member C2	1.935	74.5	144.1	0.037986
148	P04843	Dolichyl-diphosphooligosaccharide--protein glycosyltransferase subunit 1	1.932	68.2	131.8	0.000505
149	P18124	60S ribosomal protein L7	1.932	68.2	131.8	6.96E-05
150	Q9Y295	developmentally-regulated GTP-binding protein 1	1.929	68.3	131.7	0.000626
151	O60888-2	Isoform A of Protein CutA	1.927	70.3	135.5	7.9E-05
152	Q96FQ6	Protein S100-A16	1.923	68.4	131.6	0.000155
153	Q86UP2-1	Kinectin	1.92	68.5	131.5	0.000148
154	P62280	40S ribosomal protein S11	1.917	68.6	131.4	1.43E-05
155	Q9BU23-1	Lipase maturation factor 2	1.914	68.6	131.4	4.11E-05
156	P62906	60S ribosomal protein L10A	1.913	68.7	131.3	9.1E-05
157	Q92804-1	TATA-binding protein-associated factor 2N	1.909	68.7	131.3	0.000445
158	Q15393-1	Splicing factor 3B subunit 3	1.898	69	131	0.000499
159	Q6WCQ1-2	Isoform 2 of Myosin phosphatase Rho-interacting protein	1.889	69.2	130.8	0.001993
160	P46778	60S ribosomal protein L21	1.889	69.2	130.8	3.47E-05
161	Q9NRW3	DNA dC->dU-editing enzyme APOBEC-3C	1.889	69.2	130.8	2.22E-06
162	Q15459	splicing factor 3A subunit 1	1.888	71.3	134.6	0.000908
163	P13674-1	prolyl 4-hydroxylase subunit alpha-1	1.883	76	143	0.004627
164	Q7Z478	ATP-dependent RNA helicase Dhx29	1.866	69.8	130.2	0.001938
165	P05387	60S acidic ribosomal protein P2	1.861	69.9	130.1	7.97E-05
166	P08708	40S ribosomal protein S17	1.851	70.1	129.9	0.002114
167	P08621-1	U1 small nuclear ribonucleoprotein 70 kDa	1.848	70.2	129.8	0.005818
168	P28370-1	Probable global transcription activator SNF2L1	1.848	70.2	129.8	0.002725
169	P62829	60S ribosomal protein L23	1.843	70.3	129.7	0.000122
170	Q8IX12	Cell division cycle and apoptosis regulator protein 1	1.842	70.4	129.6	0.044106
171	P02795	metallothionein-2	1.839	70.5	129.5	0.006633
172	P62913	60S ribosomal protein L11	1.837	70.5	129.5	3.26E-05
173	P60468	protein transport protein Sec61 subunit beta	1.831	70.6	129.4	0.000187
174	P46782	40S ribosomal protein S5	1.826	70.8	129.2	3.42E-06

(Continued....)

Whole cell proteomic analysis of primary dystonia patients having *THAP1* mutation

Serial No	Accession	Description	Abundance Ratio: (Patient) / (Control)	Abundances (Grouped): Control	Abundances (Grouped): Patient	FDR adjusted p value
175	P49721	proteasome subunit beta type-2	1.818	71	129	0.016121
176	P61247	40S ribosomal protein S3a	1.816	71	129	2.87E-07
177	Q7KZF4	staphylococcal nuclease domain-containing protein 1	1.808	71.2	128.8	8.21E-05
178	P26599-3	Isoform 3 of Polypyrimidine tract-binding protein 1	1.803	71.4	128.6	0.00216
179	P61313-1	60S ribosomal protein L15	1.803	71.4	128.6	6.52E-05
180	P31942	Heterogeneous nuclear ribonucleoprotein H3	1.802	71.4	128.6	0.000926
181	Q96I20	PRKC apoptosis WT1 regulator protein	1.801	71.4	128.6	0.000475
182	P63173	60s ribosomal protein l38	1.8	71.4	128.6	0.000552
183	P05388	60S acidic ribosomal protein P0	1.798	71.5	128.5	5.59E-05
184	Q9Y6A9	Signal peptidase complex subunit 1	1.797	76	136.6	0.006787
185	P20908	Collagen alpha-1(V) chain	1.796	71.5	128.5	0.0005
186	P28331-2	Isoform 2 of NADH-ubiquinone oxidoreductase 75 kDa subunit, mitochondrial	1.796	71.5	128.5	8.53E-05
187	Q8NC51-3	Isoform 3 of Plasminogen activator inhibitor 1 RNA-binding protein	1.792	71.6	128.4	1.17E-09
188	P78347	General transcription factor II-I	1.79	71.7	128.3	5.73E-06
189	Q53FA7-1	Quinone oxidoreductase PIG3	1.787	71.8	128.2	0.010179
190	Q00325-1	Phosphate carrier protein, mitochondrial	1.783	71.9	128.1	0.0003
191	Q14011-2	Isoform 2 of Cold-inducible RNA-binding protein	1.782	71.9	128.1	0.001644
192	P62424	60S ribosomal protein L7a	1.781	71.9	128.1	1.28E-05
193	P62888	60S ribosomal protein L30	1.781	71.9	128.1	4.69E-06
194	O75947-1	ATP synthase subunit d, mitochondrial	1.779	72	128	0.000432
195	O60506	Heterogeneous nuclear ribonucleoprotein Q	1.772	72.1	127.9	2.92E-05
196	P08865	40S ribosomal protein SA	1.768	72.3	127.7	5.98E-07
197	P61513	60S ribosomal protein L37a	1.752	72.7	127.3	1.97E-06
198	Q9Y2W1	Thyroid hormone receptor-associated protein 3	1.748	72.8	127.2	0.001868
199	P46781	40S ribosomal protein S9	1.747	72.8	127.2	2.4E-07
200	O75094-4	Isoform 4 of Slit homolog 3 protein	1.736	75.4	130.9	2.67E-05
201	Q8N5K1	CDGSH iron-sulfur domain-containing protein 2	1.733	73.2	126.8	1.01E-05
202	Q14165	Malectin	1.727	73.3	126.7	0.002105
203	A5YKK6	CCR4-NOT transcription complex subunit 1	1.722	73.5	126.5	0.001685
204	Q92879-4	Isoform 4 of CUGBP Elav-like family member 1	1.716	73.6	126.4	0.003091
205	P82979	SAP domain-containing ribonucleoprotein	1.715	73.7	126.3	0.00079
206	P62269	40S ribosomal protein S18	1.712	73.8	126.2	0.000257
207	Q9NUQ6-3	Isoform 3 of SPATS2-like protein	1.709	78.7	134.4	0.008215
208	P08123	Collagen alpha-2(I) chain	1.709	73.8	126.2	0.000162

(Continued....)

Whole cell proteomic analysis of primary dystonia patients having *THAP1* mutation

Serial No	Accession	Description	Abundance Ratio: (Patient) / (Control)	Abundances (Grouped): Control	Abundances (Grouped): Patient	FDR adjusted p value
209	Q14498	Immunoglobulin superfamily containing leucine-rich repeat protein	1.707	86.4	147.5	0.039467
210	Q99584	Protein S100-A13	1.707	73.9	126.1	8.03E-06
211	Q9Y2H6	Fibronectin type-III domain-containing protein 3a	1.703	78.8	134.3	0.002672
212	Q9Y5S9	RNA-binding protein 8A	1.703	81.5	138.9	0.00132
213	P24390	ER lumen protein-retaining receptor 1	1.702	81.6	138.8	0.000879
214	P50402	Emerin	1.699	74.1	125.9	0.002715
215	P27635	60S ribosomal protein L10	1.69	74.3	125.7	6.44E-05
216	O94832	Unconventional myosin-Id	1.686	74.5	125.5	0.00366
217	Q12797	Aspartyl/Asparaginyl beta-hydroxylase	1.686	74.5	125.5	1.33E-06
218	P46777	60S ribosomal protein L5	1.682	74.6	125.4	0.000132
219	Q16795	NADH dehydrogenase [ubiquinone] 1 alpha subcomplex subunit 9,	1.681	74.6	125.4	0.013321
220	Q07092	collagen alpha-1(XVI) chain	1.68	82.3	138.3	0.03432
221	Q00839-2	Isoform Short of Heterogeneous nuclear ribonucleoprotein U	1.67	77.3	129.1	0.007973
222	P39019	40S ribosomal protein S19	1.66	75.2	124.8	7.35E-05
223	P53985	Monocarboxylate transporter 1	1.66	75.2	124.8	1.38E-06
224	P60900	Proteasome subunit alpha type-6	1.659	75.2	124.8	0.041585
225	P18621-3	Isoform 3 of 60S ribosomal protein L17	1.657	75.3	124.7	0.000367
226	P32969	60S ribosomal protein L9	1.654	75.4	124.6	7.85E-05
227	Q96A33-1	Coiled-coil domain-containing protein 47	1.65	75.5	124.5	8.07E-05
228	P02461	Collagen alpha-1(III) chain	1.648	75.5	124.5	0.010364
229	P63244	Guanine nucleotide-binding protein subunit beta-2-like 1	1.643	75.7	124.3	5.4E-06
230	P61353	60S ribosomal protein L27	1.64	75.8	124.2	0.000159
231	O95793	double-stranded RNA-binding protein Staufen homolog 1	1.638	75.8	124.2	0.000607
232	Q99704	docking protein 1	1.636	75.9	124.1	0.022749
233	P62753	40S RIBOSOMAL PROTEIN S6	1.634	75.9	124.1	7.67E-08
234	P15880	40S ribosomal protein S2	1.633	75.9	124.1	0.000137
235	P53999	Activated RNA polymerase II transcriptional coactivator p15	1.633	76	124	1.25E-07
236	Q9P0L0	vesicle-associated membrane protein-associated protein A	1.632	76	124	1.26E-05
237	P67812-3	Isoform 3 of Signal peptidase complex catalytic subunit SEC11A	1.631	76	124	0.000162
238	Q14157-5	Isoform 5 of Ubiquitin-associated protein 2-like	1.629	76.1	123.9	0.001595
239	Q08AF3-1	schlafen family member 5	1.627	76.1	123.9	0.000194
240	Q15005	Signal peptidase complex subunit 2	1.625	76.2	123.8	6.28E-05
241	Q9NZ01-1	Very-long-chain enoyl-CoA reductase	1.622	76.3	123.7	5.81E-05
242	P49792	E3 SUMO-protein ligase RanBP2	1.617	76.4	123.6	8.95E-06
243	Q8NF91	Nesprin-1	1.616	76.5	123.5	0.0013

(Continued....)

Whole cell proteomic analysis of primary dystonia patients having *THAP1* mutation

Serial No	Accession	Description	Abundance Ratio: (Patient) / (Control)	Abundances (Grouped): Control	Abundances (Grouped): Patient	FDR adjusted p value
244	Q96JB5-4	Isoform 4 of CDK5 regulatory subunit-associated protein 3	1.616	76.4	123.6	6.14E-07
245	Q02543	60S ribosomal protein L18a	1.612	76.6	123.4	0.000115
246	O43684	Mitotic checkpoint protein BUB3	1.611	79.1	127.5	0.025948
247	P62081	40S ribosomal protein S7	1.607	76.7	123.3	1.08E-05
248	Q96QR8	Transcriptional activator protein Pur-beta	1.606	76.7	123.3	0.001869
249	P35555	Fibrillin-1	1.605	76.8	123.2	2.81E-05
250	P23246-1	splicing factor, proline- and glutamine-rich	1.604	76.8	123.2	0.036472
251	P23396-1	40S ribosomal protein S3	1.603	76.8	123.2	1.35E-07
252	Q99442	translocation protein sec62	1.6	76.9	123.1	3.43E-05
253	P61254	60S ribosomal protein L26	1.599	77	123	9.25E-05
254	P84103	Serine/arginine-rich splicing factor 3	1.596	85.2	136.1	0.023393
255	P47895	Aldehyde dehydrogenase family 1 member A3	1.594	77.1	122.9	0.006096
256	O60841	Eukaryotic translation initiation factor 5B	1.594	77.1	122.9	1.75E-07
257	Q15113	Procollagen C-endopeptidase enhancer 1	1.59	77.2	122.8	0.001928
258	O15427	Monocarboxylate transporter 4	1.59	77.2	122.8	0.000984
259	Q14103-3	Isoform 3 of Heterogeneous nuclear ribonucleoprotein D0	1.586	77.3	122.7	0.001676
260	P10606	Cytochrome c oxidase subunit 5B, mitochondrial	1.58	77.5	122.5	0.034485
261	Q13148-1	TAR DNA-binding protein 43	1.578	80.2	126.5	0.015662
262	Q9NV17-2	Isoform 2 of ATPase family AAA domain-containing protein 3A	1.578	77.6	122.4	0.010044
263	P78344-1	Eukaryotic translation initiation factor 4 gamma 2	1.578	77.6	122.4	5.23E-06
264	Q9NSD9	Phenylalanine--tRNA ligase beta subunit	1.578	77.6	122.4	3.06E-07
265	O75643-1	U5 small nuclear ribonucleoprotein 200 kDa helicase	1.576	80.2	126.5	0.001923
266	Q16629	serine/arginine-rich splicing factor 7	1.575	77.7	122.3	2.8E-05
267	Q14498-1	RNA-binding protein 39	1.571	80.4	126.3	0.00054
268	P15144	aminopeptidase N	1.57	77.8	122.2	2.24E-09
269	P55061-2	Isoform 2 of Bax inhibitor 1	1.569	80.5	126.2	0.000562
270	P28074-1	proteasome subunit beta type-5	1.566	77.9	122.1	0.015819
271	P09012	u1 small nuclear ribonucleoprotein a	1.564	78	122	0.004248
272	Q9P0J0-2	Isoform 2 of NADH dehydrogenase [ubiquinone] 1 alpha subcomplex	1.563	78	122	0.001359
273	Q9UBM7	7-dehydrocholesterol reductase	1.558	78.2	121.8	2.1E-05
274	P18077	60S ribosomal protein L35a	1.554	78.3	121.7	0.000317
275	Q15427	Splicing factor 3b subunit 4	1.553	81	125.8	0.022865
276	P67809	Nuclease-sensitive element-binding protein 1	1.553	78.3	121.7	0.000157
277	P61978-3	Isoform 3 of Heterogeneous nuclear ribonucleoprotein K	1.551	78.4	121.6	1.34E-05
278	P51809	vesicle-associated membrane protein 7	1.548	92.2	142.7	0.043956

(Continued....)

Whole cell proteomic analysis of primary dystonia patients having *THAP1* mutation

Serial No	Accession	Description	Abundance Ratio: (Patient) / (Control)	Abundances (Grouped): Control	Abundances (Grouped): Patient	FDR adjusted p value
279	Q9Y3E5	Peptidyl-tRNA hydrolase 2, mitochondrial	1.548	78.5	121.5	0.0105
280	P16989-1	Y-box-binding protein 3	1.548	81.1	125.6	0.001056
281	Q969G5	Protein kinase C delta-binding protein	1.547	78.5	121.5	0.002993
282	Q9P0K7-4	Isoform 4 of Ankyrbin	1.541	78.7	121.3	0.000736
283	P08240-1	signal recognition particle receptor subunit alpha	1.537	78.8	121.2	0.001718
284	Q13263	Transcription intermediary factor 1-beta	1.535	78.9	121.1	0.025725
285	Q02878	60S ribosomal protein L6	1.534	78.9	121.1	0.00236
286	Q9Y2B0	Protein canopy homolog 2	1.534	78.9	121.1	3.71E-05
287	P42677	40S ribosomal protein S27	1.526	79.2	120.8	0.011837
288	P61421	V-type proton ATPase subunit d 1	1.526	79.2	120.8	5.06E-05
289	P83731	60S ribosomal protein L24	1.524	79.2	120.8	0.003528
290	P24821	Tenascin	1.522	79.3	120.7	0.002084
291	Q8WWI1-3	Isoform 3 of LIM domain only protein 7	1.521	79.3	120.7	0.045707
292	O75367-1	Core histone macro-H2A.1	1.52	79.4	120.6	0.008517
293	P98160	Basement membrane-specific heparan sulfate proteoglycan core protein	1.519	79.4	120.6	0.000594
294	Q9BVC6	Transmembrane protein 109	1.519	79.4	120.6	0.000358
295	P51153	Ras-related protein Rab-13	1.518	79.4	120.6	0.000237
296	Q15029	116 kDa U5 small nuclear ribonucleoprotein component	1.51	79.7	120.3	0.005298
297	Q8N5C1	Protein FAM26E	1.509	79.7	120.3	0.003182
298	P67870	Casein kinase II subunit beta	1.506	79.8	120.2	0.000309
299	P61009	Signal peptidase complex subunit 3	1.506	79.8	120.2	0.000226
300	Q00577	Transcriptional activator protein Pur-alpha	1.505	79.8	120.2	2.12E-05
301	P22695	Cytochrome b-c1 complex subunit 2, mitochondrial	1.502	79.9	120.1	0.007426
302	Q9H4G4	Golgi-associated plant pathogenesis-related protein 1	1.501	80	120	0.019057

Accession: UniProtKB *accession numbers*, **Fold change** was calculated as abundance Ratio (Patient/Control), Fold change ≥ 1.5 .

FDR: False discovery rate based on decoy database search. **FDR adjusted p value** ≤ 0.05 .

Whole cell proteomic analysis of primary dystonia patients having *THAP1* mutation

Table 58: Significant down-regulated proteins in primary dystonia patients having *THAP1* mutation compared to controls

Serial No	Accession	Description	Abundance Ratio: (Patient) / (Control)	Abundances (Grouped): Control	Abundances (Grouped): Patient	FDR adjusted p value
1	Q13885	Tubulin beta-2A chain	1.51	120.5	79.5	1.41529E-06
2	Q6F181-1	Anamorsin	1.51	120.5	79.5	0.00012707
3	O43707	Alpha-actinin-4	1.51	120.6	79.4	6.02553E-05
4	Q8TDQ7	Glucosamine-6-phosphate isomerase 2	1.51	120.7	79.3	3.32175E-05
5	O75190	DnaJ homolog subfamily B member 6	1.52	120.7	79.3	0.022486672
6	P0C0L4-1	Complement C4-A	1.52	120.7	79.3	9.70595E-05
7	Q15139	Serine/threonine-protein kinase D1	1.52	120.8	79.2	0.006926268
8	P60981-1	Destrin	1.52	120.9	79.1	3.8197E-05
9	Q9GZT4	serine racemase	1.52	120.9	79.1	0.003069133
10	P57764	Gasdermin-D	1.53	125.1	81.7	0.002658768
11	Q12805	EGF-containing fibulin-like extracellular matrix protein 1	1.53	121	79	0.002305574
12	Q8NF37	Lysophosphatidylcholine acyltransferase 1	1.53	121.1	78.9	0.036579412
13	Q5VW36	focadhesin	1.53	121.1	78.9	0.002473207
14	Q14240-2	Isoform 2 of Eukaryotic initiation factor 4A-II	1.53	121.2	78.8	0.012796885
15	P06396-2	Isoform 2 of Gelsolin	1.53	121.2	78.8	1.86673E-05
16	P46734-3	Isoform 2 of Dual specificity mitogen-activated protein kinase kinase 3	1.53	121.2	78.8	0.000503065
17	P32929	Cystathionine gamma-lyase	1.54	121.4	78.6	0.01372782
18	P41221	protein Wnt-5a	1.54	121.4	78.6	0.007071336
19	Q9NP97	Dynein light chain roadblock-type 1	1.54	121.5	78.5	0.00030521
20	Q5T4B2-1	Probable inactive glycosyltransferase 25 family member 3	1.54	121.5	78.5	0.00443128
21	P13473-1	Lysosome-associated membrane glycoprotein 2	1.54	121.5	78.5	4.80069E-05
22	Q95749	geranylgeranyl pyrophosphate synthase	1.55	121.7	78.3	0.002111268
23	P62861	40S ribosomal protein S30	1.55	125.8	81	0.025478733
24	Q969E4	transcription elongation factor A protein-like 3	1.56	122	78	0.001787649
25	Q8WUH1	Protein Churchill	1.56	122.1	77.9	0.012762626
26	Q9UKX7	Nuclear pore complex protein Nup50	1.56	122.1	77.9	0.005018695
27	P00747	Plasminogen	1.57	122.2	77.8	0.013037985
28	Q9UBB6-3	Isoform 3 of Neurochondrin	1.57	122.4	77.6	4.87623E-05
29	Q9H008-1	Phospholysine phosphohistidine inorganic pyrophosphate phosphatase	1.57	141.5	89.5	0.02517212
30	Q5HYK7	SH3 domain-containing protein 19	1.58	122.5	77.5	0.022276257
31	P50213-1	Isocitrate dehydrogenase [NAD] subunit alpha, mitochondrial	1.58	122.6	77.4	6.6826E-06
32	P45985-2	Isoform 2 of Dual specificity mitogen-activated protein kinase kinase 4	1.59	122.9	77.1	0.001540179
33	P51808	Dynein light chain Tctex-type 3	1.60	129.8	81	0.01854245
34	Q9UPQ0-1	LIM and calponin homology domains-containing protein 1	1.60	123.3	76.7	0.007119645

(Continued....)

Whole cell proteomic analysis of primary dystonia patients having *THAP1* mutation

Serial No	Accession	Description	Abundance Ratio: (Patient) / (Control)	Abundances (Grouped): Control	Abundances (Grouped): Patient	FDR adjusted p value
35	Q7Z4H8	KDEL motif-containing protein 2	1.61	123.6	76.4	0.001014056
36	A6NDU8	UPF0600 protein C5orf51	1.62	123.7	76.3	6.39345E-05
37	Q8NDA8-1	Maestro heat-like repeat-containing protein family member 1	1.62	123.8	76.2	0.027571703
38	Q96C36	Pyrraline-5-carboxylate reductase 2	1.62	123.8	76.2	0.001497771
39	Q14847	LIM and SH3 domain protein 1	1.62	123.8	76.2	8.98184E-06
40	Q8N3F8	MICAL-like protein 1	1.63	124	76	0.006920136
41	P56199	Integrin alpha-1	1.63	124.1	75.9	0.000366637
42	P02760	Protein AMBP	1.63	124.2	75.8	0.00361635
43	P26006-1	Isoform 2 of Integrin alpha-3	1.64	124.4	75.6	0.007567022
44	P08134	Rho-related GTP-binding protein RhoC	1.65	124.6	75.4	8.17163E-09
45	O14976	Cyclin-G-associated kinase	1.65	124.6	75.4	2.15898E-05
46	Q15942	Zyxin	1.65	124.7	75.3	2.15135E-06
47	Q9GZP4	PITH domain-containing protein 1	1.66	124.8	75.2	0.029689638
48	O75083	WD repeat-containing protein 1	1.66	124.8	75.2	2.848E-06
49	P01024	Complement C3	1.66	124.9	75.1	5.10749E-05
50	P15848	arylsulfatase B	1.67	125.2	74.8	0.004315606
51	Q12765-2	Isoform 2 of Secernin-1	1.68	125.4	74.6	1.51706E-05
52	P60510	Serine/threonine-protein phosphatase 4 catalytic subunit	1.68	125.5	74.5	0.007492527
53	Q6IAA8	regulator complex protein LAMTOR1	1.68	125.6	74.4	0.024622805
54	Q9ULH1-2	Isoform 1 of Arf-GAP with SH3 domain, ANK repeat and PH domain-	1.68	132.6	78.5	0.03333371
55	Q9BXJ4-3	Isoform 3 of Complement C1q tumor necrosis factor-related protein 3	1.69	125.7	74.3	0.001795573
56	P04278-1	Sex hormone-binding globulin	1.69	125.7	74.3	0.008287818
57	P54652	Heat shock-related 70 kDa protein 2	1.70	125.9	74.1	0.003370478
58	O95967	EGF-containing fibulin-like extracellular matrix protein 2	1.70	126	74	1.66335E-06
59	P69905	Hemoglobin subunit alpha	1.71	126.4	73.6	0.001009581
60	P48735	Isocitrate dehydrogenase [NADP], mitochondrial	1.71	126.4	73.6	0.000915406
61	P21291	Cysteine and glycine-rich protein 1	1.71	126.4	73.6	0.000355457
62	Q6AWC2-6	Isoform 6 of Protein WWC2	1.73	133.9	77.3	0.007890029
63	Q8IWA5	Choline transporter-like protein 2	1.73	130.9	75.4	0.007460154
64	Q15555	Microtubule-associated protein RP/EB family member 2	1.73	126.9	73.1	3.11029E-06
65	Q8TCD5	5'(3')-deoxyribonucleotidase, cytosolic type	1.74	127	73	0.000260217
66	Q15063-1	Periostin	1.74	127	73	4.56449E-06
67	P04745	alpha-amylase 1	1.75	127.4	72.6	0.000801013
68	P07951-3	Isoform 3 of Tropomyosin beta chain	1.75	127.4	72.6	0.000312616
69	Q562R1	Beta-actin-like protein 2	1.76	127.5	72.5	0.006949164

(Continued....)

Whole cell proteomic analysis of primary dystonia patients having *THAP1* mutation

Serial No	Accession	Description	Abundance Ratio: (Patient) / (Control)	Abundances (Grouped): Control	Abundances (Grouped): Patient	FDR adjusted p value
70	Q14156-1	protein EFR3 homolog A	1.76	143.9	81.7	0.028404889
71	P46934-4	Isoform 4 of E3 ubiquitin-protein ligase NEDD4	1.76	127.6	72.4	0.000350721
72	Q9UBY9-2	Isoform 2 of Heat shock protein beta-7	1.77	128	72	0.001637893
73	P10643	Complement component C7	1.78	128.2	71.8	6.29618E-05
74	P13284	Gamma-interferon-inducible lysosomal thiol reductase	1.78	128.2	71.8	0.010462078
75	P29536-1	Leiomodin-1	1.78	128.3	71.7	0.00899048
76	P09936	Ubiquitin carboxyl-terminal hydrolase isozyme L1	1.78	128.3	71.7	0.006681479
77	P02511	Alpha-crystallin B chain	1.79	128.5	71.5	0.001896678
78	O60331-3	Isoform 3 of Phosphatidylinositol 4-phosphate 5-kinase type-1 gamma	1.79	141.1	78.5	0.001225276
79	P05161	Ubiquitin-like protein ISG15	1.80	145	80.5	0.004694391
80	Q16853	Membrane primary amine oxidase	1.80	128.7	71.3	0.001905261
81	Q16775-1	Hydroxyacylglutathione hydrolase, mitochondrial	1.81	129	71	0.000427126
82	P34059	N-acetylgalactosamine-6-sulfatase	1.81	129.1	70.9	0.002256965
83	O75880	Protein SCO1 homolog, mitochondrial	1.83	129.3	70.7	0.011222048
84	P06396-3	Isoform 3 of Gelsolin	1.83	150	81.8	0.009155355
85	O94919	endonuclease domain-containing 1 protein	1.84	146	79.3	0.005342201
86	Q9NZN3	EH domain-containing protein 3	1.85	129.8	70.2	0.002965512
87	P01031	Complement C5	1.85	129.9	70.1	0.000552065
88	Q04756	Hepatocyte growth factor activator	1.86	130.2	69.8	0.000829066
89	P02042	Hemoglobin subunit delta	1.87	130.4	69.6	2.60123E-05
90	P04004	Vitronectin	1.87	130.4	69.6	0.004367036
91	O14558	Heat shock protein beta-6	1.87	130.6	69.4	0.000100126
92	P18065	Insulin-like growth factor-binding protein 2	1.88	130.7	69.3	0.000100711
93	P49753-1	Acyl-coenzyme A thioesterase 2, mitochondrial	1.89	130.8	69.2	1.4162E-05
94	P50583	Bis(5'-nucleosyl)-tetrphosphatase [asymmetrical]	1.89	130.8	69.2	0.0039969
95	Q9H425	Uncharacterized protein C1orf198	1.89	131	69	0.000409469
96	P12259	Coagulation factor V	1.89	131	69	0.001226171
97	Q01995	transgelin	1.91	131.3	68.7	0.000272711
98	P30837	Aldehyde dehydrogenase X, mitochondrial	1.91	131.3	68.7	0.021012467
99	P49747	Cartilage oligomeric matrix protein	1.92	131.6	68.4	0.00010474
100	P51884	Lumican	1.92	131.7	68.3	9.24494E-05
101	P36955	Pigment epithelium-derived factor	1.93	131.8	68.2	0.000914113
102	Q9NZR1	Tropomodulin-2	1.93	131.9	68.1	0.000227968
103	P69891	Hemoglobin subunit gamma-1	1.94	132	68	0.004028373

(Continued....)

Whole cell proteomic analysis of primary dystonia patients having *THAP1* mutation

Serial No	Accession	Description	Abundance Ratio: (Patient) / (Control)	Abundances (Grouped): Control	Abundances (Grouped): Patient	FDR adjusted p value
104	Q7RTS9-1	dymecilin	1.95	132.2	67.8	0.000202756
105	Q93070	Ecto-ADP-ribosyltransferase 4	1.96	132.5	67.5	3.27659E-05
106	P06132	Uroporphyrinogen decarboxylase	1.98	159.5	80.5	0.039379092
107	Q13642-5	Isoform 5 of Four and a half LIM domains protein 1	1.99	133.2	66.8	0.006809504
108	P08603-1	complement factor H	2	133.3	66.7	0.002256742
109	P02649	Apolipoprotein E	2.02	133.9	66.1	0.00020975
110	P19827-1	Inter-alpha-trypsin inhibitor heavy chain H1	2.02	134	66	9.57519E-05
111	Q7Z7L8	Uncharacterized protein C11orf96	2.05	142.5	69.3	0.038633725
112	Q96M89-1	Coiled-coil domain-containing protein 138	2.05	151.6	73.7	0.003261499
113	P00734	Prothrombin	2.09	135.3	64.7	0.000536693
114	Q7Z6K1	THAP domain-containing protein 5	2.11	135.9	64.1	0.002713378
115	Q8ND94	LRRN4 C-terminal-like protein	2.13	136.2	63.8	0.007848641
116	P05156	Complement factor I	2.15	136.7	63.3	0.0003384
117	P43652	Afamin	2.20	137.6	62.4	0.001286907
118	P04114	apolipoprotein B-100	2.20	137.7	62.3	8.47441E-05
119	O95810	Serum deprivation-response protein	2.21	141.5	63.8	0.010583647
120	P01008	Antithrombin-III	2.22	138	62	7.13331E-05
121	P08697-1	Alpha-2-antiplasmin	2.23	138.2	61.8	5.14227E-05
122	P05452	Tetranectin	2.27	138.9	61.1	0.000354265
123	P02749	Beta-2-glycoprotein 1	2.28	139.1	60.9	7.8923E-05
124	P05543	thyroxine-binding globulin	2.28	139.2	60.8	9.76862E-06
125	Q15370-2	Isoform 2 of Transcription elongation factor B polypeptide 2	2.29	139.2	60.8	0.00465149
126	Q08431	Lactadherin	2.30	139.6	60.4	0.000146128
127	P19823	Inter-alpha-trypsin inhibitor heavy chain H2	2.33	140	60	4.62438E-05
128	P01023	alpha-2-macroglobulin	2.34	140.2	59.8	1.63782E-05
129	Q06033-1	Inter-alpha-trypsin inhibitor heavy chain H3	2.36	140.5	59.5	7.27974E-05
130	Q9H8M2-5	Bromodomain-containing protein 9	2.40	141.3	58.7	0.000233613
131	Q14624-1	Inter-alpha-trypsin inhibitor heavy chain H4	2.40	141.4	58.6	0.000194717
132	P02787	Serotransferrin	2.41	141.4	58.6	1.26787E-05
133	P05362	Intercellular adhesion molecule 1	2.45	142.2	57.8	9.56537E-05
134	Q9P246-2	Isoform 2 of Stromal interaction molecule 2	2.46	142.4	57.6	4.44579E-05
135	P02771	Alpha-fetoprotein	2.5	142.9	57.1	0.000122283
136	P02753	Retinol-binding protein 4	2.52	143.2	56.8	5.54335E-05
137	P00488	Coagulation factor XIII A chain	2.54	143.6	56.4	0.000864016
138	P02765	Alpha-2-HS-glycoprotein	2.55	143.7	56.3	2.98956E-05

(Continued....)

Whole cell proteomic analysis of primary dystonia patients having *THAP1* mutation

Serial No	Accession	Description	Abundance Ratio: (Patient) / (Control)	Abundances (Grouped): Control	Abundances (Grouped): Patient	FDR adjusted p value
139	Q9Y6T7-1	Diacylglycerol kinase beta	2.60	144.6	55.4	6.49767E-05
140	Q3MJ13	WD repeat-containing protein 72	2.61	144.8	55.2	0.000655579
141	P02647	Apolipoprotein A-I	2.63	145	55	4.99209E-05
142	Q9NU22	Midasin	2.71	146.2	53.8	3.52726E-05
143	P02768-1	Serum albumin	2.78	147.1	52.9	4.89046E-05
144	P02788	Lactotransferrin	2.78	147.2	52.8	6.2331E-07
145	O95497	Pantetheinase	2.78	147.2	52.8	0.000327501
146	P04217	Alpha-1B-glycoprotein	2.84	148	52	0.000325282
147	Q6P589	Tumor necrosis factor alpha-induced protein 8-like protein 2	2.90	148.9	51.1	0.002119894
148	P02774-3	Isoform 3 of Vitamin D-binding protein	3.01	150.2	49.8	0.000151761
149	Q96A00	Protein phosphatase 1 regulatory subunit 14A	3.21	174	54	0.014208117
150	P62328	Thymosin beta-4	3.32	153.7	46.3	0.000307492
151	P20742	Pregnancy zone protein	3.87	159	41	6.84354E-05
152	Q4ZG55-1	Protein GREB1	5.20	167.8	32.2	0.000315096

Accession: UniProtKB accession numbers, **Fold change** was calculated as (abundance Ratio (Patient/Control))⁻¹, **Fold change** ≥ 1.5. **FDR:** False discovery rate based on decoy database search. **FDR adjusted p value** ≤ 0.05.

Whole cell proteomic analysis of primary dystonia patients having *THAP1* mutation

Table 59: Ingenuity pathway analysis (IPA) to identify top affected molecular pathway.

ID	Molecules in Network	Score	Focus Molecules	Top Diseases and Functions
1	Arf,CDK5RAP3,Mapk,MYBBP1A,Ribosomal 40s subunit, Rnr,RPL3,RPL5,RPL6, RPL8, RPL11, RPL12,RPL13,RPL14,RPL15,RPL23,RPL30,RPL31,RPL10A,RPLP0, RPLP1, RPLP2, RPS3, RPS5, RPS6,RPS7,RPS9,RPS11,RPS12,RPS17,RPS18,RPS21,RPS27, RPS28, SRSF1	55	31	Cancer, Cell Death and Survival, Organismal Injury and Abnormalities
2	14-3-3, CCAR1,CELF1,CIRBP,CUTA,DHX9,EDF1,Eif4g,EIF4G2,FUS,HDLBP, HNRNPA1, HNRNPAB, HNRNPC,HNRNPD,HNRNPK,HNRNPL,HNRNPR, HNRNPUL2, Holo RNA polymerase II,ILF2,ILF3,KHDRBS1,MATR3,NNT,NONO, PAWR,Pkc(s), PTBP1,RALY, SERBP1, SFPQ, SNRPA, SYNCRIP,TAF15	55	31	RNA Post-Transcriptional Modification, Protein Synthesis, Gene Expression
3	60S ribosomal subunit,AFP,AKR1C1/AKR1C2,CCDC47,CKAP4,DDRKG1,Jnk, KRTCAP2, KTN1, Rar, RPL9,RPL10,RPL17,RPL18,RPL19,RPL21,RPL24,RPL26,RPL27,RPL28, RPL34,RPL38, RPL13A, RPL18A,RPL35A,RPL37A,RPL7A,Rxr,SLC16A3,SRPRA, STT3A, SUB1,T3-TR-RXR, TFIIH,thymidine kinase	47	28	Cancer, Cell Death and Survival, Organismal Injury and Abnormalities
4	ALDH1A3,APOBEC3C,CISD2,CNOT1,EFTUD2,elastase,EMD,FARSB,Fibrin,Fibrinogen, FN1, G3BP2,H2AFY,HNRNPA3,HNRNPA2B1,ICAM1,IFI16,Interferon alpha, ISLR,LMNA, LRRC59,MDN1, PRPF19,RPL7,RPL22,SLC25A1,snRNP,SNRNP70,SNRNP200, SNRPB, SNRPD3,SYNE1,TMEM109,UBAP2L,VAPA	46	30	RNA Post-Transcriptional Modification, Cellular Assembly and Organization, Cellular Function and Maintenance
5	ALYREF,APOE,DDX17,DRG1,ERH,F13A1,Gm-csf, HNRNPA0,HNRNPH3, HNRNPU, Iti, ITIH1,ITIH2,ITIH3,ITIH4,LDL-cholesterol, LRP,MOGS,MT2A, PABPN1, PARP,PDGF BB,PI3K (complex), RBMX,RPL4,RPN2,SARNP,SRSF3,SRSF7, STAU1,TARDBP,THRAP3, transglutaminase, YBX3, ZC3H15	44	27	RNA Post-Transcriptional Modification, Molecular Transport, RNA Trafficking
6	20s proteasome,26s Proteasome,Cyclin E,DAD1,GJA1,IKBIP,LTF,MIF,N-Cadherin, NFkB (complex), NUP98,PLPP3,PRKAA,Proteasome PA700/20s,PSMA6,PSMB2, PSMB5, PURA,PURB, RBM8A, RPS2,RPS19,RPS4X,RPSA,SF3A1,SF3B1,SF3B2,SF3B3,SF3B4, Smad,SMARCA1,SMU1,SNRPA1, TNFRSF11B,YBX1	43	27	Cancer, Cell Death and Survival, Organismal Injury and Abnormalities
7	AFM,Akt,Ant,ATP5H,COX4I1,COX5A,COX5B,COX6C,CYCS,Cytochrome bc1, cytochrome-c oxidase,hexokinase.HK1,MFGE8,Mitochondrial complex 1, NDUFA4, NDUFA9,PHB, RPS3A,S100, S100A13,S100A16,SLC25A3,SLC25A5,SLC25A6,SLC25A24,TSPO, UQCRB, UQCRC1,UQCRC2, Vdac,VDAC1,VDAC2,VDAC3,VLDL	42	26	Cellular Function and Maintenance, Molecular Transport, Nucleic Acid Metabolism
8	AHSG,APOH,CAPRIN1,COL12A1,COL16A1,COL1A1,COL1A2,COL3A1,COL5A1,COL5A2, COL6A3,collagen,Collagen Alpha1,Collagen type III,Collagen type V, Cpla2, ERK1/2, FBN1, GLIPR2, HDL, Hsp27,HSPG2,P4HA1,PCOLCE,Pdi,Raf,RBP4,RRBP1, S100A10,SAA, SERPINC1, SERPINF2,TCEB2,Tcf 1/3/4,TNC	35	23	Endocrine System Disorders, Gastrointestinal Disease, Metabolic Disease

Whole cell proteomic analysis of primary dystonia patients having *THAP1* mutation

ID	Molecules in Network	Score	Focus Molecules	Top Diseases and Functions
9	BANF1,CK1,Cr3,Cyclin A, EIF5B,ERK,FMR1,G3BP1,GTF2I, H1F0,HIST1H1B, HIST1H1C,HIST1H1D,Histone H1,Histone h3,HP1BP3,Importin beta, JINK1/2, Mlc,Mlcp,MPRIIP,MTDH,PARP1,PP1 protein complex group,PP1-C, PP2A, PPP1R14A,PTRH2,RBM39,Rock,SND1,TBL2,TOR1AIP1,TRA2B,Transportin	26	20	Gene Expression, Molecular Transport, RNA Trafficking
10	ADCY,c-Src,Calmodulin,calpain,caspase,CAV1,Ck2,estrogen receptor,F2,F Actin, FKBP3, G protein alpha, GREB1, GST, H2AFZ, Histone h4, HNRNPDL, Hsp90, LIMA1, MGST1, MGST3, NADH dehydrogenase, NDUFA13, NDUFB10, NDUFS1, NUMA1, PHB2, PRKCDBP, Rac, Rb, SDPR, SLC39A7, SLIT3, tubulin (complex), VAMP7	24	19	Organismal Development, Reproductive System Development and Function, Cellular Assembly and Organization
11	Actin, Alp, Alpha 1 antitrypsin, Alpha Actinin, ANPEP, APOB, ATAD3A, ATP6V0D1, BCR (complex), CCAR2, DHCR7, DOK1, E2f, FHL1, GC, hemoglobin, HIST1H2BL, Ifn gamma, IgG, Igm, Immunoglobulin, Kallikrein, LMO7, Mek, NES, Nfat (family), PI3K (family), Rap1, Ras, RPN1, SEC61A1, SEC61B, SERPINA7, SSR1, SSR4	21	18	Developmental Disorder, Hereditary Disorder, Metabolic Disease
12	BUB3, CD3, Collagen type I, CSNK2B, DDX5, DEK, ELAVL1, Focal adhesion kinase, GNB2L1, Gsk3, HISTONE, HNRNPM, Hsp70, Integrin, MLEC, NPM1, p85 (pik3r), PRKDC, Ras homolog, RNA polymerase II, SEC11A, SEC11C, Sfk, SFXN3, signal peptidase, SPCS1, SPCS2, SPCS3, SRC (family), TCR, TRAP/Media, TRGV9, TRIM28, Ubiquitin, ZNF77	20	16	Gene Expression, RNA Post-Transcriptional Modification, DNA Replication, Recombination, and Repair
13	A2M, ALB, AMPK, Ap1, APOA1, CFH, Collagen type IV, Collagen(s), Creb, FNDC3A, FNDC3B, FSH, Ifn, IFN Beta, IL1, IMMT, KDELR1, Laminin, LDL, Lh, Mmp, NOLC1, P38 MAPK, Pdgf (complex), Pka, Pro-inflammatory Cytokine, RAB13, RANBP2, Smad1/5/8, TF, Tgf beta, TMBIM6, TMSB10/TMSB4X, TP53I3, Vegf	19	15	Organ Morphology, Reproductive System Development and Function, Endocrine System Disorders
14	APP, ASPH, ATAT1, BCLAF1, C12orf65, C16orf78, C19orf70, C4orf46, CCDC138, CCNB3, CDK2, C HID1, CNPY2, COPS5, CSAG1, DDX3X, DHX29, EPB41L4A, FBXW9, HMCES, HMGN4, KCTD18, L MF2, LRRN4CL, MAGOHB, OCEL1, OLFML2A, OSM, RPF2, SEC62, SRPK2, TECR, TRUB1, VHL, ZMAT4	15	13	Cell Cycle, Nervous System Development and Function, Hereditary Disorder
15	ACSM3, Ahr-aryl hydrocarbon, BRD4, BRD9, C3, C3-Cfb, CCL4L1/CCL4L2, CFI, CR1L, DEFA4, EHF, FKBP11, FLRT1, GPX2, Histone h3, HOXD1, KRT72, LRRC32, PEX1, PLC, PNOC, PZP, RAI14, RELA, SAA2, SAA4, SLC16A1, SLFN5, SPATS2L, STARD10, TCF, TGFB1, tretinoin, VNN1, VNN2	9	9	Decreased Levels of Albumin, Cell Death and Survival, Gastrointestinal Disease
16	15-hydroxyeicosatetraenoic acid, A1BG, ANO1, AR, Ca2+, Camkk, CAMLG, CDKN1A, CEND1, CLEC3B, COG1, D-glucose, DFNA5, DGKB, DNASE1L3, DUOX1, EGFR, GCKR, KDELR2, KDM4D, KLF16, kynurenic acid, MYO1D, NLRP10, PDIA5, PHKA1, PIGA, PPEF2, RNF149, SH2D3C, SHC4, STIM2, TMEM214, TNFRSF10B, UROD	8	8	Small Molecule Biochemistry, Reproductive System Development and Function, Cellular Assembly and Organization

Whole cell proteomic analysis of primary dystonia patients having *THAP1* mutation

Table 60: Disease and function annotation of significant up and down regulated proteins.

Categories	Diseases or Functions Annotation	p-Value*	Molecules	No. of Molecules*
RNA Post-Transcriptional Modification	processing of RNA	2.80E-38	ALB,CCAR2,CELF1,DDX17,DDX5,EFTUD2,FUS,HNRNPA0,HNRNPA1,HNRNPA2B1,HNRNPC,HNRNPD,HNRNPH3,HNRNPK,HNRNPL,HNRNPM,HNRNPU,KHDRBS1,NOLC1,NONO,NPM1,PABPN1,PRPF19,PTBP1,RBM39,RBM8A,RBMX,RPL11,RPL14,RPL26,RPL35A,RPL5,RPL7,RPS17,RPS19,RPS28,RPS6,RPS7,SF3A1,SF3B1,SF3B2,SF3B3,SF3B4,SFPQ,SNRNP200,SNRNP70,SNRPA,SRSF1,SRSF3,SRSF7,SYNCRIP,TARDBP,THRAP3,TRA2B	54
Protein Synthesis	synthesis of protein	4.98E-15	CAV1,CIRBP,CNOT1,DHX9,EIF4G2,EIF5B,ELAVL1,FARSB,FMR1,FN1,HNRNPD,HNRNPK,ILF3,KHDRBS1,NPM1,PTBP1,RPL13A,RPL19,RPL23,RPL30,RPL5,RPS3,RPS3A,RPS4X,RPS5,RPS6,RPS7,RPS9,RRBP1,SNRNP70,STAU1,SYNCRIP,YBX1	33
Cellular Growth and Proliferation	proliferation of cells	1.67E-11	A2M,AFP,AHSG,AKR1C1/AKR1C2,ALB,ANPEP,APOA1,APOB,APOE,APOH,ASPH,ATAD3A,ATP6V0D1,BCLAF1,CAPRIN1,CAV1,CCAR1,CCAR2,CDK5RAP3,CIRBP,CISD2,CNPY2,COL1A1,COL1A2,COL6A3,CSNK2B,DDX17,DDX5,DHX9,DOK1,EDF1,EIF4G2,ELAVL1,EMD,F2,FBN1,FHL1,FN1,FUS,G3BP1,GJA1,GNB2L1,H2AFY,H2AFZ,HIST1H1B,HIST1H1D,HK1,HNRNPA0,HNRNPA1,HNRNPA2B1,HNRNPAB,HNRNPC,HNRNPD,HNRNPK,HNRNPM,HNRNPR,HNRNPU,HP1BP3,HSPG2,ICAM1,IFI16,ILF2,ILF3,IMMT,KHDRBS1,LIMA1,LMNA,LT F,MFGE8,MIF,MT2A,MTDH,MYBBP1A,NDUFA13,NES,NPM1,NUMA1,NUP98,P4HA1,PARP1,PAWR,PDIA5,PHB,PRKCDBP,PRKDC,PRPF19,PSMB2,PTBP1,PURA,RAB13,RPL26,RPS19,RPS3A,RPS4X,RPS6,RPS9,RPSA,S100A10,SEC61A1,SERPINC1,SERPINF2,SF3B2,SF3B3,SFPQ,SLC16A1,SLC25A5,SLC25A6,SLIT3,SMARCA1,SND1,SNRNP200,SRSF1,SRSF3,SSR1,STAU1,STIM2,TF,THRAP3,TMSB10/TMSB4X,TNC,TNFRSF11B,TRIM28,TSPO,VAMP7,VDAC1,YBX1,YBX3	127
Gene Expression	expression of RNA	5.09E-09	A2M,ALYREF,APOE,ASPH,BCLAF1,CAV1,CCAR2,CNOT1,CNPY2,COL1A1,DDX17,DDX5,DEK,DHX9,DRG1,EDF1,EIF4G2,EIF5B,F2,FARSB,FN1,GJA1,GNB2L1,GTF2I,H1F0,H2AFY,H2AFZ,HIST1H1B,HIST1H1C,HNRNPA1,HNRNPA2B1,HNRNPC,HNRNPK,HP1BP3,IFI16,ILF2,ILF3,KHDRBS1,LMNA,MATR3,MIF,MTDH,MYBBP1A,NDUFA13,NOLC1,NPM1,PABPN1,PARP1,PAWR,PHB,PHB2,PRKDC,PTRH2,PURA,RBMX,RPL13A,RPL19,RPL30,RPL6,RP3,RPS3A,RPS4X,RPS5,RPS9,RRBP1,SEC61A1,SERPINF2,SFPQ,SMARCA1,SUB1,SYNCRIP,TAF15,TARDBP,THRAP3,TRIM28,VAPA,YBX1	77

Whole cell proteomic analysis of primary dystonia patients having *THAP1* mutation

Categories	Diseases or Functions Annotation	p-Value*	Molecules	No. of Molecules*
Cell Death and Survival	cell death	4.72E-07	A2M,AFP,ALB,ANPEP,APOA1,APOB,APOE,ATAD3A,BCLAF1,CAV1,CCAR1,CCAR2,CDK5,RAP3,CFH,CFI,CIRBP,CNPY2,COL1A1,COX5A,CYCS,DAD1,DDX17,DDX5,DEK,DHCR7,DHX9,EIF4G2,ELAVL1,F2,FN1,GJA1,GNB2L1,HIST1H1C,HK1,HNRNPA1,HNRNPC,HNRNPK,ICAM1,IFI16,ILF2,IMMT,KDELRL1,KHDRBS1,LMNA,LTF,MFGE8,MIF,MPRIP,MT2A,MTDH,MYBBP1A,NDUFA13,NPM1,NUMA1,PARP1,PAWR,PHB,PHB2,PRKCDBP,PRKDC,PRPF19,PTRH2,RANBP2,RBP4,RPLP0,RPS19,RPS3,RPS3A,RPS6,RRBP1,SERPINC1,SERPINF2,SF3A1,SF3B3,SFPQ,SLC16A1,SLC25A5,SLC25A6,SMARCA1,SND1,SRSF1,STIM2,SUB1,SYNE1,TARDBP,TF,TMBIM6,TMEM109,TMEM214,TMSB10/TMSB4X,TNC,TNFRSF11B,TP53I3,TRIM28,TSPO,VAPA,VDAC1,VDAC2,YBX1	99
Cell Death and Survival	apoptosis	6.02E-07	A2M,AFP,ALB,ANPEP,APOE,ATAD3A,BCLAF1,CAV1,CCAR1,CCAR2,CDK5,RAP3,CFH,CIRBP,COL1A1,COX5A,CYCS,DAD1,DDX17,DDX5,DHX9,EIF4G2,ELAVL1,F2,FN1,GJA1,GNB2L1,HIST1H1C,HK1,HNRNPA1,HNRNPC,HNRNPK,ICAM1,IFI16,IMMT,KHDRBS1,LTF,MFGE8,MIF,MPRIP,MT2A,MTDH,MYBBP1A,NDUFA13,NPM1,NUMA1,PARP1,PAWR,PHB,PHB2,PRKCDBP,PRKDC,PRPF19,PTRH2,RBP4,RPLP0,RPS19,RPS3,RPS3A,RPS6,RRBP1,SERPINC1,SFPQ,SLC25A5,SLC25A6,SMARCA1,SND1,SRSF1,SUB1,SYNE1,TARDBP,TF,TMBIM6,TMEM214,TMSB10/TMSB4X,TNC,TNFRSF11B,TP53I3,TRIM28,TSPO,VDAC1,VDAC2,YBX1	82
Neurological Disease	Movement Disorders	1.10E-05	A2M,AFM,ALB,APOE,COL6A3,COX5B,CYCS,DGKB,DHCR7,FARSB,FUS,GJA1,HNRNPDL,HNRNPU,ITIH4,LTF,MT2A,MTDH,NDUFA13,NPM1,P4HA1,PARP1,RBP4,RPL13,RPL13A,RPL15,RPL17,RPL3,RPL31,RPS3A,RPS4X,SERPINF2,SLC25A6,SUB1,SYNE1,TOR1AIP1,TSPO,UQCRB,UQCRC1	39
Gene Expression	transcription	4.11E-06	A2M,ALYREF,ASPH,BCLAF1,CAV1,CCAR2,CNOT1,CNPY2,COL1A1,DDX17,DDX5,DEK,DHX9,DRG1,EDF1,F2,FN1,GJA1,GNB2L1,GTF2I,H1F0,H2AFY,H2AFZ,HIST1H1B,HIST1H1C,HNRNPA1,HNRNPA2B1,HNRNPC,HNRNPK,HP1BP3,IFI16,ILF2,ILF3,LMNA,MATR3,MIF,MTDH,MYBBP1A,NDUFA13,NOLC1,NPM1,PABPN1,PARP1,PAWR,PHB,PHB2,PRKDC,PSMB2,PTRH2,PURA,RBMX,RPL12,RPL6,RPS3,SEC61A1,SERPINF2,SFPQ,SMARCA1,SUB1,TAF15,TARDBP,THRAP3,TRIM28,VAPA,YBX1	65

*p-value: Significance level of overlap. **No. of Molecules: Total no. of significant up & down regulated proteins associated with the particular disease.

Whole cell proteomic analysis of primary dystonia patients having *THAP1* mutation

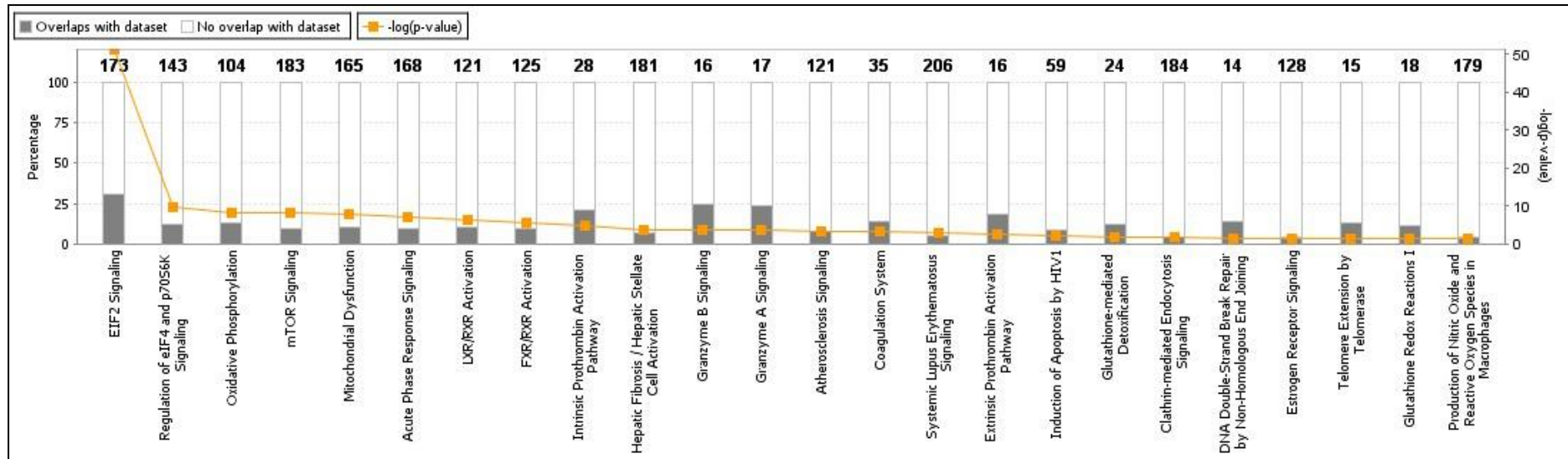
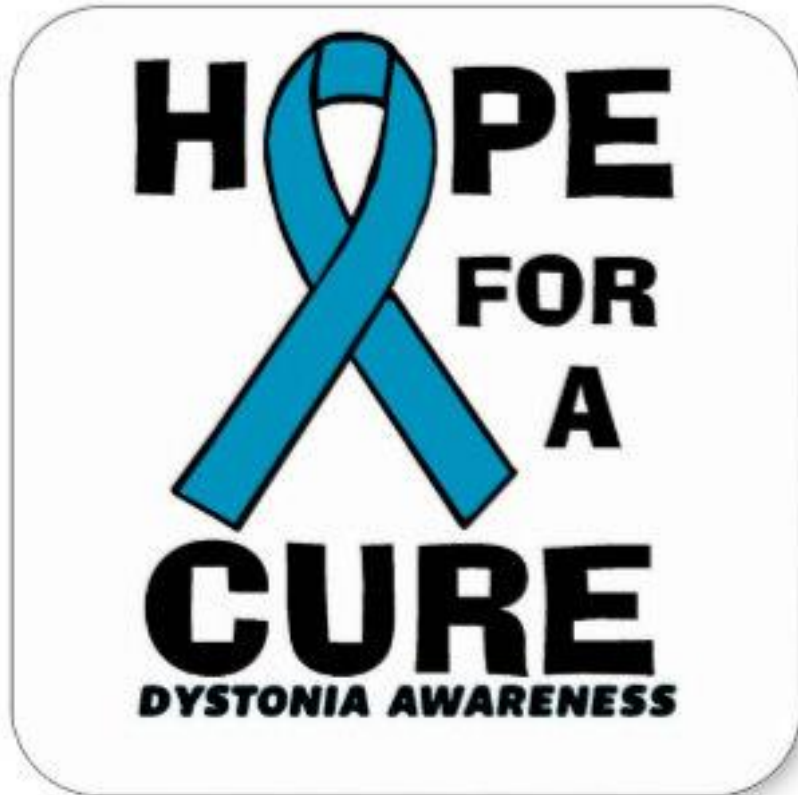


Figure 44: Top canonical pathways as identified by Ingenuity Pathway Analysis. The differentially expressed proteins are involved in these pathways which could significantly alter the pathway functions.

6.4 Discussion

To illustrate the disease pathogenesis, an unbiased whole cell proteomic profiling was carried out based on isobaric mass tag (TMTsixplex™, Thermo Scientific) followed by electron transfer dissociation (ETD) based LC-MS/MS. Subsequent data analysis identified significant 302 upregulated proteins and 152 downregulated proteins in *THAP1* mutant patients' fibroblast samples compared to control ones. Disease function and annotation of significant up and down regulated proteins identified processing of RNA, proliferation of cells, cell death and apoptosis and neurological problems (movement disorders) were the top predicted disease mechanism for primary dystonia. It has been found previously that due to *THAP1* overexpression, the cell cycle progression at G1/S phase was hampered (336) and hyocellularity was reported with abnormal morphology (322). Mutant THAP1 could trigger apoptotic cellular death as found in THAP1 mutant patients lymphoblastoid cells (335) and increased apoptotic cell death at sensorimotor region of a THAP1 mutant (*Thap1*^{C54Y/+}) knock-in mice (322). The affected movement disorder pathway includes some important associated gene products such as COL6A3 associated with DYT27 dystonia (602, 719), FUS is associated with essential tremor (720), SYNE1 for cerebellar ataxia (721), PARP1 associated with Parkinson's disease (722), TOR1AIP1 is direct interacting partner of another dystonia related protein torsinA (723), which are directly or indirectly precipitate their effect in dystonia pathogenesis. Moreover, a recent study reported that DYT1 dystonia patients derived cells are deficient of eIF2 α signalling (724), which is among the top affected canonical pathway in this proteomic study. So, the findings through this quantitative proteomic analysis actually support the previous reports and it could eventually open up a novel corridor for further exploration on primary dystonia pathogenesis.



CHAPTER 7

CONCLUSION

7.1 Summary of findings

The present study was focused on the determination of *TOR1A* and *THAP1* genetic variants and its functional contribution towards the primary dystonia pathogenesis and the identification of global alterations in transcriptome and proteome status. The Chapter 1 is focused on the overview of dystonia along with its classification, prevalence and pathophysiology. The Chapter 2 elucidated the genetics of dystonia which includes all the identified dystonia causing genes in terms of their clinical features, neuropathology, molecular genetics and molecular pathology. In this chapter, all the identified mutations in different genes found in dystonia patients have also been tabulated for efficient reference. This chapter also highlighted the possible interactions of DYT genes and their shared common molecular pathways like transcriptional regulation, stress response pathways and dopamine neurotransmission which may govern the dystonia pathogenesis.

The Chapter 3 described the experimental approaches to identify the common and rare genetic variants of *TOR1A* and *THAP1* genes among Indian primary dystonia patients. The most common Δ GAG mutation in *TOR1A* gene was found in an isolated East-Indian family, where two brothers are affected with primary generalized dystonia and the mutation was found to be inherited from their asymptomatic mother. Among the common variants in *TOR1A* gene, the minor allele of a functional SNP, rs1801968 was found to be significantly associated as risk factor with primary dystonia. Moreover, a haplotype consisting of two 3' UTR SNPs, rs1182 and rs3842225 was also found as a significant risk factor for primary dystonia pathogenesis. Genetic screening of *THAP1* gene identified two novel and one reported rare variants. The novel variants includes a small deletion (c.208-209 Δ AA;

Conclusion

p. K70VfsX15) and a 3' UTR variant (c. *157 T>C) found in a juvenile onset cervical dystonia patient and a Blepharospasm patient. The reported variant (c.427 A>G; p. M143V) was found in an early onset generalized dystonia patient, which was also previously found in an adult onset cervical dystonia patient in Germany. Taken together all variants, both the common and rare genetic variants in *TOR1A* and *THAP1* genes it appears *TOR1A* and *THAP1* could contribute considerably towards the primary dystonia pathogenesis among Indian dystonia patients.

The functional characterizations of certain *THAP1* missense mutations (R29P, L32H, H57N, L72R and M143V) were described in chapter 4. The experiments were done in an *in-vitro* cell culture system by exogeneous transfection of *THAP1* cDNA constructs. The subcellular localization was done using immunocytochemistry followed by confocal microscopy. Two of the mutants, p.R29P and p. M143V formed perinuclear inclusion bodies, whereas other mutants have normal nuclear localization as wild type *THAP1* protein. The protein stability assay was done by Cycloheximide chase assay followed by western blot, which revealed that the relative abundances of p. R29P is higher and p. M143V is lower than the wild type *THAP1* protein. The time course analysis determined that the degradation of p. R29P is higher while p. M143V is lower compared to wild type one conferring that p. M143V is more stable while p. R29P is less stable compared to wild type *THAP1* protein. The mutant *THAP1* mRNA stability was determined by actinomycin D treatment followed by qPCR, which identified the relative expression of c. T95A was significantly downregulated compared to wild type *THAP1* mRNA expression whereas the relative stability was comparable to that of wild type *THAP1*. The mutant *THAP1* repressional activity over *TOR1A* expression was assessed by dual

Conclusion

luciferase activity using *TOR1A* core promoter as a binding site for THAP1. It has been found that the L32H mutation disrupts the THAP1 repressional activity whereas the other THAP1 mutants increase the repression as evident from the decreased luciferase signal intensity. Altogether, the R29P and M143V mutations affected the normal THAP1 protein functions and functionally pathogenic for primary dystonia pathogenesis.

Whole genome gene expression analysis by RNA-seq was done in *THAP1* mutant patients' fibroblast and control fibroblast samples to identify the differentially expressed genes. Significant upregulation of 17 genes and downregulation of 38 genes have been identified with at least ≥ 1.5 fold change. The gene set enrichment analysis by Ingenuity Pathway Analysis (IPA) recognized five major dysregulated networks, which are involved in tissue development, cellular development, cell signalling, vitamin and mineral metabolism, cell death and survival. Disease and function annotation of significant up and down regulated genes enriched for neurological disease, psychological disorders, cell cycle progression, abnormal morphology of cells, quantity of cells and cell death of motor neurons. NF- κ B (complex) and ERK pathway are found to be the major hub for the dysregulated gene network.

Whole cell quantitative proteomic profiling was done for the same set of samples using *in-vitro* TMT-labelling followed by LC-MS/MS based mass spectrometry. Significant up-regulation of 302 proteins and down-regulation of 152 proteins were found with a fold change of ≥ 1.5 . The protein set enrichment analysis identified sixteen major dysregulated networks including cell death and survival, RNA post

Conclusion

transcriptional modification, cancer, gene expression, cellular function and maintenance, cell cycle, nervous system development. Disease and function annotation of significant up and down regulated protein were enriched for RNA post-transcriptional modification, protein synthesis, cellular growth and proliferation, gene expression, cell death and survival, neurological disease and gene expression. EIF2 signalling, mitochondrial dysfunction, mTOR signalling, oxidative phosphorylation, regulation of eIF4 and p70S6K signalling are revealed as the top affected canonical pathways. In combination of gene expression analysis and proteome analysis, the cell death and survival, cell cycle progression and transcriptional dysregulation were found as the common theme for the pathogenesis of primary dystonia due to *THAP1* mutation.

7.2 Future direction

The results obtained from this study could propose certain important perspectives for future dystonia research in terms of molecular genetics and underlying pathogenesis. The genetic screening part of this study identified the most common causal mutation ΔE of *TOR1A* gene in an isolated East Indian family and two novel and one reported rare variants of *THAP1* upon screening of more than 200 primary dystonia patients. The occurrence of such rare variants in these two genes arise the possibility of presence of causal genetic variants in other dystonia related genes in Indian primary dystonia patients. As India, having more than 1 billion population represents diverse genetic pool, the probability of finding the genetic variants in other dystonia genes are more likely which require an elaborate and comprehensive genetic study in primary dystonia patients. The recent advancements

Conclusion

of techniques for genetic study, such as, the exome sequencing and other high throughput next generation sequencing techniques could foster the mapping and identification of causal genetic variants in new and existing dystonia related genes. The penetrance of the causal rare variants could be governed by the other genetic common variants and their effects as SNPs or in a haplotype manner. Here in this study, the rs1801968 of *TOR1A* was revealed as a potential risk factor for primary dystonia, which also can modify the penetrance of *TOR1A* ΔE mutation. The contributing effects of the common variants are also significant for the assessment in terms of disease pathogenesis and progression. To unravel the underlying disease mechanism, the implications of the common genetic variants and the rare variants need to be understood well enough.

The functional implication of certain *THAP1* rare variants were characterized in this study and the functional abnormality of those have been discovered. Such experiments need to be done for other remaining rare variants of *THAP1* based on the functional domains and important structural motifs. This could really be helpful to understand the role of such rare variants on THAP1 protein functions, interactions with other proteins and its subsequent neurobiology. Once it will be revealed, it could effectively help to develop the genotype-phenotype correlation and therapeutic interventions based on the nature of the mutation(s). This could lead to an effective medical strategies where based on the genetic findings and phenotypic features, a drug or a combinations of drugs could be administered to ameliorate the disease course.

Here in this study, a long awaiting aspect of primary dystonia pathogenesis has been undertaken in terms of transcriptome and proteome analysis in THAP1 mutant

Conclusion

patient derived fibroblast samples. Both the analysis revealed dysregulation in some of the pivotal cellular pathways like cell death and survival, cell cycle progression, transcriptional dysregulation and neurodevelopmental disorders. This study effectively opens up a new avenue for of further research in primary dystonia pathogenesis. Further cellular experiments on these dysregulated networks could explore the actual underlying disease mechanism.

REFERENCES

1. Kernich CA. Dystonia. *The neurologist*. 2003;9(2):121-2.
2. Albanese A, Bhatia K, Bressman SB, DeLong MR, Fahn S, Fung VS, et al. Phenomenology and classification of dystonia: a consensus update. *Movement disorders : official journal of the Movement Disorder Society*. 2013;28(7):863-73.
3. Klein C, Fahn S. Translation of Oppenheim's 1911 paper on dystonia. *Movement Disorders*. 2013;28(7):851-62.
4. FRAENKEL J. DYSBASIA LORDOTICA PROGRESSIVA, DYSTONIA MUSCULORUM DEFORMANS-TORTIPELVIS. *The Journal of Nervous and Mental Disease*. 1912;39(6):261-374.
5. Herz E. Dystonia: I. Historical review; analysis of dystonic symptoms and physiologic mechanisms involved. *Archives of Neurology & Psychiatry*. 1944;51(4):305-18.
6. Marsden CD, Harrison MJ, Bunday S. Natural history of idiopathic torsion dystonia. *Adv Neurol*. 1976;14:177-87.
7. Marsden CD. The problem of adult-onset idiopathic torsion dystonia and other isolated dyskinesias in adult life (including blepharospasm, oromandibular dystonia, dystonic writer's cramp, and torticollis, or axial dystonia). *Adv Neurol*. 1976;14:259-76.
8. Fahn S. Classification of movement disorders. *Movement disorders : official journal of the Movement Disorder Society*. 2011;26(6):947-57.
9. Greene P, Kang UJ, Fahn S. Spread of symptoms in idiopathic torsion dystonia. *Movement disorders*. 1995;10(2):143-52.
10. Weiss EM, Hershey T, Karimi M, Racette B, Tabbal SD, Mink JW, et al. Relative risk of spread of symptoms among the focal onset primary dystonias. *Movement disorders*. 2006;21(8):1175-81.
11. Defazio G, Abbruzzese G, Livrea P, Berardelli A. Epidemiology of primary dystonia. *The lancet neurology*. 2004;3(11):673-8.
12. Group ESoDiEC. A prevalence study of primary dystonia in eight European countries. *Journal of neurology*. 2000;247(10):787-92.

13. Müller J, Kiechl S, Wenning G, Seppi K, Willeit J, Gasperi A, et al. The prevalence of primary dystonia in the general community. *Neurology*. 2002;59(6):941-3.
14. Pekmezović T, Ivanović N, Svetel M, Nalić D, Smiljković T, Raičević R, et al. Prevalence of primary late-onset focal dystonia in the Belgrade population. *Movement disorders*. 2003;18(11):1389-92.
15. Le K-D, Nilsen B, Dietrichs E. Prevalence of primary focal and segmental dystonia in Oslo. *Neurology*. 2003;61(9):1294-6.
16. Kandil MR, Tohamy SA, Abdel Fattah M, Ahmed HN, Farwiesz HM. Prevalence of chorea, dystonia and athetosis in Assiut, Egypt: a clinical and epidemiological study. *Neuroepidemiology*. 1994;13(5):202-10.
17. Zilber N, Korczyn A, Kahana E, Fried K, Alter M. Inheritance of idiopathic torsion dystonia among Jews. *Journal of medical genetics*. 1984;21(1):13-20.
18. Li S-c, Schoenberg BS, Wang C-c, Cheng X-m, Rui D-y, Bolis C, et al. A prevalence survey of Parkinson's disease and other movement disorders in the People's Republic of China. *Archives of neurology*. 1985;42(7):655-7.
19. Matsumoto S, Nishimura M, Shibasaki H, Kaji R. Epidemiology of primary dystonias in Japan: comparison with Western countries. *Movement disorders*. 2003;18(10):1196-8.
20. Nakashima K, Kusumi M, Inoue Y, Takahashi K. Prevalence of focal dystonias in the western area of Tottori Prefecture in Japan. *Movement disorders*. 1995;10(4):440-3.
21. Nutt JG, Muenter MD, Aronson A, Kurland LT, Melton LJ. Epidemiology of focal and generalized dystonia in Rochester, Minnesota. *Movement disorders*. 1988;3(3):188-94.
22. Defazio G, Livrea P, De Salvia R, Manobianca G, Coviello V, Anaclerio D, et al. Prevalence of primary blepharospasm in a community of Puglia region, Southern Italy. *Neurology*. 2001;56(11):1579-81.
23. Risch N, de Leon D, Ozelius L, Kramer P, Almasy L, Singer B, et al. Genetic analysis of idiopathic torsion dystonia in Ashkenazi Jews and their recent descent from a small founder population. *Nature genetics*. 1995;9(2):152-9.

References

24. Castelon Konkiewitz E, Trender-Gerhard I, Kamm C, Warner T, Ben-Shlomo Y, Gasser T, et al. Service-based survey of dystonia in Munich. *Neuroepidemiology*. 2002;21(4):202-6.
25. Butler AG, Duffey PO, Hawthorne MR, Barnes MP. An epidemiologic survey of dystonia within the entire population of northeast England over the past nine years. *Adv Neurol*. 2004;94:95-9.
26. Bhidayasiri R, Kaewwilai L, Wannachai N, Brenden N, Truong DD, Devahastin R. Prevalence and diagnostic challenge of dystonia in Thailand: a service-based study in a tertiary university referral centre. *Parkinsonism & related disorders*. 2011;17:S15-S9.
27. Asgeirsson H, Jakobsson F, Hjaltason H, Jonsdottir H, Sveinbjornsdottir S. Prevalence study of primary dystonia in Iceland. *Movement disorders*. 2006;21(3):293-8.
28. Cossu G, Mereu A, Deriu M, Melis M, Molari A, Melis G, et al. Prevalence of primary blepharospasm in Sardinia, Italy: A service-based survey. *Movement disorders*. 2006;21(11):2005-8.
29. Das SK, Banerjee TK, Biswas A, Roy T, Raut DK, Chaudhuri A, et al. Community survey of primary dystonia in the city of Kolkata, India. *Movement Disorders*. 2007;22(14):2031-6.
30. Solano Atehortua JM, Isaza Jaramillo SP, Rendón Bañol A, Buritica Henao O. Prevalence of dystonia in Antioquia, Colombia. *Neuroepidemiology*. 2016;46(2):137-43.
31. Papantonio AM, Beghi E, Fogli D, Zarrelli M, Logroscino G, Bentivoglio A, et al. Prevalence of primary focal or segmental dystonia in adults in the district of foggia, southern Italy: a service-based study. *Neuroepidemiology*. 2009;33(2):117-23.
32. Sugawara M, Watanabe S, Toyoshima I. Prevalence of dystonia in Akita prefecture in Northern Japan. *Movement disorders*. 2006;21(7):1047-9.
33. Fukuda H, Kusumi M, Nakashima K. Epidemiology of primary focal dystonias in the western area of Tottori prefecture in Japan: comparison with prevalence evaluated in 1993. *Movement disorders*. 2006;21(9):1503-6.

34. Steeves TD, Day L, Dykeman J, Jette N, Pringsheim T. The prevalence of primary dystonia: A systematic review and meta-analysis. *Movement Disorders*. 2012;27(14):1789-96.
35. Quartarone A, Rizzo V, Morgante F. Clinical features of dystonia: a pathophysiological revisitation. *Current opinion in neurology*. 2008;21(4):484-90.
36. Neychev VK, Gross RE, Lehericy S, Hess EJ, Jinnah H. The functional neuroanatomy of dystonia. *Neurobiology of disease*. 2011;42(2):185-201.
37. Garraux G, Bauer A, Hanakawa T, Wu T, Kansaku K, Hallett M. Changes in brain anatomy in focal hand dystonia. *Annals of neurology*. 2004;55(5):736-9.
38. Egger K, Mueller J, Schocke M, Brenneis C, Rinnerthaler M, Seppi K, et al. Voxel based morphometry reveals specific gray matter changes in primary dystonia. *Movement Disorders*. 2007;22(11):1538-42.
39. Etgen T, Mühlau M, Gaser C, Sander D. Bilateral grey-matter increase in the putamen in primary blepharospasm. *Journal of Neurology, Neurosurgery & Psychiatry*. 2006;77(9):1017-20.
40. Black KJ, Öngür D, Perlmutter JS. Putamen volume in idiopathic focal dystonia. *Neurology*. 1998;51(3):819-24.
41. Fabbrini G, Pantano P, Totaro P, Calistri V, Colosimo C, Carmellini Me, et al. Diffusion tensor imaging in patients with primary cervical dystonia and in patients with blepharospasm. *European journal of neurology*. 2008;15(2):185-9.
42. Colosimo C, Pantano P, Calistri V, Totaro P, Fabbrini G, Berardelli A. Diffusion tensor imaging in primary cervical dystonia. *Journal of Neurology, Neurosurgery & Psychiatry*. 2005;76(11):1591-3.
43. Blood AJ, Kuster JK, Woodman SC, Kirlic N, Makhlof ML, Multhaupt-Buell TJ, et al. Evidence for altered basal ganglia-brainstem connections in cervical dystonia. *PloS one*. 2012;7(2):e31654.
44. Yang J, Luo C, Song W, Guo X, Zhao B, Chen X, et al. Diffusion tensor imaging in blepharospasm and blepharospasm-romandibular dystonia. *Journal of neurology*. 2014;261(7):1413-24.
45. Simonyan K, Tovar-Moll F, Ostuni J, Hallett M, Kalasinsky VF, Lewin-Smith MR, et al. Focal white matter changes in spasmodic dysphonia: a combined diffusion tensor imaging and neuropathological study. *Brain*. 2008;131(2):447-59.

46. Eidelberg D. Brain networks and clinical penetrance: lessons from hyperkinetic movement disorders. *Current opinion in neurology*. 2003;16(4):471-4.
47. Carbon M, Argyelan M, Habeck C, Ghilardi MF, Fitzpatrick T, Dhawan V, et al. Increased sensorimotor network activity in DYT1 dystonia: a functional imaging study. *Brain*. 2010:awq017.
48. Kadota H, Nakajima Y, Miyazaki M, Sekiguchi H, Kohno Y, Amako M, et al. An fMRI study of musicians with focal dystonia during tapping tasks. *Journal of neurology*. 2010;257(7):1092-8.
49. Butterworth S, Francis S, Kelly E, McGlone F, Bowtell R, Sawle GV. Abnormal cortical sensory activation in dystonia: an fMRI study. *Movement disorders*. 2003;18(6):673-82.
50. Dresel C, Haslinger B, Castrop F, Wohlschlaeger AM, Ceballos-Baumann AO. Silent event-related fMRI reveals deficient motor and enhanced somatosensory activation in orofacial dystonia. *Brain*. 2006;129(1):36-46.
51. Delnooz CC, Pasman JW, Beckmann CF, van de Warrenburg BP. Task-free functional MRI in cervical dystonia reveals multi-network changes that partially normalize with botulinum toxin. *PloS one*. 2013;8(5):e62877.
52. Quartarone A, Bagnato S, Rizzo V, Siebner HR, Dattola V, Scalfari A, et al. Abnormal associative plasticity of the human motor cortex in writer's cramp. *Brain*. 2003;126(12):2586-96.
53. Quartarone A, Rizzo V, Terranova C, Morgante F, Schneider S, Ibrahim N, et al. Abnormal sensorimotor plasticity in organic but not in psychogenic dystonia. *Brain*. 2009;132(10):2871-7.
54. Weise D, Schramm A, Stefan K, Wolters A, Reiners K, Naumann M, et al. The two sides of associative plasticity in writer's cramp. *Brain*. 2006;129(10):2709-21.
55. Quartarone A, Sant'Angelo A, Battaglia F, Bagnato S, Rizzo V, Morgante F, et al. Enhanced long-term potentiation-like plasticity of the trigeminal blink reflex circuit in blepharospasm. *Journal of Neuroscience*. 2006;26(2):716-21.
56. Niethammer M, Carbon M, Argyelan M, Eidelberg D. Hereditary dystonia as a neurodevelopmental circuit disorder: evidence from neuroimaging. *Neurobiology of disease*. 2011;42(2):202-9.
57. LeDoux MS, Brady KA. Secondary cervical dystonia associated with structural lesions of the central nervous system. *Movement Disorders*. 2003;18(1):60-9.

58. Carbon M, Argyelan M, Eidelberg D. Functional imaging in hereditary dystonia. *European journal of neurology*. 2010;17(s1):58-64.
59. Argyelan M, Carbon M, Niethammer M, Uluğ AM, Voss HU, Bressman SB, et al. Cerebellothalamocortical connectivity regulates penetrance in dystonia. *Journal of Neuroscience*. 2009;29(31):9740-7.
60. Fremont R, Tewari A, Angueyra C, Khodakhah K. A role for cerebellum in the hereditary dystonia DYT1. *eLife*. 2017;6:e22775.
61. Ozelius LJ, Bressman SB. Genetic and clinical features of primary torsion dystonia. *Neurobiology of disease*. 2011;42(2):127-35.
62. Klein C, Krainc D, Schlossmacher MG, Lang AE. Translational research in neurology and neuroscience 2011: movement disorders. *Archives of neurology*. 2011;68(6):709-16.
63. Charlesworth G, Angelova PR, Bartolomé-Robledo F, Ryten M, Trabzuni D, Stamelou M, et al. Mutations in HPCA cause autosomal-recessive primary isolated dystonia. *The American Journal of Human Genetics*. 2015;96(4):657-65.
64. Hershenson J, Mencacci NE, Davis M, MacDonald N, Trabzuni D, Ryten M, et al. Mutations in the autoregulatory domain of β -tubulin 4a cause hereditary dystonia. *Annals of neurology*. 2013;73(4):546-53.
65. Lohmann K, Wilcox RA, Winkler S, Ramirez A, Rakovic A, Park JS, et al. Whispering dysphonia (DYT4 dystonia) is caused by a mutation in the TUBB4 gene. *Annals of neurology*. 2013;73(4):537-45.
66. Xiao J, Uitti RJ, Zhao Y, Vemula SR, Perlmutter JS, Wszolek ZK, et al. Mutations in CIZ1 cause adult onset primary cervical dystonia. *Annals of neurology*. 2012;71(4):458-69.
67. Charlesworth G, Plagnol V, Holmström KM, Bras J, Sheerin U-M, Preza E, et al. Mutations in ANO3 cause dominant craniocervical dystonia: ion channel implicated in pathogenesis. *The American Journal of Human Genetics*. 2012;91(6):1041-50.
68. Fuchs T, Saunders-Pullman R, Masuho I, San Luciano M, Raymond D, Factor S, et al. Mutations in GNAL cause primary torsion dystonia. *Nature genetics*. 2013;45(1):88-92.

69. Mencacci NE, Rubio-Agusti I, Zdebik A, Asmus F, Ludtmann MH, Ryten M, et al. A missense mutation in KCTD17 causes autosomal dominant myoclonus-dystonia. *The American Journal of Human Genetics*. 2015;96(6):938-47.
70. Zech M, Lam DD, Francescato L, Schormair B, Salminen AV, Jochim A, et al. Recessive mutations in the $\alpha 3$ (VI) collagen gene COL6A3 cause early-onset isolated dystonia. *The American Journal of Human Genetics*. 2015;96(6):883-93.
71. Wang J-L, Cao L, Li X-H, Hu Z-M, Li J-D, Zhang J-G, et al. Identification of PRRT2 as the causative gene of paroxysmal kinesigenic dyskinesias. *Brain*. 2011:awr289.
72. Waddy H, Fletcher N, Harding A, Marsden C. A genetic study of idiopathic focal dystonias. *Annals of neurology*. 1991;29(3):320-4.
73. Schmidt A, Jabusch H-C, Altenmüller E, Hagenah J, Brüggemann N, Lohmann K, et al. Etiology of musician's dystonia Familial or environmental? *Neurology*. 2009;72(14):1248-54.
74. Stojanović M, Cvetković D, Kostic VS. A genetic study of idiopathic focal dystonias. *Journal of neurology*. 1995;242(8):508-11.
75. Leube B, Kessler KR, Goecke T, Auburger G, Benecke R. Frequency of familial inheritance among 488 index patients with idiopathic focal dystonia and clinical variability in a large family. *Movement disorders*. 1997;12(6):1000-6.
76. LeDoux MS, Dauer WT, Warner TT. Emerging common molecular pathways for primary dystonia. *Movement Disorders*. 2013;28(7):968-81.
77. Bragg DC, Armata IA, Nery FC, Breakefield XO, Sharma N. Molecular pathways in dystonia. *Neurobiology of disease*. 2011;42(2):136-47.
78. Marsden CD, Harrison M, Bunday S. Natural history of idiopathic torsion dystonia. *Advances in neurology*. 1975;14:177-87.
79. Németh AH. The genetics of primary dystonias and related disorders. *Brain*. 2002;125(4):695-721.
80. Bressman S, Raymond D, Wendt K, Saunders–Pullman R, De Leon D, Fahn S, et al. Diagnostic criteria for dystonia in DYT1 families. *Neurology*. 2002;59(11):1780-2.
81. Grundmann K, Laubis-Herrmann U, Bauer I, Dressler D, Vollmer-Haase J, Bauer P, et al. Frequency and phenotypic variability of the GAG deletion of the DYT1 gene in an unselected group of patients with dystonia. *Archives of neurology*. 2003;60(9):1266-70.

References

82. McNaught KSP, Kapustin A, Jackson T, Jengelley TA, JnoBaptiste R, Shashidharan P, et al. Brainstem pathology in DYT1 primary torsion dystonia. *Annals of neurology*. 2004;56(4):540-7.
83. Ozelius L, Kramer PL, Moskowitz CB, Kwiatkowski DJ, Brin MF, Bressman SB, et al. Human gene for torsion dystonia located on chromosome 9q32-q34. *Neuron*. 1989;2(5):1427-34.
84. Ozelius LJ, Hewett JW, Page CE, Bressman SB, Kramer PL, Shalish C, et al. The early-onset torsion dystonia gene (DYT1) encodes an ATP-binding protein. *Nature genetics*. 1997;17(1):40-8.
85. Khan NL, Wood NW, Bhatia KP. Autosomal recessive, DYT2-like primary torsion dystonia A new family. *Neurology*. 2003;61(12):1801-3.
86. Kupke KG, Lee LV, Müller U. Assignment of the X-linked torsion dystonia gene to Xq21 by linkage analysis. *Neurology*. 1990;40(9):1438-.
87. Makino S, Kaji R, Ando S, Tomizawa M, Yasuno K, Goto S, et al. Reduced neuron-specific expression of the TAF1 gene is associated with X-linked dystonia-parkinsonism. *The American Journal of Human Genetics*. 2007;80(3):393-406.
88. Ahmad F, Davis M, Waddy H, Oley C, Marsden C, Harding A. Evidence for locus heterogeneity in autosomal dominant torsion dystonia. *Genomics*. 1993;15(1):9-12.
89. Ichinose H, Ohye T, Takahashi E-i, Seki N, Hori T-a, Segawa M, et al. Hereditary progressive dystonia with marked diurnal fluctuation caused by mutations in the GTP cyclohydrolase I gene. *Nature genetics*. 1994;8(3):236-42.
90. Lüdecke B, Dworniczak B, Bartholomé K. A point mutation in the tyrosine hydroxylase gene associated with Segawa's syndrome. *Human genetics*. 1995;95(1):123-5.
91. Fuchs T, Gavarini S, Saunders-Pullman R, Raymond D, Ehrlich ME, Bressman SB, et al. Mutations in the THAP1 gene are responsible for DYT6 primary torsion dystonia. *Nature genetics*. 2009;41(3).
92. Leube B, Hendgen T, Kessler K, Knapp M, Benecke R, Auburger G. Evidence for DYT7 being a common cause of cervical dystonia (torticollis) in Central Europe. *American journal of medical genetics*. 1997;74(5):529-32.

93. Rainier S, Thomas D, Tokarz D, Ming L, Bui M, Plein E, et al. Myofibrillogenesis regulator 1 gene mutations cause paroxysmal dystonic choreoathetosis. *Archives of Neurology*. 2004;61(7):1025-9.
94. Weber YG, Storch A, Wuttke TV, Brockmann K, Kempfle J, Maljevic S, et al. GLUT1 mutations are a cause of paroxysmal exertion-induced dyskinesias and induce hemolytic anemia by a cation leak. *The Journal of clinical investigation*. 2008;118(6):2157-68.
95. Weber Y, Kamm C, Suls A, Kempfle J, Kotschet K, Schüle R, et al. Paroxysmal choreoathetosis/spasticity (DYT9) is caused by a GLUT1 defect. *Neurology*. 2011;77(10):959-64.
96. Chen W-J, Lin Y, Xiong Z-Q, Wei W, Ni W, Tan G-H, et al. Exome sequencing identifies truncating mutations in PRRT2 that cause paroxysmal kinesigenic dyskinesia. *Nature genetics*. 2011;43(12):1252-5.
97. Zimprich A, Grabowski M, Asmus F, Naumann M, Berg D, Bertram M, et al. Mutations in the gene encoding ϵ -sarcoglycan cause myoclonus–dystonia syndrome. *Nature genetics*. 2001;29(1):66-9.
98. Kramer PL, Mineta M, Klein C, Schilling K, De Leon D, Farlow MR, et al. Rapid-onset dystonia–parkinsonism: linkage to chromosome 19q13. *Annals of neurology*. 1999;46(2):176-82.
99. de Carvalho Aguiar P, Sweadner KJ, Penniston JT, Zaremba J, Liu L, Caton M, et al. Mutations in the Na⁺/K⁺-ATPase α 3 gene ATP1A3 are associated with rapid-onset dystonia parkinsonism. *Neuron*. 2004;43(2):169-75.
100. Valente EM, Bentivoglio AR, Cassetta E, Dixon PH, Davis MB, Ferraris A, et al. DYT13, a novel primary torsion dystonia locus, maps to chromosome 1p36. 13–36.32 in an Italian family with cranial-cervical or upper limb onset. *Annals of neurology*. 2001;49(3):362-6.
101. Grimes D, Han F, Lang A, George-Hyssop PS, Racacho L, Bulman D. A novel locus for inherited myoclonus-dystonia on 18p11. *Neurology*. 2002;59(8):1183-6.
102. Camargos S, Scholz S, Simón-Sánchez J, Paisán-Ruiz C, Lewis P, Hernandez D, et al. DYT16, a novel young-onset dystonia-parkinsonism disorder: identification of a segregating mutation in the stress-response protein PRKRA. *The Lancet Neurology*. 2008;7(3):207-15.

References

103. Chouery E, Kfoury J, Delague V, Jalkh N, Bejjani P, Serre J, et al. A novel locus for autosomal recessive primary torsion dystonia (DYT17) maps to 20p11. 22–q13. 12. *Neurogenetics*. 2008;9(4):287-93.
104. Valente E, Spacey S, Wali G, Bhatia K, Dixon P, Wood N, et al. A second paroxysmal kinesigenic choreoathetosis locus (EKD2) mapping on 16q13-q22. 1 indicates a family of genes which give rise to paroxysmal disorders on human chromosome 16. *Brain*. 2000;123(10):2040-5.
105. Spacey S, Adams P, Lam P, Materek L, Stoessl A, Snutch T, et al. Genetic heterogeneity in paroxysmal nonkinesigenic dyskinesia. *Neurology*. 2006;66(10):1588-90.
106. Norgren N, Mattson E, Forsgren L, Holmberg M. A high-penetrance form of late-onset torsion dystonia maps to a novel locus (DYT21) on chromosome 2q14. 3-q21. 3. *Neurogenetics*. 2011;12(2):137-43.
107. Münchau A, Valente E, Davis M, Stinton V, Wood N, Quinn N, et al. A Yorkshire family with adult-onset cranio-cervical primary torsion dystonia. *Movement disorders*. 2000;15(5):954-9.
108. Holton J, Schneider S, Ganesharajah T, Gandhi S, Strand C, Shashidharan P, et al. Neuropathology of primary adult-onset dystonia. *Neurology*. 2008;70(9):695-9.
109. Paudel R, Kiely A, Li A, Lashley T, Bandopadhyay R, Hardy J, et al. Neuropathological features of genetically confirmed DYT1 dystonia: investigating disease-specific inclusions. *Acta neuropathologica communications*. 2014;2(1):1.
110. Kramer PL, De Leon D, Ozelius L, Risch N, Bressman SB, Brin MF, et al. Dystonia gene in Ashkenazi Jewish population is located on chromosome 9q32–34. *Annals of neurology*. 1990;27(2):114-20.
111. Kramer PL, Heiman GA, Gasser T, Ozelius LJ, de Leon D, Brin MF, et al. The DYT1 gene on 9q34 is responsible for most cases of early limb-onset idiopathic torsion dystonia in non-Jews. *American journal of human genetics*. 1994;55(3):468-75.
112. Bressman S. Genetics of dystonia. *Parkinson's Disease and Related Disorders*: Springer; 2006. p. 489-95.
113. Risch NJ, Bressman SB, Senthil G, Ozelius LJ. Intragenic Cis and Trans modification of genetic susceptibility in DYT1 torsion dystonia. *The American Journal of Human Genetics*. 2007;80(6):1188-93.

114. Kamm C, Fischer H, Garavaglia B, Kullmann S, Sharma M, Schrader C, et al. Susceptibility to DYT1 dystonia in European patients is modified by the D216H polymorphism. *Neurology*. 2008;70(23):2261-2.
115. Hewett J, Gonzalez-Agosti C, Slater D, Ziefer P, Li S, Bergeron D, et al. Mutant torsinA, responsible for early-onset torsion dystonia, forms membrane inclusions in cultured neural cells. *Human Molecular Genetics*. 2000;9(9):1403-13.
116. Hewett J, Ziefer P, Bergeron D, Naismith T, Boston H, Slater D, et al. TorsinA in PC12 cells: localization in the endoplasmic reticulum and response to stress. *Journal of neuroscience research*. 2003;72(2):158-68.
117. Kustedjo K, Bracey MH, Cravatt BF. Torsin A and its torsion dystonia-associated mutant forms are luminal glycoproteins that exhibit distinct subcellular localizations. *Journal of Biological Chemistry*. 2000;275(36):27933-9.
118. Kock N, Naismith TV, Boston HE, Ozelius LJ, Corey DP, Breakefield XO, et al. Effects of genetic variations in the dystonia protein torsinA: identification of polymorphism at residue 216 as protein modifier. *Human molecular genetics*. 2006;15(8):1355-64.
119. Vulinovic F, Lohmann K, Rakovic A, Capetian P, Alvarez-Fischer D, Schmidt A, et al. Unraveling cellular phenotypes of novel TorsinA/TOR1A mutations. *Human mutation*. 2014;35(9):1114-22.
120. Dobričić V, Kresojević N, Žarković M, Tomić A, Marjanović A, Westenberger A, et al. Phenotype of non-c. 907_909delGAG mutations in TOR1A: DYT1 dystonia revisited. *Parkinsonism & related disorders*. 2015;21(10):1256-9.
121. Zech M, Jochim A, Boesch S, Weber S, Meindl T, Peters A, et al. Systematic TOR1A non-c. 907_909delGAG variant analysis in isolated dystonia and controls. *Parkinsonism & Related Disorders*. 2016;31:119-23.
122. Cheng FB, Feng JC, Ma LY, Miao J, Ott T, Wan XH, et al. Combined occurrence of a novel TOR1A and a THAP1 mutation in primary dystonia. *Movement Disorders*. 2014;29(8):1079-83.
123. Calakos N, Patel VD, Gottron M, Wang G, Tran-Viet K-N, Brewington D, et al. Functional evidence implicating a novel TOR1A mutation in idiopathic, late-onset focal dystonia. *Journal of medical genetics*. 2009:jmg. 2009.072082.

124. LeDoux MS, Vemula SR, Xiao J, Thompson MM, Perlmutter JS, Wright LJ, et al. Clinical and genetic features of cervical dystonia in a large multicenter cohort. *Neurology Genetics*. 2016;2(3):e69.
125. Zirn B, Grundmann K, Huppke P, Puthenparampil J, Wolburg H, Riess O, et al. Novel TOR1A mutation p. Arg288Gln in early-onset dystonia (DYT1). *Journal of Neurology, Neurosurgery & Psychiatry*. 2008;79(12):1327-30.
126. Leung J, Klein C, Friedman J, Vieregge P, Jacobs H, Doheny D, et al. Novel mutation in the TOR1A (DYT1) gene in atypical, early onset dystonia and polymorphisms in dystonia and early onset parkinsonism. *Neurogenetics*. 2001;3(3):133-43.
127. Augood SJ, Martin DM, Ozelius LJ, Breakefield XO, Penney JB, Standaert DG. Distribution of the mRNAs encoding torsinA and torsinB in the normal adult human brain. *Annals of neurology*. 1999;46(5):761-9.
128. Augood SJ, Penney JB, Friberg IK, Breakefield XO, Young AB, Ozelius LJ, et al. Expression of the early-onset torsion dystonia gene (DYT1) in human brain. *Annals of neurology*. 1998;43(5):669-73.
129. Konakova M, Huynh DP, Yong W, Pulst SM. Cellular distribution of torsin A and torsin B in normal human brain. *Archives of Neurology*. 2001;58(6):921-7.
130. Siegert S, Bahn E, Kramer M, Schulz-Schaeffer W, Hewett J, Breakefield X, et al. TorsinA expression is detectable in human infants as young as 4 weeks old. *Developmental brain research*. 2005;157(1):19-26.
131. Vasudevan A, Breakefield XO, Bhide PG. Developmental patterns of torsinA and torsinB expression. *Brain research*. 2006;1073:139-45.
132. Schirmer EC, Glover JR, Singer MA, Lindquist S. HSP100/Clp proteins: a common mechanism explains diverse functions. *Trends in biochemical sciences*. 1996;21(8):289-96.
133. Muraro NI, Moffat KG. Down-regulation of torp4a, encoding the Drosophila homologue of torsinA, results in increased neuronal degeneration. *Journal of neurobiology*. 2006;66(12):1338-53.
134. Nery FC, Armata IA, Farley JE, Cho JA, Yaqub U, Chen P, et al. TorsinA participates in endoplasmic reticulum-associated degradation. *Nature communications*. 2011;2:393.

References

135. Gordon KL, Glenn KA, Gonzalez-Alegre P. Exploring the influence of torsinA expression on protein quality control. *Neurochemical research*. 2011;36(3):452-9.
136. Chen P, Burdette AJ, Porter JC, Ricketts JC, Fox SA, Nery FC, et al. The early-onset torsion dystonia-associated protein, torsinA, is a homeostatic regulator of endoplasmic reticulum stress response. *Human molecular genetics*. 2010;19(18):3502-15.
137. Konakova M, Pulst SM. Dystonia-associated forms of torsinA are deficient in ATPase activity. *Journal of molecular neuroscience*. 2005;25(1):105-17.
138. Kuner R, Teismann P, Trutzel A, Naim J, Richter A, Schmidt N, et al. TorsinA protects against oxidative stress in COS-1 and PC12 cells. *Neuroscience letters*. 2003;350(3):153-6.
139. Shashidharan P, Paris N, Sandu D, Karthikeyan L, McNaught KSP, Walker RH, et al. Overexpression of torsinA in PC12 cells protects against toxicity. *Journal of neurochemistry*. 2004;88(4):1019-25.
140. Goodchild RE, Dauer WT. The AAA+ protein torsinA interacts with a conserved domain present in LAP1 and a novel ER protein. *J Cell Biol*. 2005;168(6):855-62.
141. Torres GE, Sweeney AL, Beaulieu J-M, Shashidharan P, Caron MG. Effect of torsinA on membrane proteins reveals a loss of function and a dominant-negative phenotype of the dystonia-associated ΔE -torsinA mutant. *Proceedings of the National Academy of Sciences of the United States of America*. 2004;101(44):15650-5.
142. Gonzalez-Alegre P, Paulson HL. Aberrant cellular behavior of mutant torsinA implicates nuclear envelope dysfunction in DYT1 dystonia. *The Journal of neuroscience : the official journal of the Society for Neuroscience*. 2004;24(11):2593-601.
143. Naismith TV, Heuser JE, Breakefield XO, Hanson PI. TorsinA in the nuclear envelope. *Proceedings of the National Academy of Sciences of the United States of America*. 2004;101(20):7612-7.
144. Kamm C, Boston H, Hewett J, Wilbur J, Corey DP, Hanson PI, et al. The early onset dystonia protein torsinA interacts with kinesin light chain 1. *Journal of Biological Chemistry*. 2004;279(19):19882-92.

145. Ferrari-Toninelli G, Paccioretti S, Francisconi S, Uberti D, Memo M. TorsinA negatively controls neurite outgrowth of SH-SY5Y human neuronal cell line. *Brain research*. 2004;1012(1):75-81.
146. Hewett JW, Zeng J, Niland BP, Bragg DC, Breakefield XO. Dystonia-causing mutant torsinA inhibits cell adhesion and neurite extension through interference with cytoskeletal dynamics. *Neurobiology of disease*. 2006;22(1):98-111.
147. Augood SJ, Keller-McGandy CE, Siriani A, Hewett J, Ramesh V, Sapp E, et al. Distribution and ultrastructural localization of torsinA immunoreactivity in the human brain. *Brain research*. 2003;986(1):12-21.
148. Granata A, Schiavo G, Warner TT. TorsinA and dystonia: from nuclear envelope to synapse. *Journal of neurochemistry*. 2009;109(6):1596-609.
149. Hewett JW, Tannous B, Niland BP, Nery FC, Zeng J, Li Y, et al. Mutant torsinA interferes with protein processing through the secretory pathway in DYT1 dystonia cells. *Proceedings of the National Academy of Sciences*. 2007;104(17):7271-6.
150. Misbahuddin A, Placzek MR, Taanman JW, Gschmeissner S, Schiavo G, Cooper JM, et al. Mutant torsinA, which causes early-onset primary torsion dystonia, is redistributed to membranous structures enriched in vesicular monoamine transporter in cultured human SH-SY5Y cells. *Movement disorders*. 2005;20(4):432-40.
151. Granata A, Koo SJ, Haucke V, Schiavo G, Warner TT. CSN complex controls the stability of selected synaptic proteins via a torsinA-dependent process. *The EMBO journal*. 2011;30(1):181-93.
152. Granata A, Watson R, Collinson LM, Schiavo G, Warner TT. The dystonia-associated protein torsinA modulates synaptic vesicle recycling. *Journal of Biological Chemistry*. 2008;283(12):7568-79.
153. Südhof TC. A molecular machine for neurotransmitter release: synaptotagmin and beyond. *Nature medicine*. 2013;19(10):1227-31.
154. Xu J, Pang ZP, Shin O-H, Südhof TC. Synaptotagmin-1 functions as a Ca²⁺ sensor for spontaneous release. *Nature neuroscience*. 2009;12(6):759-66.
155. Baker K, Gordon SL, Grozeva D, van Kogelenberg M, Roberts NY, Pike M, et al. Identification of a human synaptotagmin-1 mutation that perturbs synaptic vesicle cycling. *The Journal of clinical investigation*. 2015;125(4):1670.

References

156. Müller U, Kupke KG. The genetics of primary torsion dystonia. *Human genetics*. 1990;84(2):107-15.
157. Gimenez-Roldan S, Delgado G, Marin M, Villanueva J, Mateo D. Hereditary torsion dystonia in gypsies. *Advances in neurology*. 1988;50:73.
158. Carecchio M, Reale C, Invernizzi F, Monti V, Petrucci S, Ginevrino M, et al. DYT2 screening in early-onset isolated dystonia. *European Journal of Paediatric Neurology*. 2016.
159. Kobayashi M, Takamatsu K, Saitoh S, Miura M, Noguchi T. Molecular cloning of hippocalcin, a novel calcium-binding protein of the recoverin family exclusively expressed in hippocampus. *Biochemical and biophysical research communications*. 1992;189(1):511-7.
160. Takamatsu K, Kobayashi M, Saitoh S, Fujishiro M, Noguchi T. Molecular cloning of human hippocalcin cDNA and chromosomal mapping of its gene. *Biochemical and biophysical research communications*. 1994;200(1):606-11.
161. Masaki T, Sakai E, Furuta Y, Kobayashi M, Takamatsu K. Genomic structure and chromosomal mapping of the human and mouse hippocalcin genes. *Gene*. 1998;225(1):117-24.
162. Palmer CL, Lim W, Hastie PG, Toward M, Korolchuk VI, Burbidge SA, et al. Hippocalcin functions as a calcium sensor in hippocampal LTD. *Neuron*. 2005;47(4):487-94.
163. Tzingounis AV, Kobayashi M, Takamatsu K, Nicoll RA. Hippocalcin gates the calcium activation of the slow afterhyperpolarization in hippocampal pyramidal cells. *Neuron*. 2007;53(4):487-93.
164. Lee LV, Pascasio FM, Fuentes FD, Viterbo GH. Torsion dystonia in Panay, Philippines. *Advances in neurology*. 1975;14:137-51.
165. Wilhelmsen KC, Weeks DE, Nygaard TG, Moskowitz CB, Rosales RL, Dela Paz DC, et al. Genetic mapping of "Lubag"(X-linked dystonia-parkinsonism) in a filipino kindred to the pericentromeric region of the X chromosome. *Annals of neurology*. 1991;29(2):124-31.
166. Johnston A, McKusick V. Sex-linked recessive inheritance in spastic paraplegia and parkinsonism.[Abstract]. *Proc Sec Int Cong Hum Genet*. 1963;3:1652-4.

167. Fahn S, Moskowitz C, editors. X-linked recessive dystonia and parkinsonism in Filipino males. *Annals Of Neurology*; 1988: LITTLE BROWN CO 34 BEACON STREET, BOSTON, MA 02108-1493.
168. Evidente VGH, Nolte D, Niemann S, Advincula J, Mayo MC, Natividad FF, et al. Phenotypic and molecular analyses of X-linked dystonia-parkinsonism (“lubag”) in women. *Archives of neurology*. 2004;61(12):1956-9.
169. Lee LV, Maranon E, Demaisip C, Peralta O, Borres-Icasiano R, Arancillo J, et al. The natural history of sex-linked recessive dystonia parkinsonism of Panay, Philippines (XDP). *Parkinsonism & related disorders*. 2002;9(1):29-38.
170. Evidente VGH, Gwinn-Hardy K, Hardy J, Hernandez D, Singleton A. X-linked dystonia (“Lubag”) presenting predominantly with parkinsonism: A more benign phenotype? *Movement disorders*. 2002;17(1):200-2.
171. Domingo A, Lee LV, Brüggemann N, Freimann K, Kaiser FJ, Jamora RD, et al. Woman with x-linked recessive dystonia-parkinsonism: clue to the epidemiology of parkinsonism in Filipino women? *JAMA neurology*. 2014;71(9):1177-80.
172. Evidente VGH, Advincula J, Esteban R, Pasco P, Alfon JA, Natividad FF, et al. Phenomenology of “Lubag” or X-linked dystonia–parkinsonism. *Movement disorders*. 2002;17(6):1271-7.
173. Waters C, Takahashi H, Wilhelmsen KC, Shubin R, Snow B, Nygaard T, et al. Phenotypic expression of X-linked dystonia-parkinsonism (lubag) in two women. *Neurology*. 1993;43(8):1555-.
174. Pasco PMD, Ison CV, Muñoz EL, Magpusao NS, Cheng AE, Tan KT, et al. Understanding XDP through imaging, pathology, and genetics. *International Journal of Neuroscience*. 2011;121(sup1):12-7.
175. Evidente V, Dickson D, Singleton A, Natividad F, Hardy J, Hernandez D, editors. Novel neuropathological findings in Lubag or X-linked dystonia-parkinsonism. *Movement Disorders*; 2002: WILEY-LISS DIV JOHN WILEY & SONS INC, 605 THIRD AVE, NEW YORK, NY 10158-0012 USA.
176. Goto S, Lee LV, Munoz EL, Tooyama I, Tamiya G, Makino S, et al. Functional anatomy of the basal ganglia in X-linked recessive dystonia-parkinsonism. *Annals of neurology*. 2005;58(1):7-17.

177. Goto S, Kawarai T, Morigaki R, Okita S, Koizumi H, Nagahiro S, et al. Defects in the striatal neuropeptide Y system in X-linked dystonia-parkinsonism. *Brain*. 2013;136(5):1555-67.
178. Kupke KG, Lee LV, Viterbo GH, Arancillo J, Donlon T, Müller U. X-linked recessive torsion dystonia in the Philippines. *American journal of medical genetics*. 1990;36(2):237-42.
179. Tamiya G, Makino S, Kaji R. TAF1 as the most plausible disease gene for XDP/DYT3. *The American Journal of Human Genetics*. 2007;81(2):417-8.
180. Nolte D, Niemann S, Müller U. Specific sequence changes in multiple transcript system DYT3 are associated with X-linked dystonia parkinsonism. *Proceedings of the National Academy of Sciences*. 2003;100(18):10347-52.
181. Herzfeld T, Nolte D, Müller U. Structural and functional analysis of the human TAF1/DYT3 multiple transcript system. *Mammalian Genome*. 2007;18(11):787-95.
182. Wassarman DA, Sauer F. TAFII250. *Journal of cell science*. 2001;114(16):2895-902.
183. Hisatake K, Roeder RG, Horikoshi M. Functional dissection of TFIIB domains required for TFIIB–TFIID–promoter complex formation and basal transcription activity. 1993.
184. Ruppert S, Wang EH, Tjian R. Cloning and expression of human TAFII250: a TBP-associated factor implicated in cell-cycle regulation. 1993.
185. Buchmann AM, Skaar JR, DeCaprio JA. Activation of a DNA damage checkpoint response in a TAF1-defective cell line. *Molecular and cellular biology*. 2004;24(12):5332-9.
186. Kloet SL, Whiting JL, Gafken P, Ranish J, Wang EH. Phosphorylation-dependent regulation of cyclin D1 and cyclin A gene transcription by TFIID subunits TAF1 and TAF7. *Molecular and cellular biology*. 2012;32(16):3358-69.
187. Hilton TL, Wang EH. Transcription Factor IID Recruitment and Sp1 Activation DUAL FUNCTION OF TAF1 IN CYCLIN D1 TRANSCRIPTION. *Journal of Biological Chemistry*. 2003;278(15):12992-3002.
188. Herzfeld T, Nolte D, Grznarova M, Hofmann A, Schultze JL, Müller U. X-linked dystonia parkinsonism syndrome (XDP, lubag): disease-specific sequence change DSC3 in TAF1/DYT3 affects genes in vesicular transport and dopamine metabolism. *Human molecular genetics*. 2012:dds499.

189. Parker N. Hereditary whispering dysphonia. *Journal of Neurology, Neurosurgery & Psychiatry*. 1985;48(3):218-24.
190. Wilcox RA, Winkler S, Lohmann K, Klein C. Whispering dysphonia in an Australian family (DYT4): a clinical and genetic reappraisal. *Movement Disorders*. 2011;26(13):2404-8.
191. Vemula SR, Xiao J, Bastian RW, Momčilović D, Blitzer A, LeDoux MS. Pathogenic variants in TUBB4A are not found in primary dystonia. *Neurology*. 2014;82(14):1227-30.
192. Kancheva D, Chamova T, Guergueltcheva V, Mitev V, Azmanov DN, Kalaydjieva L, et al. Mosaic dominant TUBB4A mutation in an inbred family with complicated hereditary spastic paraplegia. *Movement Disorders*. 2015;30(6):854-8.
193. Leandro-García LJ, Leskelä S, Landa I, Montero-Conde C, López-Jiménez E, Letón R, et al. Tumoral and tissue-specific expression of the major human β -tubulin isoforms. *Cytoskeleton*. 2010;67(4):214-23.
194. Gerace L. TorsinA and torsion dystonia: unraveling the architecture of the nuclear envelope. *Proceedings of the National Academy of Sciences of the United States of America*. 2004;101(24):8839-40.
195. Segawa M, Hosaka A, Miyagawa F, Nomura Y, Imai H. Hereditary progressive dystonia with marked diurnal fluctuation. *Advances in neurology*. 1975;14:215-33.
196. Nygaard T. Dopa-responsive dystonia: delineation of the clinical syndrome and clues to pathogenesis. *Advances in neurology*. 1993;60:577-85.
197. Nygaard TG, Wilhelmsen KC, Risch NJ, Brown DL, Trugman JM, Gilliam TC, et al. Linkage mapping of dopa-responsive dystonia (DRD) to chromosome 14q. *Nature genetics*. 1993;5(4):386-91.
198. Nygaard TG, Trugman JM, de Yebenes JG, Fahn S. Dopa-responsive dystonia The spectrum of clinical manifestations in a large North American family. *Neurology*. 1990;40(1):66-.
199. Furukawa Y, Lang A, Trugman J, Bird T, Hunter A, Sadeh M, et al. Gender-related penetrance and de novo GTP-cyclohydrolase I gene mutations in dopa-responsive dystonia. *Neurology*. 1998;50(4):1015-20.
200. Steinberger D, Weber Y, Korinthenberg R, Deuschl G, Benecke R, Martiniuss J, et al. High penetrance and pronounced variation in expressivity of GCH1

- mutations in five families with Dopa-responsive dystonia. *Annals of neurology*. 1998;43(5):634-9.
201. Steinberger D, Topka H, Fischer D, Müller U. GCH1 mutation in a patient with adult-onset oromandibular dystonia. *Neurology*. 1999;52(4):877-.
202. Müller U, Steinberger D, Topka H. Mutations of GCH1 in Dopa-responsive dystonia. *Journal of neural transmission*. 2002;109(3):321-8.
203. Tassin J, Dürr A, Bonnet A-M, Gil R, Vidailhet M, Lücking CB, et al. Levodopa-responsive dystonia. *Brain*. 2000;123(6):1112-21.
204. Trender-Gerhard I, Sweeney MG, Schwingenschuh P, Mir P, Edwards MJ, Gerhard A, et al. Autosomal-dominant GTPCH1-deficient DRD: clinical characteristics and long-term outcome of 34 patients. *Journal of Neurology, Neurosurgery & Psychiatry*. 2009;80(8):839-45.
205. Van Hove J, Steyaert J, Matthijs G, Legius E, Theys P, Wevers R, et al. Expanded motor and psychiatric phenotype in autosomal dominant Segawa syndrome due to GTP cyclohydrolase deficiency. *Journal of Neurology, Neurosurgery & Psychiatry*. 2006;77(1):18-23.
206. Rajput A, Gibb W, Zhong X, Shannak K, Kish S, Chang L, et al. Dopa-responsive dystonia: pathological and biochemical observations in a case. *Annals of neurology*. 1994;35(4):396-402.
207. Grötzsch H, Pizzolato G-P, Ghika J, Schorderet D, Vingerhoets F, Landis T, et al. Neuropathology of a case of dopa-responsive dystonia associated with a new genetic locus, DYT14. *Neurology*. 2002;58(12):1839-42.
208. Furukawa Y, Nygaard T, Güttlich M, Rajput A, Pifl C, DiStefano L, et al. Striatal bipterin and tyrosine hydroxylase protein reduction in dopa-responsive dystonia. *Neurology*. 1999;53(5):1032-.
209. Segawa M, Nomura Y, Nishiyama N. Autosomal dominant guanosine triphosphate cyclohydrolase I deficiency (Segawa disease). *Annals of neurology*. 2003;54(S6):S32-S45.
210. Thöny B, Heizmann CW, Mattei M-G. Human GTP-cyclohydrolase I gene and sepiapterin reductase gene map to region 14q21–q22 and 2p14–p12, respectively, by in situ hybridization. *Genomics*. 1995;26(1):168-70.
211. Ichinose H, Ohye T, Matsuda Y, Hori T-a, Blau N, Burlina A, et al. Characterization of mouse and human GTP cyclohydrolase I genes Mutations in

- patients with GTP cyclohydrolase I deficiency. *Journal of Biological Chemistry*. 1995;270(17):10062-71.
212. Wider C, Melquist S, Hauf M, Solida A, Cobb S, Kachergus J, et al. Study of a Swiss dopa-responsive dystonia family with a deletion in GCH1 redefining DYT14 as DYT5. *Neurology*. 2008;70(16 Part 2):1377-83.
213. Ichinose H, Nagatsu T. Molecular genetics of hereditary dystonia—mutations in the GTP cyclohydrolase I gene. *Brain research bulletin*. 1997;43(1):35-8.
214. Hwu WL, Chiou YW, Lai SY, Lee YM. Dopa-responsive dystonia is induced by a dominant-negative mechanism. *Annals of neurology*. 2000;48(4):609-13.
215. Naiya T, Misra AK, Biswas A, Das SK, Ray K, Ray J. Occurrence of GCH1 gene mutations in a group of Indian dystonia patients. *Journal of Neural Transmission*. 2012;119(11):1343-50.
216. Lee J-H, Ki C-S, Kim D-S, Cho J-W, Park K-P, Kim S. Dopa-responsive dystonia with a novel initiation codon mutation in the GCH1 gene misdiagnosed as cerebral palsy. *Journal of Korean medical science*. 2011;26(9):1244-6.
217. Cao L, Zheng L, Tang WG, Xiao Q, Zhang T, Tang HD, et al. Four novel mutations in the GCH1 gene of Chinese patients with dopa-responsive dystonia. *Movement Disorders*. 2010;25(6):755-60.
218. Lewthwaite A, Lambert T, Rolfe E, Olgiati S, Quadri M, Simons E, et al. Novel GCH1 variant in Dopa-responsive dystonia and Parkinson's disease. *Parkinsonism & related disorders*. 2015;21(4):394-7.
219. de la Fuente-Fernández R. Mutations in GTP-cyclohydrolase I gene and vitiligo. *The Lancet*. 1997;350(9078):640.
220. Jarman PR, Bandmann O, Marsden C, Wood N. GTP cyclohydrolase I mutations in patients with dystonia responsive to anticholinergic drugs. *Journal of Neurology, Neurosurgery & Psychiatry*. 1997;63(3):304-8.
221. Steinberger D, Korinthenberg R, Topka H, Berghäuser M, Wedde R, Müller U, et al. Dopa-responsive dystonia: mutation analysis of GCH1 and analysis of therapeutic doses of L-dopa. *Neurology*. 2000;55(11):1735-8.
222. Hagenah J, Saunders-Pullman R, Hedrich K, Kabakci K, Habermann K, Wiegers K, et al. High mutation rate in dopa-responsive dystonia: detection with comprehensive GCHI screening. *Neurology*. 2005;64(5):908-11.

223. Scola RH, Carducci C, Amaral VG, Lorenzoni PJ, Teive HA, Giovannello T, et al. A novel missense mutation pattern of the GCH1 gene in dopa-responsive dystonia. *Arquivos de neuro-psiquiatria*. 2007;65(4B):1224-7.
224. Rengmark A, Pihlstrøm L, Linder J, Forsgren L, Toft M. Low frequency of GCH1 and TH mutations in Parkinson's disease. *Parkinsonism & related disorders*. 2016;29:109-11.
225. Bandmann O, Valente E, Holmans P, Surtees R, Walters J, Wevers R, et al. Dopa-responsive dystonia: a clinical and molecular genetic study. *Annals of neurology*. 1998;44(4):649-56.
226. Opladen T, Hoffmann G, Hörster F, Hinz AB, Neidhardt K, Klein C, et al. Clinical and biochemical characterization of patients with early infantile onset of autosomal recessive GTP cyclohydrolase I deficiency without hyperphenylalaninemia. *Movement Disorders*. 2011;26(1):157-61.
227. Brüggemann N, Spiegler J, Hellenbroich Y, Opladen T, Schneider SA, Stephani U, et al. Beneficial prenatal levodopa therapy in autosomal recessive guanosine triphosphate cyclohydrolase 1 deficiency. *Archives of neurology*. 2012;69(8):1071-5.
228. Ichinose H, Ohye T, Segawa M, Nomura Y, Endo K, Tanaka H, et al. GTP cyclohydrolase I gene in hereditary progressive dystonia with marked diurnal fluctuation. *Neuroscience letters*. 1995;196(1):5-8.
229. Wu-Chou YH, Yeh TH, Wang CY, Lin JJ, Huang CC, Chang HC, et al. High frequency of multiexonic deletion of the GCH1 gene in a Taiwanese cohort of dopa-response dystonia. *American Journal of Medical Genetics Part B: Neuropsychiatric Genetics*. 2010;153(4):903-8.
230. Klein C, Hedrich K, Kabakci K, Mohrmann K, Wiegers K, Landt O, et al. Exon deletions in the GCHI gene in two of four Turkish families with dopa-responsive dystonia. *Neurology*. 2002;59(11):1783-6.
231. Markova ED, Slominsky PA, Illarioshkin SN, Miklina NI, Popova SN, Limborska SA, et al. A novel mutation in the GTP cyclohydrolase I gene associated with a broad range of clinical presentations in a family with autosomal dominant dopa-responsive dystonia. *European journal of neurology*. 1999;6(5):605-8.

232. Markova E, Slominskiĭ P, Illarioshkin S, Miklina N, Shadrina M, Popova S, et al. Molecular-genetic analysis of torsion dystonia in Russia. *Genetika*. 2000;36(7):952-8.
233. Yu L, Zhou H, Hu F, Xu Y. Two novel mutations of the GTP cyclohydrolase 1 gene and genotype–phenotype correlation in Chinese Dopa-responsive dystonia patients. *European Journal of Human Genetics*. 2013;21(7):731-5.
234. Lee J-Y, Yang HJ, Kim J-M, Jeon BS. Novel GCH-1 mutations and unusual long-lasting dyskinesias in Korean families with dopa-responsive dystonia. *Parkinsonism & related disorders*. 2013;19(12):1156-9.
235. Illarioshkin SN, Markova ED, Slominsky PA, Miklina NI, Popova SN, Limborska SA, et al. The GTP cyclohydrolase I gene in Russian families with dopa-responsive dystonia. *Archives of neurology*. 1998;55(6):789-92.
236. Nishiyama N, Yukishita S, Hagiwara H, Kakimoto S, Nomura Y, Segawa M. Gene mutation in hereditary progressive dystonia with marked diurnal fluctuation (HPD), strictly defined dopa-responsive dystonia. *Brain and Development*. 2000;22:102-6.
237. Ohta E, Funayama M, Ichinose H, Toyoshima I, Urano F, Matsuo M, et al. Novel mutations in the guanosine triphosphate cyclohydrolase 1 gene associated with DYT5 dystonia. *Archives of neurology*. 2006;63(11):1605-10.
238. Zirn B, Steinberger D, Troidl C, Brockmann K, von der Hagen M, Feiner C, et al. Frequency of GCH1 deletions in Dopa-responsive dystonia. *Journal of Neurology, Neurosurgery & Psychiatry*. 2008;79(2):183-6.
239. Furukawa Y, Kish SJ, Bebin EM, Jacobson RD, Fryburg JS, Wilson WG, et al. Dystonia with motor delay in compound heterozygotes for GTP-cyclohydrolase I gene mutations. *Annals of neurology*. 1998;44(1):10-6.
240. Hirano M, Komure O, Ueno S. A novel missense mutant inactivates GTP cyclohydrolase I in dopa-responsive dystonia. *Neuroscience letters*. 1999;260(3):181-4.
241. Mencacci NE, Isaias IU, Reich MM, Ganos C, Plagnol V, Polke JM, et al. Parkinson's disease in GTP cyclohydrolase 1 mutation carriers. *Brain*. 2014:awu179.
242. Zhang W, Zhou Z, Li X, Huang Y, Li T, Lin Y, et al. Dopa-responsive dystonia in Chinese patients: Including a novel heterozygous mutation in the GCH1 gene with

- an intermediate phenotype and one case of prenatal diagnosis. *Neuroscience Letters*. 2017.
243. Cai C, Shi W, Zeng Z, Zhang M, Ling C, Chen L, et al. GTP cyclohydrolase I and tyrosine hydroxylase gene mutations in familial and sporadic dopa-responsive dystonia patients. *PloS one*. 2013;8(6):e65215.
244. Brique S, Destée A, Lambert J-C, Mouroux V, Delacourte A, Amouyel P, et al. A new GTP-cyclohydrolase I mutation in an unusual doparesponsive dystonia, familial form. *Neuroreport*. 1999;10(3):487-91.
245. Hu FY, Xu YM, Yu LH, Ma MY, He XH, Zhou D. A novel missense mutation in GTP cyclohydrolase I (GCH1) gene causes dopa-responsive dystonia in Chinese Han population. *European journal of neurology*. 2011;18(2):362-4.
246. Hirano M, Tamaru Y, Ito H, Matsumoto S, Imai T, Ueno S. Mutant GTP cyclohydrolase I mRNA levels contribute to dopa-responsive dystonia onset. *Annals of neurology*. 1996;40(5):796-8.
247. Tamaru Y, Hirano M, Ito H, Kawamura J, Matsumoto S, Imai T, et al. Clinical similarities of hereditary progressive/dopa responsive dystonia caused by different types of mutations in the GTP cyclohydrolase I gene. *Journal of Neurology, Neurosurgery & Psychiatry*. 1998;64(4):469-73.
248. Beyer K, Lao-Villadoniga J, Vecino-Bilbao B, Cacabelos R, De la Fuente-Fernandez R. A novel point mutation in the GTP cyclohydrolase I gene in a Spanish family with hereditary progressive and dopa responsive dystonia. *Journal of Neurology, Neurosurgery & Psychiatry*. 1997;62(4):420.
249. Ikeda T, Kanmura K, Kodama Y, Sawada K, Nuno H, Hasegawa K. Segawa disease with a novel heterozygous mutation in exon 5 of the GCH-1 gene (E183K). *Brain and Development*. 2009;31(2):173-5.
250. Furukawa Y, Guttman M, Sparagana SP, Trugman JM, Hyland K, Wyatt P, et al. Dopa-responsive dystonia due to a large deletion in the GTP cyclohydrolase I gene. *Annals of neurology*. 2000;47(4):517-20.
251. Hirano M, Imaiso Y, Ueno S. Differential splicing of the GTP cyclohydrolase I RNA in dopa-responsive dystonia. *Biochemical and biophysical research communications*. 1997;234(2):316-9.

References

252. Imaiso Y, Taniwaki T, Yamada T, Yoshimura T, Hirano M, Ueno S, et al. A novel mutation of the GTP-cyclohydrolase I gene in a patient with hereditary progressive dystonidopa-responsive dystonia. *Neurology*. 1998;50(2):517-9.
253. Liu X, Zhang SS, Fang DF, Ma MY, Guo XY, Yang Y, et al. GCH1 mutation and clinical study of Chinese patients with dopa-responsive dystonia. *Movement Disorders*. 2010;25(4):447-51.
254. Nardocci N, Zorzi G, Blau N, Alvarez EF, Sesta M, Angelini L, et al. Neonatal dopa-responsive extrapyramidal syndrome in twins with recessive GTPCH deficiency. *Neurology*. 2003;60(2):335-7.
255. Garavaglia B, Invernizzi F, Carbone MLA, Viscardi V, Saracino F, Ghezzi D, et al. GTP-cyclohydrolase I gene mutations in patients with autosomal dominant and recessive GTP-CH1 deficiency: identification and functional characterization of four novel mutations. *Journal of inherited metabolic disease*. 2004;27(4):455-63.
256. Hjermind L, Johannsen L, Wevers R, Blau N, Friberg L, Regeur L, editors. A patient with dopa-responsive dystonia and juvenile Parkinson's disease. *MOVEMENT DISORDERS*; 2004: WILEY-LISS DIV JOHN WILEY & SONS INC, 111 RIVER ST, HOBOKEN, NJ 07030 USA.
257. Kim J-I, Choi JK, Lee J-W, Kim J, Ki C-S, Hong JY. A novel missense mutation in GCH1 gene in a Korean family with Segawa disease. *Brain and Development*. 2015;37(3):359-61.
258. Camargos ST, Cardoso F, Momeni P, Gurgel Gianetti J, Lees A, Hardy J, et al. Novel GCH1 mutation in a Brazilian family with dopa-responsive dystonia. *Movement Disorders*. 2008;23(2):299-302.
259. De Rosa A, Carducci C, Antonozzi I, Giovanniello T, Xhoxhi E, Criscuolo C, et al. A novel mutation in GCH-1 gene in a case of dopa-responsive dystonia. *Journal of neurology*. 2007;254(8):1133-4.
260. Bezin L, Nygaard T, Neville J, Shen H, Levine R. Reduced lymphoblast neopterin detects GTP cyclohydrolase dysfunction in dopa-responsive dystonia. *Neurology*. 1998;50(4):1021-7.
261. Leuzzi V, Carducci C, Carducci C, Cardona F, Artiola C, Antonozzi I. Autosomal dominant GTP-CH deficiency presenting as a dopa-responsive myoclonus-dystonia syndrome. *Neurology*. 2002;59(8):1241-3.

262. Sato H, Uematsu M, Endo W, Nakayama T, Kobayashi T, Hino-Fukuyo N, et al. Early replacement therapy in a first Japanese case with autosomal recessive guanosine triphosphate cyclohydrolase I deficiency with a novel point mutation. *Brain and Development*. 2014;36(3):268-71.
263. Hong K-M, Kim Y-S, Paik M-K. A novel nonsense mutation of the GTP cyclohydrolase I gene in a family with dopa-responsive dystonia. *Human heredity*. 2001;52(1):59-60.
264. Bernal-Pacheco O, Oyama G, Briton A, Singleton AB, Fernandez HH, Rodriguez RL, et al. A novel DYT-5 mutation with phenotypic variability within a Colombian family. *Tremor and Other Hyperkinetic Movements*. 2013.
265. Nitschke M, Steinberger D, Heberlein I, Otto V, Müller U, Vieregge P. Dopa responsive dystonia with Turner's syndrome: clinical, genetic, and neuropsychological studies in a family with a new mutation in the GTP-cyclohydrolase I gene. *Journal of Neurology, Neurosurgery & Psychiatry*. 1998;64(6):806-8.
266. Furukawa Y, Shimadzu M, Rajput AH, Shimuzu Y, Tagawa T, Mori H, et al. GTP-cyclohydrolase I gene mutations in hereditary progressive and dopa-responsive dystonia. *Annals of neurology*. 1996;39(5):609-17.
267. Hoenicka J, Vidal L, Godoy M, Ochoa J, Garcia de Yébenes J. New nonsense mutation in the GTP-cyclohydrolase I gene in L-DOPA responsive dystonia-parkinsonism. *Movement disorders*. 2001;16(2):364-6.
268. López-Laso E, Camino R, Mateos ME, Pérez-Navero JL, Ochoa JJ, Lao-Villadóniga JI, et al. Dopa-responsive infantile hypokinetic rigid syndrome due to dominant guanosine triphosphate cyclohydrolase 1 deficiency. *Journal of the neurological sciences*. 2007;256(1):90-3.
269. López-Laso E, Ochoa-Sepúlveda JJ, Ochoa-Amor JJ, Bescansa-Heredero E, Camino-León R, Gascón-Jiménez FJ, et al. Segawa syndrome due to mutation Q89X in the GCH1 gene: a possible founder effect in Córdoba (southern Spain). *Journal of neurology*. 2009;256(11):1816-24.
270. Teva GM, Esteban CV, Picó AN, Jover CJ, editors. GTP cyclohydrolase 1-deficient dopa-responsive hereditary dystonia. *Anales de pediatría (Barcelona, Spain: 2003)*; 2011.

References

271. Sasaki R, Naito Y, Kuzuhara S. A novel de novo point mutation in the GTP cyclohydrolase I gene in a Japanese patient with hereditary progressive and dopa responsive dystonia. *Journal of Neurology, Neurosurgery & Psychiatry*. 1998;65(6):947-.
272. Jeon BS, Jeong JM, Park SS, Kim JM, Chang YS, Song HC, et al. Dopamine transporter density measured by [¹²³I] β-CIT single-photon emission computed tomography is normal in dopa-responsive dystonia. *Annals of neurology*. 1998;43(6):792-800.
273. Von Mering M, Gabriel H, Opladen T, Hoffmann G, Storch A. A novel mutation (c. 64_65delGGinsAACC [p. G21fsX66]) in the GTP cyclohydrolase 1 gene that causes Segawa disease. *Journal of Neurology, Neurosurgery & Psychiatry*. 2008;79(2):229-.
274. Tsao C-Y. Guanine Triphosphate–Cyclohydrolase 1–Deficient Dopa-Responsive Dystonia Presenting as Frequent Falling in 2 Children. *Journal of child neurology*. 2012;27(3):389-91.
275. Bardien S, Keyser R, Lombard D, Du Plessis M, Human H, Carr J. Novel non-sense GCH1 mutation in a South African family diagnosed with dopa-responsive dystonia. *European journal of neurology*. 2010;17(3):510-2.
276. Hirano M, Tamaru Y, Nagai Y, Ito H, Imai T, Ueno S. Exon skipping caused by a base substitution at a splice site in the GTP cyclohydrolase I gene in a Japanese family with hereditary progressive dystonia/dopa-responsive dystonia. *Biochemical and biophysical research communications*. 1995;213(2):645-51.
277. Uncini A, De Angelis MV, Di Fulvio P, Ragno M, Annesi G, Filla A, et al. Wide expressivity variation and high but no gender-related penetrance in two dopa-responsive dystonia families with a novel GCH-I mutation. *Movement disorders*. 2004;19(10):1139-45.
278. Tachi N, Takahashi S, Jo M, Shinoda M. A new mutation of GCH1 in triplets family with dopa-responsive dystonia. *European journal of neurology*. 2011;18(9):1191-3.
279. Weber Y, Steinberger D, Deuschl G, Benecke R, Müller U. Two previously unrecognized splicing mutations of GCH1 in Dopa-responsive dystonia: exon skipping and one base insertion. *Neurogenetics*. 1997;1(2):125-7.

280. Potulska-Chromik A, Hoffman-Zacharska D, Łukawska M, Kostera-Pruszczyk A. Dopa-responsive dystonia or early-onset Parkinson disease—Genotype–phenotype correlation. *Neurologia i Neurochirurgia Polska*. 2016.
281. Irie S, Kanazawa N, Ryoh M, Mochizuki H, Nomura Y, Segawa M. A case of parkinsonism and dopa-induced severe dyskinesia associated with novel mutation in the GTP cyclohydrolase I gene. *Parkinsonism & related disorders*. 2011;17(10):769-70.
282. Clot F, Grabli D, Cazeneuve C, Roze E, Castelnau P, Chabrol B, et al. Exhaustive analysis of BH4 and dopamine biosynthesis genes in patients with Dopa-responsive dystonia. *Brain*. 2009;132(7):1753-63.
283. Hirano M, Yanagihara T, Ueno S. Dominant negative effect of GTP cyclohydrolase I mutations in dopa-responsive hereditary progressive dystonia. *Annals of neurology*. 1998;44(3):365-71.
284. Segawa M. Hereditary progressive dystonia with marked diurnal fluctuation. *Brain and Development*. 2011;33(3):195-201.
285. Steinberger D, Trübenbach J, Zirn B, Leube B, Wildhardt G, Müller U. Utility of MLPA in deletion analysis of GCH1 in dopa-responsive dystonia. *Neurogenetics*. 2007;8(1):51-5.
286. Ceravolo R, Nicoletti V, Garavaglia B, Reale C, Kiferle L, Bonuccelli U. Expanding the clinical phenotype of DYT5 mutations: is multiple system atrophy a possible one? *Neurology*. 2013;81(3):301-2.
287. Theuns J, Crosiers D, Debaene L, Nuytemans K, Meeus B, Sleegers K, et al. Guanosine triphosphate cyclohydrolase 1 promoter deletion causes dopa-responsive dystonia. *Movement Disorders*. 2012;27(11):1451-6.
288. Potulska-Chromik A, Hoffman-Zacharska D, Łukawska M, Kostera-Pruszczyk A. Dopa-responsive dystonia or early-onset Parkinson disease—Genotype–phenotype correlation. *Neurologia i Neurochirurgia Polska*. 2017;51(1):1-6.
289. Nagatsu T. Biopterin cofactor and monoamine-synthesizing monooxygenases. *Neurochemistry international*. 1983;5(1):27-38.
290. Thöny B, Blau N. Mutations in the BH4-metabolizing genes GTP cyclohydrolase I, 6-pyruvoyl-tetrahydropterin synthase, sepiapterin reductase, carbinolamine-4a-dehydratase, and dihydropteridine reductase. *Human mutation*. 2006;27(9):870-8.

References

291. Harada T, Kagamiyama H, Hatakeyama K. Feedback regulation mechanisms for the control of GTP cyclohydrolase I activity. *SCIENCE-NEW YORK THEN WASHINGTON*. 1993;260:1507-.
292. Kapatos G, Hirayama K, Shimoji M, Milstien S. GTP cyclohydrolase I feedback regulatory protein is expressed in serotonin neurons and regulates tetrahydrobiopterin biosynthesis. *Journal of neurochemistry*. 1999;72(2):669-75.
293. Hirayama K, Kapatos G. Nigrostriatal dopamine neurons express low levels of GTP cyclohydrolase I protein. *Journal of neurochemistry*. 1998;70(1):164-70.
294. Schiller A, Wevers R, Steenbergen G, Blau N, Jung H. Long-term course of L-dopa-responsive dystonia caused by tyrosine hydroxylase deficiency. *Neurology*. 2004;63(8):1524-6.
295. Swaans R, Rondot P, Renier W, HEUVEL L, STEENBERGEN-SPANJERS G, Wevers R. Four novel mutations in the tyrosine hydroxylase gene in patients with infantile parkinsonism. *Annals of human genetics*. 2000;64(1):25-31.
296. Craig S, Buckle V, Lamouroux A, Mallet J, Craig I. Localization of the human tyrosine hydroxylase gene to 11p15: gene duplication and evolution of metabolic pathways. *Cytogenetic and Genome Research*. 1986;42(1-2):29-32.
297. Kobayashi K, Kaneda N, Ichinose H, Kishi F, Nakazawa A, Kurosawa Y, et al. Structure of the human tyrosine hydroxylase gene: alternative splicing from a single gene accounts for generation of four mRNA types. *Journal of biochemistry*. 1988;103(6):907-12.
298. Toshiharu N, Hiroshi I. Comparative studies on the structure of human tyrosine hydroxylase with those of the enzyme of various mammals. *Comparative Biochemistry and Physiology Part C: Comparative Pharmacology*. 1991;98(1):203-10.
299. Grima B, Lamouroux A, Boni C, Julien J-F, Javoy-Agid F, Mallet J. A single human gene encoding multiple tyrosine hydroxylases with different predicted functional characteristics. *Nature*. 1987;326(6114):707-11.
300. Vrana KE, Walker SJ, Rucker P, Liu X. A carboxyl terminal leucine zipper is required for tyrosine hydroxylase tetramer formation. *J Neurochem*. 1994;63(6):2014-20.

301. Ramsey AJ, Daubner SC, Ehrlich JI, Fitzpatrick PF. Identification of iron ligands in tyrosine hydroxylase by mutagenesis of conserved histidiny residues. *Protein science : a publication of the Protein Society*. 1995;4(10):2082-6.
302. Daubner SC, Le T, Wang S. Tyrosine hydroxylase and regulation of dopamine synthesis. *Archives of biochemistry and biophysics*. 2011;508(1):1-12.
303. Chen R, Wei J, Fowler SC, Wu JY. Demonstration of functional coupling between dopamine synthesis and its packaging into synaptic vesicles. *Journal of biomedical science*. 2003;10(6 Pt 2):774-81.
304. Ribasés M, Serrano M, Fernández-Alvarez E, Pahisa S, Ormazabal A, García-Cazorla À, et al. A homozygous tyrosine hydroxylase gene promoter mutation in a patient with dopa-responsive encephalopathy: clinical, biochemical and genetic analysis. *Molecular genetics and metabolism*. 2007;92(3):274-7.
305. Wevers R, de Rijk-Van Andel J, Bräutigam C, Geurtz B, van den Heuvel LP, Steenbergen-Spanjers GC, et al. A review of biochemical and molecular genetic aspects of tyrosine hydroxylase deficiency including a novel mutation (291delC). *Journal of inherited metabolic disease*. 1999;22(4):364-73.
306. de Rijk–Van Andel J, Gabreels F, Geurtz B, Steenbergen–Spanjers G, van den Heuvel L, Smeitink J, et al. l-dopa–responsive infantile hypokinetic rigid parkinsonism due to tyrosine hydroxylase deficiency. *Neurology*. 2000;55(12):1926-8.
307. Hoffmann GF, Assmann B, Bräutigam C, Dionisi-Vici C, Häussler M, De Klerk JB, et al. Tyrosine hydroxylase deficiency causes progressive encephalopathy and dopa-nonresponsive dystonia. *Annals of neurology*. 2003;54(S6):S56-S65.
308. van den Heuvel LP, Luiten B, Smeitink JA, de Rijk-van Andel JF, Hyland K, Steenbergen-Spanjers GC, et al. A common point mutation in the tyrosine hydroxylase gene in autosomal recessive L-DOPA-responsive dystonia in the Dutch population. *Human genetics*. 1998;102(6):644-6.
309. Grattan-Smith PJ, Wevers RA, Steenbergen-Spanjers GC, Fung VS, Earl J, Wilcken B. Tyrosine hydroxylase deficiency: clinical manifestations of catecholamine insufficiency in infancy. *Movement disorders*. 2002;17(2):354-9.
310. Lüdecke B, Knappskog PM, Clayton PT, Surtees RA, Clelland JD, Heales SJ, et al. Recessively inherited L-DOPA-responsive parkinsonism in infancy caused by a

- point mutation (L205P) in the tyrosine hydroxylase gene. *Human molecular genetics*. 1996;5(7):1023-8.
311. Diepold K, Schütz B, Rostasy K, Wilken B, Hougaard P, Güttler F, et al. Levodopa-responsive infantile parkinsonism due to a novel mutation in the tyrosine hydroxylase gene and exacerbation by viral infections. *Movement disorders*. 2005;20(6):764-7.
312. Fossbakk A, Kleppe R, Knappskog PM, Martinez A, Haavik J. Functional Studies of Tyrosine Hydroxylase Missense Variants Reveal Distinct Patterns of Molecular Defects in Dopa-Responsive Dystonia. *Human mutation*. 2014;35(7):880-90.
313. Wu ZY, Lin Y, Chen WJ, Zhao GX, Xie H, Murong SX, et al. Molecular analyses of GCH-1, TH and parkin genes in Chinese dopa-responsive dystonia families. *Clinical genetics*. 2008;74(6):513-21.
314. Royo M, Daubner SC, Fitzpatrick PF. Effects of mutations in tyrosine hydroxylase associated with progressive dystonia on the activity and stability of the protein. *Proteins: Structure, Function, and Bioinformatics*. 2005;58(1):14-21.
315. Sun Z-f, Zhang Y-h, Guo J-f, Sun Q-y, Mei J-p, Zhou H-l, et al. Genetic diagnosis of two dopa-responsive dystonia families by exome sequencing. *PloS one*. 2014;9(9):e106388.
316. Stamelou M, Mencacci NE, Cordivari C, Batla A, Wood NW, Houlden H, et al. Myoclonus-dystonia syndrome due to tyrosine hydroxylase deficiency. *Neurology*. 2012;79(5):435-41.
317. Furukawa Y, Graf W, Wong H, Shimadzu M, Kish S. Dopa-responsive dystonia simulating spastic paraplegia due to tyrosine hydroxylase (TH) gene mutations. *Neurology*. 2001;56(2):260-3.
318. Bressman SB, Raymond D, Fuchs T, Heiman GA, Ozelius LJ, Saunders-Pullman R. Mutations in THAP1 (DYT6) in early-onset dystonia: a genetic screening study. *The Lancet Neurology*. 2009;8(5):441-6.
319. Djarmati A, Schneider SA, Lohmann K, Winkler S, Pawlack H, Hagenah J, et al. Mutations in THAP1 (DYT6) and generalised dystonia with prominent spasmodic dysphonia: a genetic screening study. *The Lancet Neurology*. 2009;8(5):447-52.

320. Almasy L, Bressman S, Raymond D, Kramer P, Greene P, Heiman G, et al. Idiopathic torsion dystonia linked to chromosome 8 in two Mennonite families. *Annals of neurology*. 1997;42(4):670-3.
321. Zhao Y, Xiao J, Gong S, Clara JA, LeDoux MS. Neural expression of the transcription factor THAP1 during development in rat. *Neuroscience*. 2013;231:282-95.
322. Ruiz M, Perez-Garcia G, Ortiz-Virumbrales M, Méneret A, Morant A, Kottwitz J, et al. Abnormalities of motor function, transcription and cerebellar structure in mouse models of THAP1 dystonia. *Human molecular genetics*. 2015;24(25):7159-70.
323. Cheng FB, Wan XH, Feng JC, Ma LY, Hou B, Feng F, et al. Subcellular distribution of THAP1 and alterations in the microstructure of brain white matter in DYT6 dystonia. *Parkinsonism & related disorders*. 2012;18(8):978-82.
324. Paudel R, Li A, Hardy J, Bhatia KP, Houlden H, Holton J. DYT6 dystonia: A neuropathological study. *Neurodegenerative Diseases*. 2016;16(3-4):273-8.
325. Xiomerisiou G, Houlden H, Scarmeas N, Stamelou M, Kara E, Hardy J, et al. THAP1 mutations and dystonia phenotypes: genotype phenotype correlations. *Movement Disorders*. 2012;27(10):1290-4.
326. LeDoux MS, Xiao J, Rudzińska M, Bastian RW, Wszolek ZK, Van Gerpen JA, et al. Genotype–phenotype correlations in THAP1 dystonia: Molecular foundations and description of new cases. *Parkinsonism & related disorders*. 2012;18(5):414-25.
327. Bessiere D, Lacroix C, Campagne S, Ecochard V, Guillet V, Mourey L, et al. Structure-function analysis of the THAP zinc finger of THAP1, a large C2CH DNA-binding module linked to Rb/E2F pathways. *Journal of Biological Chemistry*. 2008;283(7):4352-63.
328. Campagne S, Saurel O, Gervais V, Milon A. Structural determinants of specific DNA-recognition by the THAP zinc finger. *Nucleic acids research*. 2010;38(10):3466-76.
329. Sengel C, Gavarini S, Sharma N, Ozelius LJ, Bragg DC. Dimerization of the DYT6 dystonia protein, THAP1, requires residues within the coiled-coil domain. *Journal of neurochemistry*. 2011;118(6):1087-100.

330. Campagne S, Muller I, Milon A, Gervais V. Towards the classification of DYT6 dystonia mutants in the DNA-binding domain of THAP1. *Nucleic acids research*. 2012;40(19):9927-40.
331. Kaiser FJ, Osmanovic A, Rakovic A, Erogullari A, Uflacker N, Braunholz D, et al. The dystonia gene DYT1 is repressed by the transcription factor THAP1 (DYT6). *Annals of neurology*. 2010;68(4):554-9.
332. Gavarini S, Cayrol C, Fuchs T, Lyons N, Ehrlich ME, Girard JP, et al. Direct interaction between causative genes of DYT1 and DYT6 primary dystonia. *Annals of neurology*. 2010;68(4):549-53.
333. Lohmann K, Uflacker N, Erogullari A, Lohnau T, Winkler S, Dendorfer A, et al. Identification and functional analysis of novel THAP1 mutations. *European Journal of Human Genetics*. 2012;20(2):171-5.
334. Osmanovic A, Dendorfer A, Erogullari A, Uflacker N, Braunholz D, Rakovic A, et al. Truncating mutations in THAP1 define the nuclear localization signal. *Movement Disorders*. 2011;26(8):1565-7.
335. Vemula SR, Xiao J, Zhao Y, Bastian RW, Perlmutter JS, Racette BA, et al. A rare sequence variant in intron 1 of THAP1 is associated with primary dystonia. *Molecular Genetics & Genomic Medicine*. 2014;2(3):261-72.
336. Cayrol C, Lacroix C, Mathe C, Ecochard V, Ceribelli M, Loreau E, et al. The THAP-zinc finger protein THAP1 regulates endothelial cell proliferation through modulation of pRB/E2F cell-cycle target genes. *Blood*. 2007;109(2):584-94.
337. Mazars R, Gonzalez-de-Peredo A, Cayrol C, Lavigne A-C, Vogel JL, Ortega N, et al. The THAP-zinc finger protein THAP1 associates with coactivator HCF-1 and O-GlcNAc transferase a link between DYT6 and DYT3 dystonias. *Journal of Biological Chemistry*. 2010;285(18):13364-71.
338. De Carvalho Aguiar P, Fuchs T, Borges V, Lamar KM, Silva SMA, Ferraz HB, et al. Screening of Brazilian families with primary dystonia reveals a novel THAP1 mutation and a de novo TOR1A GAG deletion. *Movement Disorders*. 2010;25(16):2854-7.
339. da Silva-Junior FP, dos Santos CO, Silva SMCA, Barbosa ER, Borges V, Ferraz HB, et al. Novel THAP1 variants in Brazilian patients with idiopathic isolated dystonia. *Journal of the neurological sciences*. 2014;344(1):190-2.
340. Jurek M, Hoffman-Zacharska D, Koziowski D, Mądry J, Friedman A, Bal J. Intrafamilial variability of the primary dystonia DYT6 phenotype caused by p.

- Cys5Trp mutation in THAP1 gene. *Neurologia i neurochirurgia polska*. 2014;48(4):254-7.
341. Clot F, Grabli D, Burbaud P, Aya M, Derkinderen P, Defebvre L, et al. Screening of the THAP1 gene in patients with early-onset dystonia: myoclonic jerks are part of the dystonia 6 phenotype. *Neurogenetics*. 2011;12(1):87-9.
342. Houlden H, Schneider S, Paudel R, Melchers A, Schwingenschuh P, Edwards M, et al. THAP1 mutations (DYT6) are an additional cause of early-onset dystonia. *Neurology*. 2010;74(10):846-50.
343. Xiao J, Zhao Y, Bastian R, Perlmutter JS, Racette BA, Tabbal SD, et al. Novel THAP1 sequence variants in primary dystonia. *Neurology*. 2010;74(3):229-38.
344. Zittel S, Moll CK, Brüggemann N, Tadic V, Hamel W, Kasten M, et al. Clinical neuroimaging and electrophysiological assessment of three DYT6 dystonia families. *Movement Disorders*. 2010;25(14):2405-12.
345. Dobričić VS, Kresojević ND, Svetel MV, Janković MZ, Petrović IN, Tomić AD, et al. Mutation screening of the DYT6/THAP1 gene in Serbian patients with primary dystonia. *Journal of neurology*. 2013;260(4):1037-42.
346. Paisán-Ruiz C, Ruiz-Martinez J, Ruibal M, Mok KY, Indakoetxea B, Gorostidi A, et al. Identification of a novel THAP1 mutation at R29 amino-acid residue in sporadic patients with early-onset dystonia. *Movement Disorders*. 2009;24(16):2428-9.
347. Jech R, Bares M, Krepelova A, Urgosik D, Havrankova P, Ruzicka E. DYT 6-- a novel THAP1 mutation with excellent effect on pallidal DBS. *Movement disorders : official journal of the Movement Disorder Society*. 2011;26(5):924-5.
348. Miyamoto R, Koizumi H, Morino H, Kawarai T, Maruyama H, Mukai Y, et al. DYT6 in Japan—genetic screening and clinical characteristics of the patients. *Movement Disorders*. 2014;29(2):278-80.
349. Schneider SA, Ramirez A, Shafiee K, Kaiser FJ, Erogullari A, Brüggemann N, et al. Homozygous THAP1 mutations as cause of early-onset generalized dystonia. *Movement Disorders*. 2011;26(5):858-61.
350. Groen JL, Yildirim E, Ritz K, Baas F, van Hilten JJ, van der Meulen FW, et al. THAP1 mutations are infrequent in spasmodic dysphonia. *Movement Disorders*. 2011;26(10):1952.

351. Cheng FB, Ozelius LJ, Wan XH, Feng JC, Ma LY, Yang YM, et al. THAP1/DYT6 sequence variants in non-DYT1 early-onset primary dystonia in China and their effects on RNA expression. *Journal of neurology*. 2012;259(2):342-7.
352. Gajos A, Golańska E, Sieruta M, Szybka M, Liberski PP, Bogucki A. High variability of clinical symptoms in a Polish family with a novel THAP1 mutation. *International Journal of Neuroscience*. 2015;125(10):755-9.
353. Söhn AS, Glöckle N, Doetzer AD, Deuschl G, Felbor U, Topka HR, et al. Prevalence of THAP1 sequence variants in German patients with primary dystonia. *Movement Disorders*. 2010;25(12):1982-6.
354. Groen JL, Ritz K, Contarino MF, van de Warrenburg BP, Aramideh M, Foncke EM, et al. DYT6 dystonia: mutation screening, phenotype, and response to deep brain stimulation. *Movement disorders*. 2010;25(14):2420-7.
355. Cheng F, Wan X, Feng J, Wang L, Yang Y, Cui L. Clinical and genetic evaluation of DYT1 and DYT6 primary dystonia in China. *European Journal of Neurology*. 2011;18(3):497-503.
356. Giri S, Naiya T, Eqbal Z, Sankhla CS, Das SK, Ray K, et al. Genetic Screening of THAP1 in Primary Dystonia Patients of India. *Neuroscience Letters*. 2016.
357. Song W, Chen Y, Huang R, Chen K, Pan P, Yang Y, et al. Novel THAP1 gene mutations in patients with primary dystonia from Southwest China. *Journal of the neurological sciences*. 2011;309(1):63-7.
358. Bonetti M, Barzaghi C, Brancati F, Ferraris A, Bellacchio E, Giovanetti A, et al. Mutation screening of the DYT6/THAP1 gene in Italy. *Movement disorders*. 2009;24(16):2424-7.
359. Newman JR, Lehn AC, Boyle RS, Silburn PA, Mellick GD. Screening for rare sequence variants in the THAP1 gene in a primary dystonia cohort. *Movement Disorders*. 2013;28(12):1752-3.
360. Blanchard A, Roubertie A, Simonetta-Moreau M, Ea V, Coquart C, Frederic MY, et al. Singular DYT6 phenotypes in association with new THAP1 frameshift mutations. *Movement Disorders*. 2011;26(9):1775-6.
361. Miyamoto R, Ohta E, Kawarai T, Koizumi H, Sako W, Izumi Y, et al. Broad spectrum of dystonia associated with a novel thanatosis-associated protein

- domain-containing apoptosis-associated protein 1 mutation in a Japanese family with dystonia 6, torsion. *Movement Disorders*. 2012;27(10):1324-5.
362. Roussigne M, Cayrol C, Clouaire T, Amalric F, Girard J-P. THAP1 is a nuclear proapoptotic factor that links prostate-apoptosis-response-4 (Par-4) to PML nuclear bodies. *Oncogene*. 2003;22(16):2432-42.
363. Duan W, Zhang Z, Gash DM, Mattson MP. Participation of prostate apoptosis response-4 in degeneration of dopaminergic neurons in models of Parkinson's disease. *Annals of neurology*. 1999;46(4):587-97.
364. Guo Q, Fu W, Xie J, Luo H, Sells SF, Geddes J, et al. Par-4 is a mediator of neuronal degeneration associated with the pathogenesis of Alzheimer disease. *Nature medicine*. 1998;4(8):957-62.
365. Chen D-H, Matsushita M, Rainier S, Meaney B, Tisch L, Feleke A, et al. Presence of alanine-to-valine substitutions in myofibrillogenesis regulator 1 in paroxysmal nonkinesigenic dyskinesia: confirmation in 2 kindreds. *Archives of Neurology*. 2005;62(4):597-600.
366. Hempelmann A, Kumar S, Muralitharan S, Sander T. Myofibrillogenesis regulator 1 gene (MR-1) mutation in an Omani family with paroxysmal nonkinesigenic dyskinesia. *Neuroscience letters*. 2006;402(1):118-20.
367. Lee H-Y, Xu Y, Huang Y, Ahn AH, Auburger GW, Pandolfo M, et al. The gene for paroxysmal non-kinesigenic dyskinesia encodes an enzyme in a stress response pathway. *Human molecular genetics*. 2004;13(24):3161-70.
368. Stefanova E, Djarmati A, Momčilović D, Dragašević N, Svetel M, Klein C, et al. Clinical characteristics of paroxysmal nonkinesigenic dyskinesia in Serbian family with Myofibrillogenesis regulator 1 gene mutation. *Movement disorders*. 2006;21(11):2010-5.
369. Mount LA, Reback S. Familial paroxysmal choreoathetosis: preliminary report on a hitherto undescribed clinical syndrome. *Archives of Neurology & Psychiatry*. 1940;44(4):841-7.
370. Richards R, Barnett H. Paroxysmal dystonic choreoathetosis A family study and review of the literature. *Neurology*. 1968;18(5):461-.
371. Walker E. Familial paroxysmal dystonic choreoathetosis: a neurologic disorder simulating psychiatric illness. *The Johns Hopkins medical journal*. 1981;148(3):108-13.

372. Byrne E, White O, Cook M. Familial dystonic choreoathetosis with myokymia; a sleep responsive disorder. *Journal of Neurology, Neurosurgery & Psychiatry*. 1991;54(12):1090-2.
373. Demirkiran M, Jankovic J. Paroxysmal dyskinesias: clinical features and classification. *Annals of neurology*. 1995;38(4):571-9.
374. Bruno M, Lee H-Y, Auburger GW, Friedman A, Nielsen JE, Lang AE, et al. Genotype–phenotype correlation of paroxysmal nonkinesigenic dyskinesia. *Neurology*. 2007;68(21):1782-9.
375. Fink JK, Rainer S, Wilkowski J, Jones SM, Kume A, Hedera P, et al. Paroxysmal dystonic choreoathetosis: tight linkage to chromosome 2q. *American journal of human genetics*. 1996;59(1):140.
376. Fink JK, Hedera P, Mathay JG, Albin RL. Paroxysmal dystonic choreoathetosis linked to chromosome 2q: clinical analysis and proposed pathophysiology. *Neurology*. 1997;49(1):177-83.
377. Blakeley J, Jankovic J. Secondary paroxysmal dyskinesias. *Movement disorders*. 2002;17(4):726-34.
378. Djarmati A, Svetel M, Momčilović D, Kostić V, Klein C. Significance of recurrent mutations in the myofibrillogenesis regulator 1 gene. *Archives of neurology*. 2005;62(10):1641-.
379. Raskind WH, Bolin T, Wolff J, Fink J, Matsushita M, Litt M, et al. Further localization of a gene for paroxysmal dystonic choreoathetosis to a 5-cM region on chromosome 2q34. *Human genetics*. 1998;102(1):93-7.
380. Ghezzi D, Viscomi C, Ferlini A, Gualandi F, Mereghetti P, DeGrandis D, et al. Paroxysmal non-kinesigenic dyskinesia is caused by mutations of the MR-1 mitochondrial targeting sequence. *Human molecular genetics*. 2009;18(6):1058-64.
381. Mannervik B. Molecular enzymology of the glyoxalase system. *Drug metabolism and drug interactions*. 2008;23(1/2):13.
382. Vander Jagt DL. Glyoxalase II: molecular characteristics, kinetics and mechanism. *Biochemical Society Transactions*. 1993;21(2):522.
383. Shen Y, Lee H-Y, Rawson J, Ojha S, Babbitt P, Fu Y-H, et al. Mutations in PNKD causing paroxysmal dyskinesia alters protein cleavage and stability. *Human molecular genetics*. 2011;20(12):2322-32.

384. Ptacek L, Shen Y, Fu Y-H. Mutations in PNKD Causing Paroxysmal Dyskinesia Alters Protein Cleavage and Stability (IN10-1.005). *Neurology*. 2012;78(1 Supplement):IN10-1.005-IN10-1.
385. Auburger G, Ratzlaff T, Lunkes A, Nelles H, Leube B, Binkofski F, et al. A gene for autosomal dominant paroxysmal choreoathetosis/spasticity (CSE) maps to the vicinity of a potassium channel gene cluster on chromosome 1p, probably within 2 cM between D1S443 and D1S197. *Genomics*. 1996;31(1):90-4.
386. Margari L, Perniola T, Illiceto G, Ferrannini E, De Iaco M, Presicci A, et al. Familial paroxysmal exercise-induced dyskinesia and benign epilepsy: a clinical and neurophysiological study of an uncommon disorder. *Neurological Sciences*. 2000;21(3):165-72.
387. Münchau A, Valente E, Shahidi G, Eunson L, Hanna M, Quinn N, et al. A new family with paroxysmal exercise induced dystonia and migraine: a clinical and genetic study. *Journal of Neurology, Neurosurgery & Psychiatry*. 2000;68(5):609-14.
388. Suls A, Dedeken P, Goffin K, Van Esch H, Dupont P, Cassiman D, et al. Paroxysmal exercise-induced dyskinesia and epilepsy is due to mutations in SLC2A1, encoding the glucose transporter GLUT1. *Brain*. 2008;131(7):1831-44.
389. Roubergue A, Apartis E, Mesnage V, Doummar D, Trocetto J-M, Roze E, et al. Dystonic tremor caused by mutation of the glucose transporter gene GLUT1. *Journal of inherited metabolic disease*. 2011;34(2):483-8.
390. Schneider SA, Paisan-Ruiz C, Garcia-Gorostiaga I, Quinn NP, Weber YG, Lerche H, et al. GLUT1 gene mutations cause sporadic paroxysmal exercise-induced dyskinesias. *Movement Disorders*. 2009;24(11):1684-8.
391. Bovi T, Fasano A, Juergenson I, Gellera C, Castellotti B, Fontana E, et al. Paroxysmal exercise-induced dyskinesia with self-limiting partial epilepsy: a novel GLUT-1 mutation with benign phenotype. *Parkinsonism & related disorders*. 2011;17(6):479-81.
392. Afawi Z, Suls A, Ekstein D, Kivity S, Neufeld MY, Oliver K, et al. Mild adolescent/adult onset epilepsy and paroxysmal exercise-induced dyskinesia due to GLUT1 deficiency. *Epilepsia*. 2010;51(12):2466-9.
393. Brockmann K. The expanding phenotype of GLUT1-deficiency syndrome. *Brain and Development*. 2009;31(7):545-52.

394. Pascual JM, Wang D, Lecumberri B, Yang H, Mao X, Yang R, et al. GLUT1 deficiency and other glucose transporter diseases. *European journal of endocrinology*. 2004;150(5):627-33.
395. Agus DB, Gambhir SS, Pardridge WM, Spielholz C, Baselga J, Vera JC, et al. Vitamin C crosses the blood-brain barrier in the oxidized form through the glucose transporters. *Journal of Clinical Investigation*. 1997;100(11):2842.
396. Pellerin L. Brain energetics (thought needs food). *Current Opinion in Clinical Nutrition & Metabolic Care*. 2008;11(6):701-5.
397. Wang X, Michaelis EK. Selective neuronal vulnerability to oxidative stress in the brain. *Frontiers in aging neuroscience*. 2010;2:12.
398. Bruno MK, Hallett M, Gwinn-Hardy K, Sorensen B, Considine E, Tucker S, et al. Clinical evaluation of idiopathic paroxysmal kinesigenic dyskinesia: new diagnostic criteria. *Neurology*. 2004;63(12):2280-7.
399. Tomita H-a, Nagamitsu S, Wakui K, Fukushima Y, Yamada K, Sadamatsu M, et al. Paroxysmal kinesigenic choreoathetosis locus maps to chromosome 16p11. 2-q12. 1. *The American Journal of Human Genetics*. 1999;65(6):1688-97.
400. Lipton J, Rivkin MJ. 16p11. 2-related paroxysmal kinesigenic dyskinesia and dopa-responsive parkinsonism in a child. *Neurology*. 2009;73(6):479-80.
401. Liu XR, Wu M, He N, Meng H, Wen L, Wang JL, et al. Novel PRRT2 mutations in paroxysmal dyskinesia patients with variant inheritance and phenotypes. *Genes, brain, and behavior*. 2013;12(2):234-40.
402. Meneret A, Grabli D, Depienne C, Gaudebout C, Picard F, Durr A, et al. PRRT2 mutations: a major cause of paroxysmal kinesigenic dyskinesia in the European population. *Neurology*. 2012;79(2):170-4.
403. Cao L, Huang XJ, Zheng L, Xiao Q, Wang XJ, Chen SD. Identification of a novel PRRT2 mutation in patients with paroxysmal kinesigenic dyskinesias and c.649dupC as a mutation hot-spot. *Parkinsonism & related disorders*. 2012;18(5):704-6.
404. Becker F, Schubert J, Striano P, Anttonen AK, Liukkonen E, Gaily E, et al. PRRT2-related disorders: further PKD and ICCA cases and review of the literature. *Journal of neurology*. 2013;260(5):1234-44.
405. Lee YC, Lee MJ, Yu HY, Chen C, Hsu CH, Lin KP, et al. PRRT2 mutations in paroxysmal kinesigenic dyskinesia with infantile convulsions in a Taiwanese cohort. *PLoS One*. 2012;7(8):e38543.

406. Li HF, Ni W, Xiong ZQ, Xu J, Wu ZY. PRRT2 c.649dupC mutation derived from de novo in paroxysmal kinesigenic dyskinesia. *CNS neuroscience & therapeutics*. 2013;19(1):61-5.
407. Heron SE, Grinton BE, Kivity S, Afawi Z, Zuberi SM, Hughes JN, et al. PRRT2 mutations cause benign familial infantile epilepsy and infantile convulsions with choreoathetosis syndrome. *The American Journal of Human Genetics*. 2012;90(1):152-60.
408. Ji Z, Su Q, Hu L, Yang Q, Liu C, Xiong J, et al. Novel loss-of-function PRRT2 mutation causes paroxysmal kinesigenic dyskinesia in a Han Chinese family. *BMC Neurol*. 2014;14:146.
409. Li J, Zhu X, Wang X, Sun W, Feng B, Du T, et al. Targeted genomic sequencing identifies PRRT2 mutations as a cause of paroxysmal kinesigenic choreoathetosis. *Journal of medical genetics*. 2012;49(2):76-8.
410. Gardiner AR, Bhatia KP, Stamelou M, Dale RC, Kurian MA, Schneider SA, et al. PRRT2 gene mutations from paroxysmal dyskinesia to episodic ataxia and hemiplegic migraine. *Neurology*. 2012;79(21):2115-21.
411. Groffen AJ, Klapwijk T, van Rootselaar A-F, Groen JL, Tijssen MA. Genetic and phenotypic heterogeneity in sporadic and familial forms of paroxysmal dyskinesia. *Journal of neurology*. 2013;260(1):93-9.
412. van Vliet R, Breedveld G, De Rijk-Van Andel J, Brilstra E, Verbeek N, Verschuuren-Bemelmans C, et al. PRRT2 phenotypes and penetrance of paroxysmal kinesigenic dyskinesia and infantile convulsions. *Neurology*. 2012;79(8):777-84.
413. Wang K, Zhao X, Du Y, He F, Peng G, Luo B. Phenotypic overlap among paroxysmal dyskinesia subtypes: Lesson from a family with PRRT2 gene mutation. *Brain and Development*. 2013;35(7):664-6.
414. van Strien TW, van Rootselaar A-F, Hilgevoord AA, Linssen WH, Groffen AJ, Tijssen MA. Paroxysmal kinesigenic dyskinesia: cortical or non-cortical origin. *Parkinsonism & related disorders*. 2012;18(5):645-8.
415. Riant F, Roze E, Barbance C, Méneret A, Guyant-Maréchal L, Lucas C, et al. PRRT2 mutations cause hemiplegic migraine. *Neurology*. 2012;79(21):2122-4.
416. Liu Q, Qi Z, Wan X-H, Li J-Y, Shi L, Lu Q, et al. Mutations in PRRT2 result in paroxysmal dyskinesias with marked variability in clinical expression. *Journal of medical genetics*. 2012;49(2):79-82.

417. Ono S, Yoshiura K-i, Kinoshita A, Kikuchi T, Nakane Y, Kato N, et al. Mutations in PRRT2 responsible for paroxysmal kinesigenic dyskinesias also cause benign familial infantile convulsions. *Journal of human genetics*. 2012;57(5):338-41.
418. Lee H, Huang Y, Bruneau N, Roll P, Roberson E, Hermann M. Mutations in the novel protein PRRT2 cause paroxysmal kinesigenic dyskinesia with infantile convulsions. *Cell Rep*. 2012; 1: 2–12. Using whole exome sequencing in 6 samples from well-defined families with PKD and infantile seizures the authors identified PRRT2 mutations and confirmed this gene to be associated with ICCA in further 25 families with this phenotype.
419. Schubert J, Paravidino R, Becker F, Berger A, Bebek N, Bianchi A, et al. PRRT2 mutations are the major cause of benign familial infantile seizures. *Human mutation*. 2012;33(10):1439-43.
420. Schmidt A, Kumar KR, Redyk K, Grünwald A, Leben M, Münchau A, et al. Two faces of the same coin: benign familial infantile seizures and paroxysmal kinesigenic dyskinesia caused by PRRT2 mutations. *Archives of neurology*. 2012;69(5):668-70.
421. Dale RC, Gardiner A, Antony J, Houlden H. Familial PRRT2 mutation with heterogeneous paroxysmal disorders including paroxysmal torticollis and hemiplegic migraine. *Developmental Medicine & Child Neurology*. 2012;54(10):958-60.
422. Steinlein OK, Villain M, Korenke C. The PRRT2 mutation c. 649dupC is the so far most frequent cause of benign familial infantile convulsions. *Seizure*. 2012;21(9):740-2.
423. Specchio N, Terracciano A, Trivisano M, Cappelletti S, Claps D, Travaglini L, et al. PRRT2 is mutated in familial and non-familial benign infantile seizures. *European Journal of Paediatric Neurology*. 2013;17(1):77-81.
424. Hedera P, Xiao J, Puschmann A, Momčilović D, Wu SW, LeDoux MS. Novel PRRT2 mutation in an African-American family with paroxysmal kinesigenic dyskinesia. *BMC neurology*. 2012;12(1):93.
425. Ishii A, Yasumoto S, Ihara Y, Inoue T, Fujita T, Nakamura N, et al. Genetic analysis of PRRT2 for benign infantile epilepsy, infantile convulsions with choreoathetosis syndrome, and benign convulsions with mild gastroenteritis. *Brain and Development*. 2013;35(6):524-30.

426. Cloarec R, Bruneau N, Rudolf G, Massacrier A, Salmi M, Bataillard M, et al. PRRT2 links infantile convulsions and paroxysmal dyskinesia with migraine. *Neurology*. 2012;79(21):2097-103.
427. Marini C, Conti V, Mei D, Battaglia D, Lettori D, Losito E, et al. PRRT2 mutations in familial infantile seizures, paroxysmal dyskinesia, and hemiplegic migraine. *Neurology*. 2012;79(21):2109-14.
428. Scheffer IE, Grinton BE, Heron SE, Kivity S, Afawi Z, Iona X, et al. PRRT2 phenotypic spectrum includes sporadic and fever-related infantile seizures. *Neurology*. 2012;79(21):2104-8.
429. de Vries B, Callenbach PM, Kamphorst JT, Weller CM, Koelewijn SC, ten Houten R, et al. PRRT2 mutation causes benign familial infantile convulsions. *Neurology*. 2012;79(21):2154-5.
430. Okumura A, Shimojima K, Kubota T, Abe S, Yamashita S, Imai K, et al. PRRT2 mutation in Japanese children with benign infantile epilepsy. *Brain and Development*. 2013;35(7):641-6.
431. Li HF, Ni W, Xiong ZQ, Xu J, Wu ZY. PRRT2 c. 649dupC mutation derived from de novo in paroxysmal kinesigenic dyskinesia. *CNS neuroscience & therapeutics*. 2013;19(1):61-5.
432. Sheerin U-M, Stamelou M, Charlesworth G, Shiner T, Spacey S, Valente E-M, et al. Migraine with aura as the predominant phenotype in a family with a PRRT2 mutation. *Journal of neurology*. 2013;260(2):656-60.
433. Castiglioni C, López I, Riant F, Bertini E, Terracciano A. PRRT2 mutation causes paroxysmal kinesigenic dyskinesia and hemiplegic migraine in monozygotic twins. *European Journal of Paediatric Neurology*. 2013;17(3):254-8.
434. Dale RC, GRATTAN-SMITH P, Nicholson M, Peters GB. Microdeletions detected using chromosome microarray in children with suspected genetic movement disorders: a single-centre study. *Developmental Medicine & Child Neurology*. 2012;54(7):618-23.
435. Almén MS, Bringeland N, Fredriksson R, Schiöth HB. The dispanins: a novel gene family of ancient origin that contains 14 human members. *PLoS One*. 2012;7(2):e31961.

436. D'Arcangelo G, Grassi F, Ragozzino D, Santoni A, Tancredi V, Eusebi F. Interferon inhibits synaptic potentiation in rat hippocampus. *Brain research*. 1991;564(2):245-8.
437. Osen-Sand A, Catsicas M, Staple JK, Jones KA, Ayala G, Knowles J, et al. Inhibition of axonal growth by SNAP-25 antisense oligonucleotides in vitro and in vivo. *Nature*. 1993;364(6436):445.
438. Grosse G, Grosse J, Tapp R, Kuchinke J, Gorsleben M, Fetter I, et al. SNAP-25 requirement for dendritic growth of hippocampal neurons. *Journal of neuroscience research*. 1999;56(5):539-46.
439. Foncke E, Gerrits M, Van Ruissen F, Baas F, Hedrich K, Tijssen C, et al. Distal myoclonus and late onset in a large Dutch family with myoclonus–dystonia. *Neurology*. 2006;67(9):1677-80.
440. Asmus F, Gasser T. Inherited myoclonus-dystonia. *Advances in neurology*. 2004;94:113.
441. Nardocci N, Zorzi G, Barzaghi C, Zibordi F, Ciano C, Ghezzi D, et al. Myoclonus–dystonia syndrome: clinical presentation, disease course, and genetic features in 11 families. *Movement Disorders*. 2008;23(1):28-34.
442. Roze E, Apartis E, Clot F, Dorison N, Thobois S, Guyant-Marechal L, et al. Myoclonus–dystonia Clinical and electrophysiologic pattern related to SGCE mutations. *Neurology*. 2008;70(13):1010-6.
443. Kyllerman M, Forsgren L, Sanner G, Holmgren G, Wahlstrom J, Drugge U. Alcohol-responsive myoclonic dystonia in a large family: dominant inheritance and phenotypic variation. *Movement disorders : official journal of the Movement Disorder Society*. 1990;5(4):270-9.
444. Kinugawa K, Vidailhet M, Clot F, Apartis E, Grabli D, Roze E. Myoclonus-dystonia: an update. *Movement Disorders*. 2009;24(4):479-89.
445. Guettard É, Portnoi M-F, Lohmann-Hedrich K, Keren B, Rossignol S, Winkler S, et al. Myoclonus-dystonia due to maternal uniparental disomy. *Archives of neurology*. 2008;65(10):1380-5.
446. Nygaard TG, Raymond D, Chen C, Nishino I, Greene PE, Jennings D, et al. Localization of a gene for myoclonus-dystonia to chromosome 7q21-q31. *Annals of neurology*. 1999;46(5):794-8.

447. Klein C, Schilling K, Saunders-Pullman RJ, Garrels J, Breakefield XO, Brin MF, et al. A major locus for myoclonus-dystonia maps to chromosome 7q in eight families. *The American Journal of Human Genetics*. 2000;67(5):1314-9.
448. Ritz K, Van Schaik BD, Jakobs ME, Van Kampen AH, Aronica E, Tijssen MA, et al. SGCE isoform characterization and expression in human brain: implications for myoclonus–dystonia pathogenesis? *European Journal of Human Genetics*. 2011;19(4):438-44.
449. Esapa CT, Waite A, Locke M, Benson MA, Kraus M, McIlhinney RJ, et al. SGCE missense mutations that cause myoclonus-dystonia syndrome impair ϵ -sarcoglycan trafficking to the plasma membrane: modulation by ubiquitination and torsinA. *Human molecular genetics*. 2007;16(3):327-42.
450. Straub V, Ettinger AJ, Durbeej M, Venzke DP, Cutshall S, Sanes JR, et al. ϵ -Sarcoglycan replaces α -sarcoglycan in smooth muscle to form a unique dystrophin-glycoprotein complex. *Journal of Biological Chemistry*. 1999;274(39):27989-96.
451. Imamura M, Araishi K, Noguchi S, Ozawa E. A sarcoglycan–dystroglycan complex anchors Dp116 and utrophin in the peripheral nervous system. *Human Molecular Genetics*. 2000;9(20):3091-100.
452. Chan P, Gonzalez-Maeso J, Ruf F, Bishop DF, Hof PR, Sealfon SC. ϵ -Sarcoglycan immunoreactivity and mRNA expression in mouse brain. *Journal of Comparative Neurology*. 2005;482(1):50-73.
453. Ettinger AJ, Feng G, Sanes JR. ϵ -Sarcoglycan, a broadly expressed homologue of the gene mutated in limb-girdle muscular dystrophy 2D. *Journal of Biological Chemistry*. 1997;272(51):32534-8.
454. Hjermind L, Vissing J, Asmus F, Krag T, Lochmüller H, Walter M, et al. No muscle involvement in myoclonus-dystonia caused by ϵ -sarcoglycan gene mutations. *European journal of neurology*. 2008;15(5):525-9.
455. Xiao J, LeDoux MS. Cloning, developmental regulation and neural localization of rat ϵ -sarcoglycan. *Molecular brain research*. 2003;119(2):132-43.
456. Chawla G, Lin C-H, Han A, Shiue L, Ares M, Black DL. Sam68 regulates a set of alternatively spliced exons during neurogenesis. *Molecular and cellular biology*. 2009;29(1):201-13.

457. McNally EM, Ly CT, Kunkel LM. Human ϵ -sarcoglycan is highly related to α -sarcoglycan (adhalin), the limb girdle muscular dystrophy 2D gene. *FEBS letters*. 1998;422(1):27-32.
458. Holt KH, Campbell KP. Assembly of the sarcoglycan complex Insights for muscular dystrophy. *Journal of Biological Chemistry*. 1998;273(52):34667-70.
459. Lapidos KA, Kakkar R, McNally EM. The dystrophin glycoprotein complex. *Circulation research*. 2004;94(8):1023-31.
460. Bogdanik L, Framery B, Frölich A, Franco B, Mornet D, Bockaert J, et al. Muscle dystroglycan organizes the postsynapse and regulates presynaptic neurotransmitter release at the *Drosophila* neuromuscular junction. *PLoS One*. 2008;3(4):e2084.
461. Grady RM, Zhou H, Cunningham JM, Henry MD, Campbell KP, Sanes JR. Maturation and maintenance of the neuromuscular synapse: genetic evidence for roles of the dystrophin–glycoprotein complex. *Neuron*. 2000;25(2):279-93.
462. Lyons A, McQuillan K, Deighan BF, O'Reilly J-A, Downer EJ, Murphy AC, et al. Decreased neuronal CD200 expression in IL-4-deficient mice results in increased neuroinflammation in response to lipopolysaccharide. *Brain, behavior, and immunity*. 2009;23(7):1020-7.
463. Imamura M, Mochizuki Y, Engvall E, Takeda S. Epsilon-sarcoglycan compensates for lack of alpha-sarcoglycan in a mouse model of limb-girdle muscular dystrophy. *Human molecular genetics*. 2005;14(6):775-83.
464. DeBerardinis RJ, Conforto D, Russell K, Kaplan J, Kollros PR, Zackai EH, et al. Myoclonus in a patient with a deletion of the epsilon-sarcoglycan locus on chromosome 7q21. *American journal of medical genetics Part A*. 2003;121a(1):31-6.
465. Grabowski M, Zimprich A, Lorenz-Depiereux B, Kalscheuer V, Asmus F, Gasser T, et al. The epsilon-sarcoglycan gene (SGCE), mutated in myoclonus-dystonia syndrome, is maternally imprinted. *European journal of human genetics : EJHG*. 2003;11(2):138-44.
466. Muller B, Hedrich K, Kock N, Dragasevic N, Svetel M, Garrels J, et al. Evidence that paternal expression of the epsilon-sarcoglycan gene accounts for reduced penetrance in myoclonus-dystonia. *American journal of human genetics*. 2002;71(6):1303-11.

467. Valente EM, Edwards MJ, Mir P, DiGiorgio A, Salvi S, Davis M, et al. The epsilon-sarcoglycan gene in myoclonic syndromes. *Neurology*. 2005;64(4):737-9.
468. Jain P, Sharma S, van Ruissen F, Aneja S. Myoclonus-dystonia: An under-recognized entity - Report of 5 cases. *Neurology India*. 2016;64(5):980-3.
469. Raymond D, Saunders-Pullman R, de Carvalho Aguiar P, Schule B, Kock N, Friedman J, et al. Phenotypic spectrum and sex effects in eleven myoclonus-dystonia families with epsilon-sarcoglycan mutations. *Movement disorders : official journal of the Movement Disorder Society*. 2008;23(4):588-92.
470. Hess CW, Raymond D, Aguiar Pde C, Frucht S, Shriberg J, Heiman GA, et al. Myoclonus-dystonia, obsessive-compulsive disorder, and alcohol dependence in SGCE mutation carriers. *Neurology*. 2007;68(7):522-4.
471. Carecchio M, Magliozzi M, Copetti M, Ferraris A, Bernardini L, Bonetti M, et al. Defining the epsilon-sarcoglycan (SGCE) gene phenotypic signature in myoclonus-dystonia: a reappraisal of genetic testing criteria. *Movement disorders : official journal of the Movement Disorder Society*. 2013;28(6):787-94.
472. Wada T, Takano K, Tsurusaki Y, Miyake N, Nakashima M, Saitsu H, et al. Japanese familial case of myoclonus-dystonia syndrome with a splicing mutation in SGCE. *Pediatrics international : official journal of the Japan Pediatric Society*. 2015;57(2):324-6.
473. Chung EJ, Lee WY, Kim JY, Kim JH, Kim GM, Ki CS, et al. Novel SGCE gene mutation in a Korean patient with myoclonus-dystonia with unique phenotype mimicking Moya-Moya disease. *Movement disorders : official journal of the Movement Disorder Society*. 2007;22(8):1206-7.
474. Peall KJ, Kurian MA, Wardle M, Waite AJ, Hedderly T, Lin JP, et al. SGCE and myoclonus dystonia: motor characteristics, diagnostic criteria and clinical predictors of genotype. *Journal of neurology*. 2014;261(12):2296-304.
475. Hedrich K, Meyer EM, Schule B, Kock N, de Carvalho Aguiar P, Wiegers K, et al. Myoclonus-dystonia: detection of novel, recurrent, and de novo SGCE mutations. *Neurology*. 2004;62(7):1229-31.
476. Gerrits MC, Foncke EM, de Haan R, Hedrich K, van de Leemput YL, Baas F, et al. Phenotype-genotype correlation in Dutch patients with myoclonus-dystonia. *Neurology*. 2006;66(5):759-61.

477. Ritz K, Gerrits MC, Foncke EM, van Ruissen F, van der Linden C, Vergouwen MD, et al. Myoclonus-dystonia: clinical and genetic evaluation of a large cohort. *Journal of neurology, neurosurgery, and psychiatry*. 2009;80(6):653-8.
478. Schule B, Kock N, Svetel M, Dragasevic N, Hedrich K, De Carvalho Aguiar P, et al. Genetic heterogeneity in ten families with myoclonus-dystonia. *Journal of neurology, neurosurgery, and psychiatry*. 2004;75(8):1181-5.
479. Tezenas du Montcel S, Clot F, Vidailhet M, Roze E, Damier P, Jedynak CP, et al. Epsilon sarcoglycan mutations and phenotype in French patients with myoclonic syndromes. *J Med Genet*. 2006;43(5):394-400.
480. Roze E, Apartis E, Clot F, Dorison N, Thobois S, Guyant-Marechal L, et al. Myoclonus-dystonia: clinical and electrophysiologic pattern related to SGCE mutations. *Neurology*. 2008;70(13):1010-6.
481. Bonello M, Lerner A, Alusi S. Myoclonus-dystonia (DYT11) with novel SGCE mutation misdiagnosed as a primary psychiatric disorder. *Journal of the neurological sciences*. 2014;346(1):356-7.
482. Huang C-L, Lan M-Y, Chang Y-Y, Hsu C-Y, Lai S-C, Chen R-S, et al. Large SGCE deletion contributes to Taiwanese myoclonus–dystonia syndrome. *Parkinsonism & related disorders*. 2010;16(9):585-9.
483. Weissbach A, Kasten M, Grunewald A, Bruggemann N, Trillenber P, Klein C, et al. Prominent psychiatric comorbidity in the dominantly inherited movement disorder myoclonus-dystonia. *Parkinsonism & related disorders*. 2013;19(4):422-5.
484. Grunewald A, Djarmati A, Lohmann-Hedrich K, Farrell K, Zeller JA, Allert N, et al. Myoclonus-dystonia: significance of large SGCE deletions. *Human mutation*. 2008;29(2):331-2.
485. Han F, Lang AE, Racacho L, Bulman DE, Grimes DA. Mutations in the epsilon-sarcoglycan gene found to be uncommon in seven myoclonus-dystonia families. *Neurology*. 2003;61(2):244-6.
486. Cif L, Valente EM, Hemm S, Coubes C, Vayssiere N, Serrat S, et al. Deep brain stimulation in myoclonus-dystonia syndrome. *Movement disorders : official journal of the Movement Disorder Society*. 2004;19(6):724-7.
487. Asmus F, Zimprich A, Tezenas Du Montcel S, Kabus C, Deuschl G, Kupsch A, et al. Myoclonus-dystonia syndrome: epsilon-sarcoglycan mutations and phenotype. *Ann Neurol*. 2002;52(4):489-92.

488. Uruha A, Kimura K, Okiyama R. An Asian Patient with Myoclonus-Dystonia (DYT11) Responsive to Deep Brain Stimulation of the Globus Pallidus Internus. *Case Reports in Neurological Medicine*. 2014;2014:937095.
489. Szubiga M, Rudzinska M, Bik-Multanowski M, Pietrzyk JJ, Szczudlik A. A novel conserved mutation in SGCE gene in 3 unrelated patients with classical phenotype myoclonus-dystonia syndrome. *Neurological research*. 2013;35(6):659-62.
490. Zimprich A, Grabowski M, Asmus F, Naumann M, Berg D, Bertram M, et al. Mutations in the gene encoding ϵ -sarcoglycan cause myoclonus–dystonia syndrome. *Nature genetics*. 2001;29(1):66-9.
491. Tedroff K, Rolfs A, Norling A. A novel SGCE gene mutation causing myoclonus dystonia in a family with an unusual phenotype. *Acta Paediatrica*. 2012;101(2):e90-e2.
492. Fernandez-Pajarin G, Sesar A, Relova JL, Ares B, Jimenez-Martin I, Blanco-Arias P, et al. Bilateral pallidal deep brain stimulation in myoclonus-dystonia: our experience in three cases and their follow-up. *Acta neurochirurgica*. 2016;158(10):2023-8.
493. Nardocci N, Zorzi G, Barzaghi C, Zibordi F, Ciano C, Ghezzi D, et al. Myoclonus-dystonia syndrome: clinical presentation, disease course, and genetic features in 11 families. *Movement disorders : official journal of the Movement Disorder Society*. 2008;23(1):28-34.
494. Haugarvoll K, Tzoulis C, Tran GT, Karlsen B, Engelsen BA, Knappskog PM, et al. Myoclonus-dystonia and epilepsy in a family with a novel epsilon-sarcoglycan mutation. *Journal of neurology*. 2014;261(2):358-62.
495. Kock N, Kasten M, Schule B, Hedrich K, Wiegers K, Kabakci K, et al. Clinical and genetic features of myoclonus-dystonia in 3 cases: a video presentation. *Movement disorders : official journal of the Movement Disorder Society*. 2004;19(2):231-4.
496. Marechal L, Raux G, Dumanchin C, Lefebvre G, Deslandre E, Girard C, et al. Severe myoclonus-dystonia syndrome associated with a novel epsilon-sarcoglycan gene truncating mutation. *American journal of medical genetics Part B, Neuropsychiatric genetics : the official publication of the International Society of Psychiatric Genetics*. 2003;119b(1):114-7.

497. Xiao J, Nance MA, LeDoux MS. Incomplete nonsense-mediated decay facilitates detection of a multi-exonic deletion mutation in SGCE. *Clin Genet*. 2013;84(3):276-80.
498. Drivenes B, Born AP, Ek J, Dunoe M, Uldall PV. A child with myoclonus-dystonia (DYT11) misdiagnosed as atypical opsoclonus myoclonus syndrome. *European journal of paediatric neurology : EJPN : official journal of the European Paediatric Neurology Society*. 2015;19(6):719-21.
499. Asmus F, Salih F, Hjermind LE, Ostergaard K, Munz M, Kuhn AA, et al. Myoclonus-dystonia due to genomic deletions in the epsilon-sarcoglycan gene. *Ann Neurol*. 2005;58(5):792-7.
500. Borges V, Aguiar Pde C, Ferraz HB, Ozelius LJ. Novel and de novo mutations of the SGCE gene in Brazilian patients with myoclonus-dystonia. *Movement disorders : official journal of the Movement Disorder Society*. 2007;22(8):1208-9.
501. Kimura Y, Mihara M, Kawarai T, Kishima H, Sakai N, Takahashi MP, et al. Efficacy of deep brain stimulation in an adolescent patient with DYT11 myoclonus-dystonia. *Neurology and Clinical Neuroscience*. 2014;2(2):57-9.
502. Hjermind LE, Werdelin LM, Eiberg H, Krag-Olsen B, Dupont E, Sørensen SA. A novel mutation in the ϵ -sarcoglycan gene causing myoclonus-dystonia syndrome. *Neurology*. 2003;60(9):1536-9.
503. Klein C, Liu L, Doheny D, Kock N, Muller B, de Carvalho Aguiar P, et al. Epsilon-sarcoglycan mutations found in combination with other dystonia gene mutations. *Ann Neurol*. 2002;52(5):675-9.
504. Doheny D, Danisi F, Smith C, Morrison C, Velickovic M, De Leon D, et al. Clinical findings of a myoclonus-dystonia family with two distinct mutations. *Neurology*. 2002;59(8):1244-6.
505. Akbari MT, Mirfakhraie R, Zare-Karizi S, Shahidi G. Myoclonus dystonia syndrome: a novel ϵ -sarcoglycan gene mutation with variable clinical symptoms. *Gene*. 2014;548(2):306-7.
506. Misbahuddin A, Placzek M, Lennox G, Taanman JW, Warner TT. Myoclonus-dystonia syndrome with severe depression is caused by an exon-skipping mutation in the epsilon-sarcoglycan gene. *Movement disorders : official journal of the Movement Disorder Society*. 2007;22(8):1173-5.
507. Asmus F, Devlin A, Munz M, Zimprich A, Gasser T, Chinnery PF. Clinical differentiation of genetically proven benign hereditary chorea and myoclonus-

- dystonia. *Movement disorders : official journal of the Movement Disorder Society*. 2007;22(14):2104-9.
508. Kobylecki C, Damodaran D, Kerr B, Newton RW, Silverdale MA. Prominent Lower-Limb Involvement in a Family with Myoclonus-Dystonia. *Movement Disorders Clinical Practice*. 2014;1(2):115-7.
509. Foncke EM, Klein C, Koelman JH, Kramer PL, Schilling K, Muller B, et al. Hereditary myoclonus-dystonia associated with epilepsy. *Neurology*. 2003;60(12):1988-90.
510. Kuncel AM, Turner DA, Ozelius LJ, Greene PE, Grill WM, Stacy MA. Myoclonus and tremor response to thalamic deep brain stimulation parameters in a patient with inherited myoclonus-dystonia syndrome. *Clin Neurol Neurosurg*. 2009;111(3):303-6.
511. Cilia R, Reale C, Castagna A, Nasca A, Muzi-Falconi M, Barzaghi C, et al. Novel DYT11 gene mutation in patients without dopaminergic deficit (SWEDD) screened for dystonia. *Neurology*. 2014;83(13):1155-62.
512. Progression of neuropsychiatric and cognitive features due to exons 2 to 5 deletion in the epsilon-sarcoglycan gene: a case report. *Neurocase*. 2016;22(2):215-9.
513. Dobyens WB, Ozelius L, Kramer P, Brashear A, Farlow M, Perry T, et al. Rapid-onset dystonia-parkinsonism. *Neurology*. 1993;43(12):2596-.
514. Brashear A, Dobyens WB, de Carvalho Aguiar P, Borg M, Frijns CJ, Gollamudi S, et al. The phenotypic spectrum of rapid-onset dystonia-parkinsonism (RDP) and mutations in the ATP1A3 gene. *Brain*. 2007;130(Pt 3):828-35.
515. Tarsy D, Sweadner KJ, Song PC. Case 17-2010: a 29-year-old woman with flexion of the left hand and foot and difficulty speaking. *New England Journal of Medicine*. 2010;362(23):2213-9.
516. Anselm IA, Sweadner KJ, Gollamudi S, Ozelius LJ, Darras BT. Rapid-onset dystonia-parkinsonism in a child with a novel atp1a3 gene mutation. *Neurology*. 2009;73(5):400-1.
517. Pittock SJ, Joyce C, O'keane V, Hogle B, Hardiman O, Brett F, et al. Rapid-onset dystonia-parkinsonism A clinical and genetic analysis of a new kindred. *Neurology*. 2000;55(7):991-5.

References

518. Brashear A, DeLeon D, Bressman S, Thyagarajan D, Farlow M, Dobyns WB. Rapid-onset dystonia-parkinsonism in a second family. *Neurology*. 1997;48(4):1066-9.
519. Zaremba J, Mierzevska H, Lysiak Z, Kramer P, Ozelius LJ, Brashear A. Rapid-onset dystonia-parkinsonism: A fourth family consistent with linkage to chromosome 19q13. *Movement disorders*. 2004;19(12):1506-10.
520. Cook JF, Hill DF, Snively BM, Boggs N, Suerken CK, Haq I, et al. Cognitive impairment in rapid-onset dystonia-parkinsonism. *Movement disorders : official journal of the Movement Disorder Society*. 2014;29(3):344-50.
521. Brashear A, Butler IJ, Ozelius LJ, Kramer PI, Farlow MR, Breakefield XO, et al. Rapid-onset dystonia-parkinsonism: a report of clinical, biochemical, and genetic studies in two families. *Adv Neurol*. 1998;78:335-9.
522. Brashear A, Mink JW, Hill DF, Boggs N, McCall WV, Stacy MA, et al. ATP1A3 mutations in infants: a new rapid-onset dystonia-Parkinsonism phenotype characterized by motor delay and ataxia. *Developmental medicine and child neurology*. 2012;54(11):1065-7.
523. Brashear A, Mulholland GK, Zheng QH, Farlow MR, Siemers ER, Hutchins GD. PET imaging of the pre-synaptic dopamine uptake sites in rapid-onset dystonia-parkinsonism (RDP). *Movement disorders : official journal of the Movement Disorder Society*. 1999;14(1):132-7.
524. Zanotti-Fregonara P, Vidailhet M, Kas A, Ozelius LJ, Clot F, Hindie E, et al. [123I]-FP-CIT and [99mTc]-HMPAO single photon emission computed tomography in a new sporadic case of rapid-onset dystonia-parkinsonism. *J Neurol Sci*. 2008;273(1-2):148-51.
525. Svetel M, Ozelius LJ, Buckley A, Lohmann K, Brajkovic L, Klein C, et al. Rapid-onset dystonia-parkinsonism: case report. *Journal of neurology*. 2010;257(3):472-4.
526. Oblak AL, Hagen MC, Sweadner KJ, Haq I, Whitlow CT, Maldjian JA, et al. Rapid-onset dystonia-parkinsonism associated with the I758S mutation of the ATP1A3 gene: a neuropathologic and neuroanatomical study of four siblings. *Acta neuropathologica*. 2014;128(1):81-98.

527. Yang-Feng TL, Schneider JW, Lindgren V, Shull MM, Benz EJ, Jr., Lingrel JB, et al. Chromosomal localization of human Na⁺, K⁺-ATPase alpha- and beta-subunit genes. *Genomics*. 1988;2(2):128-38.
528. Ovchinnikov Yu A, Monastyrskaya GS, Broude NE, Ushkaryov Yu A, Melkov AM, Smirnov Yu V, et al. Family of human Na⁺, K⁺-ATPase genes. Structure of the gene for the catalytic subunit (alpha III-form) and its relationship with structural features of the protein. *FEBS Lett*. 1988;233(1):87-94.
529. Kamphuis DJ, Koelman H, Lees AJ, Tijssen MA. Sporadic rapid-onset dystonia–parkinsonism presenting as Parkinson's disease. *Movement disorders*. 2006;21(1):118-9.
530. Sweadner KJ, Toro C, Whitlow CT, Snively BM, Cook JF, Ozelius LJ, et al. ATP1A3 Mutation in Adult Rapid-Onset Ataxia. *PLoS One*. 2016;11(3):e0151429.
531. Kamm C, Fogel W, Wächter T, Schweitzer K, Berg D, Kruger R, et al. Novel ATP1A3 mutation in a sporadic RDP patient with minimal benefit from deep brain stimulation. *Neurology*. 2008;70(16 Part 2):1501-3.
532. Rosewich H, Ohlenbusch A, Huppke P, Schlotawa L, Baethmann M, Carrilho I, et al. The expanding clinical and genetic spectrum of ATP1A3-related disorders. *Neurology*. 2014;82(11):945-55.
533. Barbano RL, Hill DF, Snively BM, Light LS, Boggs N, McCall WV, et al. New triggers and non-motor findings in a family with rapid-onset dystonia-parkinsonism. *Parkinsonism & related disorders*. 2012;18(6):737-41.
534. Lee JY, Gollamudi S, Ozelius LJ, Kim JY, Jeon BS. ATP1A3 mutation in the first asian case of rapid-onset dystonia-parkinsonism. *Movement Disorders*. 2007;22(12):1808-9.
535. Linazasoro G, Indakoetxea B, Ruiz J, Van Blercom N, Lasa A. Possible sporadic rapid-onset dystonia–parkinsonism. *Movement disorders*. 2002;17(3):608-9.
536. Rodacker V, Toustrup-Jensen M, Vilsen B. Mutations Phe785Leu and Thr618Met in Na⁺, K⁺-ATPase, associated with familial rapid-onset dystonia parkinsonism, interfere with Na⁺ interaction by distinct mechanisms. *Journal of Biological Chemistry*. 2006;281(27):18539-48.
537. Roubergue A, Roze E, Vuillaumier-Barrot S, Fontenille MJ, Méneret A, Vidailhet M, et al. The multiple faces of the ATP1A3-related dystonic movement disorder. *Movement Disorders*. 2013;28(10):1457-9.

538. Blanco-Arias P, Einholm AP, Mamsa H, Concheiro C, Gutiérrez-de-Terán H, Romero J, et al. A C-terminal mutation of ATP1A3 underscores the crucial role of sodium affinity in the pathophysiology of rapid-onset dystonia-parkinsonism. *Human molecular genetics*. 2009;18(13):2370-7.
539. Schneider JW, Mercer RW, Gilmore-Hebert M, Utset MF, Lai C, Greene A, et al. Tissue specificity, localization in brain, and cell-free translation of mRNA encoding the A3 isoform of Na⁺, K⁺-ATPase. *Proceedings of the National Academy of Sciences*. 1988;85(1):284-8.
540. Hilgenberg LG, Su H, Gu H, O'Dowd DK, Smith MA. α 3Na⁺/K⁺-ATPase is a neuronal receptor for agrin. *Cell*. 2006;125(2):359-69.
541. Sweadner KJ. Na, K-ATPase and its isoforms: Oxford University Press, New York; 1995.
542. Blanco G, Sanchez G, Mercer RW. Comparison of the enzymatic properties of the Na, K-ATPase alpha 3 beta 1 and alpha 3 beta 2 isozymes. *Biochemistry*. 1995;34(31):9897-903.
543. Crambert G, Hasler U, Beggah AT, Yu C, Modyanov NN, Horisberger J-D, et al. Transport and pharmacological properties of nine different human Na, K-ATPase isozymes. *Journal of Biological Chemistry*. 2000;275(3):1976-86.
544. Calderon DP, Fremont R, Kraenzlin F, Khodakhah K. The neural substrates of rapid-onset Dystonia-Parkinsonism. *Nature neuroscience*. 2011;14(3):357-65.
545. Seibler P, Djarmati A, Langpap B, Hagenah J, Schmidt A, Bruggemann N, et al. A heterozygous frameshift mutation in PRKRA (DYT16) associated with generalised dystonia in a German patient. *The Lancet Neurology*. 2008;7(5):380-1.
546. Zech M, Castrop F, Schormair B, Jochim A, Wieland T, Gross N, et al. DYT16 revisited: exome sequencing identifies PRKRA mutations in a European dystonia family. *Movement disorders : official journal of the Movement Disorder Society*. 2014;29(12):1504-10.
547. Quadri M, Olgiati S, Sensi M, Gualandi F, Groppo E, Rispoli V, et al. PRKRA Mutation Causing Early-Onset Generalized Dystonia-Parkinsonism (DYT16) in an Italian Family. *Movement disorders : official journal of the Movement Disorder Society*. 2016;31(5):765-7.
548. Chen G, Ma C, Bower KA, Ke Z, Luo J. Interaction between RAX and PKR modulates the effect of ethanol on protein synthesis and survival of neurons. *Journal of Biological Chemistry*. 2006;281(23):15909-15.

549. Patel CV, Handy I, Goldsmith T, Patel RC. PACT, a stress-modulated cellular activator of interferon-induced double-stranded RNA-activated protein kinase, PKR. *Journal of Biological Chemistry*. 2000;275(48):37993-8.
550. Patel RC, Sen GC. PACT, a protein activator of the interferon-induced protein kinase, PKR. *The EMBO Journal*. 1998;17(15):4379-90.
551. Ito T, Yang M, May WS. RAX, a cellular activator for double-stranded RNA-dependent protein kinase during stress signaling. *The Journal of biological chemistry*. 1999;274(22):15427-32.
552. D'Acquisto F, Ghosh S. PACT and PKR: turning on NF- κ B in the absence of virus. *Science Signaling*. 2001;2001(89):re1-re.
553. Lee E-S, Yoon C-H, Kim Y-S, Bae Y-S. The double-strand RNA-dependent protein kinase PKR plays a significant role in a sustained ER stress-induced apoptosis. *FEBS letters*. 2007;581(22):4325-32.
554. Vaughn LS, Bragg DC, Sharma N, Camargos S, Cardoso F, Patel RC. Altered activation of protein kinase PKR and enhanced apoptosis in dystonia cells carrying a mutation in PKR activator protein PACT. *Journal of Biological Chemistry*. 2015;290(37):22543-57.
555. Uitti RJ, Maraganore D. Adult onset familial cervical dystonia: report of a family including monozygotic twins. *Movement disorders*. 1993;8(4):489-94.
556. Gilley J, Fried M. Extensive gene order differences within regions of conserved synteny between the Fugu and human genomes: implications for chromosomal evolution and the cloning of disease genes. *Human molecular genetics*. 1999;8(7):1313-20.
557. Dufke C, Hauser AK, Sturm M, Fluhr S, Wachter T, Leube B, et al. Mutations in CIZ1 are not a major cause for dystonia in Germany. *Movement disorders : official journal of the Movement Disorder Society*. 2015;30(5):740-3.
558. Ma L, Chen R, Wang L, Yang Y, Wan X. No mutations in CIZ1 in twelve adult-onset primary cervical dystonia families. *Movement disorders : official journal of the Movement Disorder Society*. 2013;28(13):1899-901.
559. Copeland NA, Sercombe HE, Ainscough JF, Coverley D. Ciz1 cooperates with cyclin-A-CDK2 to activate mammalian DNA replication in vitro. *J Cell Sci*. 2010;123(Pt 7):1108-15.

560. Coverley D, Marr J, Ainscough J. Ciz1 promotes mammalian DNA replication. *J Cell Sci.* 2005;118(Pt 1):101-12.
561. Ainscough JF, Rahman FA, Sercombe H, Sedo A, Gerlach B, Coverley D. C-terminal domains deliver the DNA replication factor Ciz1 to the nuclear matrix. *J Cell Sci.* 2007;120(Pt 1):115-24.
562. Warder DE, Keherly MJ. Ciz1, Cip1 interacting zinc finger protein 1 binds the consensus DNA sequence ARYSR(0-2)YYAC. *Journal of biomedical science.* 2003;10(4):406-17.
563. den Hollander P, Rayala SK, Coverley D, Kumar R. Ciz1, a Novel DNA-binding coactivator of the estrogen receptor alpha, confers hypersensitivity to estrogen action. *Cancer research.* 2006;66(22):11021-9.
564. Dahmcke CM, Buchmann-Moller S, Jensen NA, Mitchelmore C. Altered splicing in exon 8 of the DNA replication factor CIZ1 affects subnuclear distribution and is associated with Alzheimer's disease. *Molecular and cellular neurosciences.* 2008;38(4):589-94.
565. Judex M, Neumann E, Lechner S, Dietmaier W, Ballhorn W, Grifka J, et al. Laser-mediated microdissection facilitates analysis of area-specific gene expression in rheumatoid synovium. *Arthritis and rheumatism.* 2003;48(1):97-102.
566. Higgins G, Roper KM, Watson IJ, Blackhall FH, Rom WN, Pass HI, et al. Variant Ciz1 is a circulating biomarker for early-stage lung cancer. *Proceedings of the National Academy of Sciences of the United States of America.* 2012;109(45):E3128-35.
567. Wang DQ, Wang K, Yan DW, Liu J, Wang B, Li MX, et al. Ciz1 is a novel predictor of survival in human colon cancer. *Experimental biology and medicine (Maywood, NJ).* 2014;239(7):862-70.
568. Zhang D, Wang Y, Dai Y, Wang J, Suo T, Pan H, et al. CIZ1 promoted the growth and migration of gallbladder cancer cells. *Tumour biology : the journal of the International Society for Oncodevelopmental Biology and Medicine.* 2015;36(4):2583-91.
569. Liu T, Ren X, Li L, Yin L, Liang K, Yu H, et al. Ciz1 promotes tumorigenicity of prostate carcinoma cells. *Frontiers in bioscience (Landmark edition).* 2015;20:705-15.

570. Rahman F, Ainscough JF, Copeland N, Coverley D. Cancer-associated missplicing of exon 4 influences the subnuclear distribution of the DNA replication factor CIZ1. *Human mutation*. 2007;28(10):993-1004.
571. Xiao J, Vemula SR, Xue Y, Khan MM, Kuruvilla KP, Marquez-Lona EM, et al. Motor phenotypes and molecular networks associated with germline deficiency of Ciz1. *Experimental neurology*. 2016;283(Pt A):110-20.
572. Katoh M, Katoh M. FLJ10261 gene, located within the CCND1-EMS1 locus on human chromosome 11q13, encodes the eight-transmembrane protein homologous to C12orf3, C11orf25 and FLJ34272 gene products. *International journal of oncology*. 2003;22(6):1375-81.
573. Zech M, Gross N, Jochim A, Castrop F, Kaffe M, Dresel C, et al. Rare sequence variants in ANO3 and GNAL in a primary torsion dystonia series and controls. *Movement disorders : official journal of the Movement Disorder Society*. 2014;29(1):143-7.
574. Ma LY, Wang L, Yang YM, Feng T, Wan XH. Mutations in ANO3 and GNAL gene in thirty-three isolated dystonia families. *Movement Disorders*. 2015;30(5):743-4.
575. Stamelou M, Charlesworth G, Cordivari C, Schneider SA, Kägi G, Sheerin UM, et al. The phenotypic spectrum of DYT24 due to ANO3 mutations. *Movement Disorders*. 2014;29(7):928-34.
576. Blackburn PR, Zimmermann MT, Gass JM, Harris KG, Cousin MA, Boczek NJ, et al. A novel ANO3 variant identified in a 53-year-old woman presenting with hyperkinetic dysarthria, blepharospasm, hyperkinesias, and complex motor tics. *BMC Medical Genetics*. 2016;17(1):93.
577. Duran C, Qu Z, Osunkoya AO, Cui Y, Hartzell HC. ANOs 3-7 in the anoctamin/Tmem16 Cl⁻ channel family are intracellular proteins. *American journal of physiology Cell physiology*. 2012;302(3):C482-93.
578. Hartzell C, Putzier I, Arreola J. Calcium-activated chloride channels. *Annual review of physiology*. 2005;67:719-58.
579. Huang WC, Xiao S, Huang F, Harfe BD, Jan YN, Jan LY. Calcium-activated chloride channels (CaCCs) regulate action potential and synaptic response in hippocampal neurons. *Neuron*. 2012;74(1):179-92.

580. Vuoristo JT, Berrettini WH, Overhauser J, Prockop DJ, Ferraro TN, Ala-Kokko L. Sequence and genomic organization of the human G-protein Golfalpha gene (GNAL) on chromosome 18p11, a susceptibility region for bipolar disorder and schizophrenia. *Molecular psychiatry*. 2000;5(5):495-501.
581. Jones DT, Reed RR. Golf: an olfactory neuron specific-G protein involved in odorant signal transduction. *Science (New York, NY)*. 1989;244(4906):790-5.
582. Herve D, Le Moine C, Corvol JC, Belluscio L, Ledent C, Fienberg AA, et al. Galpha(olf) levels are regulated by receptor usage and control dopamine and adenosine action in the striatum. *The Journal of neuroscience : the official journal of the Society for Neuroscience*. 2001;21(12):4390-9.
583. Kull B, Svenningsson P, Fredholm BB. Adenosine A(2A) receptors are colocalized with and activate g(olf) in rat striatum. *Molecular pharmacology*. 2000;58(4):771-7.
584. Corvol JC, Studler JM, Schonn JS, Girault JA, Herve D. Galpha(olf) is necessary for coupling D1 and A2a receptors to adenylyl cyclase in the striatum. *J Neurochem*. 2001;76(5):1585-8.
585. Pisani A, Bernardi G, Ding J, Surmeier DJ. Re-emergence of striatal cholinergic interneurons in movement disorders. *Trends in neurosciences*. 2007;30(10):545-53.
586. Akita K, Takahashi Y, Kataoka M, Saito K, Kaneko H. Subcellular localization of a novel G protein XLG α olf. *Biochemical and Biophysical Research Communications*. 2009;381(4):582-6.
587. Kotowski SJ, Hopf FW, Seif T, Bonci A, von Zastrow M. Endocytosis promotes rapid dopaminergic signaling. *Neuron*. 2011;71(2):278-90.
588. Puthenveedu MA, Yudowski GA, von Zastrow M. Endocytosis of neurotransmitter receptors: location matters. *Cell*. 2007;130(6):988-9.
589. Vemula SR, Puschmann A, Xiao J, Zhao Y, Rudzińska M, Frei KP, et al. Role of G α (olf) in familial and sporadic adult-onset primary dystonia. *Human molecular genetics*. 2013;22(12):2510-9.
590. LeDoux MS, Vemula SR, Xiao J, Thompson MM, Perlmutter JS, Wright LJ, et al. Clinical and genetic features of cervical dystonia in a large multicenter cohort. *Neurology Genetics*. 2016;2(3):e69.

591. Ziegan J, Wittstock M, Westenberger A, Dobricic V, Wolters A, Benecke R, et al. Novel GNAL mutations in two German patients with sporadic dystonia. *Movement disorders : official journal of the Movement Disorder Society*. 2014;29(14):1833-4.
592. Miao J, Wan XH, Sun Y, Feng JC, Cheng FB. Mutation screening of GNAL gene in patients with primary dystonia from Northeast China. *Parkinsonism & related disorders*. 2013;19(10):910-2.
593. Dos Santos CO, Masuho I, da Silva-Junior FP, Barbosa ER, Silva SM, Borges V, et al. Screening of GNAL variants in Brazilian patients with isolated dystonia reveals a novel mutation with partial loss of function. 2016;263(4):665-8.
594. Saunders-Pullman R, Fuchs T, San Luciano M, Raymond D, Brashear A, Ortega R, et al. Heterogeneity in primary dystonia: lessons from THAP1, GNAL, and TOR1A in Amish-Mennonites. *Movement disorders : official journal of the Movement Disorder Society*. 2014;29(6):812-8.
595. Carecchio M, Panteghini C, Reale C, Barzaghi C, Monti V, Romito L, et al. Novel GNAL mutation with intra-familial clinical heterogeneity: Expanding the phenotype. *Parkinsonism & related disorders*. 2016;23:66-71.
596. Kumar KR, Lohmann K, Masuho I, Miyamoto R, Ferbert A, Lohnau T, et al. Mutations in GNAL: a novel cause of craniocervical dystonia. *JAMA Neurol*. 2014;71(4):490-4.
597. Putzel GG, Fuchs T, Battistella G, Rubien-Thomas E, Frucht SJ, Blitzler A, et al. GNAL mutation in isolated laryngeal dystonia. *Movement disorders : official journal of the Movement Disorder Society*. 2016;31(5):750-5.
598. Dobricic V, Kresojevic N, Westenberger A, Svetel M, Tomic A, Ralic V, et al. De novo mutation in the GNAL gene causing seemingly sporadic dystonia in a Serbian patient. *Movement disorders : official journal of the Movement Disorder Society*. 2014;29(9):1190-3.
599. Masuho I, Fang M, Geng C, Zhang J, Jiang H, Özgül RK, et al. Homozygous GNAL mutation associated with familial childhood-onset generalized dystonia. *Neurology: Genetics*. 2016;2(3):e78.
600. Kasahara K, Kawakami Y, Kiyono T, Yonemura S, Kawamura Y, Era S, et al. Ubiquitin-proteasome system controls ciliogenesis at the initial step of axoneme extension. *Nat Commun*. 2014;5:5081.

601. Speer MC, Tandan R, Rao PN, Fries T, Stajich JM, Bolhuis PA, et al. Evidence for locus heterogeneity in the Bethlem myopathy and linkage to 2q37. *Human molecular genetics*. 1996;5(7):1043-6.
602. Lohmann K, Schlicht F, Svetel M, Hinrichs F, Zittel S, Graf J, et al. The role of mutations in COL6A3 in isolated dystonia. *Journal of neurology*. 2016;263(4):730-4.
603. Groen JL, Andrade A, Ritz K, Jalalzadeh H, Haagmans M, Bradley TE, et al. CACNA1B mutation is linked to unique myoclonus-dystonia syndrome. *Human molecular genetics*. 2015;24(4):987-93.
604. Akita K, Takahashi Y, Takata N, Hashimoto M, Kataoka M, Tomigahara Y, et al. XLGalphaolf regulates expression of p27Kip1 in a CSN5 and CDK2 dependent manner. *Biochem Biophys Res Commun*. 2011;416(3-4):385-90.
605. Sako W, Morigaki R, Kaji R, Tooyama I, Okita S, Kitazato K, et al. Identification and localization of neuron-specific isoform of TAF1 in rat brain: implications for neuropathology of DYT3 dystonia. *Neuroscience*. 2011;189:100-7.
606. Mekhail K, Moazed D. The nuclear envelope in genome organization, expression and stability. *Nature reviews Molecular cell biology*. 2010;11(5):317.
607. Shimi T, Butin-Israeli V, Goldman RD. The functions of the nuclear envelope in mediating the molecular crosstalk between the nucleus and the cytoplasm. *Current opinion in cell biology*. 2012;24(1):71-8.
608. Basham SE, Rose LS. The *Caenorhabditis elegans* polarity gene *ooc-5* encodes a Torsin-related protein of the AAA ATPase superfamily. *Development*. 2001;128(22):4645-56.
609. Baptista MJ, O'Farrell C, Hardy J, Cookson MR. Microarray analysis reveals induction of heat shock proteins mRNAs by the torsion dystonia protein, TorsinA. *Neuroscience letters*. 2003;343(1):5-8.
610. Koh Y-H, Rehfeld K, Ganetzky B. A *Drosophila* model of early onset torsion dystonia suggests impairment in TGF- β signaling. *Human Molecular Genetics*. 2004;13(18):2019-30.
611. Diepkins G, Stutz F. Connecting the transcription site to the nuclear pore: a multi-tether process that regulates gene expression. *J Cell Sci*. 2010;123(12):1989-99.
612. Irvin JD, Pugh BF. Genome-wide transcriptional dependence on TAF1 functional domains. *Journal of Biological Chemistry*. 2006;281(10):6404-12.

613. Maile T, Kwoczynski S, Katzenberger RJ, Wassarman DA, Sauer F. TAF1 activates transcription by phosphorylation of serine 33 in histone H2B. *Science (New York, NY)*. 2004;304(5673):1010-4.
614. Hewett JW, Nery FC, Niland B, Ge P, Tan P, Hadwiger P, et al. siRNA knock-down of mutant torsinA restores processing through secretory pathway in DYT1 dystonia cells. *Human molecular genetics*. 2008;17(10):1436-45.
615. Bernasconi R, Molinari M. ERAD and ERAD tuning: disposal of cargo and of ERAD regulators from the mammalian ER. *Current opinion in cell biology*. 2011;23(2):176-83.
616. Sagun K, Cárcamo JM, Golde DW. Vitamin C enters mitochondria via facilitative glucose transporter 1 (Glut1) and confers mitochondrial protection against oxidative injury. *The FASEB journal*. 2005;19(12):1657-67.
617. Miyazaki I, Asanuma M. Dopaminergic neuron-specific oxidative stress caused by dopamine itself. *Acta medica Okayama*. 2008;62(3):141-50.
618. Stansley BJ, Yamamoto BK. L-dopa-induced dopamine synthesis and oxidative stress in serotonergic cells. *Neuropharmacology*. 2013;67:243-51.
619. Geller DA, Di Silvio M, Billiar TR, Hatakeyama K. GTP cyclohydrolase I is coinduced in hepatocytes stimulated to produce nitric oxide. *Biochemical and biophysical research communications*. 2000;276(2):633-41.
620. Sakai N, Kaufman S, Milstien S. Parallel induction of nitric oxide and tetrahydrobiopterin synthesis by cytokines in rat glial cells. *Journal of neurochemistry*. 1995;65(2):895-902.
621. Huang A, Zhang Y-Y, Chen K, Hatakeyama K, Keaney JF. Cytokine-stimulated GTP cyclohydrolase I expression in endothelial cells requires coordinated activation of nuclear factor- κ B and Stat1/Stat3. *Circulation research*. 2005;96(2):164-71.
622. Dai W, Jiang J, Kong W, Wang Y. Silencing MR-1 attenuates inflammatory damage in mice heart induced by AngII. *Biochemical and biophysical research communications*. 2010;391(3):1573-8.
623. Wong G, Goldshmit Y, Turnley AM. Interferon- γ but not TNF α promotes neuronal differentiation and neurite outgrowth of murine adult neural stem cells. *Experimental neurology*. 2004;187(1):171-7.
624. Quartarone A, Pisani A. Abnormal plasticity in dystonia: Disruption of synaptic homeostasis. *Neurobiology of disease*. 2011;42(2):162-70.

625. Knappskog PM, Flatmark T, Mallet J, Lūdecke B, Bartholomé K. Recessively inherited L-DOPA-responsive dystonia caused by a point mutation (Q381K) in the tyrosine hydroxylase gene. *Human molecular genetics*. 1995;4(7):1209-12.
626. Horstink C, Praamstra P, Horstink M, Berger H, Booij J, Van Royen E. Low striatal D2 receptor binding as assessed by [123I] IBZM SPECT in patients with writer's cramp. *Journal of Neurology, Neurosurgery & Psychiatry*. 1997;62(6):672-3.
627. Hierholzer J, Cordes M, Schelosky L, Richter W, Keske U, Venz S, et al. Dopamine D2 receptor imaging with iodine-123-iodobenzamide SPECT in idiopathic rotational torticollis. *Journal of Nuclear Medicine*. 1994;35(12):1921-7.
628. Asanuma K, Ma Y, Okulski J, Dhawan V, Chaly T, Carbon M, et al. Decreased striatal D2 receptor binding in non-manifesting carriers of the DYT1 dystonia mutation. *Neurology*. 2005;64(2):347-9.
629. Augood SJ, Hollingsworth Z, Albers D, Yang L, Leung J-C, Muller B, et al. Dopamine transmission in DYT1 dystonia: a biochemical and autoradiographical study. *Neurology*. 2002;59(3):445-8.
630. Song C-H, Fan X, Exeter CJ, Hess EJ, Jinnah H. Functional analysis of dopaminergic systems in a DYT1 knock-in mouse model of dystonia. *Neurobiology of disease*. 2012;48(1):66-78.
631. Hewett J, Johansen P, Sharma N, Standaert D, Balcioglu A. Function of dopamine transporter is compromised in DYT1 transgenic animal model in vivo. *Journal of neurochemistry*. 2010;113(1):228-35.
632. Carbon M, Eidelberg D. Abnormal structure-function relationships in hereditary dystonia. *Neuroscience*. 2009;164(1):220-9.
633. Park SK, Nguyen MD, Fischer A, Luke MP-S, Affar EB, Dieffenbach PB, et al. Par-4 links dopamine signaling and depression. *Cell*. 2005;122(2):275-87.
634. Beukers RJ, Booij J, Weisscher N, Zijlstra F, van Amelsvoort T, Tijssen MA. Reduced striatal D2 receptor binding in myoclonus–dystonia. *European journal of nuclear medicine and molecular imaging*. 2009;36(2):269-74.
635. Yokoi F, Dang MT, Li J, Li Y. Myoclonus, motor deficits, alterations in emotional responses and monoamine metabolism in ϵ -sarcoglycan deficient mice. *Journal of Biochemistry*. 2006;140(1):141-6.
636. Zhang L, Yokoi F, Parsons DS, Standaert DG, Li Y. Alteration of striatal dopaminergic neurotransmission in a mouse model of DYT11 myoclonus-dystonia. *PLoS One*. 2012;7(3):e33669.

637. Lombroso C, Fischman A. Paroxysmal non-kinesigenic dyskinesia: pathophysiological investigations. *Epileptic disorders: international epilepsy journal with videotape*. 1999;1(3):187-93.
638. Lee H-y, Nakayama J, Xu Y, Fan X, Karouani M, Shen Y, et al. Dopamine dysregulation in a mouse model of paroxysmal nonkinesigenic dyskinesia. *The Journal of clinical investigation*. 2012;122(2):507-18.
639. Brashear A, Butler IJ, Hyland K, Farlow MR, Dobyns WB. Cerebrospinal fluid homovanillic acid levels in rapid-onset dystonia-parkinsonism. *Annals of neurology*. 1998;43(4):521-6.
640. Brashear A, Farlow M, Butler I, Kasarskis E, Dobyns WB. Variable phenotype of rapid-onset dystonia-parkinsonism. *Movement disorders*. 1996;11(2):151-6.
641. Ashmore LJ, Hrizo SL, Paul SM, Van Voorhies WA, Beitel GJ, Palladino MJ. Novel mutations affecting the Na, K ATPase alpha model complex neurological diseases and implicate the sodium pump in increased longevity. *Human genetics*. 2009;126(3):431-47.
642. Sun Y, Dong Z, Khodabakhsh H, Chatterjee S, Guo S. Zebrafish chemical screening reveals the impairment of dopaminergic neuronal survival by cardiac glycosides. *PLoS one*. 2012;7(4):e35645.
643. Zhuang X, Belluscio L, Hen R. G(olf)alpha mediates dopamine D1 receptor signaling. *The Journal of neuroscience : the official journal of the Society for Neuroscience*. 2000;20(16):Rc91.
644. Naiya T, Biswas A, Neogi R, Datta S, Misra A, Das S, et al. Clinical characterization and evaluation of DYT1 gene in Indian primary dystonia patients. *Acta neurologica scandinavica*. 2006;114(3):210-5.
645. Hettich J, Ryan SD, Souza ON, Saraiva Macedo Timmers LF, Tsai S, Atai NA, et al. Biochemical and cellular analysis of human variants of the DYT1 dystonia protein, TorsinA/TOR1A. *Human mutation*. 2014;35(9):1101-13.
646. Fasano A, Nardocci N, Elia AE, Zorzi G, Bentivoglio AR, Albanese A. Non-DYT1 early-onset primary torsion dystonia: Comparison with DYT1 phenotype and review of the literature. *Movement disorders*. 2006;21(9):1411-8.
647. Kamm C, Castelon-Konkiewitz E, Naumann M, Heinen F, Brack M, Nebe A, et al. GAG deletion in the DYT1 gene in early limb-onset idiopathic torsion dystonia in Germany. *Movement disorders*. 1999;14(4):681-3.

648. Schmidt A, Altenmüller E, Jabusch H-C, Lee A, Wiegers K, Klein C, et al. The GAG deletion in Tor1A (DYT1) is a rare cause of complex musician's dystonia. *Parkinsonism & related disorders*. 2012;18(5):690-1.
649. Tuffery-Giraud S, Cavalier L, Roubertie A, Guittard C, Carles S, Calvas P, et al. No evidence of allelic heterogeneity in the DYT1 gene of European patients with early onset torsion dystonia. *Journal of medical genetics*. 2001;38(10):e35-e.
650. Brassat D, Camuzat A, Vidailhet M, Feki I, Jedynak P, Klap P, et al. Frequency of the DYT1 mutation in primary torsion dystonia without family history. *Archives of neurology*. 2000;57(3):333-5.
651. Lebre A-S, Durr A, Jedynak P, Ponsot G, Vidailhet M, Agid Y, et al. DYT1 mutation in French families with idiopathic torsion dystonia. *Brain*. 1999;122(1):41-5.
652. Hjermind LE, Werdelin LM, Sorensen S. Inherited and de novo mutations in sporadic cases of DYT1-dystonia. *European Journal of Human Genetics*. 2002;10(3):213-6.
653. Zorzi G, Garavaglia B, Invernizzi F, Girotti F, Soliveri P, Zeviani M, et al. Frequency of DYT1 mutation in early onset primary dystonia in Italian patients. *Movement disorders*. 2002;17(2):407-8.
654. Major T, Svetel M, Romac S, Kostić VS. DYT1 mutation in primary torsion dystonia in a Serbian population. *Journal of neurology*. 2001;248(11):940-3.
655. Valente E, Warner T, Jarman P, Mathen D, Fletcher N, Marsden C, et al. The role of DYT1 in primary torsion dystonia in Europe. *Brain*. 1998;121(12):2335-9.
656. Gajos A, Piaskowski S, Sławek J, Ochudło S, Opala G, Łobińska A, et al. Phenotype of the DYT1 mutation in the TOR1A gene in a Polish population of patients with dystonia. A preliminary report. *Neurologia i neurochirurgia polska*. 2006;41(6):487-94.
657. O'Riordan S, Cockburn D, Barton D, Lynch T, Hutchinson M. Primary torsion dystonia due to the Tor1A GAG deletion in an Irish family. *Irish journal of medical science*. 2002;171(1):31-2.
658. Ritz K, Groen JL, Kruisdijk JJ, Baas F, Koelman JH, Tijssen MA. Screening for dystonia genes DYT1, 11 and 16 in patients with writer's cramp. *Movement Disorders*. 2009;24(9):1390-2.
659. Giri S, Biswas A, Das SK, Ray K, Ray J. Molecular basis of DYT1 and DYT6 primary dystonia in Indian patients. *Molecular Cytogenetics*. 2014;7(1):1.

660. Akbari MT, Zand Z, Shahidi GA, Hamid M. Clinical features, DYT1 mutation screening and genotype-phenotype correlation in patients with dystonia from Iran. *Medical Principles and Practice*. 2012;21(5):462-6.
661. Matsumoto S, Nishimura M, Kaji R, Sakamoto T, Mezaki T, Shimazu H, et al. DYT1 mutation in Japanese patients with primary torsion dystonia. *Neuroreport*. 2001;12(4):793-5.
662. Im J-H, Ahn T-B, Kim KB, Ko S-B, Jeon BS. DYT1 mutation in Korean primary dystonia patients. *Parkinsonism & related disorders*. 2004;10(7):421-3.
663. Lin Y-W, Chang H-C, Chou Y-HW, Chen R-S, Hsu W-C, Wu W-S, et al. DYT1 mutation in a cohort of Taiwanese primary dystonias. *Parkinsonism & related disorders*. 2006;12(1):15-9.
664. Yang J-F, Wu T, Li J-Y, Li Y-J, Zhang Y-L, Chan P. DYT1 mutations in early onset primary torsion dystonia and Parkinson disease patients in Chinese populations. *Neuroscience letters*. 2009;450(2):117-21.
665. Zhang SS, Fang DF, Hu XH, Burgunder JM, Chen XP, Zhang YW, et al. Clinical feature and DYT1 mutation screening in primary dystonia patients from South-West China. *European Journal of Neurology*. 2010;17(6):846-51.
666. Slominsky PA, Markova ED, Shadrina MI, Illarioshkin SN, Miklina NI, Limborska SA, et al. A common 3-bp deletion in the DYT1 gene in Russian families with early-onset torsion dystonia. *Human mutation*. 1999;14:269-.
667. Camargo CHF, Camargos ST, Raskin S, Cardoso FEC, Teive HAG. Genetic evaluation for TOR1-A (DYT1) in Brazilian patients with dystonia. *Arquivos de neuro-psiquiatria*. 2014;72(10):753-6.
668. Müller U. The monogenic primary dystonias. *Brain*. 2009;132(8):2005-25.
669. Spatola M, Wider C. Overview of primary monogenic dystonia. *Parkinsonism & related disorders*. 2012;18:S158-S61.
670. Kaffe M, Gross N, Castrop F, Dresel C, Gieger C, Lichtner P, et al. Mutational screening of THAP1 in a German population with primary dystonia. *Parkinsonism & related disorders*. 2012;18(1):104-6.
671. Van Gerpen JA, LeDoux MS, Wszolek ZK. Adult-onset leg dystonia due to a missense mutation in THAP1. *Movement Disorders*. 2010;25(9):1306-7.
672. Fahn S, Eldridge R. Definition of dystonia and classification of the dystonic states. *Advances in neurology*. 1976;14:1.

673. Johns MB, Paulus-Thomas JE. Purification of human genomic DNA from whole blood using sodium perchlorate in place of phenol. *Analytical biochemistry*. 1989;180(2):276-8.
674. Sambrook J, Fritsch E, Maniatis T. 1989 *Molecular Cloning A Laboratory Manual*. Cold Spring Harbor Laboratory Press, Cold Spring Harbor, NY; 1989.
675. Rozen S, Skaletsky H. Primer3 on the WWW for general users and for biologist programmers. *Bioinformatics methods and protocols*. 1999:365-86.
676. Sanger F, Nicklen S, Coulson AR. DNA sequencing with chain-terminating inhibitors. *Proceedings of the National Academy of Sciences of the United States of America*. 1977;74(12):5463-7.
677. Tatusova TA, Madden TL. BLAST 2 Sequences, a new tool for comparing protein and nucleotide sequences. *FEMS microbiology letters*. 1999;174(2):247-50.
678. Adzhubei I, Jordan DM, Sunyaev SR. Predicting functional effect of human missense mutations using PolyPhen-2. *Current protocols in human genetics*. 2013;Chapter 7:Unit7.20.
679. Kumar P, Henikoff S, Ng PC. Predicting the effects of coding non-synonymous variants on protein function using the SIFT algorithm. *Nature protocols*. 2009;4(7):1073-81.
680. Schwarz JM, Cooper DN, Schuelke M, Seelow D. MutationTaster2: mutation prediction for the deep-sequencing age. *Nat Meth*. 2014;11(4):361-2.
681. Liu X, Jian X, Boerwinkle E. dbNSFP v2.0: a database of human non-synonymous SNVs and their functional predictions and annotations. *Human mutation*. 2013;34(9):E2393-402.
682. Rosner BA. *Fundamentals of Biostatistics*: Thomson-Brooks/Cole; 2006.
683. Zuker M. Mfold web server for nucleic acid folding and hybridization prediction. *Nucleic Acids Research*. 2003;31(13):3406-15.
684. Barrett JC, Fry B, Maller J, Daly MJ. Haploview: analysis and visualization of LD and haplotype maps. *Bioinformatics*. 2005;21(2):263-5.
685. Hahn LW, Ritchie MD, Moore JH. Multifactor dimensionality reduction software for detecting gene-gene and gene-environment interactions. *Bioinformatics*. 2003;19(3):376-82.
686. Opal P, Tintner R, Jankovic J, Leung J, Breakefield XO, Friedman J, et al. Intrafamilial phenotypic variability of the DYT1 dystonia: from asymptomatic TOR1A gene carrier status to dystonic storm. *Movement disorders*. 2002;17(2):339-45.

References

687. Ikeuchi T, Shimohata T, Nakano R, Koide R, Takano H, Tsuji S. A case of primary torsion dystonia in Japan with the 3-bp (GAG) deletion in the DYT1 gene with a unique clinical presentation. *Neurogenetics*. 1999;2(3):189-90.
688. Caputo M, Irisarri M, Perandones C, Alechine E, Pellene LA, Roca CU, et al. Analysis of D216H polymorphism in Argentinean patients with primary dystonia. *Journal of neurogenetics*. 2013;27(1-2):16-8.
689. Groen JL, Ritz K, Tanck MW, Warrenburg BP, Hilten JJ, Aramideh M, et al. Is TOR1A a risk factor in adult-onset primary torsion dystonia? *Movement Disorders*. 2013;28(6):827-31.
690. Wang L, Duan C, Gao Y, Xu W, Ding J, Liu VT, et al. Lack of association between TOR1A and THAP1 mutations and sporadic adult-onset primary focal dystonia in a Chinese population. *Clinical neurology and neurosurgery*. 2016;142:26-30.
691. Frédéric MY, Clot F, Blanchard A, Dhaenens CM, Lesca G, Cif L, et al. The p. Asp216His TOR1A allele effect is not found in the French population. *Movement Disorders*. 2009;24(6):919-21.
692. Sharma N, Franco RA, Kuster JK, Mitchell AA, Fuchs T, Saunders-Pullman R, et al. Genetic evidence for an association of the TOR1A locus with segmental/focal dystonia. *Movement Disorders*. 2010;25(13):2183-7.
693. Chen Y, Burgunder JM, Song W, Huang R, Shang HF. Assessment of D216H DYT1 polymorphism in a Chinese primary dystonia patient cohort. *European Journal of Neurology*. 2012;19(6):924-6.
694. Chen Y, Chen K, Burgunder J-M, Song W, Huang R, Zhao B, et al. Association of rs1182 polymorphism of the DYT1 gene with primary dystonia in Chinese population. *Journal of the neurological sciences*. 2012;323(1):228-31.
695. Kamm C, Asmus F, Mueller J, Mayer P, Sharma M, Muller U, et al. Strong genetic evidence for association of TOR1A/TOR1B with idiopathic dystonia. *Neurology*. 2006;67(10):1857-9.
696. Defazio G, Matarin M, Peckham EL, Martino D, Valente EM, Singleton A, et al. The TOR1A polymorphism rs1182 and the risk of spread in primary blepharospasm. *Movement Disorders*. 2009;24(4):613-6.

697. Xiromerisiou G, Dardiotis E, Tsironi EE, Hadjigeorgiou G, Ralli S, Kara E, et al. THAP1 mutations in a Greek primary blepharospasm series. *Parkinsonism & related disorders*. 2013;19(3):404-5.
698. Sabogal A, Lyubimov AY, Corn JE, Berger JM, Rio DC. THAP proteins target specific DNA sites through bipartite recognition of adjacent major and minor grooves. *Nature structural & molecular biology*. 2010;17(1):117-23.
699. Grundmann K, Reischmann B, Vanhoutte G, Hübener J, Teismann P, Hauser T-K, et al. Overexpression of human wildtype torsinA and human Δ GAG torsinA in a transgenic mouse model causes phenotypic abnormalities. *Neurobiology of disease*. 2007;27(2):190-206.
700. Sobell HM. Actinomycin and DNA transcription. *Proceedings of the National Academy of Sciences*. 1985;82(16):5328-31.
701. Lange A, McLane LM, Mills RE, Devine SE, Corbett AH. Expanding the definition of the classical bipartite nuclear localization signal. *Traffic*. 2010;11(3):311-23.
702. Goldberg AL. Protein degradation and protection against misfolded or damaged proteins. *Nature*. 2003;426(6968):895-9.
703. Ciechanover A, Kwon YT. Degradation of misfolded proteins in neurodegenerative diseases: therapeutic targets and strategies. *Experimental & molecular medicine*. 2015;47(3):e147.
704. Guo L, Giasson BI, Glavis-Bloom A, Brewer MD, Shorter J, Gitler AD, et al. A cellular system that degrades misfolded proteins and protects against neurodegeneration. *Molecular cell*. 2014;55(1):15-30.
705. Miyazawa S. Selection maintaining protein stability at equilibrium. *Journal of theoretical biology*. 2016;391:21-34.
706. Ling S-C, Albuquerque CP, Han JS, Lagier-Tourenne C, Tokunaga S, Zhou H, et al. ALS-associated mutations in TDP-43 increase its stability and promote TDP-43 complexes with FUS/TLS. *Proceedings of the National Academy of Sciences*. 2010;107(30):13318-23.
707. Lian X, Guo J, Gu W, Cui Y, Zhong J, Jin J, et al. Genome-Wide and Experimental Resolution of Relative Translation Elongation Speed at Individual Gene Level in Human Cells. *PLoS Genet*. 2016;12(2):e1005901.
708. Dobin A, Davis CA, Schlesinger F, Drenkow J, Zaleski C, Jha S, et al. STAR: ultrafast universal RNA-seq aligner. *Bioinformatics*. 2013;29(1):15-21.

709. Hanash S. Disease proteomics. *Nature*. 2003;422(6928):226-32.
710. Altelaar AM, Munoz J, Heck AJ. Next-generation proteomics: towards an integrative view of proteome dynamics. *Nature Reviews Genetics*. 2013;14(1):35-48.
711. Zhao Y-Y, Lin R-C. UPLC-MS E application in disease biomarker discovery: the discoveries in proteomics to metabolomics. *Chemico-biological interactions*. 2014;215:7-16.
712. Martin JN, Bair TB, Bode N, Dauer WT, Gonzalez-Alegre P. Transcriptional and proteomic profiling in a cellular model of DYT1 dystonia. *Neuroscience*. 2009;164(2):563-72.
713. Thompson A, Schäfer J, Kuhn K, Kienle S, Schwarz J, Schmidt G, et al. Tandem mass tags: a novel quantification strategy for comparative analysis of complex protein mixtures by MS/MS. *Analytical chemistry*. 2003;75(8):1895-904.
714. Dayon L, Hainard A, Licker V, Turck N, Kuhn K, Hochstrasser DF, et al. Relative quantification of proteins in human cerebrospinal fluids by MS/MS using 6-plex isobaric tags. *Analytical chemistry*. 2008;80(8):2921-31.
715. Li Z, Adams RM, Chourey K, Hurst GB, Hettich RL, Pan C. Systematic comparison of label-free, metabolic labeling, and isobaric chemical labeling for quantitative proteomics on LTQ Orbitrap Velos. *Journal of proteome research*. 2012;11(3):1582-90.
716. Renuse S, Chaerkady R, Pandey A. Proteogenomics. *Proteomics*. 2011;11(4):620-30.
717. Smith PK, Krohn RI, Hermanson G, Mallia A, Gartner F, Provenzano M, et al. Measurement of protein using bicinchoninic acid. *Analytical biochemistry*. 1985;150(1):76-85.
718. Wiechelman KJ, Braun RD, Fitzpatrick JD. Investigation of the bicinchoninic acid protein assay: identification of the groups responsible for color formation. *Analytical biochemistry*. 1988;175(1):231-7.
719. Jochim A, Zech M, Gora-Stahlberg G, Winkelmann J, Haslinger B. The clinical phenotype of early-onset isolated dystonia caused by recessive COL6A3 mutations (DYT27). *Movement Disorders*. 2015.
720. Wu YR, Foo JN, Tan LC, Chen CM, Prakash KM, Chen YC, et al. Identification of a novel risk variant in the FUS gene in essential tremor. *Neurology*. 2013;81(6):541-4.

References

721. Izumi Y, Miyamoto R, Morino H, Yoshizawa A, Nishinaka K, Udaka F, et al. Cerebellar ataxia with SYNE1 mutation accompanying motor neuron disease. *Neurology*. 2013;80(6):600-1.
722. Brighina L, Riva C, Bertola F, Fermi S, Saracchi E, Piolti R, et al. Association analysis of PARP1 polymorphisms with Parkinson's disease. *Parkinsonism & related disorders*. 2011;17(9):701-4.
723. Naismith TV, Dalal S, Hanson PI. Interaction of torsinA with its major binding partners is impaired by the dystonia-associated Δ GAG deletion. *Journal of Biological Chemistry*. 2009;284(41):27866-74.
724. Rittiner JE, Caffall ZF, Hernández-Martinez R, Sanderson SM, Pearson JL, Tsukayama KK, et al. Functional Genomic Analyses of Mendelian and Sporadic Disease Identify Impaired eIF2 α Signaling as a Generalizable Mechanism for Dystonia. *Neuron*. 2016;92(6):1238-51.

Appendix I

List of Publications pertaining for this thesis

1. **Giri S**, Biswas A, Das SK, Ray K, Ray J. Molecular basis of *DYT1* and *DYT6* primary dystonia in Indian patients. *Molecular Cytogenetics* 2014 7(Suppl 1):P121.
2. **Giri S**, Naiya T, Eqbal Z, Sankhla CS, Das SK, Ray K, Ray J. Genetic screening of THAP1 in primary dystonia patients of India. *Neurosci Lett.* 2016 Nov 29. pii: S0304-3940(16)30928-4.

Manuscripts

1. **Giri S**, Biswas A, Das SK, Ray K, Ray J. Primary generalized dystonia due to *TOR1A* Δ GAG mutation in an Indian family with intrafamilial clinical heterogeneity. (manuscript in preparation)
2. **Giri S**, Roy S, Ghosh A, Sankhla CS, Das SK, Ray K, Ray J. Association between *GCH1* polymorphism and sporadic primary dystonia in an Indian case-control group. (manuscript in preparation)
3. **Giri S**, Das SK, Ray K, Ray J. Common polymorphism of *TOR1A* may be predisposed as a risk factor for Indian primary dystonia patients. (manuscript in preparation)

Appendix II

Papers presented in international and national conferences:

1. **Oral presentation** entitled as “Role of *TOR1A* & *THAP1* genetic variants in primary dystonia pathogenesis and it’s functional implications” on the occasion of **4th Annual symposium of Calcutta Consortium of Human Genetics** held at Jhargram, West Bengal during **12th – 13th November, 2016**.
2. **Presented a poster** entitled “Genetic analysis of *TOR1A* & *THAP1* genes in Indian primary dystonia patients” on the occasion of **4th Asian and Oceanian Parkinson’s Disease and Movement Disorders Congress** organized by International Parkinson and Movement Disorder Society during **28th - 30th November, 2014** at Pattaya, Thailand. (**Abstract published in Movement Disorder journal**).
3. **Presented a poster** entitled “Molecular Basis of *DYT1* and *DYT6* Primary Dystonia in Indian Patients” on the occasion of **International Conference on human genetics & 39th Annual Meeting of Indian Society of Human genetics** held at Ahmedabad, India during **22nd – 25th January, 2014**. (**Abstract published in Molecular Cytogenetics; doi: 10.1186/1755-8166-7-S1-P121**).
4. **Presented a poster** entitled “Genetic Analysis for Molecular Pathogenesis of Primary Dystonia Patients in India” on the occasion of **International Update on Movement Disorder** held at Siliguri, India during **14th – 16th February, 2014**.
5. **Oral presentation** entitled “Genetic analysis of primary torsion dystonia among Indian patients” on the occasion of **Neuroupdate** held at Kolkata, India during **22nd – 23rd September, 2012**.
6. **Oral presentation** of “Genetic analysis of primary torsion dystonia patients of Eastern India” on the occasion of **Annual symposium of Indian Academy of**

Neurosciences (IAN), Kolkata Chapter held at Kolkata, India during **6th September, 2013**.

7. **Presented a poster** entitled “Screening of *THAP1* gene to identify mutations in primary dystonia patients of India” on the occasion of **Frontiers in Modern Biology organised** by Indian Institute of Science Education and Research (IISER) – Kolkata held at Kolkata during **9th – 10th November, 2013**.
8. **Oral presentation** of “Molecular Basis of Primary Dystonia among Indian Patients” on the occasion of annual meeting of **Society of Biological Chemists (SBC)** – Kolkata Chapter held at Kolkata, India during **26th April, 2014**.

Active participation in scientific workshop/symposium

1. Actively participated in **National Workshop on Proteomics** for hands-on training in **Isothermal Titration Calorimetry (ITC)** during **23rd - 25th February, 2015** organized by DBT-CU-IPLS in Calcutta University, Kolkata, India.
2. Actively participated in **Indo-British Neurosciences symposium** organized by Institute of Neurosciences, Kolkata (INK) on **1st December, 2013**.
3. Actively participated in a hands-on training workshop on “**Chromatography – the catapult for unraveling the facts of nature**” organized by Department of Botany, University of Calcutta during **26th – 27th December, 2013**.
4. Actively participated in the workshop on “**PCR based strategies for genetic testing**” on **23rd January, 2014** as a part of International Conference on Human Genetics & 39th Annual meeting of Indian Society of Human Genetics held at Ahmedabad, India.

Appendix III

Awards & achievements:

1. Secured the **second position** for oral presentation in a young scientist forum of 4th Annual symposium of Calcutta Consortium of Human Genetics held at Jhargram, West Bengal during 12th – 13th November, 2016.
2. Awarded as **Fulbright-Nehru Doctoral Research Fellow** for the 2015 - 2016 academic session from United States - India Educational Foundation (USIEF) jointly sponsored by Govt. of India and Department of State, USA.
3. Recipient of "**Travel Grant**" award for presentation of research work entitled "Genetic Analysis of *TOR1A* & *THAP1* genes in Indian Primary Dystonia Patients" in the 4th Asian and Oceanian Parkinson's Disease and Movement Disorders Congress (*AOPMC*) held at Pattaya, Thailand during 28th - 30th November, 2014.
4. Secured the **third position** for poster presentation in a young scientist forum held in International Update on Movement Disorder held at Siliguri, India during 14th – 16th February, 2014.
5. Qualify for **National Eligibility Test (NET)** examination in 2011 for Life science organized by University grant Commission - Council of Scientific & Industrial Research (UGC-CSIR), Govt. of India.
6. Awarded with **Gold medal for securing the First (1st) position** with First Class in **M.Sc University examination**.

Member of professional societies

1. Life member of Indian Academy of Neurosciences, India.
2. Life member of Society of Biological Chemists, India.
3. Annual student member of Calcutta Consortium of Human Genetics, India.
4. Annual student member of International Parkinson and Movement Disorder Society.